The role of PAK6 in HGF-induced prostate cancer cell migration

Fram, Sally

Awarding institution:
King's College London

Title: The role of PAK6 in HGF-induced prostate cancer cell migration

Author: Sally Fram

The role of PAK6 in HGF-induced prostate cancer cell migration

Sally Teresa Fram

Division of Cancer Studies
King's College London

Submitted to fulfil the requirements of the degree of PhD

I declare that the work presented in this thesis is the work of the author and others' work is fully acknowledged where included

Acknowledgements

I would like to thank my supervisor, Claire Wells, for her supervision and guidance as well as her invaluable advice throughout the course of my PhD. I would also like to thank my second supervisor Anne Ridley for all her help and advice.

I would also like to thank Andrew Whale for all his technical assistance, particularly in the Molecular Biology aspect of the project. Thank you to all the members of the Wells' lab - Anna Dart, Fariesha Hashim, Fahim Ismail, Helen King and Nicole Taylor; and to the many others that have helped in the completion of this work.

To Anna and Fariesha – my fellow 'powerpuff' girls! I'll miss all our laughs and jokes, this whole experience would not have been the same without you both. Thanks for being such great friends; I hope to share many more fun times with you both in the future. Fariesha, we did it! Anna, thank you so much for all your help and motivating words during the writing of this thesis – you've been amazing!

I would also like to thank my friends and family for their constant love and support. I owe the greatest thank you to my mum and dad who always strived to provide the best for me, especially throughout my education. The opportunity of pursuing a PhD would not have been possible without them.

Words cannot express how grateful I am to my husband, Stu. Thank you for believing in me and for all your patience, encouragement and unconditional love throughout the PhD. You have celebrated with me during the highs and comforted me during the lows - I could not have done this without you.

To my late father, Freddy; you fought and lost your battle to cancer during my A-levels and what you endured led me to pursue a career in science and eventually a PhD in cancer research. You were the best dad anyone could wish for; always smiling, always caring. I know that this achievement would have made you so proud and happy and I wish that you could have been here to share it with me. I dedicate this thesis in the loving memory of my dad.

Abstract

Cell migration plays a significant role in carcinoma metastasis in which cancer cells move from the primary site and establish tumours at a secondary location. During tumour progression cancer cells can assume a migratory phenotype which is characterised by cell-cell dissociation and single cells adopting a migratory morphology. Hepatocyte growth factor (HGF) signalling is known to induce cell-cell dissociation and is associated with prostate carcinoma progression.

HGF-induced cell-cell dissociation and migration require the activity of the Rho family GTPases RhoA, Rac1 and Cdc42 and their effector proteins, p21-activated kinases (PAKs), which are a family of mammalian serine/threonine protein kinases. PAK6, a PAK family member, is over-expressed in prostate cancer but little is known about its function in cells. This project investigated the potential role of PAK6 downstream of HGF in DU145 colony-forming prostate cancer cells. These cells exhibit prominent epithelial-cadherin (E-cadherin)-associated cell-cell junctions and 'scatter' upon HGF stimulation.

Studies described here show that HGF addition increases PAK6 autophosphorylation and that PAK6 depletion inhibits HGF-induced DU145 cell scattering where these cells retain junctional E-cadherin. Moreover, PAK6 over-expression induces cell elongation and colony escape in unstimulated DU145 cells and PAK6 localises to E-cadherin positive cell junctions. Functional studies identified IQ motif containing GTPase activating protein 1 (IQGAP1) as a PAK6 binding partner in DU145 cells. Furthermore, PAK6 interacts with IQGAP1 in an HGF-dependent manner and both proteins act synergistically to induce cell colony escape. Additional studies suggest a complex relationship between IQGAP1, PAK6 and E-cadherin during HGF-induced junctional disassembly where IQGAP1 mediates PAK6 activity.

The work presented here demonstrates that PAK6 has an important function during HGF-induced cancer cell-cell dissociation.

Table of contents

List of tables

List of figures

Abbreviations

[γ-^{32}P]	Gamma-phosphorus 32-labelled
2D	2-Dimensional
3D	3-Dimensional
AID	Autoinhibitory domain
AJs	Adherens junctions
AR	Androgen receptor
Arp2/3	Actin-related protein 2/3
ATP	Adenosine triphosphate
DAPI	4', 6-diamidino-2-phenylindole
E. coli	Escherichia coli
E-cadherin	Epithelial-cadherin
ECM	Extracellular matrix
EGF	Epidermal growth factor
(E)GFP	(Enhanced) green fluorescent protein
EGFR	Epidermal growth factor receptor
EL cells	Mouse L fibroblasts stably expressing E-cadherin
EMT	Epithelial to mesenchymal transition
ERK1	Extracellular receptor kinase 1
ERK2	Extracellular receptor kinase 2
F-actin	Filamentous actin
FBS	Foetal bovine serum
G-actin	Globular actin
GAPDH	Glyceraldehyde 3-phosphate dehydrogenase
GDP	Guanosine diphosphate
GEF(s)	Guanine nucleotide exchange factor(s)
GRD	Ras GTPase-activating protein (GAP)-related domain
GTP	Guanosine triphosphate
HGF	Hepatocyte growth factor
IQGAP (1-3)	IQ motif containing GTPase activating protein (isoforms 1-3)
LBD	Ligand binding domain

MAPK	Mitogen activated protein kinase
Mbt	Mushroom bodies tiny
MDCK	Madin-Darby Canine Kidney
MEK1	Mitogen-activated protein kinase/extracellular signal-regulated kinase kinase 1
MEK2	Mitogen-activated protein kinase/extracellular signal-regulated kinase kinase 2
mRFP1/RFP	Monomeric red fluorescent protein
PAK(s)	p21-activated kinase(s)
PBD	p21-binding domain
siRNA	Short interfering RNA
WB	Western blotting/immunoblotted
WCL	Whole cell lysate(s)
WT	Wild-type
XFP	GFP/mRFP1 tagged
X-PAK5	*Xenopus* PAK4 homologue
α-catenin	Alpha-catenin
β-catenin	Beta-catenin

Chapter 1
Introduction

Chapter 1 – Introduction

1.1 Cell migration

1.1.1 The importance of cell migration

Cell migration is a dynamic process that is required during various physiological activities such as morphogenesis (Vasilyev et al., 2009; Zhang et al., 2011), wound healing (Krawczyk, 1971; Ortonne et al., 1981; Schneider et al., 2010) and immune responses (Tomura et al., 2010; Tomura et al., 2008). Moreover, cell movement is involved in several diseases including atherosclerosis (Prescott et al., 1989; Vogt et al., 2008) and rheumatoid arthritis (McInnes et al., 1996; Shadidi et al., 2002). Cell migration also plays a significant role in carcinoma metastasis (Chaffer and Weinberg, 2011).

1.1.2 The role of the actin cytoskeleton during cell migration

During cell migration, the ability to re-organise the actin cytoskeleton is a fundamental requirement as the actin cytoskeleton is responsible for the changes in cell shape and the generation of forces that are required for cells to migrate (Hall, 1998). Actin filament turnover is important for the regulation of the actin cytoskeleton. Actin exists in two forms, a monomeric form, termed globular actin (G-actin), and a polymeric form known as filamentous actin (F-actin) (Straub, 1943). The G-actin monomer acts as a position of nucleation to generate F-actin filaments in a process termed polymerisation (Mommaerts, 1952). The F-actin generated by polymerisation is in a head-to-tail orientation (Wegner, 1976). Furthermore, the nucleation of G-actin monomers occurs more readily at the 'barbed' end of actin filaments (Pollard and Borisy, 2003). Thus the actin filaments exhibit polarity and are arranged with their fast-growing ends pointing towards the plasma membrane and this enables directed actin extension (Small et al., 1978).

Lamellipodia and filopodia are both products of this actin dependent protrusion and contribute to cell motility (Ridley, 2011). Lamellipodia can be characterised by their flat and broad morphology; in contrast, filopodia are recognised as finger-like projections (Small et al., 2002). In the body of the cell actin filaments are arranged as anti-parallel fibers, termed stress fibers; these fibers create the contractile forces that are required during cell movement (Katoh et al., 2001). Indeed, experiments using photoactivatable

caged-fluorescent actin demonstrated the rapid turnover of actin subunits within the lamellipodium of migrating cells (Theriot and Mitchison, 1991). More recently, fluorescence localization after photobleaching (FLAP) was employed as a novel method to monitor actin localisation and dynamics at the leading edge of migrating cells (Dunn et al., 2002). Fluorescence recovery after photobleaching (FRAP) studies have also been used to show that actin and actin-related protein 2/3 (Arp2/3) complex turnover both occur at the lamellipodial tip of motile cells (Lai et al., 2008). The Arp2/3 complex is important in facilitating the extension of actin and the production of branched actin filaments at the front of a migrating cell (Mullins et al., 1998). To achieve prolonged cell migration the actin-rich membrane protrusions that are created in the direction of movement must be stabilised by attachment of the cell to the underlying extracellular matrix (ECM) at the leading edge (Friedl and Wolf, 2003; Ridley, 2011). These adhesions then go on to generate sites of cell contraction which propel the cell forward (Ridley et al., 2003). In conjunction, to allow translocation, cell-ECM adhesions must be disrupted at the rear of the cell (Lauffenburger and Horwitz, 1996).

1.1.2.1 The role of cell-substratum adhesions during cell migration

Integrin-mediated signalling plays an important role in cell attachment to the ECM during cell migration (Huttenlocher and Horwitz, 2011). Integrins are cell surface receptors for ECM proteins, such as collagen I (Di Lullo et al., 2002; Mizuno et al., 2000) and fibronectin (Garćia and Boettiger, 1999), as well as collagen V (Ruggiero et al., 1994) and laminins (Kikkawa et al., 2000). Integrins are ubiquitously expressed (Virtanen et al., 1990) and the aberrant expression and behaviour of integrins has been associated with carcinoma metastasis including that of the breast (Taherian et al., 2011), prostate (Gorlov et al., 2009; McCabe et al., 2007) and pancreas (Hosotani et al., 2002).

1.1.3 Carcinoma metastasis

Although many biological processes require cell migration, this study is focussed on the movement of prostate cancer cells. Human cancers are mainly found to be epithelial in origin and this is true of prostate cancer; where the majority of prostate cancers manifest from the peripheral region of the prostate gland (McNeal, 1969) (**figure 1.1A**) and are predominantly adenocarcinoma in type, originating from the glandular epithelial tissue (**figure 1.1B**) (Shen and Abate-Shen, 2010). Cancer cell migration is a pre-requisite for metastasis and metastatic disease is the main cause of death in patients with malignant

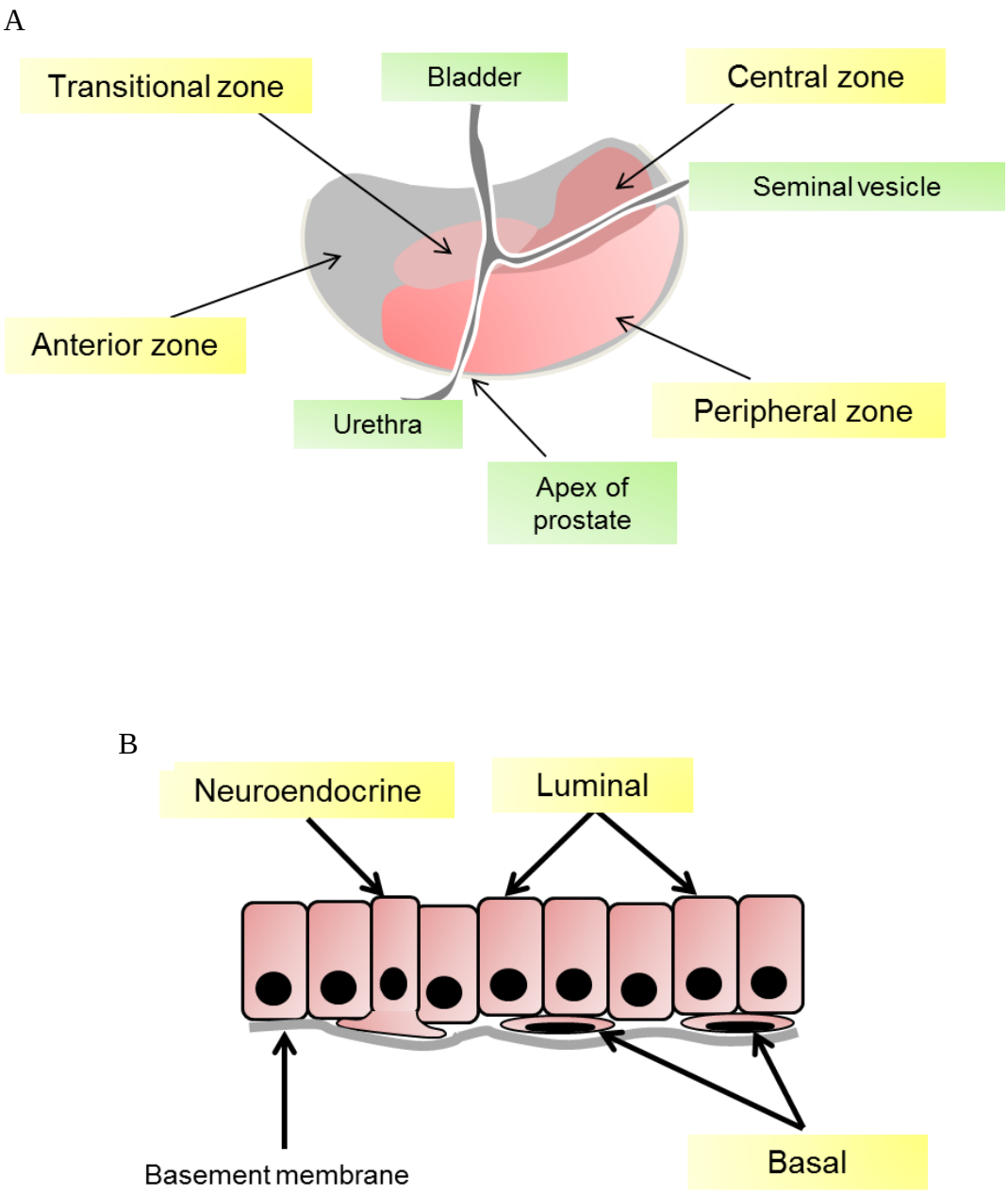

Figure 1.1 The architecture of the prostate gland. A) Schematic illustrating the different regions within the prostate gland which can be divided into four main regions termed the peripheral zone, transitional zone, central zone and the anterior fibromuscular zone as indicated (McNeal, 1988; Timms, 2008). The location of the bladder, seminal vesicles and urethra in relation to the prostate are also marked. The prostate gland is adjoined to the upper portion of the urethra. This figure is adapted from (www.harvardprostateknowledge.org/prostate-basics). **B)** The prostate gland is composed of different types of epithelial cells. Basal cells rest on the underlying basement membrane, beneath columnar luminal cells (Long et al., 2005). Neuroendocrine cells are interspersed within the epithelium with predominant incidence within the basal cell layer (Hudson, 2004). This figure is adapted from (Wang et al., 2009).

cancer (Jemal et al., 2008). Metastasis is a multi-stage process, as illustrated in **figure 1.2**. At the primary site following oncogenic transformation, cancer cells proliferate aberrantly (Fidler, 2003). The growing tumour expands and eventually requires support from a new capillary network developed from pre-existing vasculature in a process termed angiogenesis (Folkman, 1971; Folkman et al., 1963; Greene, 1941). Within the primary tumour, a selective group of tumour cells may undergo an epithelial to mesenchymal transition (EMT)-like process (Gabbert et al., 1985); EMT involves the loss of intercellular adhesivity and the dissociation of cells from the primary tumour mass, where these cells subsequently adopt a motile phenotype (Yilmaz and Christofori, 2009). Cells that have undergone EMT are then able to cross the basement membrane, migrate through the stroma and subsequently enter into the lymphatic or the vascular systems in a process termed intravasation (Wyckoff et al., 2000). Those cancer cells that survive the hostile environment of the circulatory system then exit into the surrounding tissue, in a process termed extravasation (Cameron et al., 2000; Luzzi et al., 1998). These cells must then instigate and sustain growth to produce micrometastases (Luzzi et al., 1998).

The location of distal metastasis is often defined by the site of the primary tumour and in patients with prostate cancer there is a predominance of skeletal metastases (Bubendorf et al., 2000). Indeed, numerous reports have shown that bone marrow secondary micrometastasis is favoured by prostate cancers (Ellis et al., 2003; Pantel et al., 1995; Pantel et al., 1997; Tsingotjidou et al., 2001). The metastatic cascade is actually rather inefficient and only a small proportion of disseminating cells have the capacity to proliferate and generate a macroscopic tumour (Cameron et al., 2000; Luzzi et al., 1998). Nevertheless, metastasis is still incurable and deadly (Duffy et al., 2008) and thus it is important to establish the mechanisms involved in this process for the development of future anti-metastatic therapies.

1.1.4 Differences in 2-Dimensional and 3-Dimensional cancer cell migration

There are two principle methods by which cancer cells are observed to migrate *in vivo*; collective cell migration and single cell migration (Friedl and Gilmour, 2009). Collective migration can be characterised by the collective movement of cell clusters (Farooqui and Fenteany, 2005; Vaughan and Trinkaus, 1966). This clustering phenotype

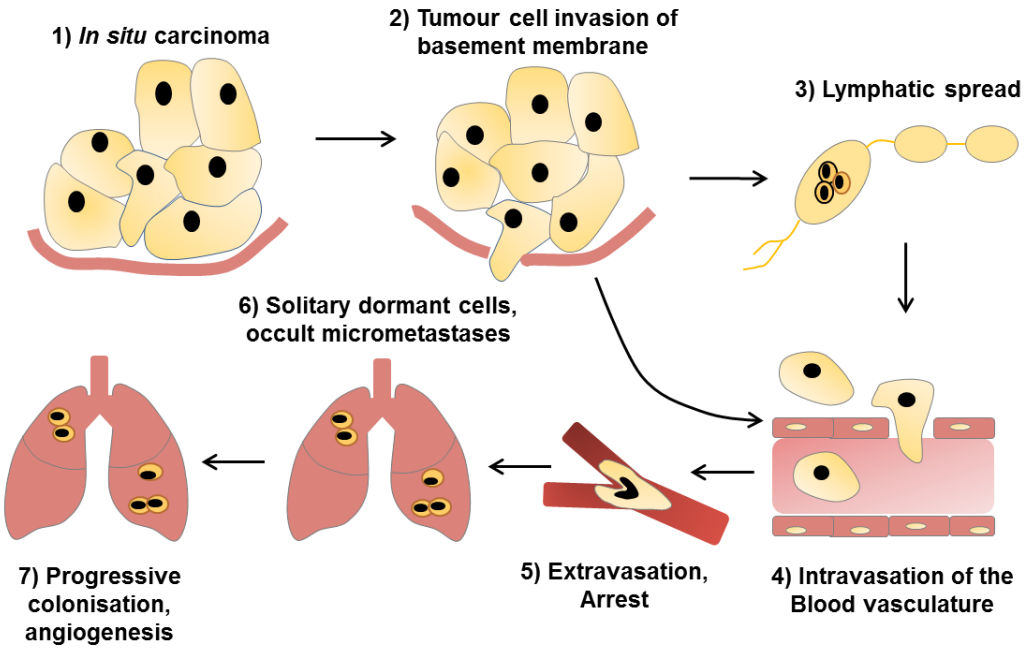

Figure 1.2 The different stages involved in carcinoma metastasis. 1) *In situ* cancer is supported by the underlying basement membrane. 2) Changes in cell-cell adhesions and cell-matrix adhesions, re-organisation of the actin cytoskeleton and basement membrane degradation instigate tumour cell movement from the primary site. 3) The dissociated tumour cells can then disseminate via the lymphatic system or 4) the blood vasculature. 5) The circulating tumour cells exit the circulation into the surrounding tissue (extravasation). 6) Occult micrometastases may develop and 7) gradually form metastases with angiogenic properties. This figure is adapted from (Steeg, 2003).

has been implicated in many invasive forms of cancer (Alexander et al., 2008; Friedl et al., 1995; Hegerfeldt et al., 2002; Iwanicki et al., 2011; Nabeshima et al., 2000). The migration of individual cancer cells has been extensively studied *in vitro* using 2-Dimensional (2D) substratums, and more recently in 3-Dimensional (3D) matrices. Numerous studies have now established that there is variation in cancer cell behaviour between 2D and 3D substratums (Sahai, 2007). For example, cells can present different morphologies; PC3 prostate carcinoma cells are observed as single cells when seeded onto 2D surfaces (Bright et al., 2009) but these cells form spheroids when grown in a 3D matrix (Härmä et al., 2010; Ivascu and Kubbies, 2006). In addition, changes in cancer cell polarity and morphogenesis (Itoh et al., 2007), gene expression (Ghosh et al., 2005), tumour cell growth (Liu et al., 2004) and variations in the effects of growth factor stimulation (Brinkmann et al., 1995) have also been reported between 2D substratums and 3D matrices. 3D studies have also revealed that within single migration populations, cancer cells exhibit either an amoeboid motility where cells are phenotypically rounded or a mesenchymal mode of migration where cells are elongated in appearance; furthermore, cancer cells can switch between these two forms of motility (Sahai and Marshall, 2003). Such studies have highlighted the need for more 3D models of cell migration and invasion.

In prostate cancer, a number of different cell lines have been routinely used to monitor migration in 2D including DU145 (Bright et al., 2009) and PC3 (Ahmed et al., 2008) cells. Moreover, more recently efforts have been made to develop 3D model systems. A 3D model system was implemented to demonstrate that matrix metalloproteinases can change the morphology of LNCaP prostate cancer cells from multi-cellular structures to possessing a fibroblast-like phenotype (Cao et al., 2008), but there was no evidence of active migration. DU145 cells have been reported to migrate through a 3D matrix (Zaman et al., 2006) and following the studies presented here a recent publication demonstrated that DU145 cells can be stimulated to form elongated ‘sprouts’ in a 3D matrix (van Leenders et al., 2011); however again active migration was not reported.

1.2 Growth factor-stimulated cell migration in cancer

1.2.1 Growth factor signalling in cancer

Growth factor signalling is known to be involved in the aberrant regulation of cell migration that is characteristic of invasive cancer cells (Alper et al., 2001; Jeffers et al., 1996; Lu et al., 2001). Specifically, epidermal growth factor (EGF) has been implicated in promoting cell movement in prostate carcinomas (Zhou et al., 2006) and the invasive potential of DU145 cells increases downstream of EGF (Turner et al., 1996). Other growth factors, such as hepatocyte growth factor (HGF), are also involved in cancer progression (Fujiuchi et al., 2003).

1.2.2 HGF

HGF is a multi-functional polypeptide that has both mitogenic (Clark, 1994; Gmyrek et al., 2001) and motogenic (Cantley et al., 1994; Niranjan et al., 1995) properties and was identified as a ligand for c-Met, a tyrosine kinase receptor (Bottaro et al., 1991; Nakamura et al., 1989). The binding of HGF to c-Met triggers receptor kinase activation and in turn initiates various signal transduction pathways that can affect, for example, cell adhesion status (Trusolino et al., 2000) and re-organisation of the actin cytoskeleton (Ridley et al., 1995; Royal et al., 2000; Wells et al., 2005). HGF is also involved in oncogenic signalling as illustrated in **figure 1.3** (Peruzzi and Bottaro, 2006). Early studies indicated that HGF was important for liver regeneration in hepatocytes (Hamanoue et al., 1992; Ishii et al., 1995). Indeed, HGF knockout mice are embryonic lethal (Schmidt et al., 1995). Initial investigations implicated HGF in cell migration; HGF was originally termed as scatter factor for its ability to induce cell-cell dissociation in colony-forming epithelial cells, as well as promoting the migration potential of single cells (Stoker, 1989; Stoker et al., 1987; Stoker and Perryman, 1985).

HGF elicits the scattering and invasion of pancreatic and bladder carcinoma cells into collagen gels (Weidner et al., 1990). A similar result was observed for Caco-2 colon carcinoma cells; these cells exhibited an increased ability to invade matrigel upon HGF addition (Kermorgant et al., 2001). It has also been demonstrated that HGF increases the invasiveness of breast cancer cells (Trusolino et al., 2000). In addition, HGF has been extensively studied in prostate carcinoma (Fujiuchi et al., 2003; Gmyrek et al., 2001).

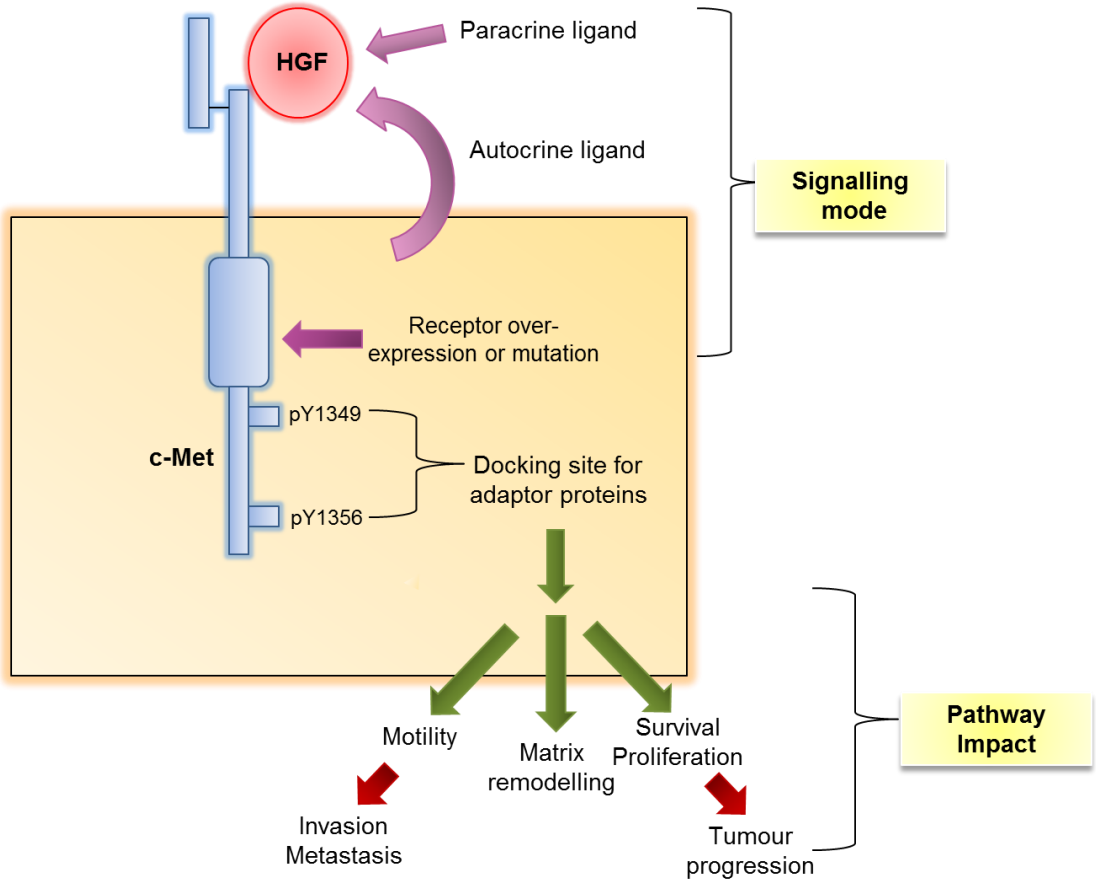

Figure 1.3 HGF and its receptor c-Met in oncogenic signalling. Oncogenic signalling through c-Met is associated with altered paracrine HGF levels and subsequent c-Met over-expression (Peruzzi and Bottaro, 2006). Signalling can also occur though the generation of autocrine HGF; pathway stimulation contributes to invasion, metastasis and tumour progression (Peruzzi and Bottaro, 2006). Tyrosine phosphorylation of residues Y1349 and Y1356 is required for the biological function of c-Met and mediates the interaction of multiple substrates with the receptor (Lai et al., 2009). This figure is adapted from (Peruzzi and Bottaro, 2006).

1.2.2.1 HGF signalling in prostate carcinoma

Oncogenic signalling via c-Met commonly occurs through paracrine (Knowles et al., 2009) or autocrine (Toiyama et al., 2011) HGF-induced activation of c-Met (**figure 1.3**). Moreover, c-Met is over-expressed in prostate cancer cells (van Leenders et al., 2002). More recently, it has been shown that an increase in the percentage of c-Met-expressing prostate cancer cells significantly correlates with the development of bone metastases (Colombel et al., 2011).

HGF stimulation increases the proliferation of prostate cancer cells (Gmyrek et al., 2001) and their ability to invade through a matrix (Fujiuchi et al., 2003; Nishimura et al., 1999; Parr et al., 2001). It has also been shown that HGF promotes the migration potential of prostate cancer cells (Ahmed et al., 2008; Parr et al., 2001). This growth factor has also been implicated in inducing cell scattering and migration in DU145 cells (Davies et al., 2004; Miura et al., 2001; Wells et al., 2005).

1.2.2.2 HGF-induced cell scattering

HGF-induced cell scattering requires the disruption of cell-cell junctions. Cell-cell contact disassembly is a process that occurs as a consequence of the re-organisation of the actin cytoskeleton and subsequent cell spreading (Ridley et al., 1995). A group of proteins, known as Rho GTPases, are activated by HGF and are pivotal in mediating the actin re-modelling that is required for the cell-cell dissociation in response to HGF (Royal et al., 2000). The binding of HGF to its receptor c-Met triggers a loss of stress fibres and a reduction in prominent actin filaments in colony-forming cells (Wells et al., 2005). HGF-induced activation of c-Met also promotes the formation of filopodia and lamellipodia mediated by the Rho GTPases Cdc42 and Rac1, respectively (Royal et al., 2000). These actin-rich protrusions are required for cell spreading, a process that precedes, and is important for, cell-cell junction disassembly (Ridley et al., 1995; Royal et al., 2000).

It has also been demonstrated that c-Met co-localises with E-cadherin (Kamei et al., 1999), a junctional protein central to the stabilisation of cell-cell adhesions (Gumbiner et al., 1988), at cell-cell contact sites in Madin-Darby Canine Kidney (MDCK) cells in the absence of HGF stimulation (Kamei et al., 1999). Upon HGF addition, cell-cell junction disassembly in these cells was coupled with the endocytosis of both c-Met and

E-cadherin and this process was mediated, in part, by phosphatidylinositol 3-kinase (PI3K) (Kamei et al., 1999). Similarly, other studies have shown that PI3K is required during HGF-induced cell spreading and subsequent cell-cell junction breakdown in MDCK cells (Potempa and Ridley, 1998; Royal et al., 2000; Royal and Park, 1995). Thus the re-modelling of the actin cytoskeleton, in addition to the localisation of c-Met and E-cadherin, are important factors during HGF-induced cell-cell adhesion disruption.

Cell scattering can be characterised by the loss of cell-cell junctions and resultant cell-cell dissociation, where cells that have escaped the cell colony are elongated and migratory in morphology (Clark, 1994; Stoker, 1989; Stoker et al., 1987; Stoker and Perryman, 1985). Cell scattering also involves the loss of junctional localisation of cell adhesion proteins (Bellovin et al., 2005; Miura et al., 2001). Since the cell scattering studies of Stoker and Perryman (Stoker and Perryman, 1985), a number of groups have reported that DU145 prostate cancer cells display these characteristics in response to HGF stimulation (Bright et al., 2009; Humphrey et al., 1995; Miura et al., 2001; Wells et al., 2005). Cell scattering as a result of HGF stimulation has also been reported in colony-forming HT29 colon adenocarcinoma cells (Herrera, 1998). The HGF-induced cell scatter assay is therefore a useful model that can be used to study cell-cell dissociation and cancer cell migration in response to HGF.

1.3 Cell-cell dissociation in cancer metastasis

During cell-cell dissociation and dissemination some cancer cells may exhibit properties reminiscent of EMT (Greenburg and Hay, 1982). EMT is important during normal development; for example, in vertebrates it is well established that EMT is necessary during neural crest cell migration (Ahlstrom and Erickson, 2009) and gastrulation (Nakaya et al., 2008).

Non-transformed epithelial cells can be characterised by their non-motile phenotype combined with strong cell-cell adhesions and cell-substratum adhesions (Chaffer and Weinberg, 2011). It is thought that when these cells become transformed during cancer, apical-basal polarity is lost and intercellular cell-cell adhesion sites are weakened (Royer and Lu, 2011) (**figure 1.4**). The initial stages of the cell-cell dissociation process

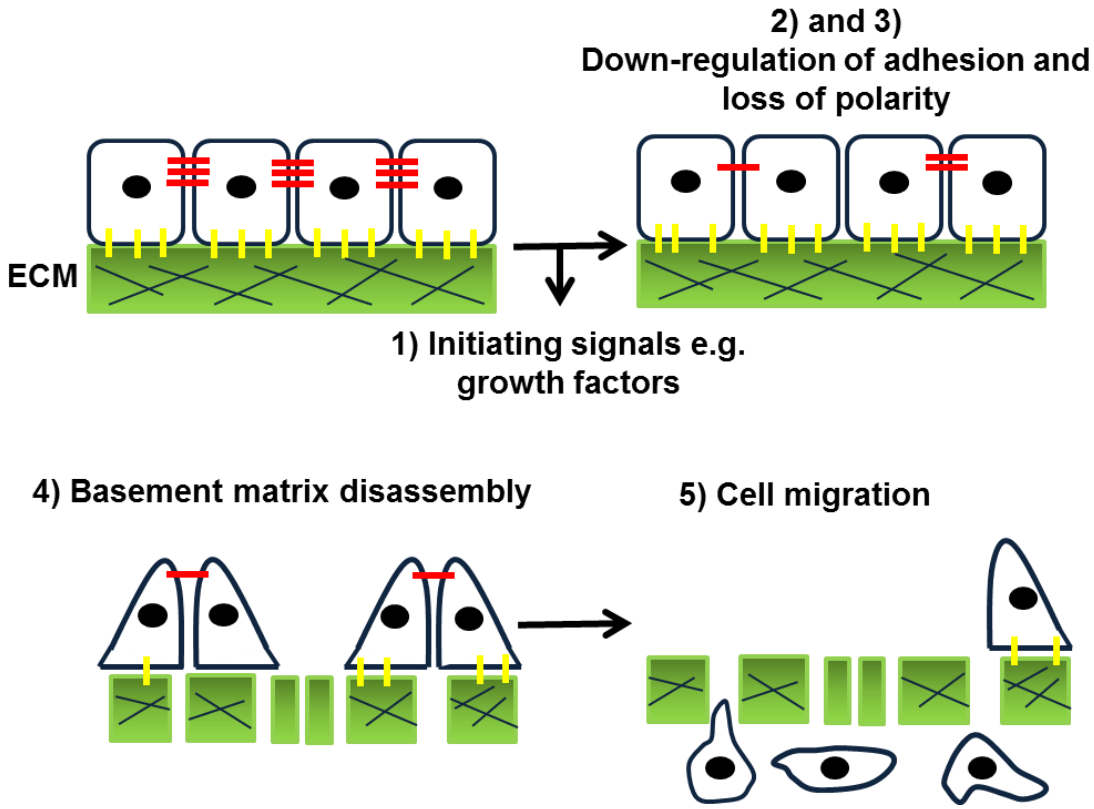

Figure 1.4 A selection of cancer cells undergo an EMT-like process during carcinoma progression. 1) Initiating factors such as growth factors instigate the 2) and 3) weakening of cell-cell junctions and the loss of cell polarity. 4) Degradation of the basement membrane and changes in cell-ECM adhesions allows 5) tumour cell escape from the primary site. This figure is adapted from (Levayer and Lecuit, 2008).

requires the disassembly of junctions between neighbouring cells and this is mediated, in part, by the re-organisation of junctional complexes.

1.3.1 Adherens junctions

Intercellular junctions are important in the maintenance of epithelial tissue structure; these junctional formations include tight junctions, adherens junctions (AJs) and desmosomes (Farquhar and Palade, 1963). AJs were initially identified in mammalian tissues using electron microscopy (Farquhar and Palade, 1963) and are responsible for cell adhesions between neighbouring epithelial cells (Gumbiner et al., 1988). Several reports have demonstrated that AJs are dynamic structures when examined *in vitro* and *in vivo* (Cavey et al., 2008; de Beco et al., 2009; Fujita et al., 2002; Pilot et al., 2006). The modulation of AJs is important during development (Shimamura and Takeichi, 1992; Vestweber and Kemler, 1984) and during disease processes such as carcinoma metastasis (Ceteci et al., 2007; Perl et al., 1998).

1.3.2 Structure of adherens junctions

The type I transmembrane proteins of AJs, cadherins, were originally identified as molecules required for the formation of adhesive cell-cell contacts (Gallin et al., 1983; Takeichi, 1977; Tanihara et al., 1994; Yoshida and Takeichi, 1982). The cell surface protein epithelial-cadherin (E-cadherin), an extensively studied member of the cadherin family, is the principle component of AJs in epithelial cells (Boller et al., 1985; Gumbiner et al., 1988). The loss of E-cadherin expression has been linked to cancer progression (Birchmeier and Behrens, 1994). Early studies tracking the movement of E-cadherin green fluorescent protein (GFP) fusion proteins using time-lapse microscopy and photobleach recovery analysis shed light on the steps thought to be required in epithelial cell-cell adhesion formation (Adams et al., 1998). This multi-stage process was shown to involve the assembly and development of E-cadherin clusters at adjoining cell membranes of adjacent cells, followed by the rapid re-organisation of actin and these E-cadherin clusters, thereby inducing tight cell colony formation (Adams et al., 1998).

E-cadherin possesses extensive intra- and extracellular domains and it has been established that the extracellular domain of one E-cadherin molecule associates with the extracellular domain of another E-cadherin molecule on an adjacent cell (Gumbiner et

al., 1988; Nose et al., 1988). In contrast, the cytoplasmic portion of E-cadherin interacts with cytosolic proteins such as catenins (Kemler and Ozawa, 1989). E-cadherin interacts with beta-catenin (β-catenin) (Aberle et al., 1994) and β-catenin sequentially binds to alpha-catenin (α-catenin) (Herrenknecht et al., 1991). Therefore, β-catenin acts as a linker between E-cadherin and α-catenin (Jou et al., 1995). α-catenin interacts with actin directly via its C-terminal region (Rimm et al., 1995) or indirectly via actin-related proteins such as alpha-actinin (α-actinin) (Knudsen et al., 1995), thereby linking E-cadherin to the actin cytoskeleton. However, more recent studies have shown that α-catenin is incapable of interacting with actin filaments whilst bound to the E-cadherin-β-catenin complex (Drees et al., 2005; Yamada et al., 2005), even when α-actinin is present (Yamada et al., 2005). Thus it has been suggested that α-catenin possesses a dual mode of action in cell-cell adhesion dynamics (Drees et al., 2005).

A third member of the catenin family, p120 catenin, also binds to E-cadherin (Daniel and Reynolds, 1995; Jou et al., 1995; Shibamoto et al., 1995) through the juxtamembrane domain within the cytoplasmic tail of E-cadherin (Ohkubo and Ozawa, 1999; Reynolds et al., 1996; Thoreson et al., 2000; Yap et al., 1998). p120 catenin is thought to mediate the stabilisation of cadherin complexes; indeed, p120 depletion in A431 human cervical cancer colony-forming cells resulted in E-cadherin degradation and the loss of cell-cell adhesivity (Davis et al., 2003). The expression levels of α- and β-catenin were also diminished in p120 catenin depleted cells; p120 catenin is therefore required for the maintenance of E-cadherin-mediated adhesion (Davis et al., 2003). Moreover, when the interaction between E-cadherin and p120 catenin is uncoupled, p120 catenin no longer localises to cell-cell junctions (Thoreson et al., 2000). p120 catenin modulates the strength of E-cadherin-mediated adhesions (Thoreson et al., 2000) and knockdown of p120 catenin in prostate cancer cells leads to cell-cell junction dissolution (Kümper and Ridley, 2010). In contrast however, it has also been reported that p120 catenin may negatively modulate intercellular adhesiveness (Aono et al., 1999; Ohkubo and Ozawa, 1999). The structure of adherens junctions encompassing E-cadherin, β-catenin, α-catenin and p120 catenin is illustrated in **figure 1.5**.

It is evident that the E-cadherin-catenin complex is important in the maintenance of AJs; aberrant expression or function of these proteins has been implicated in cancer cell dissemination. For example, *in vitro* work has shown that human cancer cells that are

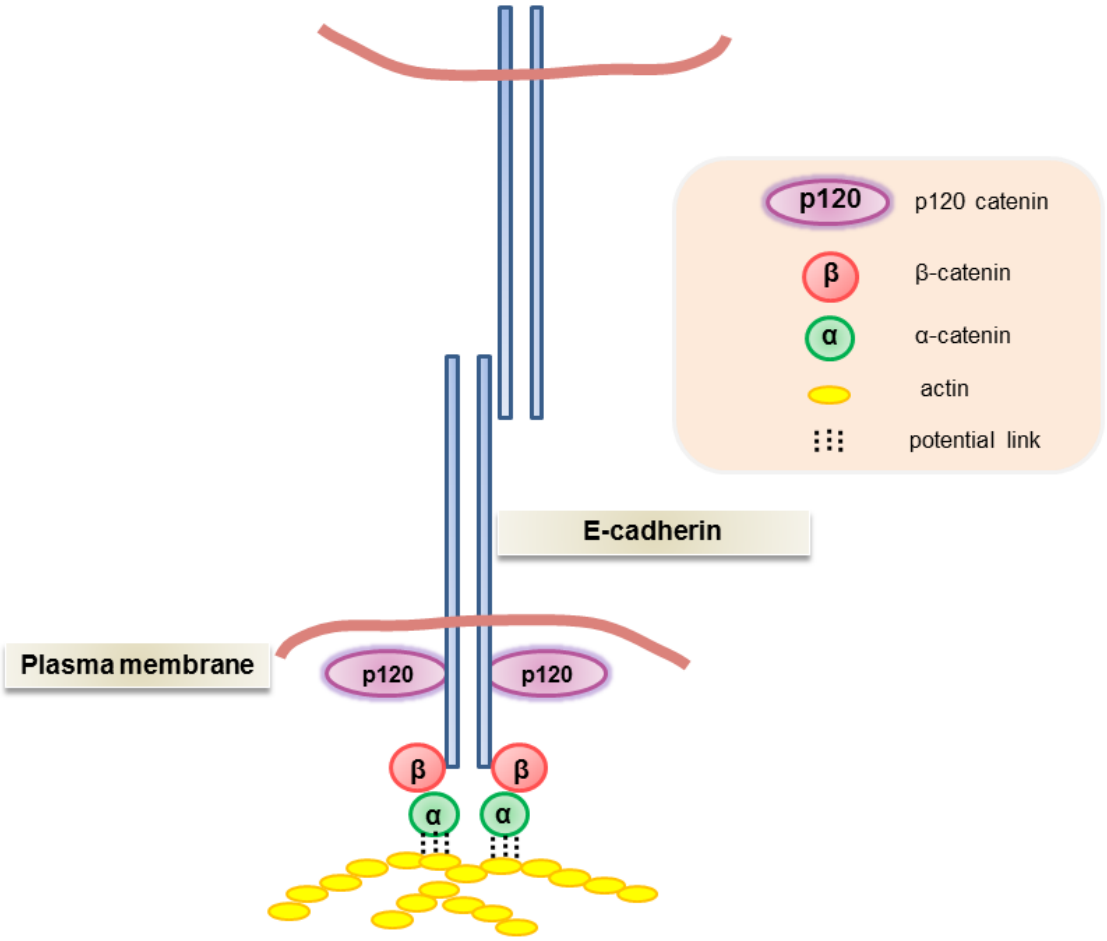

Figure 1.5 The structure of adherens junctions. This schematic illustrates the dimeric association of E-cadherin and its interactions with the cytosolic proteins α-catenin, β-catenin and p120 catenin to form an adhesive structure. It is historically thought that α-catenin links the E-cadherin-β-catenin complex to the actin cytoskeleton. However, a recent study has shown that α-catenin is unable to bind β-catenin and actin simultaneously (Drees et al., 2005; Yamada et al., 2005). This figure is adapted from (D'Souza-Schorey, 2005).

epithelioid in appearance express E-cadherin and are typically non-invasive forms of cancer, whilst the loss of E-cadherin expression correlates with invasiveness and a fibroblastoid cell morphology (Frixen et al., 1991). In the presence of low forces that mimic those found in the lymphatic system, E-cadherin-negative cancer cells exhibit an increased propensity to dissociate from cell aggregates when compared to E-cadherin-positive tumour cells (Byers et al., 1995). These results suggest that the absence of E-cadherin would promote cell-cell dissociation from a tumour mass in the presence of forces that are characteristically detected in the lymphatic system (Byers et al., 1995). The loss of E-cadherin, β-catenin and α-catenin expression is thought to contribute to the development of breast carcinoma (de Leeuw et al., 1997) and the stabilisation of E-cadherin and catenins at cell-cell contact sites reduces the invasiveness of cancer cells (Swaminathan and Cartwright, 2011). Whilst the assembly and disassembly of AJs is important during the cell-cell dissociation process, actin cytoskeletal re-organisation is also required for the detachment of adjacent cells and their subsequent ability to migrate. Both the re-organisation of the actin cytoskeleton associated with junctional disruption and the actin cytoskeletal dynamics associated with cell migration are known to be mediated by the activity of Rho family GTPases.

1.4 Rho family GTPases are central to cell migration dynamics

RhoA (Madaule and Axel, 1985), Rac1 (Didsbury et al., 1989) and Cdc42 (Munemitsu et al., 1990) are ~ 21 kDa small GTPase proteins of the Ras superfamily that act as 'molecular switches' capable of regulating downstream signal transduction pathways by modulating their effector proteins (Ellenbroek and Collard, 2007). These proteins have been implicated in various cellular processes including cell growth and proliferation (Qiu et al., 1997), cytoskeletal re-organisation (Nobes and Hall, 1995; Ridley et al., 1992), as well as adhesion and migration (Nobes and Hall, 1999; Zhao et al., 2000). In addition, these GTPases are also known to be regulated by HGF stimulation (Royal et al., 2000; Wells et al., 2005) and have been implicated in HGF-induced cell migration (Ridley et al., 1995; Wells et al., 2005).

In initial Rho GTPase studies, Swiss 3T3 cells microinjected with activated RhoA exhibited changes in cell morphology where elongated protrusions from the cell body were observed (Paterson et al., 1990). Subsequently it was revealed that active mutants

of RhoA and Rac1 instigate the generation of stress fibers (Ridley and Hall, 1992) and lamellipodia (Ridley et al., 1992) respectively, in fibroblasts. Further investigations revealed a role for Cdc42 in the induction of filopodia (Kozma et al., 1995; Nobes and Hall, 1995). RhoA, Rac1 and Cdc42 are thus central in actin remodelling during cell movement. As cell migration is a pre-requisite for cancer cell progression, these Rho GTPases have been implicated in cancer invasion and metastasis (Ellenbroek and Collard, 2007).

Rac1 is responsible for lamellipodial protrusion at the leading edge of the cell (Nobes and Hall, 1999) and for focal adhesion formation (Nobes and Hall, 1995), which are both required for cell movement. More recently, the fluorescence activation indicator for Rho proteins (FLAIR) system (Chamberlain et al., 2000; Kraynov et al., 2000) was used to show that active Rac1 also accumulates at the rear of motile neutrophils (Gardiner et al., 2002) and is required for retraction of the trailing edge in addition to the already established role of Rac1 at the leading edge of the cell (Gardiner et al., 2002). Cdc42 induces filopodia generation at the front of a migrating cell (Nobes and Hall, 1995). The expression of dominant-negative Cdc42 disrupts chemotaxis, the directional sensing of a cell, in macrophages (Allen et al., 1998). It was originally thought that RhoA promoted the contractility of the motor protein myosin to induce the generation of stress fibers and cell-ECM adhesions at the rear of the cell (ChrzanowskaWodnicka and Burridge, 1996). Activated RhoA promotes detachment of the trailing edge of the cell by the modulation of these integrin-based cell-ECM adhesions (Alblas et al., 2001). However in recent biosensor studies active RhoA was detected at the protruding edge of moving cells (Heasman et al., 2010; Kurokawa and Matsuda, 2005; Pertz et al., 2006). In addition, RhoA, Rac1 and Cdc42 all accumulate in lamellipodia during protrusion of the cell (Machacek et al., 2009). It was postulated that RhoA functions in protrusion generation at the leading edge of motile cells by instigating actin polymerisation, whilst Rac1 and Cdc42 contribute to protrusion extension by modulating cell adhesion (Machacek et al., 2009). **Figure 1.6** depicts the cell migration process regulated by Rac1, RhoA and Cdc42.

1.4.1 GDP/GTP cycle

Ligand-activated cell surface receptors can initiate Rho GTPase activation; G-protein coupled receptors (GPCRs) as well as cytokine, tyrosine kinase and adhesion receptors

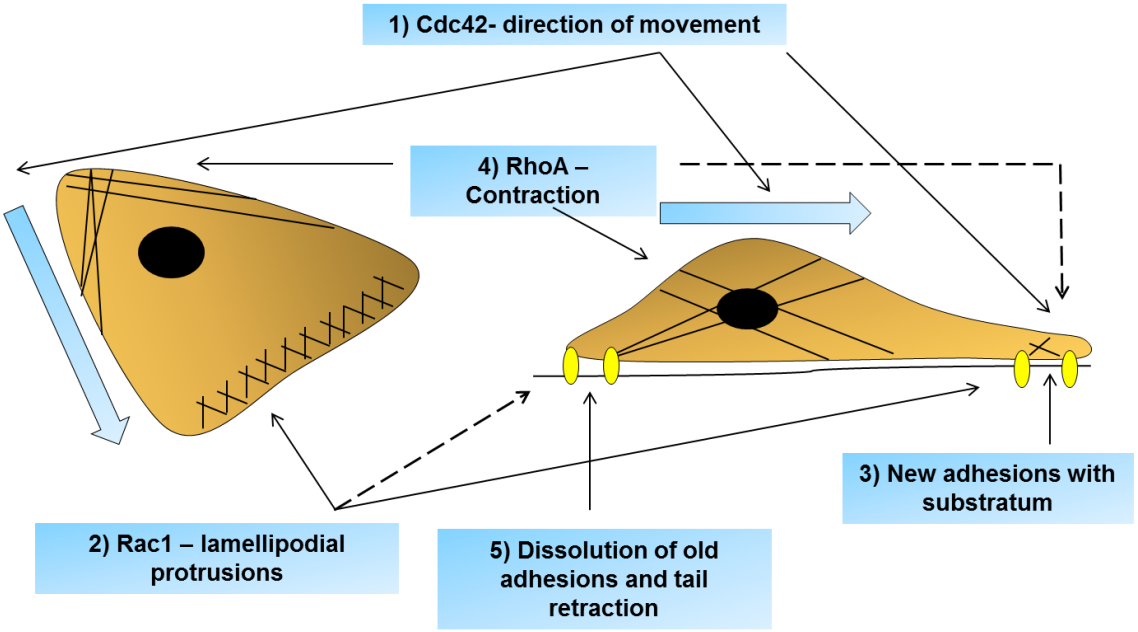

Figure 1.6 RhoA, Rac1 and Cdc42 during single cell migration. Dashed arrows represent recent studies indicating that active Rac1 also localises and functions at the cell rear (Gardiner et al., 2002) and that active RhoA has been detected at the leading edge of a migrating cell (Heasman et al., 2010; Kurokawa and Matsuda, 2005; Machacek et al., 2009; Pertz et al., 2006). This figure is adapted from (Raftopoulou and Hall, 2004).

are known to be involved in this process (Parri and Chiarugi, 2010). Intracellularly, RhoA, Rac1 and Cdc42 switch between being bound to guanosine triphosphate (GTP) which renders them active or bound to guanosine diphosphate (GDP) which renders them inactive (Heasman and Ridley, 2008) (**figure 1.7**). In contrast to these typical Rho GTPases, Rnd proteins (Fiegen et al., 2002; Foster et al., 1996; Garavini et al., 2002; Nobes et al., 1998), RhoV (Aspenström et al., 2007) and RhoH (Li et al., 2002; Schmidt-Mende et al., 2010) are not regulated by a GDP/GTP switch.

In the instance of RhoA, Rac1 and Cdc42, when signals are lacking from either the exterior or interior of the cell, these Rho GTPases are retained in their inactive GDP-bound form in the cytoplasm by guanine nucleotide dissociation inhibitors (GDIs) (Tcherkezian and Lamarche-Vane, 2007). Receptor activation induces the release of the GTPases from GDIs, which in turn allows Rho GTPase translocation from the cytosol to the plasma membrane (DerMardirossian and Bokoch, 2005). Proximity to the membrane allows GDP/GTP exchange by guanine nucleotide exchange factors (GEFs) and triggers the association of activated RhoA, Rac1 and Cdc42 with their effector proteins (Rossman et al., 2005). A third group of proteins, GTPase activating proteins (GAPs), have the ability to accelerate the inherent GTPase activity of Rho family proteins resulting in the cessation of signal transduction (Bernards and Settleman, 2004). In addition to their roles in cell motility, Rac1, Cdc42 and RhoA also have established roles in the modulation of AJs.

1.4.2 Activity of Rho GTPases at cell-cell junctions

1.4.2.1 Assembly and maintenance of junctions

It is well established that Rac1 is involved in the assembly of E-cadherin-mediated cell-cell adhesion sites (Ehrlich et al., 2002; Hoshino et al., 2004; Kovacs et al., 2002a; Kovacs et al., 2002b). RhoA has also been implicated in cell-cell junction formation; it was recently reported that RhoA depletion in neural progenitor cells induced the disruption of AJs (Katayama et al., 2011). The inhibition of RhoA by C3 transferase, a known inhibitor of endogenous Rho proteins, impaired the maintenance of E-cadherin-based cell-cell adhesions in MDCK cells (Takaishi et al., 1997). The over-expression of a dominant-negative Rac1 mutant decreases the prevalence of E-cadherin and β-catenin at cell-cell junctions, whilst an activated Rac1 mutant elicits the opposite effect (Takaishi et al., 1997). In addition, Rac1 and RhoA are required for stable cell-cell

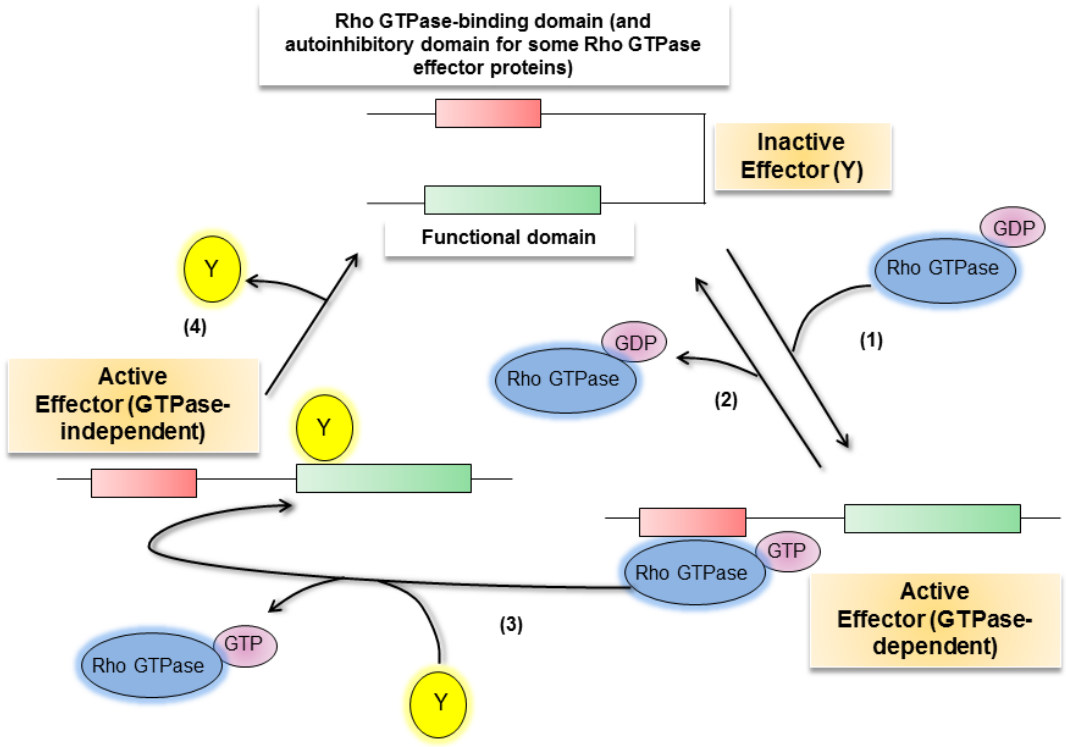

Figure 1.7 The GDP/GTP cycle. (Y represents the effector protein) (1) Binding of Rho GTPases releases intramolecular autoinhibition. Rho GTPase effectors regulated by autoinhibition include PAKs, WASP and Dia proteins. However, not all Rho GTPase effectors are regulated by an autoinhibitory mechanism. (2) GTP hydrolysis renders the effector inactive. (3) The effector may be modified by a phosphorylation event that stabilises effector activity even after the GTPase is removed. (4) The effector is inactivated through the removal of the modification thus rendering the effector inactive. This figure is adapted from (Bishop and Hall, 2000).

adhesion formation in human keratinocytes (Braga et al., 1997). In MDCK II cells, active Cdc42 increases E-cadherin and β-catenin levels at cell-cell junctions and inhibits HGF-induced disruption of intercellular junctions (Kodama et al., 1999).

1.4.2.2 Disassembly of junctions

There are several reports that implicate Rho GTPases in cell junction disassembly. Activation of Rac1 and Cdc42 abolished the multi-cellular organisation of T47D breast carcinoma cells in a 3D collagen matrix (Keely et al., 1997) and active Rac1 disrupts cell-cell adhesions in human keratinocytes (Braga et al., 2000) and pancreatic carcinoma cells (Hage et al., 2009). The induction of EMT in human proximal tubular epithelial cells, characterised by reduced E-cadherin expression and the adoption of a fibroblastic morphology, was dependent on RhoA, Rac1 and Cdc42 signalling (Patel et al., 2005). In contrast, it has been reported that the level of active Rac1 diminishes following HGF stimulation which is thought to be important during MDCK II cell-cell junction disassembly and cell-cell dissociation induction (Fukata et al., 2001; Palacios and D'Souza-Schorey, 2003). The discrepancy in the role of Rho GTPases in the assembly and disassembly of junctions indicates the complex nature of junctional dynamics. Nevertheless, Rac1 and Cdc42 are both known to interact with isoform 1 of the IQ motif containing GTPase activating protein (IQGAP) family of proteins (Kuroda et al., 1996), which has already been shown to play a role in cell-cell junction disassembly downstream of HGF (Fukata et al., 2001).

1.5 IQGAP1

1.5.1 IQGAP family of proteins

The IQGAP group of proteins have been isolated in various organisms, such as yeast (Epp and Chant, 1997; Lippincott and Li, 1998), *Xenopus* (Yamashiro et al., 2003) and mammals (Weissbach et al., 1994) where they possess distinct functions. To date, three variants of human IQGAP have been identified – IQGAP1, IQGAP2 and IQGAP3; IQGAP1 was the first to be defined in 1994 (Weissbach et al., 1994), followed shortly by the discovery of IQGAP2 (Brill et al., 1996). IQGAP3 was the last to be described in 2007 (Wang et al., 2007). The function of IQGAP1 in humans has been extensively studied (Briggs and Sacks, 2003; Brown and Sacks, 2006); this report will focus on human IQGAP1.

1.5.2 Domain structure of IQGAP1

Human IQGAP1 is a large multi-domain protein (**figure 1.8**) that is 1657 amino acids (approximately 189 kDa) in size (Weissbach et al., 1994). This protein has numerous binding partners including extracellular receptor kinase 1 and 2 (ERK1 and ERK 2), mitogen- activated protein kinase/extracellular signal-regulated kinase kinase 1 and 2 (MEK1 and MEK2) (Roy et al., 2004; Roy et al., 2005) and the EGF receptor (EGFR) (McNulty et al., 2011).

IQGAP1 is composed of an N-terminal calponin homology domain (CHD), followed by a large coiled coil domain (Johnson et al., 2009). Downstream of the large coiled region is a polyproline interacting domain (WW domain) and an IQ domain, composed of four concurrent repeats of the IQ motif (Briggs and Sacks, 2003). The N-terminal region of IQGAP1 is thought to aid the homo-dimerisation of this protein (Ren et al., 2005). The GAP-related domain (GRD) is located downstream of the IQ region and encompasses the Cdc42 binding site (Mataraza et al., 2003a). It has been reported that IQGAP1 interacts with both Cdc42 (Hart et al., 1996) and Rac1 (Kuroda et al., 1996). The most C-terminal region of IQGAP1 contains a RasGAP_C-terminus (RGCt) domain that is known to interact with a diverse range of proteins (White et al., 2011) including E-cadherin (Kuroda et al., 1998; Li et al., 1999) and β-catenin (Kuroda et al., 1998). Although this domain is considerably similar in sequence to the catalytic region of Ras-GAPs (Weissbach et al., 1994), IQGAP1 does not function as a traditional GTPase-activating protein; in fact *in vitro* studies have shown that IQGAP1 stabilises Cdc42 in its GTP-bound active conformation (Ho et al., 1999; Swart-Mataraza et al., 2002).

1.5.3 IQGAP1 in cancer

Changes in the localisation of IQGAP1, as well as elevated expression levels, have been documented in numerous cancer tissues and tumour cell lines (Johnson et al., 2009). IQGAP1 over-expression has been detected in colorectal (Nabeshima et al., 2002) and hepatocellular (Chen et al., 2010) cancer cells, as well as in head and neck squamous cancer cells (Patel et al., 2008). In addition, the highly metastatic MDA-MB-231 human breast cancer cells displayed a 2.7 fold elevation in IQGAP1 levels, when assessed against the less invasive MCF7 breast cancer cells (Jadeski et al., 2008). DNA array analysis of highly metastatic melanoma cells revealed genes, including IQGAP1, that

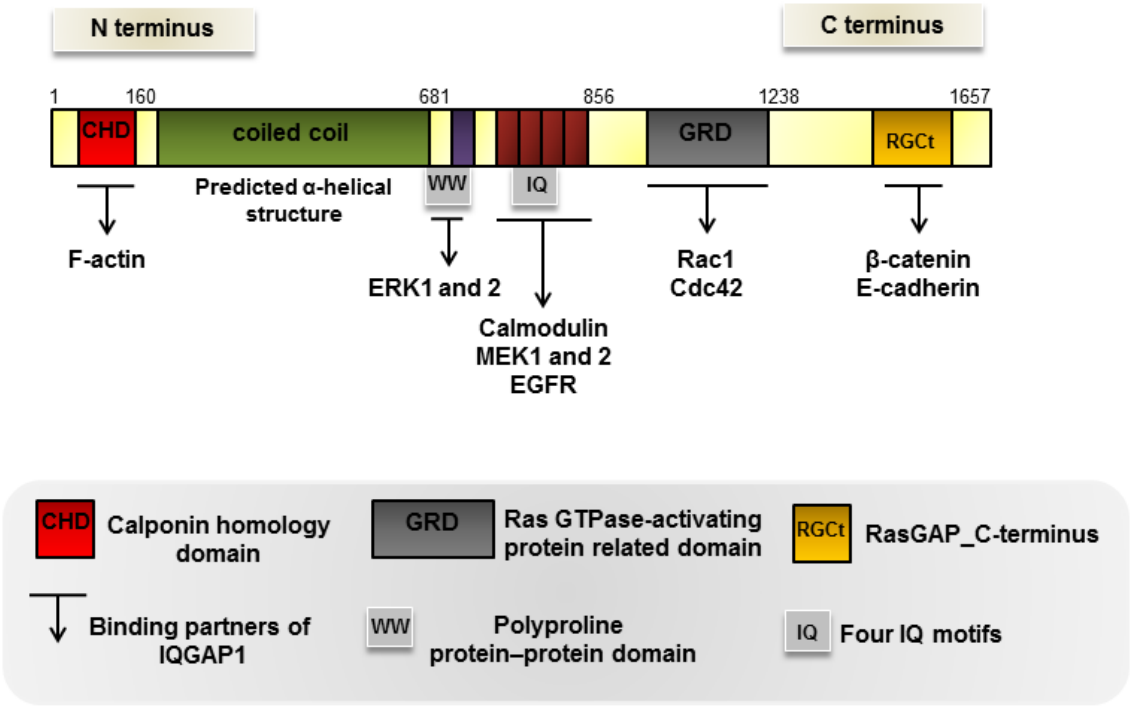

Figure 1.8 The domain structure of IQGAP1. Schematic illustrating the multi-domain structure of IQGAP1 and some of the binding partners identified for this protein. This figure is adapted from (Johnson et al., 2009; White et al., 2011).

were associated with the development of metastasis (Clark et al., 2000). As well as increased expression of IQGAP1 in cancer, several studies have implicated IQGAP1 specifically in cancer cell migration. In MCF7 breast cancer cells, the interaction between IQGAP1 and Cdc42 elevates the level of active Cdc42 (Mataraza et al., 2003b). Furthermore, increased expression of IQGAP1 promotes cell motility and this event is reliant on Cdc42 and Rac1 (Mataraza et al., 2003b). IQGAP1 accumulates at the leading edge of HGF-stimulated cells (Hu et al., 2009) and depletion of this protein inhibits the migration of glioma (Hu et al., 2009), breast cancer (Mataraza et al., 2003b) and ovarian cancer (Bourguignon et al., 2005; Dong et al., 2008) cells. However, the role of IQGAP1 in prostate cancer cell migration has yet to be elucidated.

1.5.4 IQGAP1 in cell junction modulation

Studies have shown that IQGAP1 plays a significant role in the stability and integrity of AJs by its interaction with E-cadherin. Indeed, IQGAP1 co-localises with E-cadherin at cell junction sites in MCF7 breast cancer cells and is involved in the impairment of E-cadherin-mediated adhesion (Li et al., 1999) and in cell junction dissociation downstream of HGF (Fukata et al., 2001). IQGAP1 also induces cell-cell dissociation in mouse L fibroblasts stably expressing E-cadherin (EL cells); in these cells, IQGAP1 was shown to bind to β-catenin and displace α-catenin from the functional E-cadherin-β-catenin junctional complex (Kuroda et al., 1998). It was therefore speculated that IQGAP1-mediated displacement of α-catenin resulted in a loss of intercellular adhesivity (Kuroda et al., 1998). Indeed, GTP-bound Cdc42 and Rac1 negatively regulate IQGAP1 function by inhibiting its interaction with β-catenin and in turn obstructing α-catenin dissociation (Fukata et al., 1999). However, more recently, evidence has emerged to suggest that the displacement of α-catenin from β-catenin might not be associated with junctional disruption (Drees et al., 2005). The role of the β-catenin-α-catenin interaction during junctional disassembly is therefore not fully elucidated. However others have shown that in the absence of functional α-catenin, mouse F9 teratocarcinoma cells exhibit a scattered phenotype (Maeno et al., 1999).

In contrast to the proposed role of IQGAP1 in promoting cell-cell junction disassembly, it has also been shown that IQGAP1 actually enhances cell-cell adhesion in cells by its ability to cross-link actin filaments in the presence of high levels of Rac1/Cdc42 activity (Noritake et al., 2004); furthermore, the authors proposed a model for IQGAP1-

mediated cell junction stabilisation as illustrated in **figure 1.9**. Thus the role of IQGAP1 in junctional dynamics is still not clearly understood and furthermore, IQGAP1 activity downstream of HGF has yet to be investigated in colony-forming prostate cancer cells.

Recently, a member of the p21-activated kinase (PAK) family, PAK6, was identified as a putative IQGAP1 binding protein (Kaur et al., 2008). PAKs are effectors of the Rho family GTPases Rac1 and Cdc42 (Manser et al., 1994). As such, these proteins have been implicated in the regulation of both cancer cell adhesion and migration (Whale et al., 2011).

1.6 PAKs

PAKs are a group of highly conserved mammalian serine/threonine protein kinases (Eswaran et al., 2008). To date, six human isoforms of PAK have been documented and these have been separated into two groups centred around their structure and function (Arias-Romero and Chernoff, 2008). PAKs 1–3 have been classified as group I and PAKs 4-6 constitute group II (Jaffer and Chernoff, 2002). PAKs are involved in various cellular events such as gene transcription (Stanley, 2007), hormone signalling (Holm et al., 2006; Lee et al., 2002; Rayala et al., 2006; Schrantz et al., 2004), cell morphology changes (Manser et al., 1997; Qu et al., 2001; Zeng et al., 2000), programmed cell death (apoptosis) (Cotteret et al., 2003; Huang et al., 2009) and cell migration (Ahmed et al., 2008; Bright et al., 2009).

1.6.1 Expression of PAKs 1-6 in cancer

In human tissue, PAK expression has been observed in many different tissue types. PAK1 and PAK3 expression has been detected in the brain and PAK2 is ubiquitously expressed (Manser et al., 1995; Manser et al., 1994; Martin et al., 1995; Teo et al., 1995). PAK4 is expressed in various tissues including that of the spleen, ovary, colon and prostate (Abo et al., 1998). PAK5 is highly expressed in the brain (Dan et al., 2002; Pandey et al., 2002) and PAK6 is found in the prostate, testis and brain, as well as in the kidney and placenta (Callow et al., 2002; Kaur et al., 2008; Yang et al., 2001). Altered expression of the group I PAK, PAK1, has been documented in many types of cancer including that of the brain (Aoki et al., 2007), breast (Bostner et al., 2007), liver (Ching et al., 2007), kidney (O'Sullivan et al., 2007), colon (Carter et al., 2004), bladder

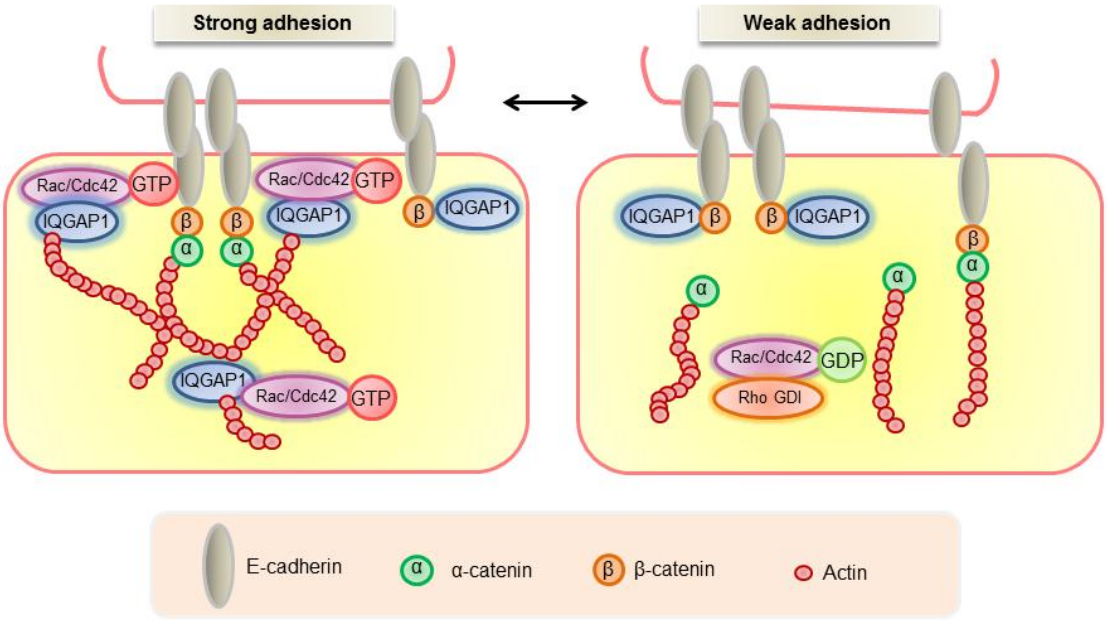

Figure 1.9 A proposed model for the modulation of intercellular adhesion strength involving IQGAP1. This figure illustrates the potential function of IQGAP1, Rac1 and Cdc42 in conferring strong or weak cell-cell adhesions at junctional sites. IQGAP1 is thought to stabilise junctions by its actin cross-linking ability which is enhanced by its interaction with activated Rho GTPases. The actin cross-linking function of IQGAP1 was postulated to link the E-cadherin-β-catenin complex to the actin cytoskeleton via α-catenin. A reduction in activated Rac1 or Cdc42 levels releases IQGAP1 and allows this protein to bind to the E-cadherin-β-catenin complex. This triggers the release of α-catenin from the complex, leading to weak cell-cell adhesions and subsequent cell-cell dissociation. This figure is adapted from (Noritake et al., 2005).

(Ito et al., 2007) and ovary (Davidson et al., 2008). Recently, elevated phospho-PAK2 expression was reported in tumours of the ovary (Siu et al., 2010). Increased PAK4 levels has been documented in various cancer cell lines including those of the breast and prostate (Callow et al., 2002). PAK5 over-expression has been observed in colorectal cancer (Gong et al., 2009). An increased level of PAK6 expression has been detected in both breast and prostate cancer cells (Kaur et al., 2008). In contrast, low PAK6 staining was reported in non-cancerous prostate epithelium (Kaur et al., 2008).

The expression of PAK6 has been linked to prostate cancer-associated pathways. For example, the aberrant expression of PAK6 enhances the survival of prostate cancer cells which suggests that PAK6 may be involved in the modulation of apoptosis (Li et al., 2005a), similar to other PAKs including PAK2 (Vilas et al., 2006), PAK4 (Gnesutta et al., 2001) and PAK5 (Cotteret et al., 2003). In addition, the suppression of PAK6, in conjunction with irradiation, reduces the survival of PC3 and DU145 prostate cancer cells (Zhang et al., 2009). PAK6 inhibition induces a decrease in the phosphorylation of a pro-apoptotic member of the B-cell lymphoma 2 (Bcl-2) family, bcl-2 antagonist of cell death (BAD), at serine 211, which may contribute to the survival of these cells in a PAK6 knockdown background (Zhang et al., 2009). In contrast, PAK6 may act as a tumour suppressor in prostate cancer (Wang et al., 2005) as the PAK6 gene was found to be hyper-methylated (Wang et al., 2005); hyper-methylated genes are frequently associated with the inhibition of tumour growth (He et al., 2003). Furthermore, in knockout studies, no defects were noted for PAK6 knockout mice, and PAK5/PAK6-double-knockout mice were unaffected in their viability and fertility (Nekrasova et al., 2008). However, these double-knockout mice were impaired in their learning and memory capabilities (Nekrasova et al., 2008).

1.6.2 Structure of PAKs 1-6

It is well established that PAKs 1-3 possess a distinctive N-terminal region that encompasses a conserved p21-binding domain (PBD) and an autoinhibitory domain (AID) (Burbelo et al., 1995; Manser et al., 1995; Manser et al., 1994; Teo et al., 1995). PAKs 1-3 are highly similar in sequence; they exhibit approximately 88% sequence homology in their PBD regions when compared to one another, whilst their kinase domains are over 90% identical in sequence (Jaffer and Chernoff, 2002). It has been shown that the AID overlaps with the PBD and is important in the regulation of basal

kinase activity for the group I proteins (Lei et al., 2000). Active Cdc42 and Rac1 are known to bind to the PBD (Bagrodia et al., 1995; Sells et al., 1997; Zhao et al., 1998) which increases PAK autophosphorylation and kinase activity (Manser et al., 1994; Martin et al., 1995). The N-terminal regulatory domain of PAKs 1-3 characteristically holds a number of proline-rich motifs, which act as binding sites for proteins that contain src-homology 3 (SH3) domains; for example, the motif located at the extreme N-terminal region of PAK1 promotes the binding of the adaptor protein Nck (Bokoch et al., 1996). The second proline-rich region is capable of interacting with growth-factor-receptor-bound-protein 2 (Grb2) (Puto et al., 2003). PAK1 also interacts with the PAK-interacting exchange factor (PIX) (Manser et al., 1998) which is thought to mediate the translocation of a PAK1-Nck complex to the plasma membrane upon receptor activation (Lu et al., 1997).

Group II PAKs possess a C-terminal kinase domain and an N-terminal PBD domain, similar to group I PAKs (Abo et al., 1998; Dan et al., 2002; Lee et al., 2002). However, the sequences vary between the two groups. For example, the kinase region of PAK6 resembles that of PAKs 1-5, whilst the homology of this protein to PAK1 is only 50% when compared to 80% with its group member, PAK4 (Lee et al., 2002). PAK6 and PAK4 are structurally different from group I PAKs and do not appear to have an identifiable AID (Jaffer and Chernoff, 2002). In contrast, PAK5 has been shown to possess an inhibitory region that is approximately 120 amino acids in size (Ching et al., 2003).

Whilst PAK6 and its group II family members do not possess any SH3 binding domains in their N-terminal regulatory region that is characteristic of PAKs 1-3 (Lee et al., 2002), group II PAKs do possess a number of proline-rich regions between the PBD and the kinase domain of the protein (Wells and Jones, 2010). PAK4 possesses a GEF interacting domain via which GEF-H1 interacts (Callow et al., 2005). This GEF is able to promote GDP to GTP exchange for Rac1 and RhoA but not Cdc42 (Ren et al., 1998). Whilst a GEF interacting domain has not been identified in PAK6, this kinase is unique from PAKs 1-5 in that it possesses a FXXMF motif which associates directly with the androgen receptor (AR) ligand binding domain (LBD) (van de Wijngaart et al., 2006). Whilst PAK6 (Lee et al., 2002), similar to PAK1 (Wang et al., 2002), binds to the alpha isoform of the estrogen receptor (ER-α), PAK6 is the only PAK family member that

interacts with the AR (Yang et al., 2001). The AR is important in the differentiation of epithelial prostate cells (Donjacour and Cunha, 1993) and has been implicated in the development of prostate cancer (Han et al., 2005; Massie et al., 2011). The similarities and differences between the structures of group I and II PAKs are demonstrated in **figure 1.10**.

1.6.3 Regulation of PAK activity

It has been established that the kinase activity of PAKs 1-3 is enhanced by the binding of the active form of the Rho GTPases, Rac1 and Cdc42 to the PBD (Manser et al., 1994; Martin et al., 1995). Group I PAKs exist as a dimer in an autoinhibited inactive state where the AID from one PAK molecule is bound to the catalytic domain of the other PAK within the dimer (Lei et al., 2000). The binding of active Cdc42 or Rac1 to the PBD relieves this autoinhibitory conformation and induces a number of conformational changes that trigger the release of the AID from the catalytic region, rendering the kinase active (Lei et al., 2000; Parrini et al., 2002). Group I PAKs can also be activated through pathways that do not require GTPases, for example by interacting with the lipid sphingosine (Bokoch et al., 1998).

In contrast to group I PAKs, the mechanism of regulation for group II PAKs has yet to be fully elucidated. PAKs 4-6 preferentially interact with the active form of Cdc42, but kinase activity is not thought to be enhanced by this association (Abo et al., 1998; Dan et al., 2002; Lee et al., 2002); although there is one report that activated Cdc42 can increase the autophosphorylation levels of glutathione S-transferase (GST) tagged PAK5 (Ching et al., 2003). As the interaction between PAK6 and the GTP-bound form of Cdc42 does not increase PAK6 kinase activity (Schrantz et al., 2004), it is possible that this association modulates PAK6 localisation as observed for PAK4 (Abo et al., 1998) and *Xenopus* PAK5 *(*X-PAK5), the Xenopus PAK4 homologue (Cau et al., 2001). It has been reported that PAK6 interacts with the atypical Rho GTPase family member, RhoV (Shepelev and Korobko, 2012), which has 52% sequence homology to Cdc42 (Aronheim et al., 1998). However, RhoV does not change PAK6 phosphorylation levels at the predicted autophosphorylation site, serine 560 (Schrantz et al., 2004; Shepelev and Korobko, 2012). Moreover, full-length PAK6 exhibits less kinase activity in comparison to a truncated version of PAK6 containing only the protein's kinase domain (Yang et al., 2001).

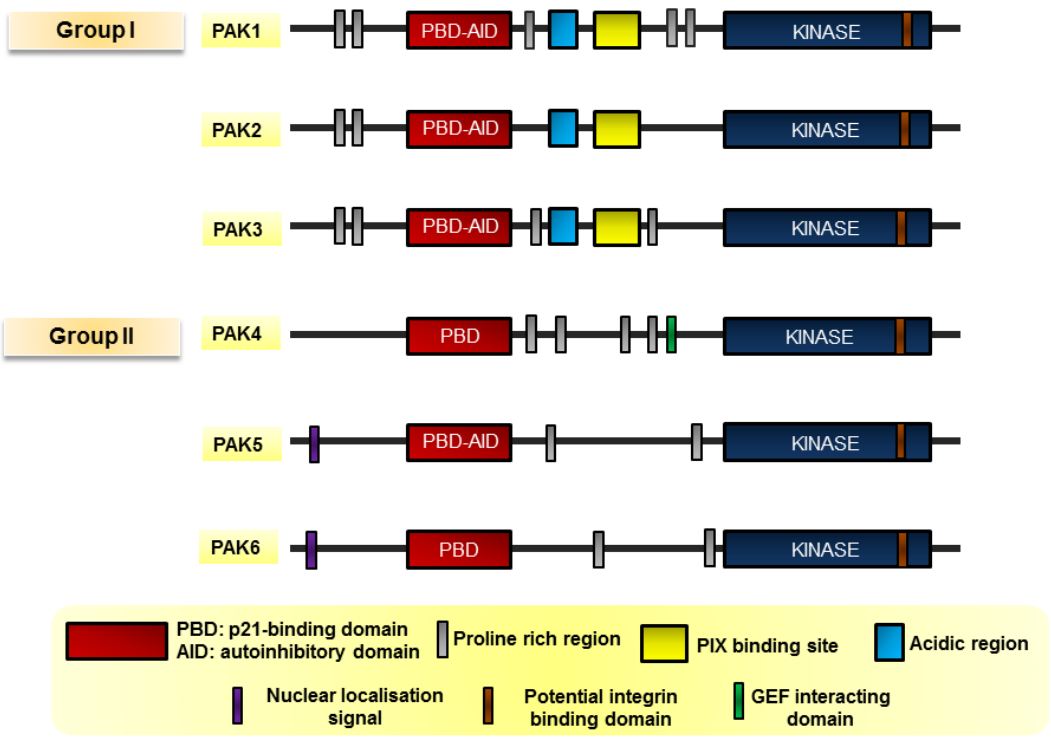

Figure 1.10 The domain structure of Group I and II PAKs. PAKs 1-6 have been divided into two groups based on their sequence homology. All PAK isoforms possess an N-terminal PBD and C-terminal kinase domain. There is variation in structure in the region between the PBD and kinase domain of PAKs. This figure is adapted from (Arias-Romero and Chernoff, 2008; Wells and Jones, 2010).

PAK6 kinase activity can also be regulated by the p38 mitogen activated protein kinase (MAPK) signalling cascade (Kaur et al., 2005). Phosphorylation by p38 MAPK and mitogen activated protein kinase kinase 6 (MKK6) activates PAK6; furthermore autophosphorylation of PAK6 at serine 560 is required for MKK6-facilitated activation (Kaur et al., 2005). In addition, the results obtained from kinase activity studies suggest that the AR may also play a part in regulating PAK6 kinase activity (Lee et al., 2002).

1.6.4 PAKs and cancer cell migration

Group I PAKs were initially implicated in cell movement as a consequence of their aptitude to induce membrane ruffling (Sells et al., 1997) as well as the inhibitory effect on cell migration induced by a dominant-negative PAK1 mutant (Kiosses et al., 1999). PAK1 also phosphorylates cytoskeletal-associated proteins such as actin-related protein 2/3 complex 41 kDa (p41-Arc), a component of the Arp2/3 complex which contributes to breast cancer cell migration (Vadlamudi et al., 2004).

PAK1 has been shown to promote cell migration in colon cancer (Huynh et al., 2010). More recently, PAK1 was found to be over-expressed in gastric cancer cells and its presence enhances cell motility in these cells whilst the depletion of PAK1 inhibits this phenotype (Li et al., 2012). Group I PAKs have also been implicated in cancer cell motility downstream of growth factor stimulation. DU145 cell motility is inhibited in PAK1, but not PAK2, short interfering RNA (siRNA) knockdown cells upon HGF stimulation (Bright et al., 2009). In ovarian cancer cells, PAK1 and PAK2 are over-expressed and cell motility is enhanced by their presence (Siu et al., 2010). In contrast, whilst it has been recently suggested that PAK3 somatic mutations may contribute to cancer tumourigenesis (Greenman et al., 2007), very little is known on the function of PAK3 in cancer cell migration.

There is extensive evidence that supports a role for PAK4 in cancer cell motility. For example, PAK4 depletion reduces the velocity of migrating DU145 cells stimulated with HGF (Wells et al., 2010). In PC3 prostate carcinoma cells, PAK4 depletion induced a similar effect on cell motility upon HGF stimulation (Ahmed et al., 2008). Whilst PAK5 has been implicated in promoting neurite outgrowth downstream of Rho GTPases (Dan et al., 2002), and has also found to be localised in filopodia (Wu and Frost, 2006), the knowledge on PAK5 function in cancer cell migration is limited.

Nevertheless, PAK5 somatic mutations have been detected in a human cancer genome screen (Greenman et al., 2007) and increased PAK5 expression in colorectal cancer cells impairs cell adhesivity and promotes cell migration on collagen I (Gong et al., 2009).

PAK6 binds RhoV (Shepelev and Korobko, 2012), a protein that has been implicated in the modulation of cytoskeletal dynamics (Aronheim et al., 1998). Interestingly, HGF induces a reduction in RhoV gene expression in DU145 cells (van Leenders et al., 2011); thus it could be speculated that RhoV may be involved in HGF signalling. There is also one report in the literature that PAK6 interacts with IQGAP1 in breast cancer cells (Kaur et al., 2008). Whilst these PAK6 binding proteins have been implicated in cancer cell migration, the role of PAK6 in this process has yet to be investigated. Nevertheless, PAK6 has been implicated in other cancer-related phenotypes. For example, prostate cancer progression and invasiveness was inhibited in PAK6 siRNA-treated PC3, DU145 and LAPC4 prostate cancer cell lines (Wen et al., 2009). Furthermore, prostate cancer cell growth *in vivo* was suppressed upon PAK6 depletion; this effect was increased in the presence of the anti-tumour compound, docetaxel (Wen et al., 2009). As docetaxel acts as a microtubule stabilising agent (Altmann and Gertsch, 2007), it was proposed that PAK6 may be involved in the modulation of cytoskeletal dynamics (Wen et al., 2009). Moreover, MKK6 activates PAK6 (Kaur et al., 2005) and the increased expression of MKK6 is associated with invasiveness in osteosarcoma (Nakano et al., 2003). Whilst there is emerging evidence for the involvement of PAK6 in cancer, its role in cancer cell dissemination has yet to be defined.

1.6.5 PAKs in cell junction modulation

Whilst the role of group I PAKs in cancer cell migration has been studied extensively, their role in cell-cell dissociation has not been examined in such depth. However, it has been reported that activated group I PAKs can re-localise to cell-cell junctions (Stockton et al., 2004). PAK1 is thought to be an essential component in the modulation of E-cadherin integrity and junctional stabilisation downstream of Rac1 in keratinocytes (Lozano et al., 2008). PAK1 phosphorylates β-catenin and facilitates the disruption of the E-cadherin-β-catenin interaction (He et al., 2008). In addition, it has been shown that the presence of PAK1 kinase dead and constitutively active mutants can stimulate MDCK cell scattering (Zegers et al., 2003), a process that requires the dissolution of

intercellular adhesions. It has also been postulated that PAK1 is required for the intercellular breakdown of junctions downstream of HGF in DU145 cells (Bright et al., 2009).

Recent work has implicated group II PAKs in intercellular junction modulation. PAK4 was found to be required for the maturation of nascent apical junctions in human bronchial epithelial cells (Wallace et al., 2010). Moreover, PAK4 accumulated at sites of cell contact and this junctional localisation was reliant on the presence of Cdc42 (Wallace et al., 2010). It has been shown that the activated form of mushroom bodies tiny (Mbt), the *Drosophila* homologue of group II PAKs, is localised at AJs and is involved in the cell-cell dissociation process during eye maturation (Menzel et al., 2008; Menzel et al., 2007; Schneeberger and Raabe, 2003). Mbt activation interfered with the interaction between β-catenin and E-cadherin and thereby reduced intercellular adhesion in *Drosophila* (Menzel et al., 2008). In addition, X-PAK5 also localises at cell junction sites and modulates cell adhesion (Faure et al., 2005). A recent report has also demonstrated that PAK4 interacts with β-catenin, implicating this kinase in β-catenin re-localisation and signalling (Li et al., 2011). Additionally, an interaction with p120 catenin and group II PAKs has been documented; this association was more pronounced with PAK5 when compared to PAK4 and PAK6 (Wong et al., 2010). Furthermore, p120 catenin was phosphorylated by PAK4 and PAK5 both *in vitro* and *in vivo*, however the ability of PAK6 to phosphorylate p120 catenin was not tested (Wong et al., 2010). It has also been reported that the PAK6 binding protein RhoV (Shepelev and Korobko, 2012) modulates E-cadherin localisation at cell junctions in zebrafish (Tay et al., 2010). Thus whilst PAK6 interacts with proteins associated with the modulation of AJs, the potential role of PAK6 in this process has yet to be explored.

It is known that PAK6 exhibits abundant localisation in the mitochondria (Cotteret et al., 2003). Additionally, intracellular localisation of PAK6 has been detected in the cytoplasm and at the plasma membrane of HeLa cells (Lee et al., 2002), as well as in the nucleus of prostate cells (Yang et al., 2001). It was recently shown that over-expressed PAK6 localises at punctate cytoplasmic structures in HeLa B and NCI-H1299 lung cancer cells (Shepelev and Korobko, 2012). However, PAK6 has yet to be localised to cell-cell junctions.

1.7 Hypothesis

PAK6 is over-expressed in prostate cancer and this kinase interacts with IQGAP1, a scaffold protein implicated in cancer cell-cell dissociation and cell migration. Furthermore, PAKs have been implicated in cancer cell migration downstream of HGF stimulation. Thus it was hypothesised that PAK6 is involved during HGF-induced prostate cancer cell migration.

1.8 Aims of the project

The aim of this project is to investigate the importance of PAK6 downstream of growth factor-induced cell-cell dissociation and migration in prostate cancer cells. To facilitate studies of PAK6 biology, a 2D scatter assay will be optimised and subsequently developed into a 3D scatter assay. The effect of PAK6 over-expression and depletion on growth factor-induced prostate cancer cell-cell dissociation and migration will then be monitored using the scatter assay. In parallel, PAK6 interacting partner(s) which are relevant to cell-cell dissociation and migration will be isolated using GST pulldown assays and immunoprecipitation (IP) protocols. Finally, the relationship between PAK6 and identified interacting partner(s) will be characterised and explored in the context of growth factor-induced cell scattering.

Chapter 2
Materials and Methods

Chapter 2 – Materials and Methods

2.1 Materials

2.1.1 General materials

2-Amino-2-hydroxymethyl-propane-1**,**3-diol (Tris)-Base/

Hydrochloric acid (HCL) (Sigma-Aldrich, UK)

3-N-morpholino propane sulfonic acid (MOPs) (Sigma-Aldrich, UK)

4-(2-hydroxyethyl)-1-piperazineethanesulfonic acid (Hepes) (GIBCO®, Invitrogen, UK)

4', 6-diamidino-2-phenylindole (DAPI) (Sigma-Aldrich, UK)

Acrylamide (30%) (Severn Biotech Ltd, UK)

Adenosine triphosphate (ATP) (Millipore, UK)

Agarose (Invitrogen, UK)

Alexa Fluor® 488 goat anti-mouse (Invitrogen, UK)

Alexa Fluor® 568 goat anti-mouse (Invitrogen, UK)

Alexa Fluor® 633 Phalloidin (Invitrogen, UK)

Ammonium persulfate (APS) (Sigma-Aldrich, UK)

Ampicillin (Sigma-Aldrich, UK)

Aprotinin (Sigma-Aldrich, UK)

BD Matrigel^{TM} Matrix (BD Biosciences, UK)

Beta (β)-mercaptoethanol (Sigma-Aldrich, UK)

Bovine serum albumin (BSA) (VWR International, UK)

Bromophenol blue (Bio-Rad, UK)

Calcium phosphate transfection kit (Invitrogen, UK)

Carbenicillin (Sigma-Aldrich, UK)

Control siRNA oligonucleotide (non-silencing) (Qiagen Ltd, UK)

Dimethyl sulfoxide **(**DMSO) (Sigma-Aldrich, UK)

Dithiothreitol (DTT) (Sigma-Aldrich, UK)

DNA ladder (New England Biolabs, UK)

Dulbecco's modified Eagle's medium (DMEM)+GlutaMAX^{TM} (GIBCO®, Invitrogen, UK)

Dulbecco's phosphate-buffered saline (DPBS) (GIBCO®, Invitrogen, UK)

EGF (Recombinant Human) (R&D systems, USA)

Enhanced chemiluminescence (ECL) Plus western blotting detection system (Amersham Biosciences, UK)

Ethidium bromide (Thermo Fisher Scientific, UK)

Ethylenediaminetetraacetic acid (EDTA) (Sigma-Aldrich, UK)

Fibronectin (Sigma-Aldrich.UK)

FluorSave™ Reagent (Calbiochem, UK)

Foetal bovine serum (FBS) (GIBCO®, Invitrogen, UK)

FuGene HD (Roche, UK)

Fuji Medical X ray film, Super RX (Fuji Film, Japan)

Gateway™ LR and BP Clonase™ Enzyme Mix (Invitrogen, UK)

Gentamicin (Sigma-Aldrich, UK)

Glutaraldehyde (Sigma-Aldrich, UK)

Glutathione Sepharose™ 4 Fast Flow beads (Amersham Biosciences, UK)

Glycerol (Sigma-Aldrich, UK)

Glycine (Sigma-Aldrich, UK)

Hepes, free acid, ULTROL grade (Calbiochem, UK)

HGF (Recombinant Human) (R&D systems, USA)

HiPerfect (Qiagen Ltd, UK)

Histone H1 (Millipore, UK)

Kanamycin (Invitrogen, UK)

L-Arabinose (Sigma-Aldrich, UK)

Leupeptin (Sigma-Aldrich, UK)

Lipofectamine 2000 (Invitrogen, UK)

Lithium chloride (LiCl) (Fisons Scientific Apparatus, UK)

Luria-agar (L-agar) (Sigma-Aldrich, UK)

Luria-broth (L-broth) (Invitrogen, UK)

Magnesium acetate (Sigma-Aldrich, UK)

Magnesium chloride ($MgCl_2$) (Sigma-Aldrich, UK)

MAX Efficiency® DH5α™ Competent Escherichia coli (E. coli) Cells (Invitrogen, UK)

Molecular biology enzymes (New England Biolabs, UK)

Nitrocellulose membrane (Perkin Elmer, USA)

Octylphenoxypolyethoxyethanol/Nonidet™ P40 substitute (NP-40) (Sigma-Aldrich, UK)

One Shot® BL21-AI Competent *E. coli* Cells (Invitrogen, UK)

One Shot® TOP10 Chemically Competent *E. coli* Cells (Invitrogen, UK)

OptiMEM (GIBCO®, Invitrogen, UK)

PAK6 siRNA oligonucleotide 1 (Oligo 1) (Ambion, USA)

PAK6 siRNA oligonucleotide 2 (Oligo 2) (Thermo Scientific Dharmacon, UK)

Paraformaldehyde (PFA) (Sigma-Aldrich, UK)

pDEST^{TM}15 (Invitrogen, UK)

pDONOR^{TM} 207 (Invitrogen, UK)

Penicillin/Streptomycin (Sigma-Aldrich, UK)

Phenylmethylsulfonylfluoride (PMSF) (Sigma-Aldrich, UK)

Phosphate buffered saline (PBS) tablets (Oxoid Limited, UK)

Phusion enzyme (Finnzymes, UK)

Pierce® ECL western blotting substrate (Thermo Scientific, USA)

Protein G Sepharose^{TM} 4 Fast Flow beads (Amersham Biosciences, UK)

Protein marker (Biorad, USA)

Purelink^{TM} Hi Pure Plasmid mini-prep kit (Invitrogen, UK)

QIAGEN HiPerfect transfection reagent (Qiagen Ltd, UK)

QIAGEN Plasmid maxi-prep kit (Qiagen Ltd, UK)

QIAquick gel extraction kit (Qiagen Ltd, UK)

QuikChange^{TM} Site-Directed mutagenesis Kit (Stratagene, USA)

Rat tail collagen, Type I (BD Biosciences, UK)

Roswell Park Memorial Institute (RPMI)-1640 medium (GIBCO®, Invitrogen, UK)

Sodium chloride (NaCl) (Sigma-Aldrich, UK)

Sodium dodecyl sulphate (SDS) (Sigma-Aldrich, UK)

Sodium fluoride (NaF) (Alfa Aesar, UK)

Sodium orthovanadate (Na_3VO_4) (Sigma-Aldrich, UK)

Sodium pyrophosphate (BDH Chemicals, UK)

Sucrose (Sigma-Aldrich, UK)

Super optimal broth with catabolite repression (SOC) media (Invitrogen, UK)

Tetramethylrhodamine isothiocyanate (TRITC)-Phalloidin (Sigma-Aldrich, UK)

Tris-base (Sigma-Aldrich, UK)

Triton X-100 (VWR International, UK)

Trypsin/EDTA (GIBCO®, Invitrogen, UK)

Tween 20 (VWR International, UK

2.1.2 Plasmids

Construct	Vector backbone	Source
GFP-PAK6 wild-type (WT)	pEGFP-C1 (Clontech, UK) modified for use in Gateway™ Technology by Kerry Shea, King's College London)	Generated by the author
mRFP1/ RFP-PAK6 wild-type	pDEST (modified for use in Gateway™ Technology by Kerry Shea, King's College London)	Generated by the author
Myc-PAK6 wild-type	pCMV6-Myc	Kind gift from Jonathan Chernoff, Fox Chase Cancer Center, Philadelphia, USA
GST-PAK6 wild-type	pDEST™15 (Invitrogen)	Generated by the author
GFP-PAK6 Kinase active (S531N)	pEGFP-C1 (Clontech, UK) modified for use in Gateway™ Technology by Kerry Shea, King's College London	Generated by the author
GFP-PAK6 Kinase dead (K436A)	pEGFP-C1 (Clontech, UK) modified for use in Gateway™ Technology by Kerry Shea, King's College London	Generated by the author
GFP-PAK6 predicted autophosphorylation site mutant (S560E)	pEGFP-C1 (Clontech, UK) modified for use in Gateway™ Technology by Kerry Shea, King's College London	Generated by the author
HA-Cdc42-V12	pCMV5	Kind gift from Maddy Parsons, King's College London
GFP-IQGAP1 wild-type	pEGFP-C1	Kind gift from David Sacks, Department of Laboratory Medicine, NIH, Bethesda, USA
RFP-PAK6 C-terminal mutant	pDEST (modified for use in Gateway™ Technology by Kerry Shea, King's College London)	Generated by the author
RFP-PAK6 N-terminal mutant	pDEST (modified for use in Gateway™ Technology by Kerry Shea, King's College London)	Generated by the author

Myc-IQGAP1 N-terminal mutant	pcDNA3	Kind gift from David Sacks, Department of Laboratory Medicine, NIH, Bethesda, USA
Myc-IQGAP1 C-terminal mutant	pcDNA3	Kind gift from David Sacks, Department of Laboratory Medicine, NIH, Bethesda, USA
GFP-PAK6 C-terminal mutant	pEGFP-C1 (Clontech, UK) modified for use in Gateway™ Technology by Kerry Shea, King's College London	Generated by the author
GST-IQGAP1 (amino acids 717-863)	pGEX4T	Kind gift from David Sacks, Department of Laboratory Medicine, NIH, Bethesda, USA
GST-IQGAP1 (amino acids 162-671)	pGEX4T	Kind gift from David Sacks, Department of Laboratory Medicine, NIH, Bethesda, USA
GFP-IQGAP1 dominant-negative	pEGFP-C1	Kind gift from David Sacks, Department of Laboratory Medicine, NIH, Bethesda, USA

Table 2.1 Construct list

2.1.3 Antibodies

Antibody	Company	Source	Application	Dilution
Anti-c-Met (C-12) Cat# sc-10	Santa Cruz	Rabbit	Western Blotting	1: 500
Anti-c-Myc (9E10) Cat# sc-40	Santa Cruz	Mouse	Western Blotting and Immunoprecipitation	1: 250
Anti-Cdc42 Cat# 2462	Cell Signaling Technology	Rabbit	Western Blotting	1: 500
Anti-E-cadherin (HECD-1) Cat# GTX21416	GeneTex	Mouse	a) Western Blotting b) Immuno-fluorescence	a) 1: 500 b) 1: 500
Anti-EGFR Cat# 2232	Cell Signaling Technology	Rabbit	Western Blotting	1: 500
Anti-ERK1/2 Cat# 9102	Cell Signaling Technology	Rabbit	Western Blotting	1: 2000

Anti-GAPDH Cat# MAB374	Millipore	Mouse	Western Blotting	1: 20000
Anti-GFP Cat# 11814460001	Roche	Mouse	Western Blotting and Immunoprecipitation	1: 200
Anti-GST (GST-2) Cat# G1160	Sigma-Aldrich	Mouse	Western Blotting	1: 10000
Anti-HA (Y-11) Cat# sc-805	Santa Cruz	Rabbit	Western Blotting	1: 500
Anti-IQGAP1 Cat# 2293	Cell Signaling Technology	Rabbit	Western Blotting	1: 500
Anti-PAK1 Cat# 2602	Cell Signaling Technology	Rabbit	Western Blotting	1: 1000
Anti-PAK2 Cat# 2608	Cell Signaling Technology	Rabbit	Western Blotting	1: 2000
Anti-PAK4 Cat# 3242	Cell Signaling Technology	Rabbit	Western Blotting	1: 500
Anti-PAK4	In-house Affinity purified	Rabbit	Western Blotting	1: 2000
Anti-PAK6 Cat# ST1108	Calbiochem	Rabbit	Western Blotting	1: 500
Anti-Paxillin (349) Cat# 610051	BD Transduction Laboratories	Mouse	Immunofluorescence	1: 50
Anti-phospho-ERK1/2 (p44/42 MAPK, Thr202/Tyr204) (E10) Cat# 9106	Cell Signaling Technology	Mouse	Western Blotting	1: 1000
Anti-phospho-PAK4 (ser474)/PAK5 (ser602)/PAK6 (ser560) Cat# 3241	Cell Signaling Technology	Rabbit	Western Blotting	1: 1000
Anti-RFP Cat# 632393	Living Colors	Rabbit	Western Blotting and Immunoprecipitation	1: 1000
Anti-β-tubulin (clone TUB 2.1) Cat#T4026	Sigma-Aldrich	Mouse	Western Blotting	1: 1000

Table 2.2 Primary antibodies

Antibody	Company	Source	Dilution
Horseradish peroxidase (HRP)-conjugated anti mouse	Dako	Goat	1: 1000 - 1: 10000
HRP-conjugated anti rabbit	Dako	Goat	1: 1000 - 1: 2000

Table 2.3 Secondary antibodies

2.1.4 Buffers

Blocking solution: 5% w/v milk powder or 5% w/v BSA in Tris buffered saline (TBS)-Tween

DNA loading buffer: 40% w/v sucrose, 0.25% w/v bromophenol blue

Freeze down buffer for GST protein beads: 50% v/v glycerol, 20 mM Tris-HCL pH 7.6, 100 mM NaCl, 1 mM DTT

NP-40 lysis buffer: 0.5% v/v NP-40, 30 mM sodium pyrophosphate, 50 mM Tris-HCL pH 7.6, 150 mM NaCl, 0.1 mM EDTA and protease inhibitor cocktail

Protease inhibitor cocktail: 50 mM NaF, 1 mM Na_3VO_4, 1 mM PMSF, 10 µg/ml leupeptin, 1 µg/ml aprotinin and 1 mM DTT

Sodium dodecyl sulphate-polyacrylamide gel electrophoresis (SDS-PAGE) running buffer (10x): 250 mM Tris-base, 1.92 M Glycine, 1% w/v SDS. Dilute to 1x with distilled water (dH_2O)

SDS-PAGE transfer buffer (10x): 250 mM Tris-base, 1.92 M Glycine. Make up 1x transfer buffer fresh on the day by diluting to 1x and adding methanol to a final concentration of 20% v/v.

SDS-PAGE sample buffer (2x): 100 mM Tris-HCL pH 6.8, 4% w/v SDS, 20% v/v glycerol, 0.2% w/v bromophenol blue, 1: 50 β-mercaptoethanol

Tris acetate EDTA (TAE) buffer (1x): 40 mM Tris acetate, 1 mM EDTA

TBS-Tween: 25 mM Tris-HCL pH 7.6, 50 mM NaCl, 0.1% v/v Tween 20

PBS-Tween: PBS, 0.1% v/v Tween 20

Stripping buffer: 25 mM glycine pH 2, w/v 1% SDS

Coomassie blue stain: 50% v/v methanol, 10% v/v acetic acid, 0.025% w/v coomassie blue

Coomassie destain: 12.5% v/v isopropanol, 10% v/v acetic acid

Kinase buffer: 50 mM Tris-HCL pH 7.5, 10 mM $MgCl_2$, 1 mM DTT

LiCl buffer: 0.5 M LiCl, 20 mM Tris pH 8

Kinase cocktail solution: 2.5 mM Hepes pH 7.4 (Calbiochem, UK), 50 mM magnesium acetate, 0.5 mM ATP

Kinase assay reaction buffer (5x): 40 mM MOPs pH 7, 1 mM EDTA

2.2 Methods

2.2.1 Molecular biology

Transformation of *Escherichia coli* cells

The heat shock method was used to transform DH5α and Top10 strains of *E. coli* with DNA plasmids. These competent *E. coli* cells, typically stored at -80^{o}C, were allowed to thaw out on ice prior to transformation. 1 µl of plasmid DNA was then added to the bacteria and this transformation mixture was placed on ice for 30 minutes, followed by incubation at 42^{o}C for exactly 20 seconds or 30 seconds for DH5α or Top10 cells, respectively. The transformed bacteria were then placed on ice for a further 2 minutes, supplemented with 950 µl of SOC media (supplied with the competent cells) and incubated in a shaking incubator at 37^{o}C for one hour. Subsequently, the transformed bacteria were plated onto L-agar containing the appropriate antibiotic and incubated at 37^{o}C overnight.

Purification of plasmid DNA

Plasmid DNA was isolated and purified from *E. coli* cells using the QIAGEN maxi-prep kit and the Purelink^{TM} mini-prep kit. L-broth supplemented with the appropriate antibiotic was inoculated with transformed bacteria and incubated in a shaking incubator overnight at 37^{o}C. The concentrations of antibiotic used were typically 7 µg/ml for gentamicin, 30 µg/ml for kanamycin and 100 µg/ml for ampicillin. Mini-prep kits were employed to purify up to 20 µg plasmid DNA from 5 ml L-broth. Maxi-prep kits were utilised to purify up to 500 µg plasmid DNA from 200 ml L-broth. The plasmid DNA was eluted in water and stored at -20^{o}C for future use.

Restriction digests of plasmid DNA

A restriction digest reaction typically contained 0.5–1 µg of plasmid DNA, 10–20 units of restriction endonuclease (New England Biolabs (NEB)) and 1x NEB buffer in a total volume of 15 µl. The reaction was then incubated for one hour at the optimum temperature for the restriction endonuclease being used. 2 µl of DNA loading buffer was used to terminate the reaction. The restriction digest products were then resolved on an agarose gel.

Resolving DNA fragments on an agarose gel

A 1% w/v TAE agarose gel supplemented with 0.5 µg/ml ethidium bromide was used to resolve DNA fragments. DNA loading buffer was added to the DNA products and 10–20 µl of sample was loaded, alongside a DNA marker, into a well of the agarose gel. The gel was covered with 1x TAE buffer and the DNA was migrated through the gel at 140V. The DNA marker was used to verify the size of the DNA fragments present and these fragments were visualised under ultraviolet (UV) light.

Generation of tagged PAK6 constructs

Polymerase chain reaction (PCR)

The Gateway™ Technology system (Invitrogen, UK) was used to generate tagged PAK6 constructs. Myc-PAK6 wild-type plasmid was used as the DNA template in the production of PAK6 DNA flanked by *att*B sequences; the addition of *att*B sequences was required to allow for subsequent cloning into Gateway™ vectors. PAK6 DNA flanked by *att*B sequences was produced by PCR amplification (see **Appendix 1** for primer sequences). The PCR reaction was performed using Phusion DNA polymerase in the supplied reaction buffer. Each reaction was set up using 500 ng template DNA, 5% v/v DMSO, 0.2 mM of each deoxyribonucleotide triphosphate (dNTP) and 300 nM of forward and reverse primers (primers were ordered from Thermo Fisher Scientific, Germany). The total reaction volume in a 0.2 ml PCR tube was 50 µl. The specific conditions used for the PCR reaction for DNA amplification are displayed in **table 2.5.**

Cycle(s)	Process	Conditions
1	Pre-incubation	95ºC, 5 minutes
35	Denaturation	95ºC, 1 minute
	Annealing	48ºC and 55ºC, 1 minute
	Extension	74ºC, 1 minute 30 seconds
1	Final Extension	74ºC, 10 minutes

Table 2.4 Conditions for PCR amplification of PAK6

PAK6 mutants were generated using the same conditions shown in **table 2.5**; however the extension times were varied depending on the size of the PAK6 region being amplified. PCR amplification was also used to generate GFP tagged C-terminal PAK6

and mRFP1 tagged N- and C-terminal PAK6 mutant constructs as appropriate (see **Appendix 1** for primer sequences).

Gel purification of DNA fragments

PCR products were resolved on a 1% w/v TAE agarose gel supplemented with 0.5 µg/ml ethidium bromide and the DNA was visualised under low intensity UV light. The fragment of interest was excised from the gel with a razor and the DNA purified from the agarose using a QIAquick gel extraction kit. The purified DNA was eluted in water and then stored at -20°C for subsequent use.

Construction of PAK6 entry clone

In order to generate a PAK6 entry clone, a Gateway™ BP recombination reaction was conducted between the pDONR™ 207 vector and the *att*B sequence flanked PAK6 PCR product in accordance with the manufacturer's instructions. The BP reaction was incubated for 1 hour at room temperature. Subsequently, proteinase K was added and the reaction mixture was incubated at 37 ºC for 10 minutes to terminate the reaction. The BP reaction mixture was then transformed into TOP10 *E. coli* cells and the bacteria were plated onto L-agar supplemented with the appropriate antibiotic and incubated overnight at 37ºC. Colonies were then selected and the plasmid DNA was purified. The presence of PAK6 in individual colonies was verified by restriction digest. PAK6-positive clones were subsequently sequenced by Eurofins MWG Operon using primers that anneal to the gateway sequence upstream of the PAK6 gene (primers 19 and 20, primers were ordered from Thermo Fisher Scientific, Germany, see **Appendix 1** for primer sequences). An internal primer was also generated to sequence the entirety of PAK6 (see **Appendix 1** for primer sequence).

Construction of PAK6 expression clone

In order to generate GST, GFP and RFP-PAK6 expression plasmids, a Gateway™ LR recombination reactions were performed between the pENTR (PAK6) entry clone and pDEST™15 (Invitrogen, UK), modified pEGFP-C1 (Clontech, UK) (for use in the Gateway™ Technology system) and pDEST (mRFP1/RFP) in accordance with the manufacturer's instructions. The LR reaction was incubated for 1 hour at room temperature. Subsequently, proteinase K was added and the reaction mixture was incubated at 37 ºC for 10 minutes to terminate the reaction. The reaction was then

transformed into TOP10 *E. coli* cells as described in previously. The plasmid DNA purified from the individual colonies was then sequenced by Eurofins MWG Operon using sequencing primers (primers were ordered from Thermo Fisher Scientific, Germany, see **Appendix 1** for primer sequences).

Purification of GST-fusion proteins

E. coli BL21-A1 cells were transformed with GST expression plasmids. The transformed bacteria were cultured in L-broth to which 100 µg/ml of ampicillin was added. The cultures were incubated overnight in a shaking incubator at 37ºC. The following day, the bacterial cultures were diluted 1 in 100 into 200 ml of L-broth and grown for approximately 2 hours for the optical density to reach 0.6. The bacterial cultures were subsequently induced overnight at 20ºC with the appropriate % of L-Arabinose. The overnight cultures were then centrifuged at 6000 revolutions per minute (rpm) for 15 minutes to pellet the bacteria. The pelleted bacteria were re-suspended in 15 ml of a PBS: protease inhibitor cocktail. Sonication was used to disrupt the cells and this was followed by the removal of cell debris using centrifugation (4800 rpm for 10 minutes). GST beads were pre-washed three times with a PBS: protease inhibitor cocktail and added to the supernatant prior to incubation for two hours at 4ºC. The beads were then pelleted by centrifugation at 500 x gravity (x g) for 5 minutes and washed three times in a PBS: protease inhibitor cocktail at 2000 rpm for 2 minutes per wash. The beads were stored in freeze down buffer at -80^{o}C.

Site-Directed mutagenesis

Site-Directed mutagenesis was used to construct potential kinase active (S531N and S560E) mutants and a kinase dead (K436A) mutant of PAK6. Mutagenic primers were designed using the Stratagene QuikChange® Site-Directed mutagenesis primer design programme (see **Appendix 1** for primer sequences).

The PCR reactions were performed using 1 µl of *PfuTurbo* DNA polymerase (2.5 U/µl) in the supplied reaction buffer. Each PCR reaction was performed using 100 ng of template DNA (PAK6 entry clone), 0.2 mM of each dNTP and 300 nM of mutagenic forward and reverse primers. The total reaction volume in a 0.2 ml PCR tube was typically 50 µl. The specific conditions used for the PCR reactions are shown in **table 2.5**.

Cycle(s)	Conditions
1	95ºC, 30 seconds
18	95ºC, 30 seconds
	55ºC, 1 minute
	68ºC, 1 min/ kilobase (kb) of plasmid length

Table 2.5 Conditions for Site-Directed mutagenesis PCR

Following thermocycling, 1 µl of Dpn 1 restriction enzyme (10 U/µl) was added to the PCR reaction and mixed thoroughly. The reaction was then immediately incubated at 37 ºC for 2 hours to digest the parental supercoiled double-stranded DNA. 1 µl of the Dpn1-treated DNA was transformed into separate 50 µl aliquots of XL1-Blue supercompetent cells. The XL1-Blue supercompetent cells, typically stored at -80^{o}C, were thawed out slowly on ice prior to transformation. 1µl of plasmid DNA was then added to the bacteria and this transformation mixture was placed on ice for 30 minutes, followed by incubation at 42^{o}C for exactly 45 seconds. The transformed bacteria were then returned to the ice for a further 2 minutes. 500 µl of SOC media was added to the transformed bacteria and incubated at 37^{o}C with shaking for one hour. The bacteria were then plated onto L-agar containing the appropriate antibiotic and incubated at 37^{o}C overnight. The plasmid DNA purified from the individual colonies was sequenced using sequencing primers (primers were ordered from Thermo Fisher Scientific, Germany, see **Appendix 1** for primer sequences). DNA from positive colonies was then used to perform a Gateway^{TM} LR recombination reaction between the mutagenic pENTR (PAK6) entry clone and the pEGFP-C1 (Clontech, UK) destination vector, modified for use in the Gateway^{TM} Technology system, according to manufacturer's instructions.

2.2.2 Mammalian cell culture

DU145 human prostate cancer cells (obtained from Claire Wells, King's College London) and DU145 enhanced GFP (EGFP) cells (a kind gift from Yolanda Calle, King's College London) were cultured in 10% FBS, 90% RPMI-1640 with L-Glutamine and penicillin-streptomycin. HT29 human colon cancer cells and HEK293 human embryonic kidney cells, both obtained from Claire Wells, King's College London, were cultured in 10% FBS, 90% DMEM+GlutaMAX^{TM}, penicillin-

streptomycin, 4.5 g/L D-Glucose, 25 mM Hepes media. All media were warmed before use to 37^{o}C. All cell lines were cultured at 37^{o}C in a tissue culture incubator with humidified air, supplemented with CO_2 to 5% over atmospheric levels. Cells were passaged and maintained at sub-confluent levels. During cell passaging the growth medium was removed and the cells were washed with 5 ml PBS prior to incubation with 1 ml trypsin/EDTA at 37^{o}C until the adherent cells had detached. 4 ml of 10% FBS in RPMI-1640 or 10% FBS DMEM+GlutaMAX^{TM} media (as appropriate) was then added to the cells. Cells were pelleted by centrifugation at 1000 rpm for 5 minutes. The media was carefully removed and the cell pellet re-suspended in 10% FBS media. An appropriate dilution of these cells was subsequently added to 10% FBS media in a fresh tissue culture flask to give a total volume of 10 ml.

2.2.3 Transient transfection

FuGene HD

Cells were plated at an appropriate density the day before transfection (**table 2.7**) in 10% FBS media. A transfection reaction was set up by the addition of a specific concentration of DNA to serum-free OptiMEM media and then incubated at room temperature for 5 minutes. Following this, typically three times the volume of FuGene HD to DNA was added. To allow for complex formation, the mixture was then incubated for 30 minutes at room temperature, in accordance with the manufacturer's instructions. The serum-containing media was replaced with serum-free OptiMEM. After 30 minutes, the DNA: FuGene HD complexes were added to the cells. Following five hours, the OptiMEM media was replaced with fresh medium (containing 10% FBS).

Lipofectamine 2000

Cells were plated at an appropriate density the day before transfection (**table 2.7**) in the appropriate 10% FBS media. To set up a transfection reaction, 3 µl of lipofectamine 2000 was diluted in 100 µl serum-free OptiMEM media. In a separate eppendorf, 3 µg of DNA was added to 100 µl serum-free OptiMEM media. The mixtures were left at room temperature for 5 minutes. Following this, the lipofectamine 2000: OptiMEM mix was added dropwise to the DNA: OptiMEM mix and then incubated at room temperature for 15 minutes. Prior to the addition of the DNA: lipofectamine 2000 complexes to the cells, serum-containing media (10% FBS) was replaced with serum-

free media. The cells were then incubated with the transfection reagents for seven hours before the replacement of the serum-free media with the appropriate 10% FBS media.

Cells	Cell Density	Transfection Reagent	Concentration of DNA (µg): Volume of FuGene HD used (µl)	Constructs Transfected using this protocol
DU145	$2x10^4$ /ml	FuGene HD	1: 3	GFP control vector All GFP/RFP-tagged constructs used
DU145	$5x10^4$ /ml	FuGene HD	1: 6	GFP-IQGAP1 WT Co-expression of GFP-IQGAP1 WT and RFP-PAK6 WT
HT29	$1x10^5$ /ml	Lipofectamine 2000	N/A	GFP control vector All GFP-tagged constructs used
HEK293	$1x10^5$ /ml	Calcium Phosphate	N/A	All tagged constructs transfected into HEK293 cells

Table 2.6 Optimised transient transfection protocols

Calcium phosphate transfection

Cells were seeded at a density of $1x10^5$ /ml (**table 2.7**) and then incubated at 37°C for 24 hours. The medium was changed 3-4 hours prior to transfection. The transfection reaction was set up using the conditions described in **table 2.8**.

10cm tissue culture dish (10 ml)	2cm tissue culture dish (2 ml)
To tube A add: 36 µl 2M $CaCl_2$ 20 µg DNA Make volume to 300 µl with sterile water **To tube B add:** 300 µl 2x Hepes buffered saline (HBS)	**To tube A add:** 7.2 µl 2M $CaCl_2$ 4 µg DNA Make volume to 60 µl with sterile water **To tube B add:** 60 µl 2x Hepes buffered saline (HBS)

Table 2.7 Calcium phosphate transfection conditions

The calcium chloride ($CaCl_2$), DNA and water mixture was added dropwise to the 2x HBS with aeration until depleted. The transfection complex was then incubated at room temperature for 30 minutes. The transfection mix was then added dropwise to the cells, dispersed and incubated at 37°C overnight. The medium was then replaced with fresh medium and incubated for 24 hours.

HiPerfect for siRNA transfections

Cells were plated at an appropriate density the day before transfection (**table 2.9**) in 10% FBS media. To set up a transfection reaction, 75 nM (for PAK6 siRNA oligo 1) or 225 nM (for PAK6 siRNA oligo 2) was diluted in serum-free OptiMEM media to give a total volume of 100 µl (see **Appendix 2** for siRNA target sequences). Equal concentrations of control siRNA as PAK6 siRNA were used. To this, 12 µl of HiPerfect was added. The transfection mix was then incubated at room temperature for 30 minutes. The transfection mix was subsequently added dropwise to the cells and incubated at 37°C for 72 hours.

		Scatter assay	Whole cell lysates
Cells	**siRNA oligonucleotide(s)**	**Cell density**	**Cell density**
DU145	Control	$0.5x10^4$ /ml	$1x10^5$ /ml
DU145	Oligo 1	$1x10^4$ /ml	$1x10^5$ /ml
DU145	Oligo 2	$0.5x10^4$ /ml	$2x10^5$ /ml
HT29	Control and Oligo 1	$1x10^4$ /ml	$1x10^5$ /ml

Table 2.8 Optimised HiPerfect transfection protocol for siRNA transfections

2.2.4 Cell lysis

Cells were washed twice in PBS and lysed on ice in 0.5% NP-40 lysis buffer supplemented with a protease inhibitor cocktail for 10 minutes. The whole cell lysates were then scraped and centrifuged for 10 minutes at 13000 x g for 10 minutes to remove cell debris. The supernatant was removed and placed in a fresh tube for storage. 10 µl of 2x SDS Gel sample buffer (GSB) was added to the lysates and the samples boiled at 90ºC for 3 minutes.

2.2.5 Immunoprecipitation

Typically 5 µl of the appropriate IP antibody was added to the lysis supernatant (see **section 2.2.4**) and incubated overnight at 4ºC on a rotating wheel. The following day, protein G beads were washed three times in lysis buffer. The beads were re-suspended in an appropriate volume of lysis buffer prior to adding 30 µl of bead slurry to each IP sample. The samples were then incubated for 1 hour on a rotating wheel at 4˚C. Each IP, and untransfected (UT) control, was pulse spun following incubation and washed three times with lysis buffer. 2x GSB was added to each sample and boiled at 90°C for 3 minutes.

2.2.6 Gel electrophoresis and immunoblotting

Proteins were loaded onto appropriate % gels and electrophoresed. Proteins were then blotted onto nitrocellulose membranes. The blots were then blocked in 5% milk or 5% BSA/TBS-Tween as appropriate for one hour at room temperature and incubated with primary antibodies overnight at 4°C. Blots were then washed for three 10 minute

washes with 0.1% TBS-Tween. Blots were then incubated with HRP-conjugated secondary antibodies for one hour at room temperature. Blots were then subjected to a further three 10 minute washes with 0.1% TBS-Tween. If re-probing was required, the blots were incubated in stripping buffer for 15 minutes which was then removed and replaced with fresh stripping buffer for a further 15 minutes. The blots were then washed with 0.1% PBS-Tween for 5 minutes. Subsequently the blots were blocked for 1 hour in 5% milk or 5% BSA/TBS-Tween as appropriate and incubated overnight with primary antibodies at 4°C.

2.2.7 *In vitro* kinase assay

The immune complexes were prepared as described in **section 2.2.5**, washed three times with lysis buffer, once with lithium chloride wash buffer and once with a kinase buffer wash. A kinase cocktail solution was diluted 1:1 with dH_2O. 10 µl per sample of this was transferred to a separate eppendorf. To a new eppendorf, 10 µl per sample of dH_2O, 5 µl of histone H1 and 5 µl of 5x reaction buffer per sample was added. 1.25 µl of gamma-phosphorus 32-labelled ([γ-^{32}P]) ATP per sample was then added to the kinase cocktail: dH_2O mix. 10 µl per sample from this was transferred to the reaction buffer: histone H1: dH_2O mix, resulting in the complete kinase reaction mix. To each sample 25 µl of the complete kinase reaction mix was added. The samples were then incubated at 30°C for 30 minutes with gentle mixing every 10 minutes. 10 µl of 2x GSB was added to each sample to stop the reaction and the samples were boiled at 100°C for 3 minutes. Histone H1 or XFP-tagged immunoprecipitated proteins were used as substrates as appropriate.

2.2.8 GST pulldown assays

Cells were seeded at $2x10^5$ /ml in each 10cm tissue culture dish and were grown in 10% FBS RPMI-1640 for 48 hours. Cells were then lysed with 1 ml lysis buffer (0.5% NP-40 lysis buffer supplemented with a protease inhibitor cocktail) per 10cm tissue culture dish or serum-starved in 0.5% FBS RPMI-1640 for 24 hours prior to lysis. They were either unstimulated or stimulated with HGF (500 ng/ml) for specific time points as required before lysis. GST beads, pre-washed with the lysis buffer: protease inhibitor cocktail, were used to pre-clear the lysates for one hour prior to incubation with GST purified protein beads (also pre-washed in the lysis buffer: protease inhibitor cocktail) for two hours at 4ºC on a rotating wheel. Subsequently, the unbound fractions were

discarded and the beads were washed three times in the lysis buffer: protease inhibitor cocktail prior to the addition of 25 µl of 2x SDS sample loading buffer. The samples were then boiled for 10 minutes at 90ºC and loaded onto the appropriate % polyacrylamide gels and were immunoblotted (WB).

For GST pulldown assays in the presence of over-expressed XFP-tagged constructs cells were seeded at $1x10^5$ /ml in each 10cm tissue culture dish and were grown in 10% FBS media for 24 hours and each dish was transfected with the appropriate XFP-tagged construct using the calcium phosphate transfection kit (see **section 2.2.3**). Following 24 hours the media was replaced and incubated for a further 24 hours. Cells were then lysed as usual.

Typically 5 µl of the GST alone expression plasmid or 200 µl of GST fusion proteins were used per sample in the GST pulldown assays.

2.2.9 Immunofluorescence

Preparation of coverslips

13 mm diameter No. 1 glass coverslips were placed in a solution containing 40% of 1 M HCL and 60% of 96% ethanol overnight, gently rinsed three times in dH_2O and then boiled. The coverslips were then rinsed a further six times with dH_2O. Excess water was drained and the coverslips were incubated in an oven at 150°C overnight for sterilisation before being used.

a. Rat tail collagen type I coated coverslips

A 50 µg/ml solution of rat tail collagen type I (hereafter referred to as collagen I) was prepared in 20 mM acetic acid under sterile conditions. 100 µl of the mix was added to each 13 mm coverslip and incubated at room temperature for 1 hour. The coverslips were then washed twice with sterile PBS and were then ready for use.

b. Fibronectin coated coverslips

10 µl of fibronectin was added to 1 ml sterile PBS. 100 µl of the mix was added to each 13 mm coverslip and incubated at room temperature for 45 minutes. The coverslips were then washed twice with sterile PBS and were then ready for use.

c. 2D matrigel coated coverslips

Matrigel was allowed to thaw on ice. A 1 in 100 dilution of the matrigel in serum-free media was set up. 100 µl of the mix was added to each 13 mm coverslip and incubated at 37°C for 1 hour. The coverslips were then washed twice with sterile PBS and were then ready for use.

Immunofluorescent labelling

Cells were fixed with 4% PFA in PBS at room temperature for 20 minutes and washed three times with PBS before being permeabilised with 0.2% Triton X-100/PBS for 5 minutes. Cells were then washed three times with PBS. For F-actin alone (this includes XFP-tagged expressing cells), cells were incubated at room temperature for 1 hour with TRITC-Phalloidin (1 in 1000 dilution in 3% BSA-PBS) or Phalloidin 633 (1 in 200 dilution in 3% BSA-PBS). The coverslips were then washed twice with PBS and once with dH_2O before being mounted in 10 µl FluorSave^{TM} Reagent on glass slides.

For Paxillin or E-cadherin staining, cells were blocked in 3% BSA-PBS for 30 minutes. They were then washed three times with PBS and incubated at room temperature for 2 hours with an anti-paxillin antibody (1 in 50 dilution in 3% BSA-PBS) or with an anti-E-cadherin antibody (1 in 50 dilution in 3% BSA-PBS). Cells were then washed three times with PBS and incubated with Alexa Fluor® 488 or 568 goat anti-mouse antibody (1 in 200 dilution in 3% BSA-PBS) in addition to TRITC-Phalloidin (1 in 1000 in 3% BSA-PBS) or Phalloidin 633 (1 in 200 dilution in in 3% BSA-PBS). Coverslips were then washed and mounted as described for F-actin staining alone. Images were collected on an Olympus IX71 inverted microscope, or a Carl Zeiss LSM510 META laser scanning confocal microscope.

2.2.10 Time-lapse microscopy

Cells seeded into six-well plates and supplemented with 20 mM Hepes (Invitrogen, UK) were placed on the automated and heated stage of an Olympus IX71 microscope. Cell images were collected using a Retiga SRV CCD camera, where a frame was captured at 5 minute intervals over 24 hours from each of the six wells using Image-Pro Plus software (supplied by MAG, UK). Following acquisition, the time-lapse sequences were displayed as a movie and saved as AVI files. These files could then be used to manually track cells for the whole of the time-lapse sequence using Motion Analysis software

(ANDOR IQ Technology, Belfast, UK). This resulted in the generation of a sequence of position co-ordinates corresponding to each cell in each frame which was subsequently saved as Cel files. A total of 30-60 cells were tracked over 3 independent films per condition. The Cel files were then subjected to mathematical analysis using Mathematica 6.0™ notebooks developed in-house by Prof. G. Dunn and Prof. G. Jones to obtain the mean migration speed and statistical significance, which was accepted for $P \leq 0.05$.

2.2.11 Cell scatter assay in a 3D matrix

The Lab-Tek® chambered #1.0 8 chamber borosilicate coverglass system (Nunc, USA) was used. 100 µl of matrigel was added to the bottom of all 8 wells. This was allowed to set at 37ºC for 1 hour. 2 µl of matrigel and 98 µl of collagen I was mixed with $2.4x10^4$ DU145 cells in a 100 µl suspension. This was left to set at 37ºC overnight. Once set, chamber wells were supplemented with 100 µl 10% FBS RPMI-1640 media and subsequently every other day. Following one week, media was removed and cells were fixed with 4% PFA and 0.25% glutaraldehyde in PBS at room temperature for 20 minutes and washed three times with PBS before being permeabilised with 0.2% Triton X-100/PBS for 5 minutes. Cells were then washed three times with PBS and incubated at room temperature for 1 hour with TRITC-Phalloidin diluted 1 in 1000 in 3% BSA-PBS for F-actin staining. For DAPI staining, cells were incubated with 3 µm DAPI diluted in PBS and left at room temperature for 5 minutes and washed three times with PBS. Images were collected on a Carl Zeiss LSM510 META laser scanning confocal microscope.

For live-cell imaging of cells, the chamber was set up as described above. Following a week, the chamber wells were washed 3 times with PBS and serum-starved with 0.5% FBS RPMI-1640 media. Following 24 hours, cells were stimulated with HGF (500 ng/ml) and left at 37ºC for a further 48 hours. Unstimulated cells were serum-starved 24 hours prior to filming. The cells were then filmed for 24 hours using the set up described in **section 2.2.10**.

2.2.12 HGF-and EGF-induced cell scatter assay on 2D substratum

Cells were seeded onto coverslips at a density of $0.5x10^4$ /ml and allowed 48 hours to form colonies. Cells were serum-starved with 0.5% FBS media 24 hours. The media

was not changed prior to growth factor stimulation. Cells were then fixed with 4% PFA after 24 hours.

HGF-induced cell scattering quantification

Cells were counted and cell counts of starved versus starved plus HGF stimulation were compared. The % of scattered cells per experiment was calculated using the following:

Unscattered + attempted scatter + scattered = n
Scattered/n x 100 = % of scattered cells

The % of attempted scatter cells per experiment was calculated using the following:
Unscattered + attempted scatter + scattered = n
Attempted scatter/n x 100 = % of attempted scatter cells

2.2.13 Data analysis

Image processing and cell shape analysis

Image J software was used to elucidate the morphology of each cell by manually drawing around individual cells and then processing the data to give elongation ratios and cell spread areas. In order to determine the elongation ratio of a cell, Image J shape analysis software divides the shortest cell diameter by the longest. Therefore, the ratio for an elongated cell morphology generated by Image J is a small numerical value. Hence, in order to aid graphical representation of the results acquired, all elongation ratio values have been subtracted from one and all spread areas have been multiplied by 1000.

Densitometry Analysis

The autoradiographs were saved as TIF files in Adobe Photoshop CS5 and ANDOR IQ Technology software was used to quantify desired protein levels. In this analysis system it was assumed that 0 is black and the maximal value is 255 at 8 bits per pixel. These values were then used to calculate the mean fold value.

Chapter 3
Development of an HGF-induced 3D cell scatter assay

Chapter 3 – Development of an HGF-induced 3D cell scatter assay

3.1 Introduction

It has long been established that growth factors can promote cell migration both *in vitro* and *in vivo*. Indeed, HGF is known to be a mitogenic (Clark, 1994) and motogenic (Cantley et al., 1994; Niranjan et al., 1995) growth factor that is important during normal development. HGF signalling is also implicated in prostate carcinoma metastasis (Fujiuchi et al., 2003; Gmyrek et al., 2001; Wells et al., 2005) and the HGF receptor c-Met is known to be over-expressed in prostate cancer (van Leenders et al., 2002).

HGF was found to induce cell scattering in colony-forming MDCK cells and was thereafter used as an EMT model (Stoker and Perryman, 1985). Subsequently, other cells have been shown to respond to HGF, including DU145 prostate cancer cells (Davies et al., 2004; Wells et al., 2005). Cell scattering involves cell-cell dissociation and the loss of junctional E-cadherin localisation (Miura et al., 2001). As such, the HGF-induced DU145 scatter model has been used in live-cell imaging to show the migration of single DU145 cells in response to HGF and to observe and track actin cytoskeletal changes, as well as modifications in intercellular adhesions, downstream of HGF stimulation (Bright et al., 2009; Wells et al., 2005).

During tumour cell invasion and metastasis, cancer cells must acquire a migratory phenotype to move through the 3D environment of the ECM. It has been documented that tumour cells exhibit different properties in 2D and 3D substrata (Sahai, 2007). Therefore, 3D model systems are being employed to investigate cell migration in an environment similar to that found *in vivo* (Yamazaki et al., 2009; Zaman et al., 2006).

In this chapter, the 2D HGF-induced scatter assay has been further optimised (Fram et al., 2011) and an attempt has been made to translate this assay into a 3D model. In addition, other cell types and growth factors have been tested for their cell scattering potential.

3.2 Results

3.2.1 DU145 cells scatter in response to HGF stimulation

It has been previously reported that HGF stimulation elicits scattering in colony-forming DU145 cells (Wells et al., 2005). To confirm the ability of HGF to induce DU145 cell scattering, DU145 cells were maintained in low serum prior to HGF stimulation for 4 and 24 hours. DU145 cells grew as colonies in serum-starved conditions (minus HGF) with tight cell-cell junctions and prominent E-cadherin localisation at the junctions (**figure 3.1**). Following 4 hours HGF stimulation, colony edge cells began to dissociate and this was characterised by a change in their cell morphology and a reduction in E-cadherin staining localised at the cell-cell junctions (**figure 3.1, arrows**). Twenty four hours after HGF addition, the majority of the DU145 cells had scattered and exhibited an elongated migratory phenotype with little or no E-cadherin staining visible at cell-cell boundaries (**figure 3.1**). These observations were consistent with previous reports that E-cadherin re-localises from cell-cell junctions to the cytosol upon HGF stimulation (Miura et al., 2001).

3.2.2 Optimal HGF-induced DU145 cell scattering occurs after 2-5 weeks of culturing

A robust HGF-induced scatter assay requires cells that grow as tight colonies in the absence of HGF. The efficiency of HGF-induced DU145 cell scattering may be affected by continual cell culturing. Therefore, an optimal time window for tight colony formation in the absence of HGF, as well as cell scatter induction in the presence of HGF, needed to be defined.

DU145 cells were plated at a low density to favour the growth of cell colonies (**figure 3.2A, minus HGF**) (see **section 2.2.12**). Serum-starved DU145 cells were then stimulated with HGF to induce cell-cell dissociation and independent migration (**figure 3.2A, plus HGF**). This experiment was repeated in exactly the same manner over 7 weeks using cells from the same population. The efficiency of the DU145 cell scatter response to HGF stimulation was found to change with time. The optimum time for scattering was defined as the point at which the scattered cell count was at its lowest in the low serum conditions and the scatter response was at its highest following HGF addition (**figure 3.2B**). A time window for HGF-induced DU145 cell scattering of

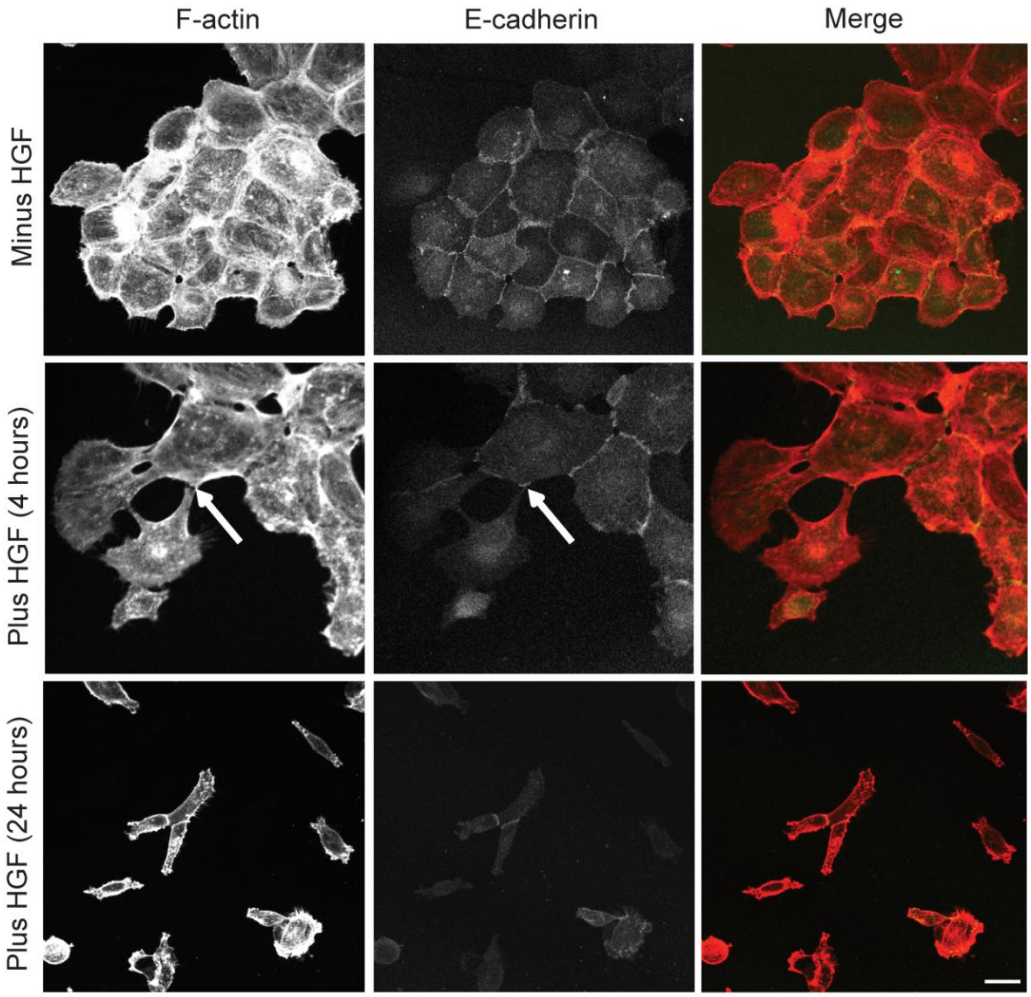

Figure 3.1 HGF induces scattering in DU145 cells. Cells were serum-starved (minus HGF) for 24 hours prior to 4 hours or 24 hours HGF (10 ng/ml) stimulation (plus HGF). Cells were then fixed and labelled for E-cadherin and F-actin. Arrow marks point of cell-cell dissociation (plus HGF (4 hours), Actin) and reduction in junctional E-cadherin staining (plus HGF (4 hours), E-cadherin). Images shown are representative of 3 independent experiments. Bar = 10 µm.

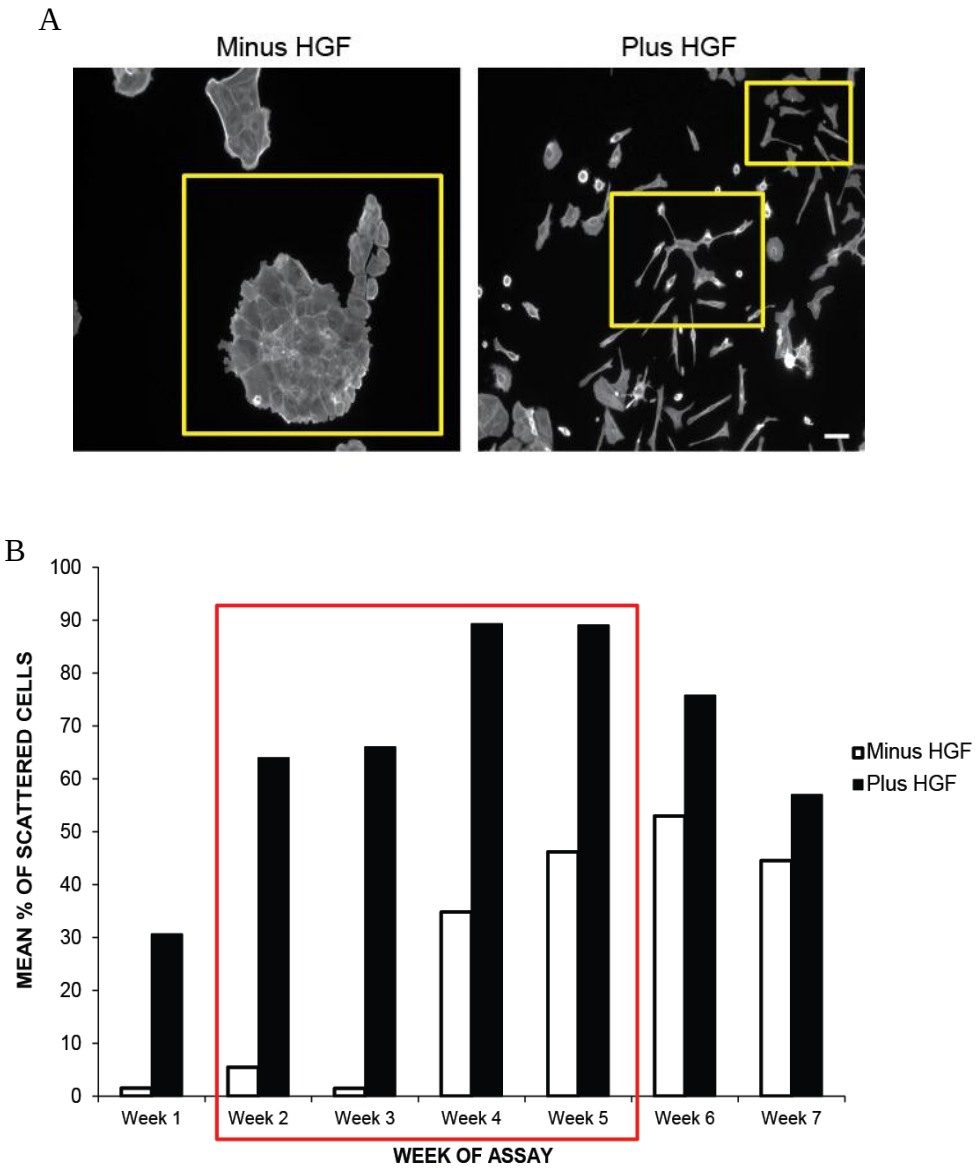

Figure 3.2 Optimisation of the HGF-induced scattering model in DU145 cells. A) The HGF-induced DU145 scatter assay was conducted. Cells were serum-starved for 24 hours and were either left untreated (minus HGF) or were treated with HGF (plus HGF) (10 ng/ml). After 24 hours the cells were fixed and stained for F-actin. Images illustrate categorisation of the DU145 cells minus and plus HGF. Unscattered = cells in a colony as marked (minus HGF). One cell adjoined to another was also classed as within a cell colony, even if these cells were detached from the remainder of the colony. Attempted Scatter = cells remain attached to one another but also exhibit an elongated phenotype and there is some loss of cell-cell junctions as indicated in centre (plus HGF). Scattered = loss of cell-cell junctions and single cells with an elongated migratory phenotype as indicated at top right (plus HGF). **B)** The HGF-induced DU145 scatter assay was conducted over 7 weeks and the mean % of scattered cells was calculated. The optimum time for scattering was deduced as marked. Bar = 10 µm.

between 2-5 weeks of culturing following cell recovery from cryogenic storage was deemed optimal and therefore, was used in all subsequent experiments (Fram et al., 2011).

3.2.3 Effect of substratum on HGF-induced DU145 cell scattering

It has been reported that the rigidity of the underlying ECM can affect the migratory behaviour of cells (Lo et al., 2000). Matrigel, collagen and fibronectin are commonly used in 2D and 3D *in vitro* cell migration assays to examine tumour cell migration and metastasis. The ECM environment of connective tissues is rich in collagen I; thus this type of collagen is the most commonly used for *in vitro* studies (Hooper et al., 2006). Matrigel is employed as its composition resembles that of basement membranes and is a mixture of various proteins that is particularly rich in collagen V and laminins (Hooper et al., 2006). Lastly, fibronectin is a suitable component in migration assays as this ECM protein is secreted by a number of cell types (Hershkoviz et al., 1992; Lam et al., 2003; Peters et al., 1990; Tse et al., 2011). Prior to attempting to establish a 3D scatter assay, the effect of matrix composition on HGF-induced cell scattering was quantified using serum (glass coverslips placed in 10% FBS media for 48 hours prior to serum-starving), fibronectin, collagen I and 2D matrigel coated coverslips.

Serum-starved, unstimulated DU145 cells seeded on all the tested substrata possessed prominent actin fibers with paxillin-rich cell-substratum adhesion sites around the entirety of the cell colony (**figure 3.3A**). No obvious change in adhesions or morphology was visible between the different substrata. All of the tested substrata supported cell scattering upon addition of HGF to a significant level, notably on collagen I substratum, when compared to the minus HGF control cells (**figure 3.3B**).

3.2.4 Effect of substratum on DU145 cell speed upon HGF stimulation

Live-cell imaging was employed to directly examine the migration of single DU145 cells in response to HGF and to compare the migration speed of these scattering cells on the different substrata. The migration paths for HGF-stimulated DU145 cells were manually tracked and processed. The migration of individual cell tracks were plotted and shifted to an origin of (x0, y0) (**figure 3.4A**). As a control, serum-starved DU145 cells were filmed in the absence of HGF for all the substratum tested. In these conditions, cells within the colony were still in contact with each other following 24

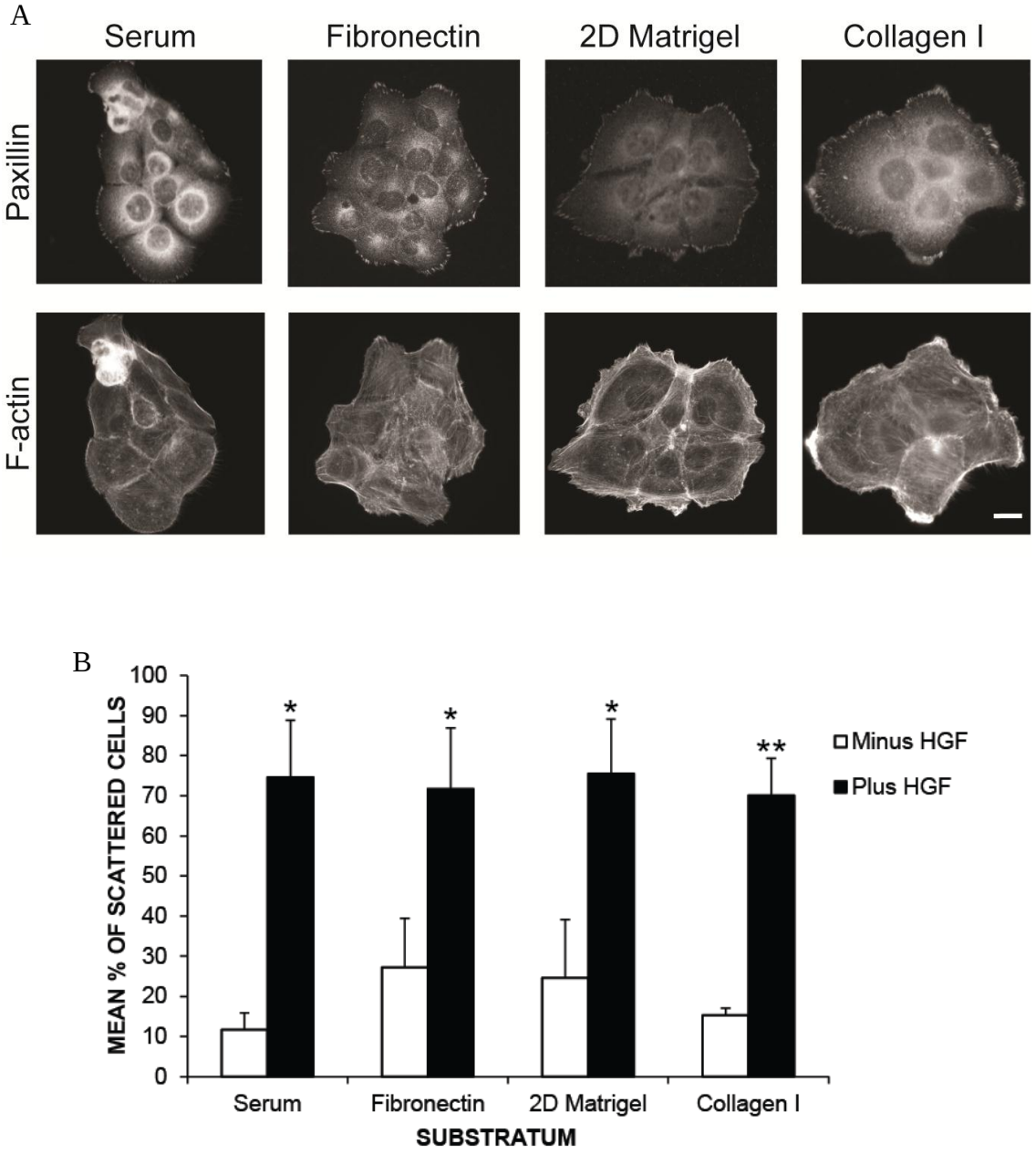

Figure 3.3 Variation in HGF-induced DU145 cell scattering response on different 2D substratum. A) DU145 cells seeded onto serum, fibronectin, 2D matrigel and collagen I coated coverslips were serum-starved for 24 hours, fixed and then labelled for paxillin and F-actin in the absence of HGF addition. **B)** The HGF-induced DU145 scatter assay was conducted using serum, fibronectin, 2D matrigel and collagen I coated coverslips. Cells were serum-starved for 24 hours prior to HGF (10 ng/ml) stimulation. After 24 hours cells were fixed and stained for F-actin. Scattered = loss of cell-cell junctions and single cells with an elongated migratory phenotype. Cells were counted and cell counts of minus HGF versus plus HGF were compared. The mean % of scattered cells and the standard error of the mean were calculated over 3 independent experiments for each substratum. Statistical significance compared with minus HGF cells was calculated using Student's *t*-test; *, $P < 0.05$ **, $P < 0.005$. Bar = 10 µm.

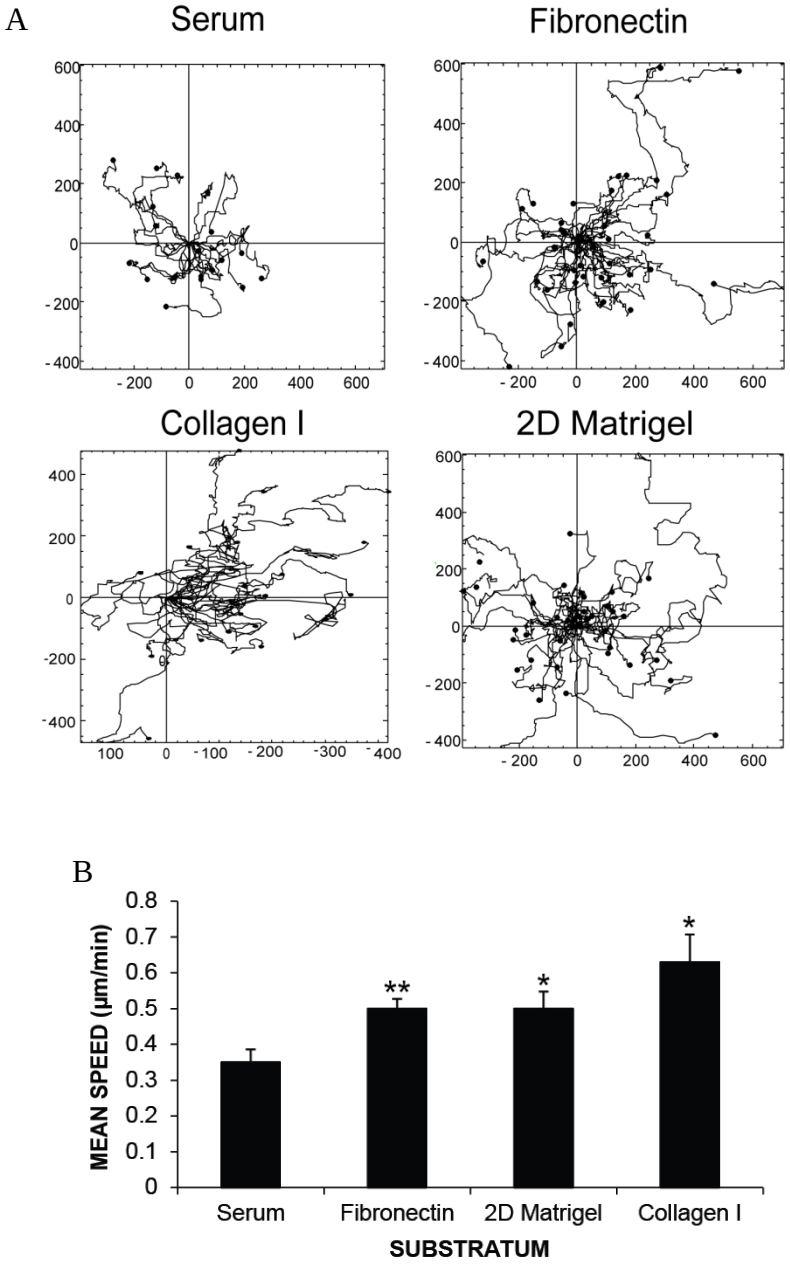

Figure 3.4 Effect of 2D substratum on DU145 cell migration speed upon HGF stimulation. A) DU145 cells seeded onto serum, fibronectin, 2D matrigel and collagen I coated coverslips were then serum-starved for 24 hours, stimulated with HGF (10 ng/ml) and filmed for 24 hours at 5 minute intervals using phase-contrast time-lapse microscopy. All colony edge cells were then tracked using ANDOR IQ Technology software and processed in Mathematica©. Plots of individual cell tracks are displayed centered at (x0,y0). **B)** The mean migration speed and the standard error of the mean (SEM) for 3 independent experiments for each substratum were calculated for cells tracked in (A). Statistical significance compared with serum substratum was calculated using Student's *t*-test; *, $P \leq 0.05$ **, $P \leq 0.005$.

hours filming (see **movie 1** for representative movie and **Appendix 3**). DU145 cells displayed a significant increase in mean migratory speed following HGF addition on fibronectin (0.5 μm/min ± 0.027 SEM), 2D matrigel (0.5 μm/min ± 0.048 SEM) and collagen I (0.63 μm/min ± 0.077 SEM) when compared to serum-coated substratum (0.35 μm/min ± 0.036 SEM) (**figure 3.4B** and see **movie 2** for representative movie and **Appendix 3**). DU145 cells seeded onto collagen I exhibited a higher mean migration speed when compared to all the substrata used, suggesting that collagen I, in the presence of HGF stimulation, increases the migration potential of DU145 cells.

3.2.5 DU145 cells scatter in response to EGF stimulation

EGF signalling is important in the progression of prostate cancer; indeed, the frequency of bone metastases was hindered upon the inhibition of EGFR signalling *in vivo* (Angelucci et al., 2006). EGF, like HGF, has been shown to enhance prostate cancer cell migration (Zhou et al., 2006). EGF has also been shown to enhance the invasive potential of DU145 prostate carcinoma cells (Turner et al., 1996) and, following the completion of these studies, this growth factor was reported to induce the disassembly of cell-cell boundaries in DU145 cells (Gan et al., 2010). However unlike HGF, EGF has not been tested in a prostate cancer cell scatter assay. Prior to performing the DU145 scatter assay with EGF, DU145 whole cell lysate was immunoblotted for EGFR to confirm its expression in this cell line. EGFR was found to be expressed in DU145 cells (**figure 3.5A**).

EGF was found to be able to induce cell scattering in DU145 cells (**figure 3.5B, plus EGF**). Serum, fibronectin and collagen I substratum all supported the scattering effect when compared to serum-starved control cells (minus EGF) (**figure 3.5C**). However unlike HGF, the addition of EGF was not enough to significantly increase the scattering potential of cells on 2D matrigel coated substratum, when compared to serum-starved conditions (minus EGF) (**figures 3.3B** and **3.5C**).

3.2.6 HGF induces cell scattering in HT29 cells

It has been reported that HGF also induces the scattering of HT29 colon adenocarcinoma cells; however, this scattering effect induced by HGF was not quantified (Herrera, 1998). Therefore, to complement the use of DU145 cells, and to provide a scatter model from a different cell type, HT29 cells were tested for their

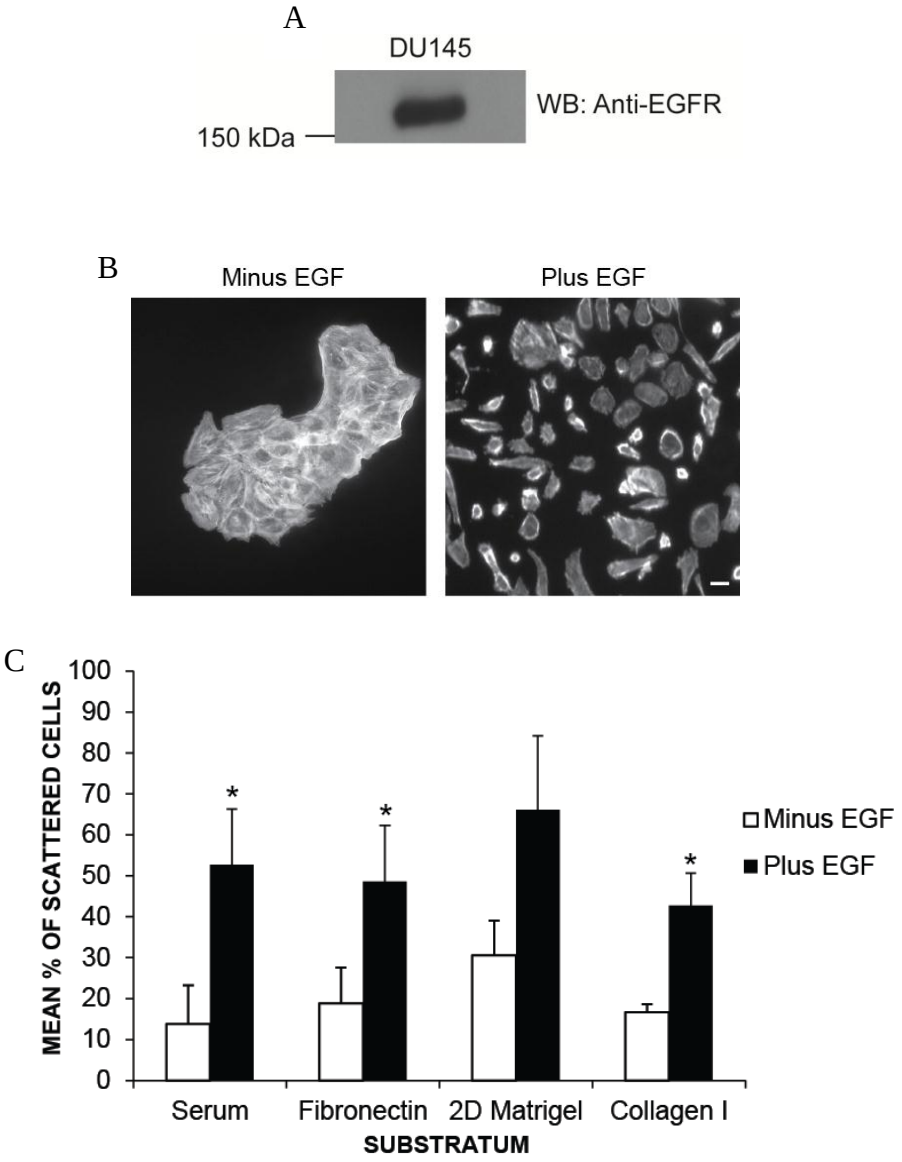

Figure 3.5 EGF induces DU145 cell scattering. A) DU145 whole cell lysate was immunoblotted for EGFR. **B)** The EGF-induced DU145 scatter assay was conducted. Cells seeded onto glass coverslips were serum-starved for 24 hours, and were then either left untreated (minus EGF) or were treated with EGF (plus EGF) (100 ng/ml). After 24 hours the cells were fixed and stained for F-actin. **C)** DU145 cells were seeded onto serum, fibronectin, 2D matrigel or collagen I coated coverslips and treated as described in (B). Cells were counted and scattered cell counts of serum-starved versus plus EGF stimulation were compared. Scattered = loss of cell-cell junctions and single cells with an elongated migratory phenotype as discernible in (B) (plus EGF). The mean % of scattered cells and the standard error of the mean were calculated over 3 independent experiments for each substratum. Statistical significance compared with minus EGF cells was calculated using Student's *t*-test; *, $P < 0.05$. Bar = 10 µm.

scattering potential downstream of HGF. HT29 cells are morphologically similar to DU145 cells in that they form multi-cellular colonies. Expression of the HGF receptor, c-Met, was confirmed in the HT29 cell line (**figure 3.6A**). Initial assays using HGF at a concentration of 10 ng/ml induced a minimal scatter response (**figure 3.6B**). However it was evident that the cells were attempting to scatter upon addition of the growth factor when the serum-starved (minus HGF) and attempted scatter cell counts were compared (**figure 3.6B**). In order to optimise the HT29 scatter assay, the time of stimulation was increased from 24 hours to 48 hours. However no difference was observed when compared to 24 hours HGF addition (data not shown).

Closer examination of western analysis revealed that a higher level of c-Met receptor expression was present in the HT29 cells when compared to DU145 cells (**figure 3.6A**). Thus it was speculated that an increased concentration of HGF may be required to occupy the higher level of c-Met receptor that was detected. Hence a range of HGF concentrations were tested for their affect on HT29 cell scattering (**figure 3.6C**). A P value of < 0.05 was obtained, when compared to control cells (0 ng/ml), when concentrations of 30 ng/ml and 120 ng/ml HGF were used. Moreover, a more significant P value of < 0.0005 following the addition of 60 ng/ml HGF was obtained when compared to control cells (0 ng/ml). Thus 60 ng/ml was used for subsequent HT29 cell investigations. Morphological changes were induced when HT29 cells were stimulated with HGF (60 ng/ml) and the scatter response was represented by cell-cell dissociation and independent migration (**figure 3.6D, plus HGF**). Whilst a higher expression level of c-Met was observed in the HT29 cells when compared to DU145 cells, it could be speculated that the surface level of c-Met is lower on HT29 cells. This could in part account for the reduced scattering obsesrved in response to HGF treatment in this cell line when compared to DU145 cells.

3.2.7 Effect of substratum on HGF-induced HT29 cell scattering

Previous work showed that DU145 cell scattering was supported on multiple matrices (**figure 3.3B**). Therefore, the ability of the different matrices to support HGF-induced HT29 cell scattering was also tested. Serum-starved, unstimulated HT29 cells seeded on serum, fibronectin, 2D matrigel and collagen I coated coverslips all possessed prominent actin fibers with paxillin staining discernible around the entire edge of the

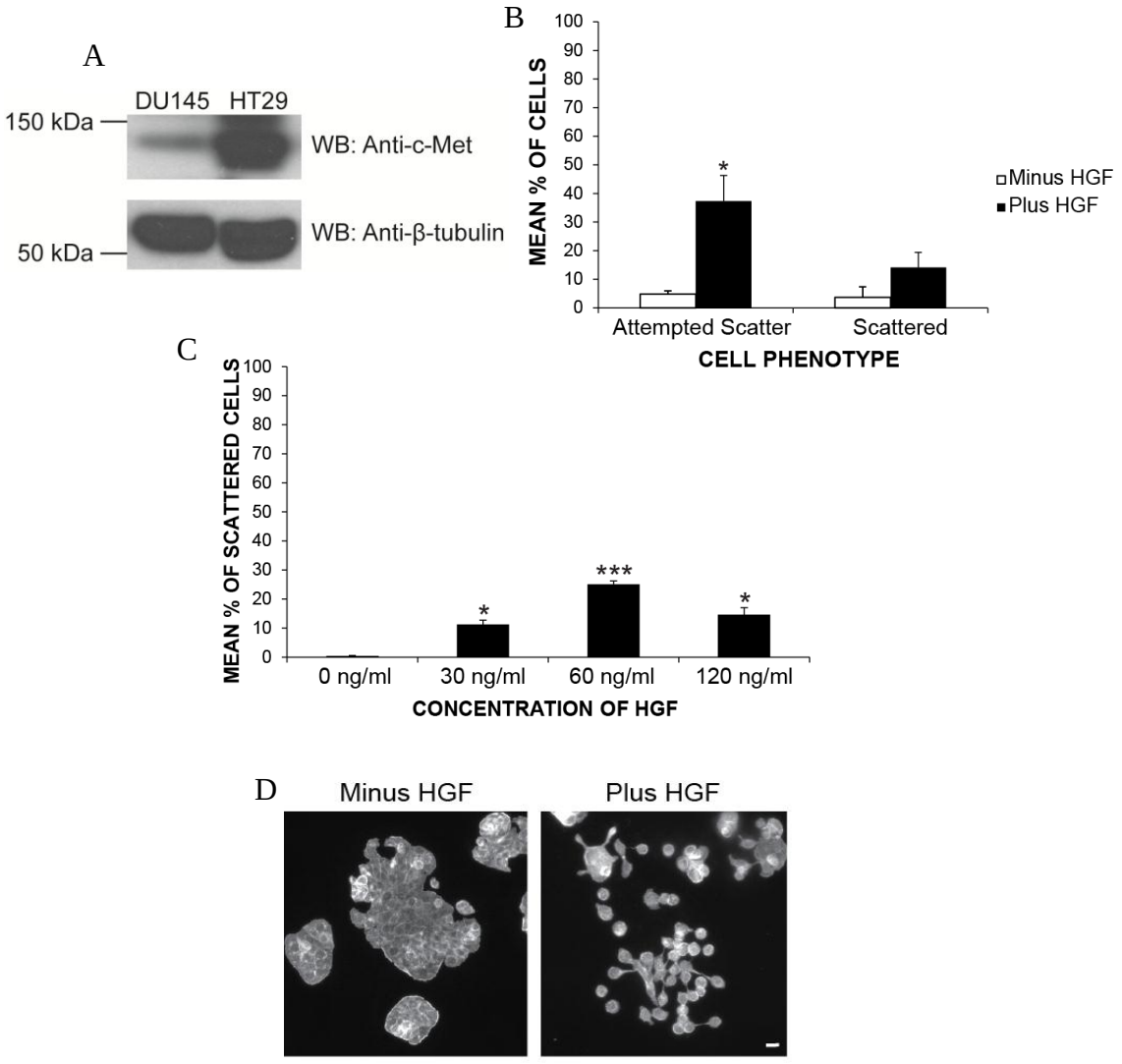

Figure 3.6 Optimisation of HGF-induced HT29 cell scattering. A) DU145 and HT29 whole cell lysates were immunoblotted for c-Met expression and for β-tubulin as a loading control. **B)** The HGF-induced scatter assay was conducted using HT29 cells. Cells were seeded onto glass coverslips and serum-starved for 24 hours prior to 24 hours HGF (10 ng/ml) stimulation. Cells were then fixed and stained for F-actin. Cells were counted and cell counts of serum-starved versus serum-starved plus HGF were compared. Attempted Scatter = cells remain attached to one another but also exhibit an elongated phenotype and there is some loss of cell-cell junctions. Scattered = loss of cell-cell junctions and single cells with an elongated migratory phenotype. **C)** The HT29 scatter assay was repeated as described in (B) using varying concentrations of HGF as indicated. **D)** Serum-starved (minus HGF) and HGF-stimulated (plus HGF) (60 ng/ml) HT29 cells were stained for F-actin as described in (B). In (B) the mean % of cells and in (C) the mean % of scattered cells and the standard error of the mean were calculated over 3 independent experiments. Statistical significance compared with minus HGF cells was calculated using Student's *t*-test; *, $P < 0.05$ ***, $P < 0.0005$. Bar = 10 µm.

cell colony (**figure 3.7A**). This was consistent with the morphology observed previously for DU145 cells (**figure 3.3A**). Analysis of the HGF-induced scatter assay results demonstrated that all substrata tested supported cell scattering, with the most significant level of scattering observed on serum and collagen I (**figure 3.7B**). Interestingly, the mean percentage of scattered cells in unstimulated conditions (minus HGF) was significantly lower for all the substrata tested using HT29 cells when compared to DU145 cells (**figures 3.3B** versus **3.7B**).

3.2.8 Optimisation of the HGF-induced scatter assay in a 3D matrix

Although 2D cell migration assays can deliver useful characterisation of cell behaviour and help to identify key regulatory proteins, 2D assays do not closely reflect the *in vivo* environment. Therefore, to complement the 2D studies conducted, a 3D model of HGF-induced cell migration was attempted. DU145 cells were chosen for the 3D model instead of HT29 cells as DU145 cells were more responsive to HGF in 2D (**figure 3.3** versus **figures 3.6** and **3.7**). HGF was chosen as the growth factor stimulant as it appeared to be a more effective cell scattering inducer than EGF (**figure 3.3B** versus **figure 3.5C**).

The first objective was to identify a matrix composition that would support the formation of cell colonies and allow serum-starvation without significant cell scattering. Following matrix composition trials (data not shown), and based on the previous data obtained in chapter 3, it was established that a matrix of 98% collagen I and 2% 2D matrigel best supported colony growth (**figure 3.8A, grow** and **minus HGF**). Cell colonies were easily identified by prominent actin staining coupled with multiple DAPI stained nuclei in both basal and serum-starved conditions. Sometimes, in 3D matrix assays, the cells imaged are actually adhered to the bottom of the well. Therefore, to ensure that the cell colonies detected were fully embedded within the matrix, images were captured where cell colonies were found to be present across different planes within the same 3D matrix field of view (**figure 3.8B**). Whilst colonies of DU145 cells were detected in the 3D matrix, full lumen formation was not observed. DU145 cells are metastatic epithelial cells, thus it is possible that these cells have lost properties that are typical of non-transformed epithelial cells and have acquired mesenchymal-like characteristics. Therefore, DU145 cells may not be able to form a full lumen. In order to

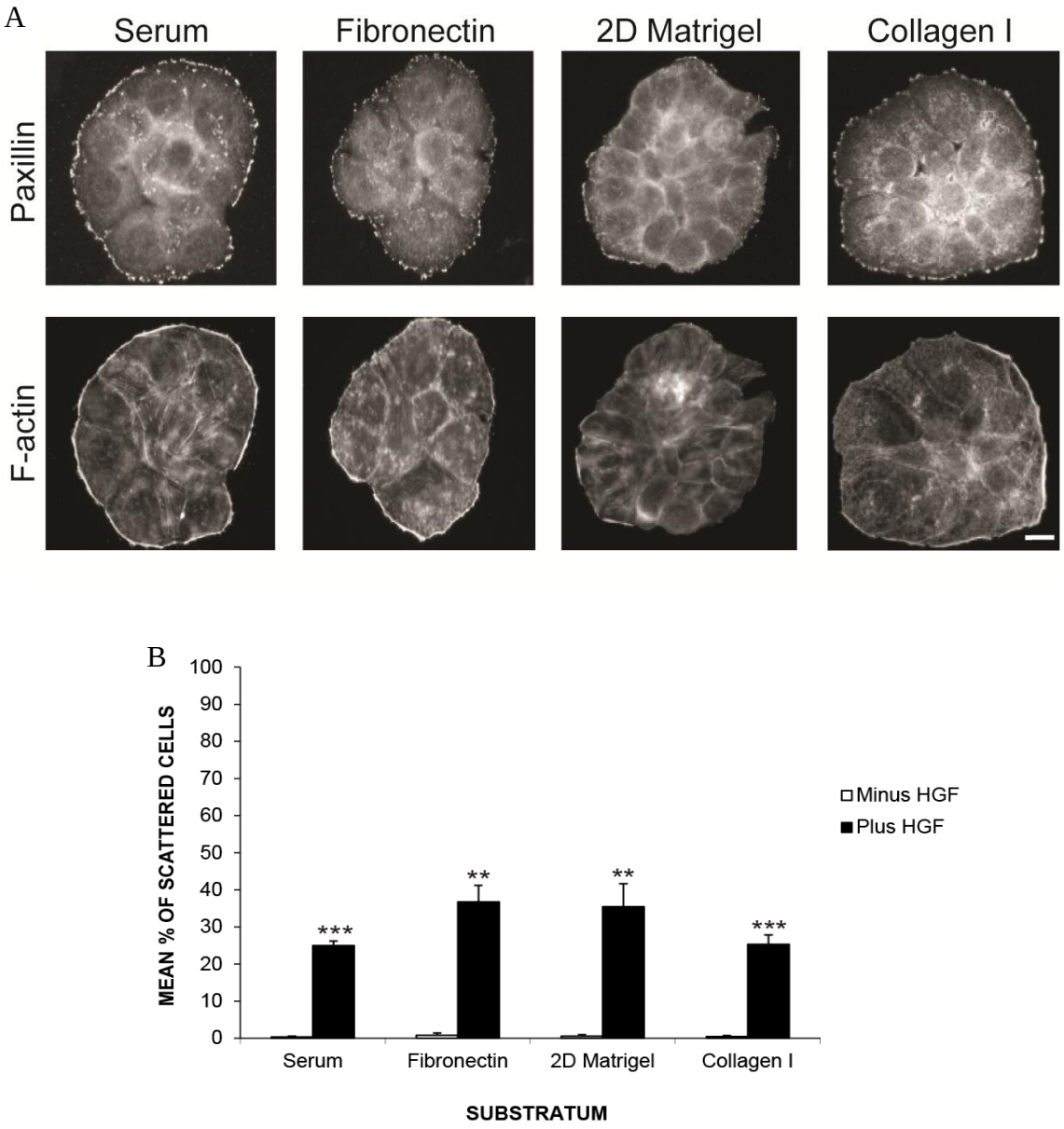

Figure 3.7 Variation in HGF-induced HT29 cell scattering response on different 2D substratum. A) HT29 cells seeded onto serum, fibronectin, 2D matrigel and collagen I coated coverslips were serum-starved for 24 hours, fixed and then labelled for paxillin and F-actin in the absence of HGF. **B)** The HGF-induced HT29 scatter assay was conducted using serum, fibronectin, 2D matrigel and collagen I coated coverslips. Cells were serum-starved for 24 hours prior to HGF (60 ng/ml) stimulation. After 24 hours cells were fixed and stained for F-actin. Cells were counted and cell counts of starved versus starved plus HGF stimulation were compared. Scattered = loss of cell-cell junctions and single cells with an elongated migratory phenotype. The mean % of scattered cells and the standard error of the mean were calculated over 3 independent experiments for each substratum. Statistical significance compared with minus HGF cells was calculated using Student's *t*-test; **, $P < 0.005$, ***, $P < 0.0005$. Bar = 10 µm.

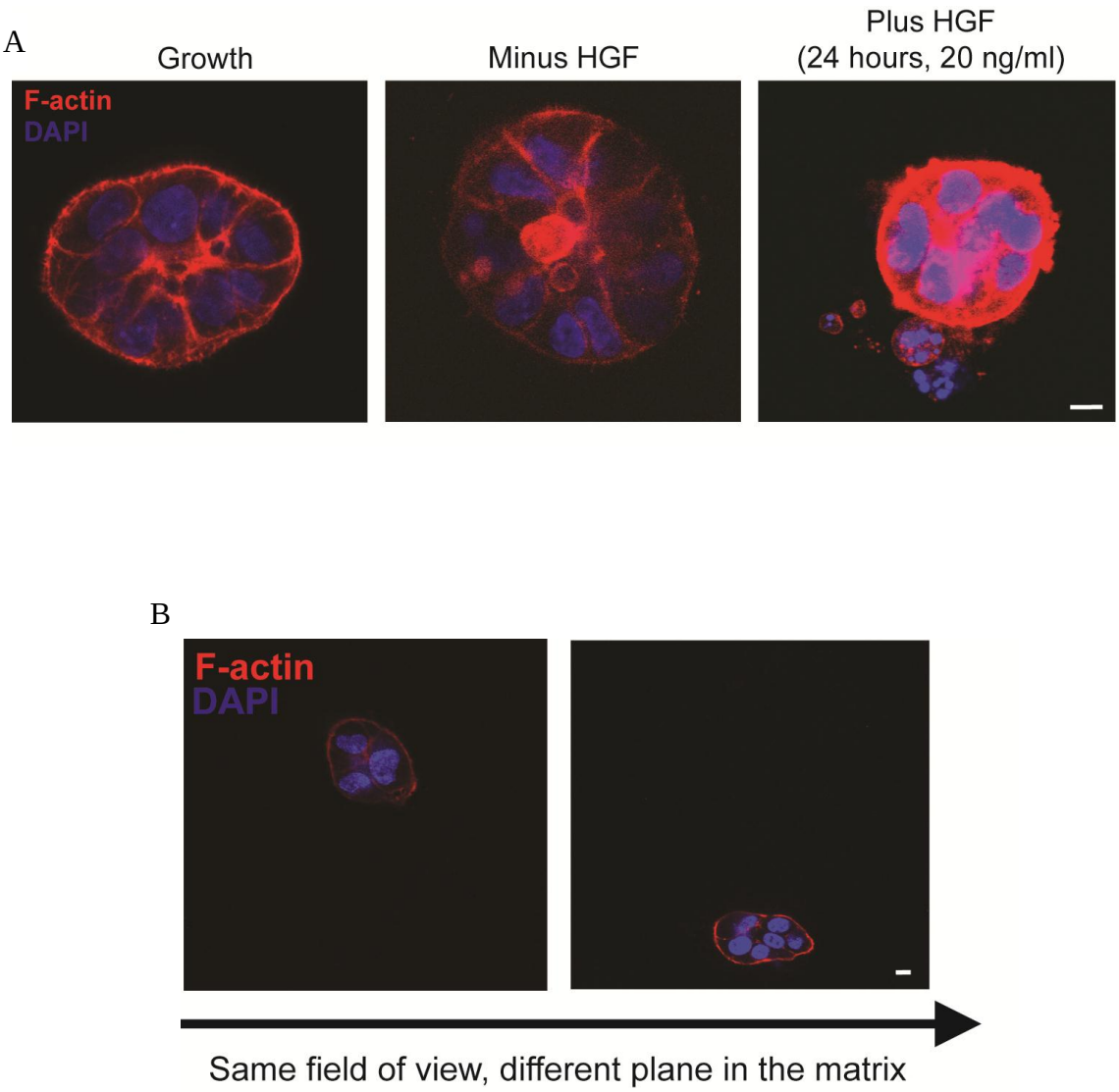

Figure 3.8 DU145 cells are able to form colonies and respond to HGF in a 3D matrix. A) DU145 cells were grown in a 98% collagen I and a 2% matrigel 3D matrix (see **section 2.2.11**). Following one week, cells were either left in growth conditions (Growth) (10% FBS), serum-starved (minus HGF) (0.5% FBS) for 24 hours or serum-starved 24 hours prior to HGF stimulation (20 ng/ml) for 24 hours. Cells were then fixed and stained for F-actin and for cell nuclei. **B)** DU145 cells were treated as described in (A) but were maintained in 10% FBS grow media. Cells were fixed and stained for F-actin and for cell nuclei. The images displayed were captured in the same field of view but in a different plane in the matrix. In (A) and (B) the images were collected as single images using confocal microscopy and are representative of 3 independent experiments. Bar = 10 µm.

test this hypothesis, non-transformed epithelial cells could be used as a control in the 3D assay (for example, MDCK cells), as well as other metastatic epithelial cancer cell lines.

The second objective was to be able to induce cell scattering within this 3D matrix. DU145 cell colonies in the 3D matrix were serum-starved and stimulated with HGF. Following 24 hours stimulation with 20 ng/ml HGF, there was some evidence of colony breakdown, where the F-actin distribution around the colony periphery was undulating in appearance (**figure 3.8A, plus HGF**). This may correspond to the ruffling of the colony edge cells that is known to occur following HGF stimulation in 2D DU145 HGF-induced scatter assays (Wells et al., 2005). Live-cell imaging was then used to attempt to analyse cell migration of DU145 cells embedded in a 3D matrix. However, preliminary results were difficult to interpret due to the limitation of only being able to film these cells in phase-contrast (data not shown).

3.2.9 HGF increases the migration potential of DU145 cells in a 3D matrix

To mitigate technical difficulties associated with imaging cell scattering in phase-contrast, DU145 cells stably expressing EGFP were employed. To confirm that these cells had the same morphology and response to HGF as wild-type DU145 cells, the 2D DU145 scatter assay was conducted as previously described (see **section 3.2.2**). In the absence of HGF these cells grew in tight colonies (**figure 3.9A, minus HGF)**. Upon 24 hours HGF stimulation (10 ng/ml), cell-cell contacts were diminished and single cells were visible and were exhibiting an elongated phenotype (**figure 3.9A, plus HGF**). Furthermore, there was significant scattering induction by HGF in these cells when compared to serum-starved conditions (**figures 3.9A** and **3.9B**). These observations were consistent with the results obtained previously for wild-type DU145 cells on serum-coated substratum (**figure 3.3B**).

The DU145 EGFP stable cell line was then used to assess the migration potential of DU145 cells in a 3D matrix in the absence and presence of HGF using live-cell imaging. Different HGF stimulation time points, as well as different concentrations of HGF were investigated in an attempt to induce cell migration in these cells (data not shown). The optimal concentration of HGF was found to be 500 ng/ml. In addition, DU145 EGFP cells embedded in the matrix were stimulated with HGF for 72 hours (filming occurred between 48-72 hours).

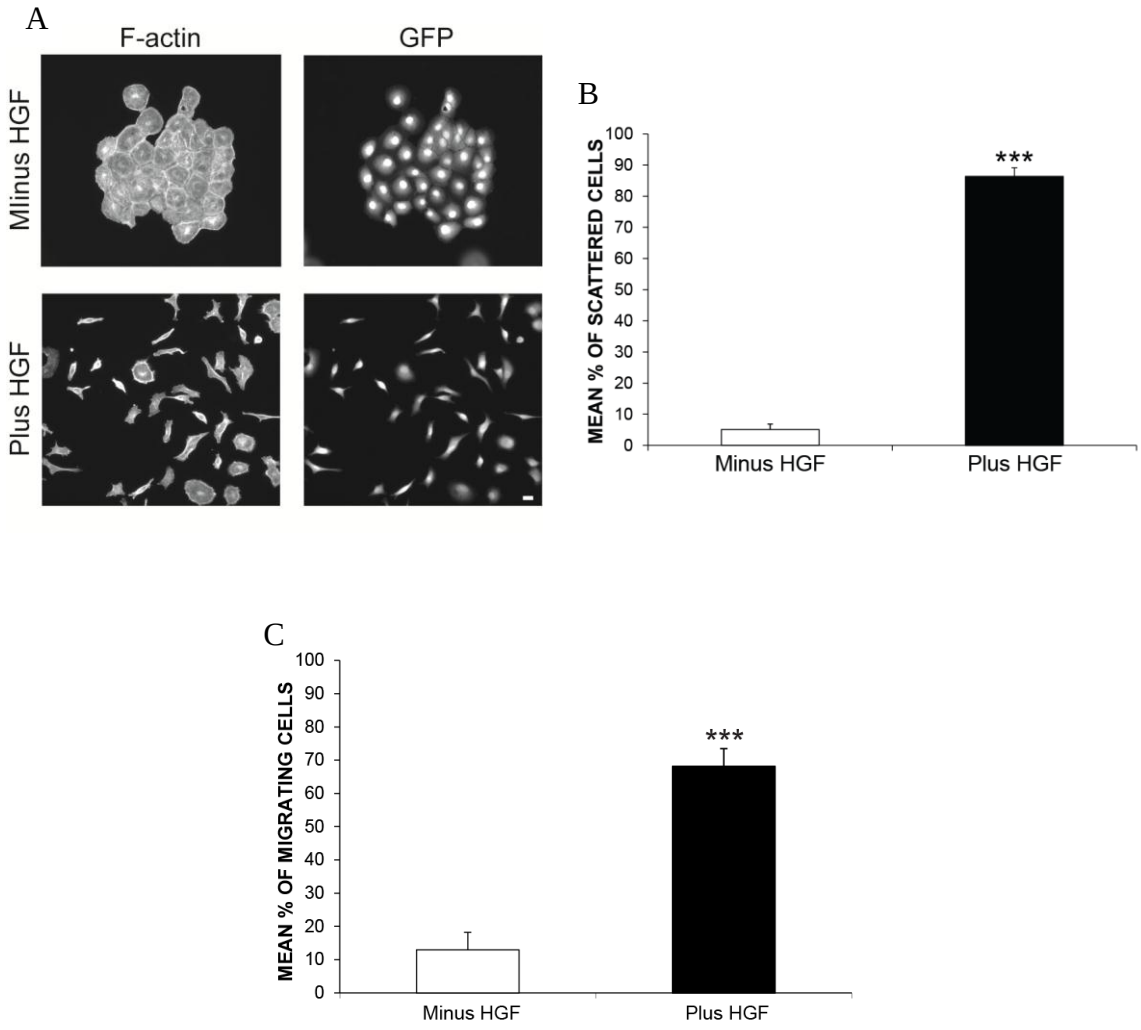

Figure 3.9 HGF increases the percentage of migrating DU145 cells. A) The HGF-induced scatter assay was conducted using DU145 cells stably expressing an EGFP lentiviral vector. Cells seeded onto glass coverslips were serum-starved for 24 hours and then left untreated (minus HGF) or stimulated with HGF (plus HGF) (10 ng/ml). After 24 hours cells were fixed and stained for F-actin. **B)** Cells from (A) were counted and cell counts of serum-starved cells versus plus HGF-stimulated cells were compared. Scattered = loss of cell-cell junctions and single cells with an elongated migratory phenotype as indicated in (A) (plus HGF). **C)** EGFP lentiviral vector expressing DU145 cells were seeded into a 98% collagen I and a 2% matrigel 3D matrix and treated in preparation for live-cell imaging (see **section 2.2.11**). Serum-starved cells in the absence of HGF were also filmed. A migrating cell was measured by the translocation of one cell body and 90 cells for each condition were analysed. In (B) and (C) the mean % of scattered cells and the mean % of migrating cells, respectively, were compared between minus and plus HGF. The standard error of the mean was also calculated over 3 independent experiments. Statistical significance compared with minus HGF cells was calculated using Student's *t*-test; ***, $P < 0.0005$. Bar = 10 µm.

The percentage of migrating cells in the absence and presence of HGF was calculated. A migrating cell in the 3D matrix was measured by the translocation of one cell body. When compared to minus HGF control cells (**figure 3.9C** and see **movies 3PC** and **3G** for representative movies and **Appendix 3**), a significantly higher percentage of cells stimulated with HGF were migrating (**figure 3.9C** and see **movies 4PC** and **4G** for representative movies and **Appendix 3**).

3.3 Discussion

In this chapter, the use of cell scatter assays has been further developed. The optimal culture time for the HGF-induced DU145 scatter assay has been determined and the assay has been extended to investigate different growth factors and a range of matrix compositions (Fram et al., 2011). It has been demonstrated that both HGF and EGF induce DU145 cell scattering. Moreover, HGF is able to induce cell scattering in the colon adenocarcinoma cell line, HT29, on different matrix compositions. Furthermore, all the substrata tested supported the HGF-induced cell scatter assay. The optimised 2D model system has also been expanded to develop a DU145 HGF-induced cell scattering assay in 3D.

Studies described here have shown that serum-starved DU145 cells became more scattered over time and displayed a reduction in their ability to form multi-cellular colonies; thus a maximum culture time was established. It is possible that prolonged culturing of these cells induces the release of endogenous growth factors. This in turn may contribute to an increase in the activity of the cells, and hence reduce their ability to form cell colonies. In support of this, it has been published that DU145 cells exhibit self-sufficiency in growth factors such as EGF which contributes to the activation of DU145 cells *in vitro* (Tillotson and Rose, 1991). In addition, DU145 cells are known to possess the ability to secrete quantifiable levels of nerve growth factor (NGF) (Geldof et al., 1997), which is a key autocrine signal for cancer growth and metastasis (Dollé et al., 2003).

There is evidence that the scattering potency of HGF in cells is regulated by the extracellular and basement matrices that encompass the cells (Herrera, 1998). A pre-requisite of the ability of colony-forming cells to induce the morphological modifications reminiscent of EMT is their capacity to spread on the underlying ECM (Ridley et al., 1995). Cell spreading is known to be modulated by Rho GTPases (Ridley et al., 1995) and integrin-mediated signalling (Herrera, 1998). Rho GTPases are required for the re-organisation of the actin cytoskeleton during cell movement (Ridley et al., 1995) and integrins play an important role in mediating the attachment of cells to the ECM (Huttenlocher and Horwitz, 2011).

HGF-induced DU145 cell scattering was maximal on a collagen I substratum. DU145 cells are known to express a number of matrix interacting integrin proteins including α3, α5 and α6 integrin and the subunits β1, β3 and β4, where β1 is the most prevelant (Witkowski et al., 1993). Moreover, aberrant expression of integrins has been reported in prostate cancer (Bonkhoff et al., 1993; Schmelz et al., 2002). The differences observed in DU145 HGF-induced cell scattering may be as a result of varying integrin expression. Rabinovitz et al. demonstrated that higher expression levels of the α6 integrin in DU145 cells elevated the cell migration velocity of these cells on a laminin substratum (Rabinovitz et al., 1995). Furthermore, HGF-induced MDCK cell scattering increases on collagen I; it was speculated that the integrin α2β1 may facilitate this effect (de Rooij et al., 2005; Sander et al., 1998).

The HGF-induced DU145 cell migration speed was highest on collagen I substratum when compared to the DU145 cell velocity on serum substratum. A number of factors are involved in determining cell migration velocity including ligand and receptor levels and their affinity to bind to one another, as well as cytoskeletal interactions (Huttenlocher et al., 1996; Palecek et al., 1997). The turnover of integrin-mediated adhesions between the cell and ECM is necessary for cell migration to occur (Huttenlocher and Horwitz, 2011). It has been proposed that optimal cell migration velocity is achieved when integrins and ECM proteins are intermediately expressed, resulting in an intermediate level of adhesivity between the cell and ECM (DiMilla et al., 1993; Palecek et al., 1997). DU145 cells are known to express the fibronectin integrin α5β1 (Witkowski et al., 1993), as well as intermediate levels of the collagen I integrin, α2β1 (Patrawala et al., 2007). Therefore, the presence of an intermediate level of collagen I and this integrin may account for the maximal migration speed of DU145 cells on this substratum.

It has been proposed that the efficiency of cell scattering may be linked with cell adhesivity rather than the cell migration speed (de Rooij et al., 2005). MDCK cells exhibited the highest migration speed but the lowest cell scattering count on laminin 1 substratum when compared to collagen I and fibronectin (de Rooij et al., 2005). However, this does not correlate with the work presented here, where high migration speed and increased cell scattering efficiency were both associated with the same matrix composition.

In order to develop the range of the 2D scatter assay, the scattering potential of the growth factor EGF was tested, as EGF is known to increase the invasiveness of DU145 cells (Turner et al., 1996). All the substrata tested, except for 2D matrigel, supported the EGF-induced scatter assay to a significant level in DU145 cells. Indeed, following completion of these studies, it was reported that the addition of EGF stimulates cell-cell junction disassembly and leads to a reduction in E-cadherin localisation at junctional sites (Gan et al., 2010). On 2D matrigel substratum, a higher percentage of single DU145 cells were observed under serum-starved conditions when compared to the other substrata that were assessed. The matrigel used in the scatter assay was composed of a complex mixture of proteins and growth factors. Thus DU145 cells may have been activated by these growth signals and hence exhibited a reduced ability to form colonies on a 2D matrigel surface. This hypothesis could be tested by using a growth factor reduced form of matrigel. Nevertheless, the inability of EGF to induce cell scattering on 2D matrigel when compared to HGF may suggest that EGF is a less effective cell scattering inducer than HGF.

To support this theory, it has been demonstrated that HGF repeatedly elicited a stronger migratory response than EGF in primary rat hepatocytes (Stolz and Michalopoulos, 1994). In addition, EGF-treated cells were morphologically less spread than those stimulated with HGF (Stolz and Michalopoulos, 1994). Moreover, HGF was found to stimulate the phosphorylation of two specific cytoskeletal-related proteins, whilst EGF showed a diminished ability to do so (Stolz and Michalopoulos, 1994). Thus it was speculated that in the hepatocyte cytoskeleton HGF and EGF activate different cell signalling pathways, and hence exhibit variation in motogenic capabilities (Stolz and Michalopoulos, 1994). This may account for the reduction in cell scattering observed here between HGF and EGF-treated DU145 cells.

As HT29 cells grow as tight colonies with extensive cell-cell junctions and c-Met expression levels are elevated in these cells when compared to DU145 cells, a higher concentration of HGF was required to obtain efficient scattering. Consistent with DU145 cells, all substrata supported the HGF-induced scatter assay; however HT29 cells did not scatter as effectively when compared to DU145 cells, possibly due to the tightness of these cells in the absence of HGF stimulation. HT29 cells were reported to scatter downstream of HGF stimulation on serum and collagen I coated substratum

(Herrera, 1998). However HT29 cells were unable to scatter on a laminin surface and this was linked to a defect in cell spreading (Herrera, 1998). The addition of phorbol 12-myristate 13-acetate (PMA) was able to reinstate HT29 cell spreading on this substratum, and this process was integrin dependent (Herrera, 1998).

In addition, HT29 cells exhibited the highest scattering potential on collagen I substratum, possibly due to an increase in integrin expression on HT29 cell surfaces that bind to collagen I. Indeed it has been shown that the highly metastatic form of HT29 cells, HT29LMM cells express the collagen receptor integrin α2β1 (Rosenow et al., 2008). In contrast, expression of the fibronectin binding integrin α5β1 was reduced in this cell line (Rosenow et al., 2008).

It was demonstrated in this chapter that DU145 cells embedded in a predominantly collagen type I 3D matrix form multi-cellular colonies with distinct cell boundaries and discernible nuclei within the cell colony. Following completion of these studies, it was reported that DU145 cells exhibit similar morphologies in a type I collagen 3D matrix to those observed in chapter 3 (Sugiyama et al., 2010). The morphology of colony-forming MDCK cells has been analysed in 3D gels for many years (McAteer et al., 1987); moreover, in a recent study, the morphology of MDCK cells embedded in a type I collagen 3D matrix (Raghavan et al., 2010) was alike to that observed here for DU145 cells.

However, in contrast, it has also been shown that DU145 cells grown in a 100% collagen I 3D matrix form multi-cellular structures with a fibroblast-like morphology (Härmä et al., 2010). This contrast in morphology reported in Härmä et al.'s study to the work presented here for DU145 cells embedded in a 3D collagen I matrix could be accounted for by a number of factors; the manner in which the type I collagen matrix is prepared, the concentration used and the conditions implemented for the 3D collagen I matrix to polymerise (Artym and Matsumoto, 2010). These factors will dictate how cells interact with the 3D matrix and the cell morphology they exhibit (Artym and Matsumoto, 2010). In addition, the time period that the cells are left in the 3D matrix may also influence their cell morphology. For example, it has been shown that prostate cancer PC3 cells in a 3D matrigel matrix form multi-cellular colonies following 9 days

incubation in a 3D matrix; however at day 13, these cells developed distinct and multiple projections (Härmä et al., 2010).

In this chapter, increasing the concentration of HGF to 500 ng/ml and incubating the cells with HGF for up to 72 hours was required to achieve a detectable DU145 cell response. However, although cell locomotion could be observed, the magnitude of scattering was small. The muted responses in 3D could be due to some of the HGF binding to the 3D matrix, as was observed for HGF-stimulated MDCK cells; this would delay growth factor transportation through the matrix and subsequently the onset of HGF stimulation (Raghavan et al., 2010). Indeed, it has been demonstrated that MDCK cell colonies positioned at the bottom of a collagen I gel failed to respond to HGF stimulation, even after 72 hours, whilst projections were observed from cell colonies embedded in the upper planes of the 3D matrix (Raghavan et al., 2010). Alternatively, although serum-starved, DU145 cells embedded in the matrix in chapter 3 were exposed to small levels of growth factor from the matrigel. The use of growth factor reduced matrigel may have better synchronised the response of these cells to HGF stimulation.

Due to time constraints, the 3D scatter assay could not be fully optimised. In the Zaman et al. study, 3D DU145 cell motility assays were conducted where the authors methodically changed matrigel and fibronectin concentrations, as well as β1 integrin expression levels (Zaman et al., 2006). From these assays it was proposed that the equilibrium of adhesion and contractile forces determines DU145 cell migration velocity at a certain matrigel density (Zaman et al., 2006). Thus in this chapter, although initial investigations have shown that DU145 cells can migrate in a 3D matrix downstream of HGF, it may be useful to, for example, examine integrin expression levels in relation to the matrix used in order to develop this assay further.

In summary, EGF- and HGF-induced cell scattering models have been developed in 2D and an attempt has been made to establish a 3D DU145 cell scattering model downstream of HGF stimulation.

3.3.1 Future work

In the future, it would be useful to optimise the 3D migration assay. In order to achieve an accurate representation of DU145 cell morphology and their response to HGF treatment in a 3D matrix, control cell lines, both metastatic and non-metastatic cells, would need to be analysed. In conjunction with this, the effect of changes in matrix rigidity on DU145 cell morphology in the absence and presence of HGF could be examined. This could be conducted by, for example, changing the pH and temperature at which collagen I polymerises; this will influence the thickness of the collagen fibers formed and in turn the rigidity of the matrix.

In this chapter, the HGF-induced scatter response was reduced in the HT29 cells when compared to DU145 cells. Furthermore, the expression of the HGF receptor c-Met was increased in HT29 cells when compared to the level of expression in DU145 cells. Thus it could be speculated that whilst HT29 cells express a higher level of c-Met, a large proportion of the receptor may be internalised rather than located on the cell surface; this could thereby account for the reduced response to HGF treatment in the HT29 cells. Therefore, it would be useful to examine and compare the surface levels of c-Met in both these cell lines. Techniques such as biotinylation and antibody labelling could be used to deduce this.

Chapter 4
PAK6 is required for HGF-induced cell-cell dissociation

Chapter 4 – PAK6 is required for HGF-induced cell-cell dissociation

4.1 Introduction

In chapter 3, in both 2D and 3D assays, HGF was chosen as the migration inducing stimulation. HGF is known to activate a variety of intracellular signalling cascades via activation of the c-Met receptor; many of which are related to actin cytoskeletal re-organisation (Ridley et al., 1995). PAKs are known to regulate the actin cytoskeleton and it has been reported that some PAK family members are required for HGF-induced migration (Ahmed et al., 2008; Bright et al., 2009; Royal et al., 2000; Royal and Park, 1995). Indeed, PAK1 knockdown but not PAK2 knockdown reduced HGF-induced cell scattering in DU145 cells (Bright et al., 2009). However the effect of PAK1 and PAK2 over-expression on DU145 cell morphology and cell junction integrity was not assessed.

PAK4 is also known to be activated upon HGF stimulation in MDCK cells (Wells et al., 2002) and mediates HGF-induced prostate cancer cell migration (Ahmed et al., 2008). Furthermore, PAK4 knockdown blocks HGF-induced DU145 cell scattering (Wells et al., 2010). PAK4 knockdown cells were able to dissociate their junctions; however cell migration was inhibited due to an increase in the incidence and size of focal adhesions (Wells et al., 2010). In addition, the effect of PAK4 over-expression on cell morphology in MDCK cells in unstimulated and HGF-stimulated conditions was examined; a kinase active PAK4 mutant induced cell shape changes only in the presence of HGF (Wells et al., 2002).

PAK6 is known to be expressed in DU145 cells (Wells et al., 2010; Yang et al., 2001). Furthermore, increased PAK6 expression has been detected in prostate cancer cells (Kaur et al., 2008). PAK6 was first detected in a screen to identify proteins that interact with the AR (Yang et al., 2001). In addition, it has been reported that siRNA knockdown of PAK6 inhibits prostate cancer growth (Wen et al., 2009). However, the role of PAK6 in cancer cell migration and more specifically HGF-induced migration has yet to be elucidated.

In this chapter, the aim was to deduce whether PAK6 plays a role in cell migration downstream of growth factor stimulation. Wild-type and mutant PAK6 expression

vectors were constructed as tools to assay the morphological effects of PAK6 over-expression in cells, whilst siRNA was used to examine the effects of PAK6 knockdown on cancer cell migration.

4.2 Results

4.2.1 PAK6 is endogenously expressed in DU145 and HT29 cells

Previous work had utilised an antibody that recognises both PAK4 and PAK6 to detect PAK6 in DU145 cells (Wells et al., 2010). Initial experiments aimed to identify a PAK6 specific antibody able to efficiently detect endogenous PAK6. A panel of five commercial antibodies were screened and tested (data not shown). Of the antibodies tested, the anti-PAK4 antibody (Cell Signaling Technology) hereafter referred to as anti-PAK4/PAK6, recognised two distinct bands correlating to PAK4 and PAK6. The upper band detected with the anti-PAK4/PAK6 antibody was validated as PAK6 using Myc-tagged PAK6 over-expressed protein (**figure 4.1A**). The anti-PAK6 specific antibody (Calbiochem) detected one band at the correct size for PAK6 and hence did not cross react with PAK4. Both antibodies were selected for future studies.

Both antibodies were utilised to investigate the levels of endogenous PAK6 protein expression in DU145 and HT29 cells. In these cell types, PAK6 was found to be present at 75 kDa using the anti-PAK4/PAK6 antibody (**figure 4.1B**). The anti-PAK6 specific antibody was able to detect endogenous PAK6 expression in HT29 and DU145 cells (**figure 4.1C**).

4.2.2 HGF but not EGF stimulation increases PAK6 autophosphorylation levels

PAKs have been implicated as important effector proteins downstream of growth factor induced signalling, where they are involved in various cellular processes such as cancer cell migration (Bright et al., 2009; Wells et al., 2010). DU145 and HT29 migration assays described previously (see **sections 3.2.2, 3.2.5** and **3.2.6**) rely on HGF or EGF stimulation. The effect of HGF and EGF stimulation on PAK6 autophosphorylation levels was therefore examined using a phospho-specific antibody from Cell Signaling Technology. This antibody detects phosphorylation of PAK6 at serine 560 in the kinase domain. This residue in PAK6 is thought to be an autophosphorylation site homologous to threonine 423 (T423) in PAK1 (Schrantz et al., 2004) and serine 474 (S474) in PAK4 (Abo et al., 1998). Using this phospho-specific antibody, endogenous PAK6 autophosphorylation levels increased upon HGF stimulation in DU145 cells (**figure 4.2A**). This antibody also detects phosphorylation of PAK4 at S474 and PAK5 at serine 602. The levels of PAK4 autophosphorylation were also elevated (**figure 4.2A**), which

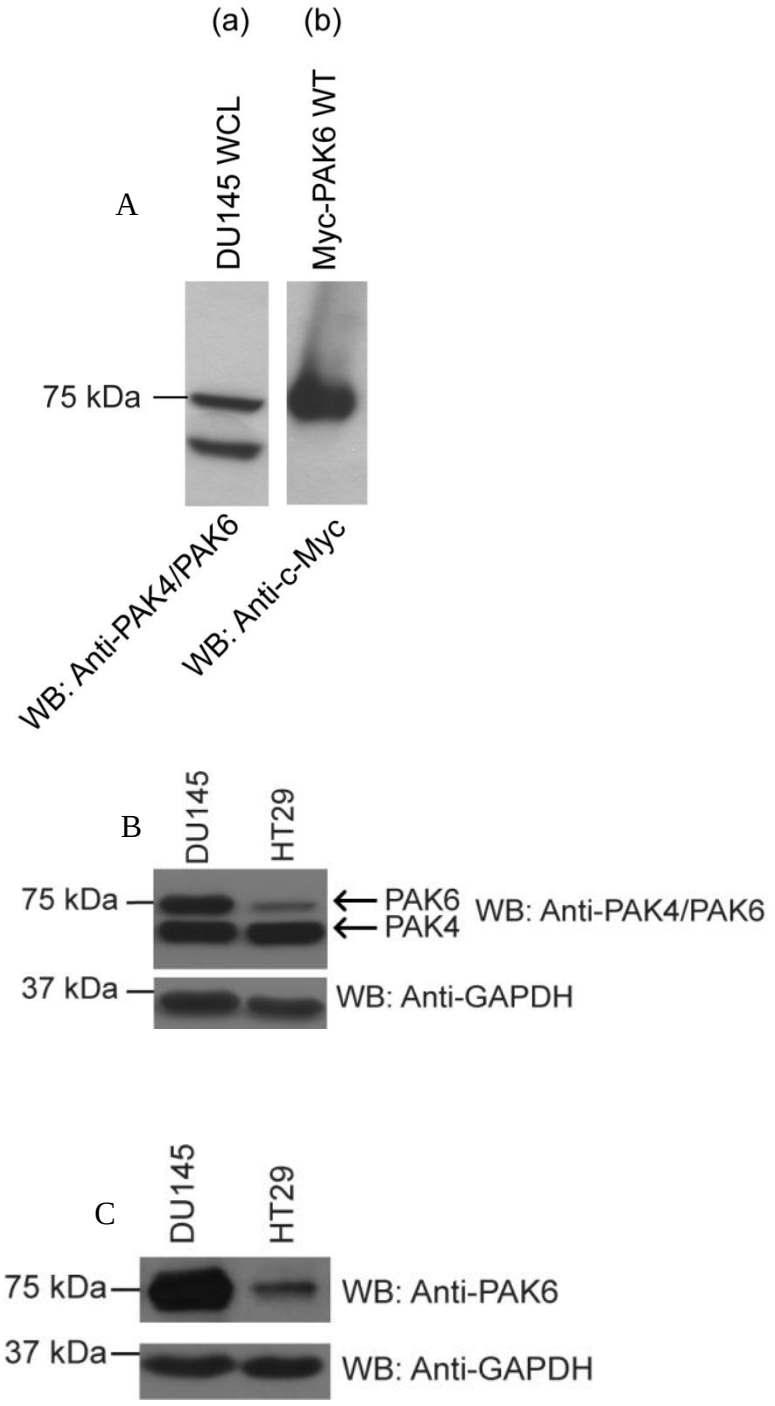

Figure 4.1 Testing of PAK6 antibodies for detecting endogenous PAK6. A) (a) DU145 whole cell lysate (WCL) was immunoblotted for PAK4/PAK6 expression using an anti-PAK4 antibody that recognises PAK6 (anti-PAK4/PAK6 antibody). (b) HEK293 cells expressing WT Myc-PAK6 were lysed and the lysate immunoblotted for PAK6 expression using an anti-c-Myc antibody. **B)** Whole cell lysates for the indicated cell lines were immunoblotted using the anti-PAK4/PAK6 antibody. **C)** Whole cell lysates for the indicated cell lines were immunoblotted using an anti-PAK6 specific antibody. In (B) and (C) lysates were immunoblotted for GAPDH as a loading control. The blots shown are representative of 3 independent experiments.

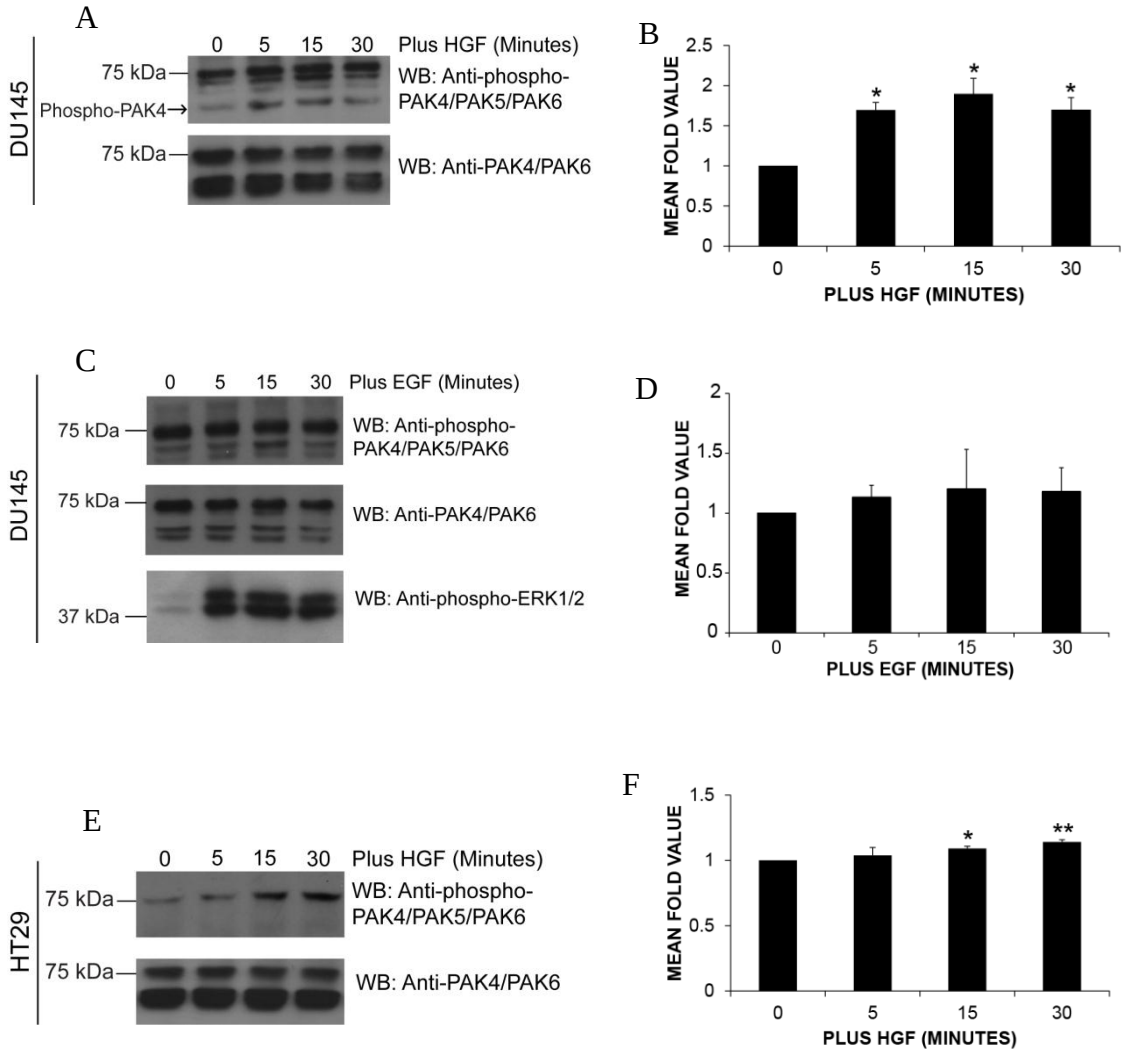

Figure 4.2 HGF stimulation increases PAK6 autophosphorylation levels in DU145 and HT29 cancer cell lines but EGF stimulation has no effect in DU145 cells. A) DU145 cells were seeded at a density that correlated with the HGF-induced scatter assay. Cells were serum-starved 48 hours after plating for 24 hours. Cells were then left unstimulated (0 minutes) or stimulated with HGF (10 ng/ml) for 5, 15 and 30 minutes prior to lysis. Lysates were immunoblotted for levels of PAK6 autophosphorylation at serine 560 using a phospho-PAK4/PAK5/PAK6 antibody. Blots were re-probed for total PAK6 expression using an anti-PAK4/PAK6 antibody. **B)** Changes in PAK6 autophosphorylation levels at serine 560 were quantified from (A). **C)** DU145 cells were treated as in (A) but stimulated with EGF (100 ng/ml). Lysates were also immunoblotted for phospho-ERK1/2 levels. **D)** Changes in PAK6 autophosphorylation levels at serine 560 were quantified from (C). **E)** HT29 cells were seeded and treated as described in (A) but stimulated with 60 ng/ml HGF. **F)** Changes in PAK6 autophosphorylation levels at serine 560 were quantified from (E). In (B), (D) and (F), the mean fold value representing the autophosphorylation of PAK6 in response to HGF or EGF stimulation and the standard error of the mean were calculated over 3 independent experiments. Statistical significance compared with minus HGF (0 minutes) cells was calculated using Student's *t*-test: *, $P < 0.05$, **, $P < 0.005$.

is consistent with previous reports (Wells et al., 2010). The increase in PAK6 phospho levels was significant following 5, 15 and 30 minutes HGF stimulation when compared to serum-starved cells (0 minutes) (**figure 4.2B)**. Interestingly, a relatively high level of PAK6 autophosphorylation was observed under serum-starved conditions (0 minutes) when compared to PAK4 autophosphorylation levels (**figure 4.2A**).

In **figure 4.2A**, the dublet at 75 kDa was quantified as the total signal for phospho-PAK6 due to the reduced sensitivity of the densitometry quantification method that was used. Thus there are some drawbacks with measuring and comparing the varying levels of protein from autoradiographs as was conducted for analysing the western blot data obtained in **figure 4.2**. Firstly, with densitometry analysis, there is a limited dynamic range, where protein bands with higher signals can become saturated. This therefore leads to inaccuracies in the quantification of the level of protein between different samples on the same autoradiograph. In order to more accurately quantify the level of protein on the same western blot, digital imaging can be used. For example, a charge-coupled device (CCD) camera can be implemented. This alternative method of imaging allows for a wider linear dynamic range where higher signals are not saturated. Thus, a more accurate quantification of the level of protein expression on the same western blot can be achieved.

In contrast to HGF, EGF stimulation did not increase endogenous phospho-PAK6 levels (**figures 4.2C** and **4.2D**). As a control, the blot was also probed for phospho-ERK1/2, which is known to be activated downstream of EGF, to confirm that EGF signalling pathways were activated. Due to the lack of PAK6 autophosphorylation in response to EGF, as well as the decreased scattering potential of EGF in DU145 cells as described in chapter 1 (see **section 3.2.5**), this growth factor was excluded from future PAK6 investigations in cell migration. The remainder of the project focussed on PAK6 function downstream of HGF signalling.

To validate the response of PAK6 to HGF observed in DU145 cells, colony-forming HT29 cells were also tested. Endogenous PAK6 phospho levels were significantly elevated when compared to serum-starved cells (0 minutes) following 15 and 30 minutes HGF stimulation (**figures 4.2E** and **4.2F**). This was consistent with the time points of increased phospho-PAK6 levels observed upon HGF addition in the DU145

cells (**figures 4.2A** and **4.2B**). Whilst it is clear that HGF increases the phosphorylation status of PAK6 at serine 560, the identification of PAK6 substrates is lacking in the literature; only one study has shown that PAK6 is able to phosphorylate the AR (Schrantz et al., 2004).

4.2.3 Sub-cloning of PAK6 into GFP, mRFP1 and GST expression vectors

PAK6 is expressed in both DU145 and HT29 cells. Furthermore, PAK6 autophosphorylation is elevated downstream of HGF in these cell lines. It might therefore be speculated that PAK6 plays a role in the cellular response to HGF observed in chapter 3. Therefore, to facilitate PAK6 functional studies, fluorophore-tagged PAK6 expression constructs were generated.

The Gateway™ Technology system (see **section 2.2.1**) was utilised to generate GFP, mRFP1 and GST PAK6 expression constructs. In order to insert PAK6 DNA into the Gateway™ Technology system, WT Myc-PAK6 was used as the DNA template for PCR. The PCR was performed using primers possessing a 25 base pair (bp) *att*B1 sequence at the 5' end and an *att*B2 sequence at the 3' end of the sequence. The cloning of PAK6 and the Gateway™ Technology system used is outlined in **figure 4.3A**. PAK6 was successfully amplified by PCR and was visible as a 2046 bp product (**figure 4.3B**). In order to insert the amplified PAK6 PCR product into the pDONOR™ 207 entry clone, a BP recombination reaction was performed (see **section 2.2.1**). Restriction digest reactions were then carried out using the EcoRV restriction endonuclease to verify the presence of PAK6 in the entry clone (**figure 4.3C**). In addition, the PAK6 containing entry clone was sequenced to confirm that no mutations had arisen in the DNA sequence during the cloning process. PAK6 was then shuttled into GFP and mRFP1 expression vectors using an LR recombination reaction as outlined in **figure 4.3A** and then sequenced (see **section 2.2.1)**. In addition, the Gateway™ Technology cloning system was also used to generate C-terminal GFP and N- and C-terminal mRFP1 PAK6 truncated mutant constructs in order to assess the functions of the different domains of PAK6 (see **Appendix 1** for primer sequences).

Wild-type GST tagged PAK6 (GST-PAK6) was also generated using the Gateway™ methodology to investigate PAK6 protein-protein interactions in GST pulldown assays. GST-PAK6 and GST alone were protein purified following the shuttling of

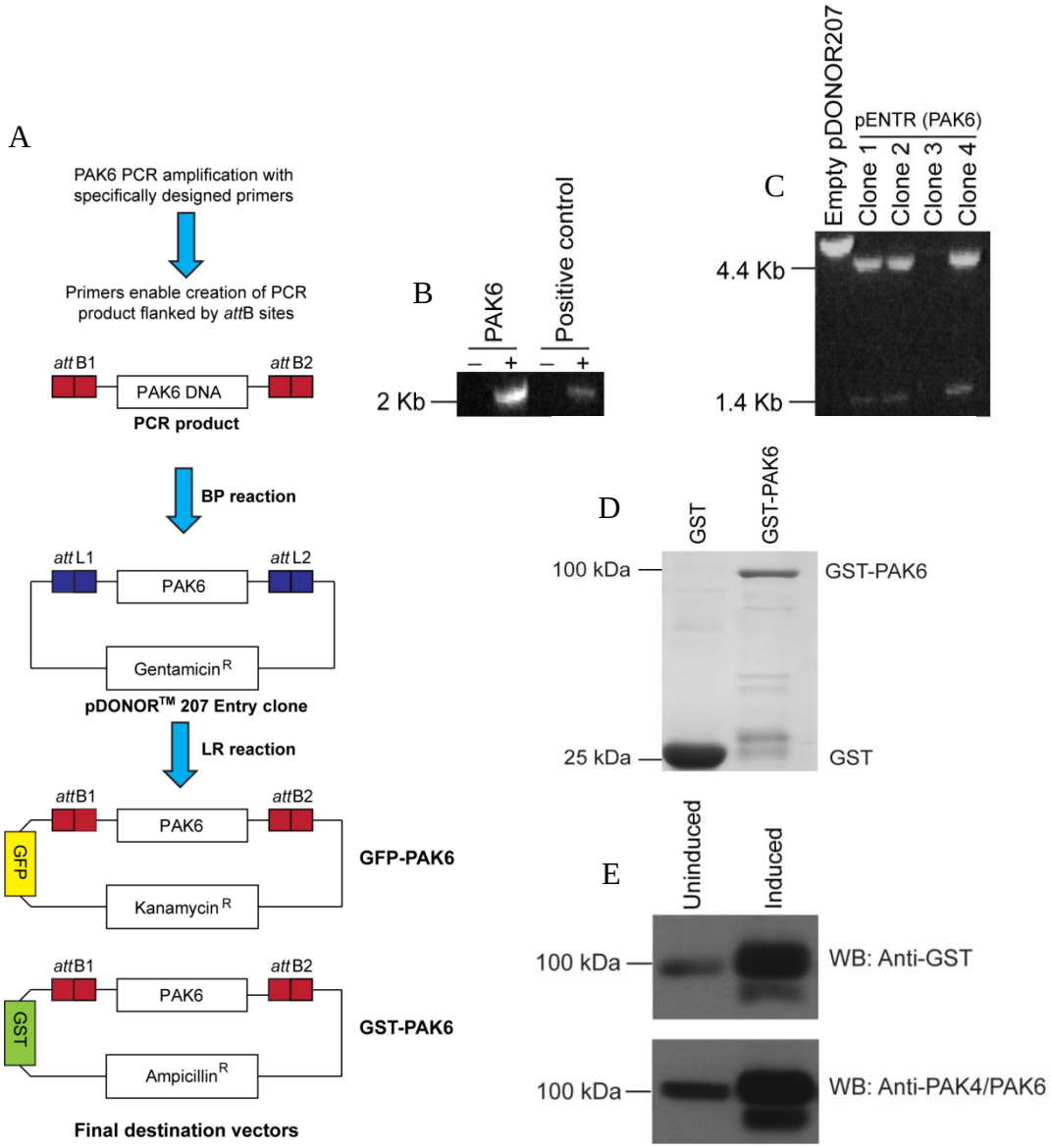

Figure 4.3 Generation of PAK6 constructs using the Gateway™ Technology system. A) Schematic representation of the Gateway™ Technology system used to construct GFP and GST vectors expressing PAK6. BP and LR recombination reactions were used to shuttle the desired DNA into the expression vectors. *att* = attachment site, ^{R} = resistance. Figure adapted from (Gateway™ Technology instruction manual, 2002). **B)** *att*B flanked gene specific primers were used to amplify human PAK6 DNA in a PCR reaction alongside positive (+) and negative controls (-) and subjected to gel electrophoresis. **C)** Restriction digest reactions were performed using the EcoRV restriction enzyme and subjected to gel electrophoresis to confirm the presence of PAK6 following the BP reaction. This enzyme cuts the vector once to linearise it, and if PAK6 is present, cuts PAK6 once resulting in the production of 2 fragments (4.4 kb and 1.4 kb). **D)** E. *coli* BL21-A1 cells transformed with the GST and GST-PAK6 expression plasmids were grown to mid-log phase and protein expression was induced with 0.2% and 0.05% L-Arabinose, respectively, overnight at 20ºC. The gel was stained with coomassie blue to visualise the protein bands present. **E)** Induced GST-PAK6 from (D) was electrophoresed against an uninduced bacterial lysate. Blots were immunoblotted for detection of GST-PAK6 using a GST specific antibody and an anti-PAK4/PAK6 antibody as indicated.

PAK6 into a GST expression vector using an LR recombination reaction (see **section 2.2.1**). Protein expression was induced for both GST-PAK6 and GST (**figure 4.3D**). Induced GST-PAK6 was also visualised by immunoblotting, with an uninduced bacterial lysate as a control (**figure 4.3E**).

4.2.4 Validation of wild-type, kinase active and kinase dead PAK6 kinase activity

Kinase mutants are useful tools in characterising proteins that possess kinase activity. Thus GFP-PAK6 kinase active and kinase dead mutants were generated using Site-Directed mutagenesis (see **section 2.2.1**) and were shuttled into suitable expression vectors using Gateway^{TM} Technology (see **section 2.2.1**).

Three mutant PAK6 constructs were generated; S560E (serine to glutamic acid mutation) and S531N (serine to asparagine mutation) as potentially active forms of PAK6, and K436A (lysine to alanine mutation), a proposed kinase dead form of PAK6 (Schrantz et al., 2004). As serine 560 is a predicted autophosphorylation site for PAK6 (based on homology to PAK1), mutating this residue may induce an increase in PAK6 kinase activity (Schrantz et al., 2004). The S531N mutation is thought to stabilise the catalytic loop region in the kinase domain of PAK6 (Schrantz et al., 2004) and is analogous to the PAK4 activation site (S445N) (Qu et al., 2001; Schrantz et al., 2004). The K436A residue change is located within the activation loop of the kinase domain and is thought to obstruct ATP binding and thereby inhibit PAK6 kinase activity (Schrantz et al., 2004). Whilst it has yet to be established, it has been predicted that PAK6, alike to its group members, is constitutively active (Kaur et al., 2005; Schrantz et al., 2004).

A radioactive *in vitro* kinase assay confirmed that the kinase dead mutant possessed no exogenous or autophosphorylation kinase activity (**figure 4.4**), as has already been documented (Schrantz et al., 2004). The S560E PAK6 mutant construct did not exhibit an increase in kinase activity when compared to WT PAK6 (**figure 4.4**) even though this is accepted as the autophosphorylation site. In fact the activity of the S560E PAK6 mutant was actually lower than WT PAK6. This is consistent with another study (Kaur et al., 2005). Interestingly however, autophosphorylation was detected for the S560E mutant which suggests that PAK6 possesses other autophosphorylation sites (**figure 4.4**). In contrast, the S531N PAK6 mutant displayed an increase in its ability

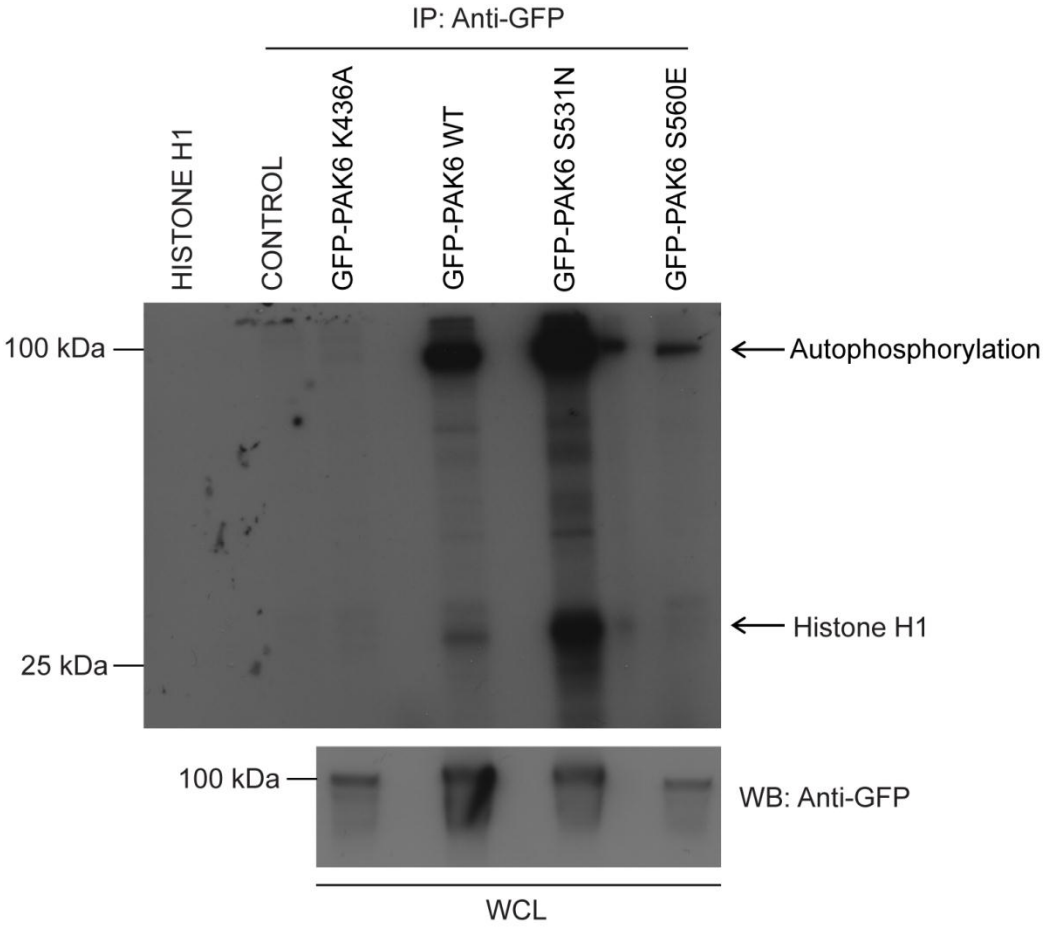

Figure 4.4 Kinase activity of PAK6 mutants. HEK293 cells were transfected with the indicated full-length GFP-PAK6 mutants. The cells were lysed and PAK6 was immunoprecipitated using an anti-GFP antibody (IP) from cell lysates. The kinase activity of the PAK6 mutants was determined with an *in vitro* kinase assay in the presence of [γ-^{32}P] ATP and using histone H1 as a substrate. Whole cell lysates (WCL) were immunoblotted using an anti-GFP antibody as a loading control. The blots shown are representative of 3 independent experiments.

to phosphorylate histone H1 when compared to WT PAK6 (**figure 4.4**). This mutant also exhibited an increased level of autophosphorylation when compared to WT PAK6, as consistent with previous reports (Schrantz et al., 2004). Therefore, the S531N mutant was used as the kinase active form of PAK6 and the K436A mutant was used as the kinase dead for future investigations.

4.2.5 PAK6 interacts with constitutively active Cdc42

Cdc42 is known to be activated by HGF (Royal et al., 2000) and the active form of Cdc42 is known to bind to PAK6 (Lee et al., 2002). Thus the PAK6 derivatives generated were tested for their ability to bind to Cdc42-V12 using an IP protocol. All of the PAK6 derivatives were able to bind Cdc42-V12 irrespective of the levels of kinase activity (**figure 4.5**).

4.2.6 DU145 cell morphology is affected by PAK6 over-expression

Having generated and characterised PAK6 expression constructs, PAK6 was over-expressed in DU145 cells to monitor the effect on cell morphology. The levels of the over-expressed PAK6 mutants were approximately 50% higher than the level of endogenous PAK6. WT PAK6 expressing DU145 cells were found to be significantly more elongated in phenotype when compared to GFP control cells under serum-starved conditions (**figures 4.6A** and **4.6C**). Importantly, GFP control transfected cells were not significantly different in shape when compared to untransfected cells (**figures 4.6A** and **4.6B**). Cells expressing the kinase active form of PAK6, S531N, were also significantly more elongated than GFP control cells, although not to the same degree as WT PAK6 expressing cells (**figures 4.6A** and **4.6C**). However, DU145 cells expressing the kinase dead mutant of PAK6, K436A, were not significantly elongated when compared to GFP control cells (**figures 4.6A** and **4.6C**). Interestingly, cells expressing WT PAK6 exhibited a further significant increase in cell elongation after HGF stimulation, when compared to WT PAK6 expressing cells in the absence of HGF (**figure 4.6A**). Interestingly, an increased level of active Cdc42 was co-immunoprecipitated with the K436A PAK6 mutant when compared to WT and S531N PAK6 (**figure 4.5**). Given that K436A PAK6 expressing DU145 cells did not exhibit an increase in cell elongation when compared to GFP control cells, unlike WT and S531N PAK6 (**figures 4.6A** and **4.6C**), it could be speculated that the K436A mutant may induce the inactivation of Cdc42.

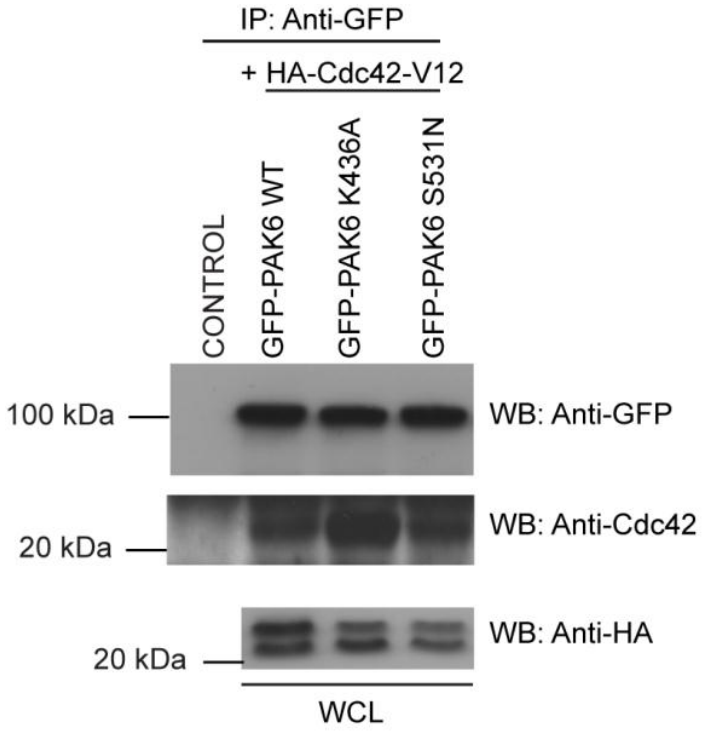

Figure 4.5 Over-expressed PAK6 interacts with Cdc42-V12. HEK293 cells were co-transfected with the indicated GFP-PAK6 mutants and HA-Cdc42-V12. The cells were lysed and over-expressed PAK6 was immunoprecipitated using an anti-GFP antibody (IP). IPs were immunoblotted using anti-GFP and anti-Cdc42 antibodies as indicated. Whole cell lysates (WCL) were immunoblotted using an anti-HA antibody as a loading control. The blots shown are representative of 3 independent experiments.

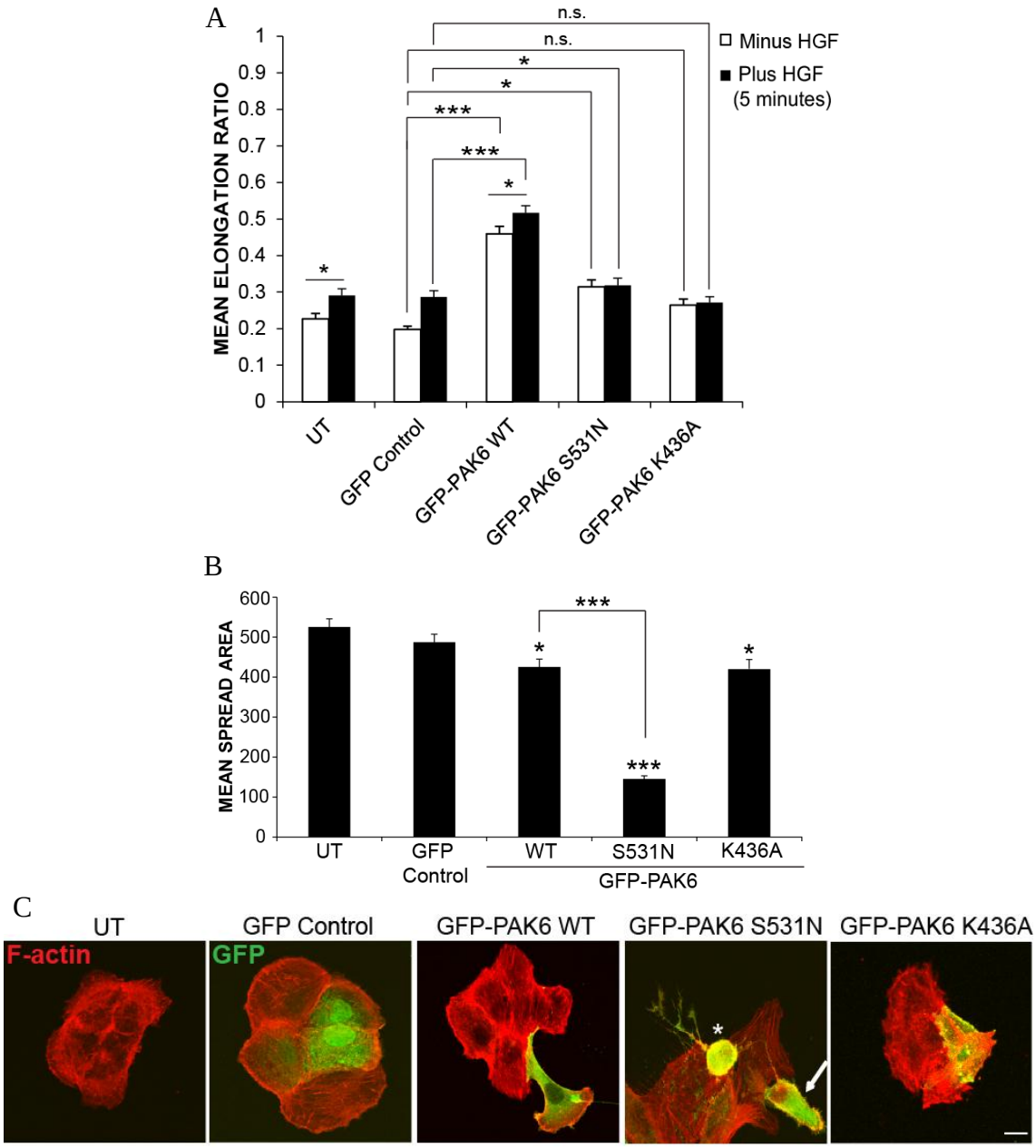

Figure 4.6 PAK6 over-expression induces morphological changes in DU145 cells. A) and **B)** DU145 cells were transfected with GFP control vector or GFP-PAK6 mutants as indicated. Untransfected cells (UT) were treated in the same manner. After 24 hours, cells were serum-starved for 24 hours. Cells were then either left unstimulated (minus HGF) or stimulated with HGF (plus HGF) for 5 minutes. Cells were then fixed and stained for F-actin. Shape analysis was performed on the cells using Image J to determine the elongation ratio and cell spread area as indicated. **C)** F-actin stained DU145 cells transfected as indicated were imaged using confocal microscopy. * = S531N PAK6 expressing cell with rounded phenotype. Arrow = S531N PAK6 expressing cell with elongated phenotype. In (A) and (B) 110 cells over 3 independent experiments were analysed. Statistical significance compared with GFP control cells (unless otherwise indicated) was calculated using Student's *t*-test; *, $P < 0.05$, *** $P < 0.0005$. n.s. = not significant. Bar = 10 µm.

This could account for, in part, the difference in cell phenotype observed between the PAK6 mutants. In contrast, the cell spread area of WT PAK6 expressing cells was significantly reduced when compared to GFP control expressing cells, as was that of K436A PAK6 expressing cells (**figures 4.6B** and **4.6C**). S531N PAK6 expressing cells also exhibited a decrease in cell spread area, and this effect was more pronounced when compared to WT PAK6 over-expression (**figures 4.6B** and **4.6C**). This phenotype observed for the S531N PAK6 mutant is consistent with previous reports for the active form of PAK4 (Wells et al., 2002).

4.2.7 PAK6 kinase activity is required for efficient cell colony escape

Having established that WT PAK6 over-expression in DU145 cells induced morphological changes, the elongated phenotype of these cells was examined more closely. In contrast to GFP control expressing cells, it was discernible that WT PAK6 expressing cells were detaching from neighbouring cells and were no longer contained within the cell colony (**figure 4.6C**). In order to investigate this observation further, untransfected DU145 cells and those expressing GFP control, WT, S531N, and K436A PAK6 mutant constructs were scored based on whether they were present in a cell colony versus escaping the cell colony. A cell escaping a colony was defined as either greater than 50% of the cell body perimeter detached from the neighbouring cell(s), cells already escaped from a colony and exhibiting 100% dissociation from the neighbouring cell(s) or cells in a different plane to the underlying cell colony (**figure 4.7A**). The colony escape phenotype was classed as the same for cells escaping from the middle of periphery of the cell colony and they were quantified in the same manner.

In serum-starved cells, GFP control expressing cells remained in colonies to a similar level as untransfected cells (data not shown). In contrast, the percentage of WT and S531N PAK6 expressing cells retained in colonies was significantly reduced when compared to GFP control cells (**figure 4.7B**). Furthermore, an increase in kinase activity was found to correlate with an increase in the induction of cell colony escape. Indeed, a greater percentage of WT PAK6 expressing cells were within a cell colony when compared to S531N PAK6 expressing cells, the latter being the more active derivative of PAK6 (**figures 4.4** and **4.7B**). Moreover, cells expressing the kinase dead mutant of PAK6, K436A, were found predominantly within a cell colony (**figure 4.7B**). In

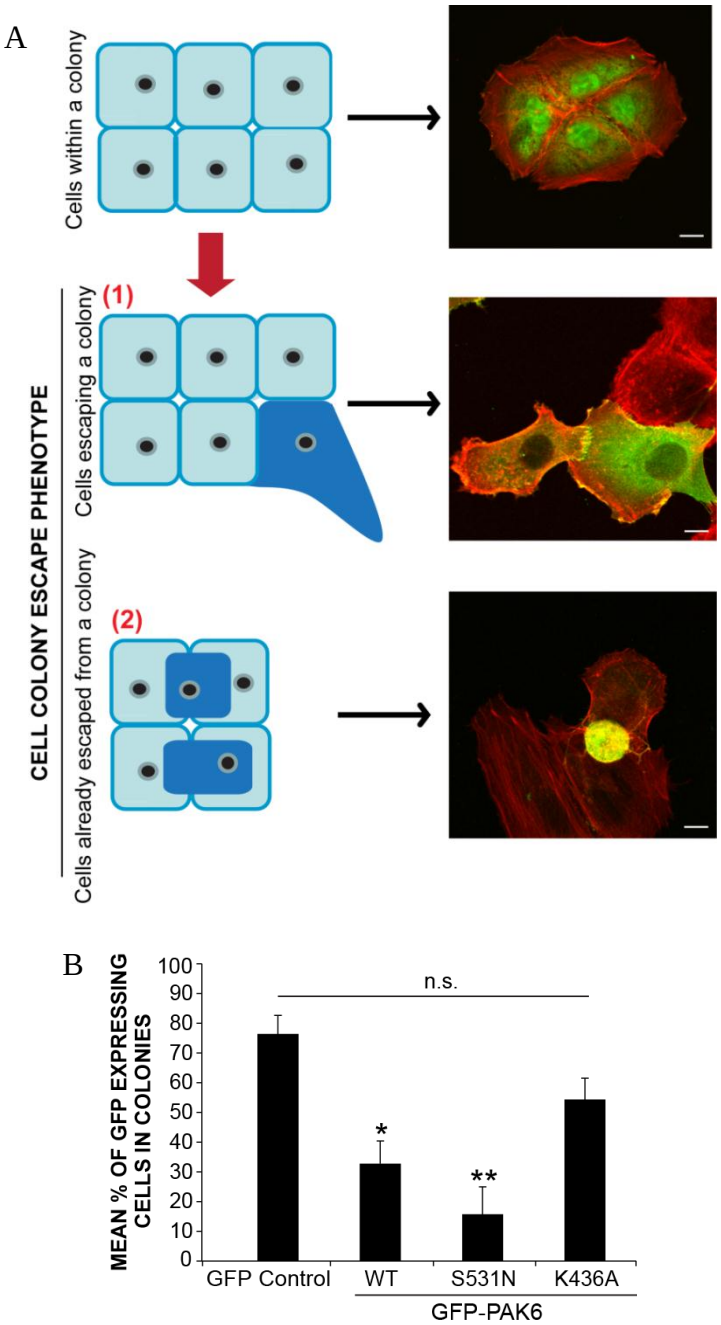

Figure 4.7 PAK6 induces cell colony escape in DU145 cells. A) Schematic illustrating colony escape phenotypes observed upon PAK6 over-expression in DU145 cells. (1) = cells escaping a colony defined as greater than 50% of the cell body perimeter detached from the neighbouring cell(s). (2) = cells already escaped from a colony defined as cells exhibiting 100% dissociation from the neighbouring cell(s) or cells in a different plane to the underlying cell colony. In (1) and (2) cells were quantified in the same manner. **B)** DU145 cells were transfected with GFP control vector or GFP-PAK6 mutants as indicated. After 24 hours, the cells were serum-starved for 24 hours and then fixed and stained for F-actin. The mean % of GFP expressing cells in colonies was calculated for 110 cells per condition over 3 independent experiments. Statistical significance compared with GFP control cells was calculated using Student's *t*-test; *, $P < 0.05$, **, $P < 0.005$. n.s. = not significant. Bar = 10 µm.

addition, HT29 cells over-expressing WT PAK6 were also able to induce colony escape to a significant level when compared to GFP control cells (**figure 4.8**). To further investigate the cell colony escape phenotype of PAK6 expressing DU145 cells, time-lapse microscopy was used to perform imaging of WT GFP-PAK6 cells to see if the cell colony escape event could be captured in live cells. Following 11 hours, it was discernible that a DU145 cell expressing PAK6 was elongated in shape (**figure 4.9, arrows**). Cell colony escape of the PAK6 expressing cell was difficult to detect as the majority of non-expressing DU145 cells exhibited a rounded phenotype leading to disrupted cell colony morphology. This is most likely due to the sub-optimal transfection-induced conditions that these cells were exposed to for a prolonged time frame. However, in contrast to non-expressing DU145 cells, the PAK6 expressing cell was still elongated and independently migrating 16 hours following transfection (**figure 4.9, arrows** and see **movies 5PC** and **5G** for representative movies and **Appendix 3**).

Subsequently, attempts were made to see if the same effect could be captured using the 3D assay described in chapter 3. However, whilst WT PAK6 expressing cells were successfully embedded in the matrix, no significant cell movement or cell shape changes were observed under serum-starved conditions during a 24 hour time-lapse movie (data not shown).

4.2.8 HGF-induced cell scattering is inhibited in DU145 and HT29 PAK6 knockdown cell populations

HGF-driven cell scattering requires the dissolution of cell-cell adhesions (**figure 3.1**). Given that PAK6 can drive cell-cell dissociation, PAK6 may act downstream of HGF during a cell scatter response. Thus it might also be reasoned that a loss of PAK6 would hinder this process. Two different siRNA oligonucleotides were employed to knockdown PAK6 (**figure 4.10)**. The level of PAK6 was significantly reduced when compared to PAK6 levels in control siRNA lysates and did not affect PAK1, PAK2 or PAK4 expression **(figure 4.10**). No significant difference in PAK6 expression levels was detected between untransfected mock and control siRNA-treated DU145 and HT29 cells (**figures 4.10B** and **4.10D**). However, whilst PAK6 knockdown was achieved, this was a challenging process that required the optimisation of siRNA concentrations and the cell densities used. Furthermore, PAK6 knockdown in the DU145 cells was

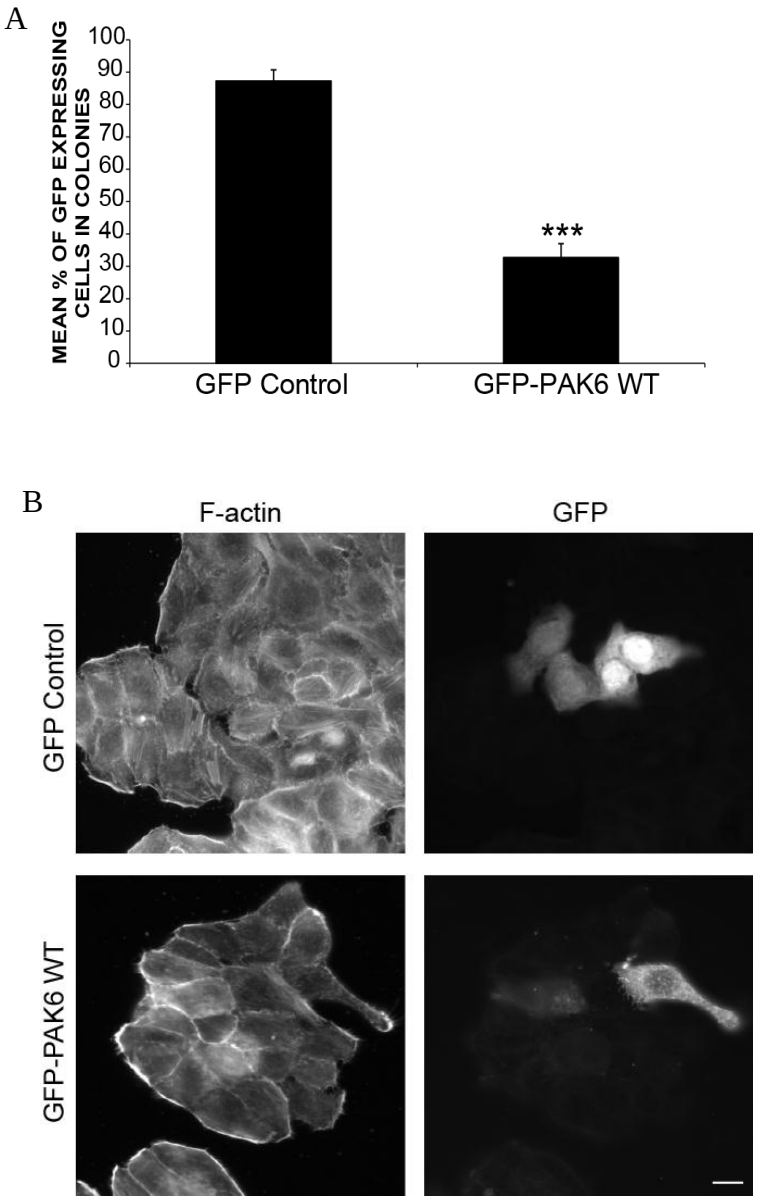

Figure 4.8 PAK6 induces cell colony escape in HT29 cells. A) HT29 cells were transfected with GFP control vector or WT GFP-PAK6. Following 24 hours, the cells were serum-starved for 24 hours. The cells were fixed and stained for F-actin. The % of GFP expressing cells present within a colony was calculated. A cell escaping a colony was defined as either greater than 50% of the cell body perimeter detached from the neighbouring cell(s), cells already escaped from a colony and exhibiting 100% dissociation from the neighbouring cell(s) or cells in a different plane to the underlying cell colony. **B)** Cells were treated as described in (A) and imaged using fluorescence microscopy. In (A) the mean % of GFP expressing cells in colonies was calculated for 110 cells per condition over 3 independent experiments. Statistical significance compared with GFP control cells was calculated using Student's *t*-test; ***, $P < 0.0005$. Bar = 10 µm.

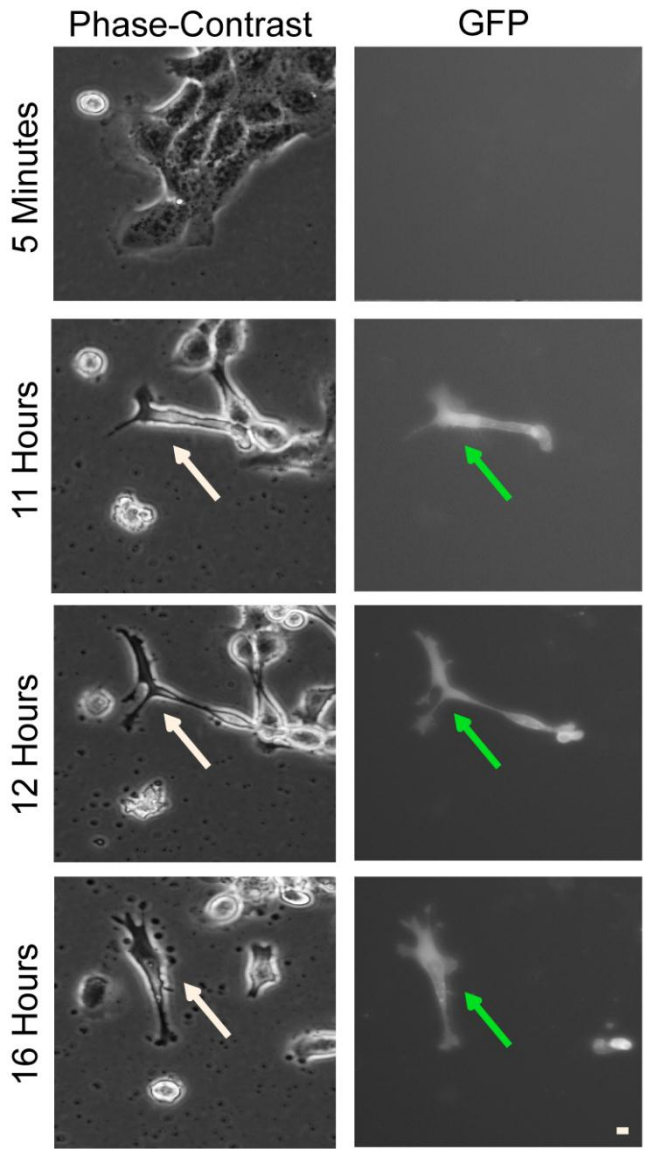

Figure 4.9 Live-cell imaging of WT GFP-PAK6 in DU145 cells. DU145 cells were transfected with WT GFP-PAK6. Cells were immediately filmed for 24 hours at 5 minute intervals using phase-contrast and GFP fluorescence time-lapse microscopy. Still images from the film at varying time points were taken to show a WT GFP-PAK6 expressing cell elongating (arrows). The images shown are representative of 3 independent experiments. Bar = 10 µm.

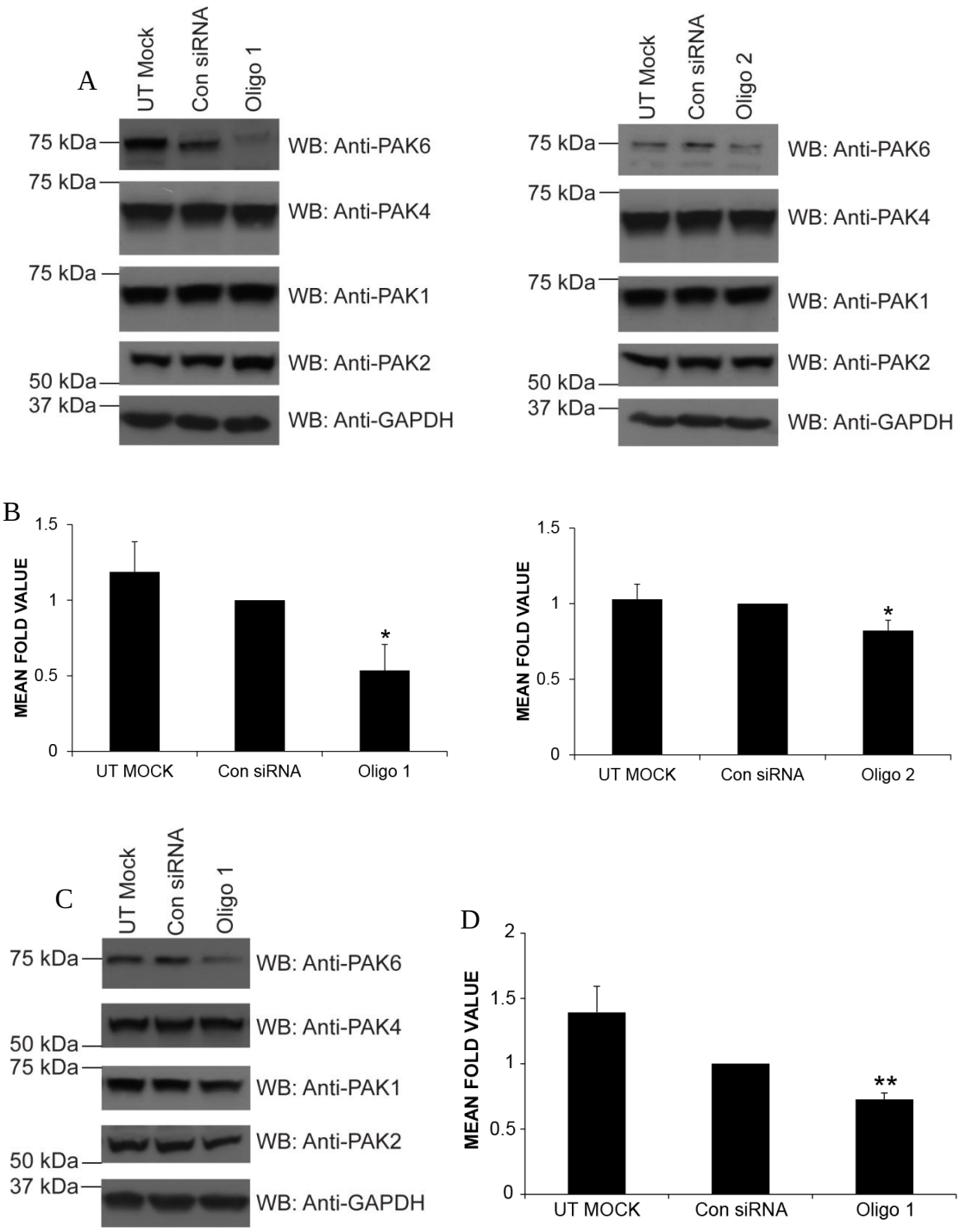

Figure 4.10 PAK6 siRNA knockdown in DU145 and HT29 cells. A) DU145 cells were transfected with PAK6 siRNA (Oligo 1 or 2) or control siRNA (Con siRNA), lysed after 72 hours and immunoblotted for PAK6 using a PAK6 specific antibody and for GAPDH as a loading control. Lysates were also immunoblotted for PAK4 using an in-house affinity purified PAK4 specific antibody and for PAK1 and PAK2 as controls for specific knockdown. **B)** Quantification of blots from (A). **C)** HT29 cells were treated as described in (A). **D)** Quantification of blots from (C). In (B) and (D) the mean fold value and the standard error of the mean were calculated over 3 independent experiments. Statistical significance compared between Con siRNA and UT Mock or PAK6 siRNA (Oligo 1 or 2) was calculated using Student's *t*-test: *, $P < 0.05$, **, $P < 0.005$.

particularly difficult when compared to the HT29 cell line. There are a number of reasons that could account for this. Firstly, PAK6 expression at an mRNA level may be significantly higher in the DU145 cells; indeed PAK6 protein expression was observed to be lower in the HT29 cell line when compared to DU145 cells (**figures 4.1B** and **4.1C**). Furthermore, it has been proposed that PAK6 has anti-apoptotic functions in prostate cancer cells (Zhang et al., 2009). Moreover, PAK6 was classed as a 'difficult to silence' gene in an siRNA screen where the central region of PAK6 mRNA was found to be highly difficult to target using siRNA knockdown (Bergauer et al., 2009).

Control siRNA DU145 cells exhibited a normal degree of cell-cell dissociation upon HGF stimulation; however the ability of the PAK6 knockdown cell populations to scatter in response to HGF was significantly reduced (**figures 4.11A** and **4.11B**). Moreover, PAK6 knockdown cells exhibited similar elongation ratios in the absence and presence of HGF (4 hours stimulation) (**figure 4.11C**), whilst untransfected and control siRNA cells were significantly more elongated following 4 hours HGF stimulation (**figure 4.11C**); a characteristic response of DU145 cells to HGF. Thus PAK6 knockdown cells appeared to possess a defect in cell elongation upon HGF addition. Consistent with these findings in DU145 cells, HT29 cells transfected with control siRNA scattered upon HGF stimulation (**figure 4.11D, Con siRNA**). However PAK6 siRNA-transfected HT29 cells exhibited a significantly diminished ability to scatter in response to HGF addition (**figures 4.11D** and **4.11E**).

4.2.9 PAK6 knockdown affects cell-cell junction integrity and E-cadherin localisation in DU145 cells

Closer examination of PAK6 siRNA colonies in the presence of HGF suggested that these cells were not disassembling their cell-cell junctions, a normal initial HGF response (**figure 3.1**) (Fram et al., 2011; Wells et al., 2005). E-cadherin is a junctional epithelial marker and a key component of cell-cell junction integrity (Gumbiner et al., 1988). Therefore, its distribution in control siRNA and PAK6 knockdown cells was examined downstream of HGF stimulation.

Control siRNA cells were undergoing dissociation after 4 hours HGF stimulation, with minimal E-cadherin staining visible at sites of cell-cell contact (**figure 4.12A**). In addition, the control siRNA cells were elongated after 24 hours HGF addition, with no

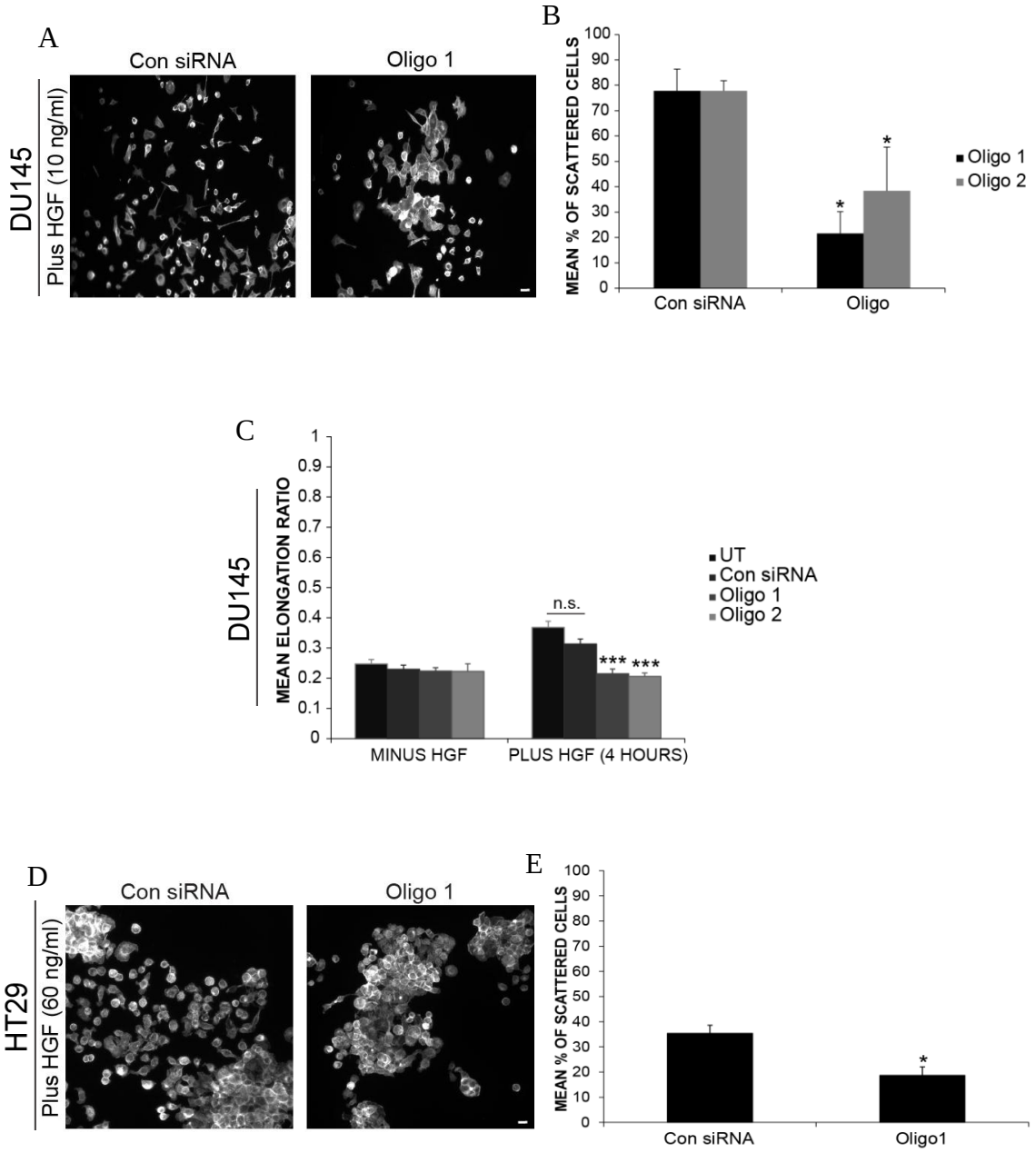

Figure 4.11 PAK6 siRNA knockdown reduces HGF-induced cell scattering in colony-forming cells. A) DU145 cells were transfected with PAK6 siRNA (Oligos 1 and 2) or control siRNA (Con siRNA). Following 72 hours, cells were serum-starved for 24 hours and stimulated with HGF (10 ng/ml) for a further 24 hours. The cells were fixed and stained for F-actin. **B)** DU145 cells were counted and cell counts of Con siRNA versus PAK6 siRNA were compared. Scattered = loss of cell-cell junctions and single cells with an elongated migratory phenotype. **C)** Cells were seeded and treated as described in (A) but left unstimulated (minus HGF) or stimulated with HGF for 4 hours and were then fixed and stained for F-actin. Cells were subjected to Image J analysis to determine the cell elongation ratio. **D)** HT29 cells were treated as in (A) but stimulated with 60 ng/ml HGF. **E)** Scattered cells were quantified as in (B). In (B), (C) and (E) the mean values and the standard error of the mean were calculated over 3 independent experiments. Statistical significance compared with Con siRNA cells was calculated using Student's *t*-test; *, $P < 0.05$, ***, $P < 0.0005$. n.s. = not significant. Bar = 10 µm.

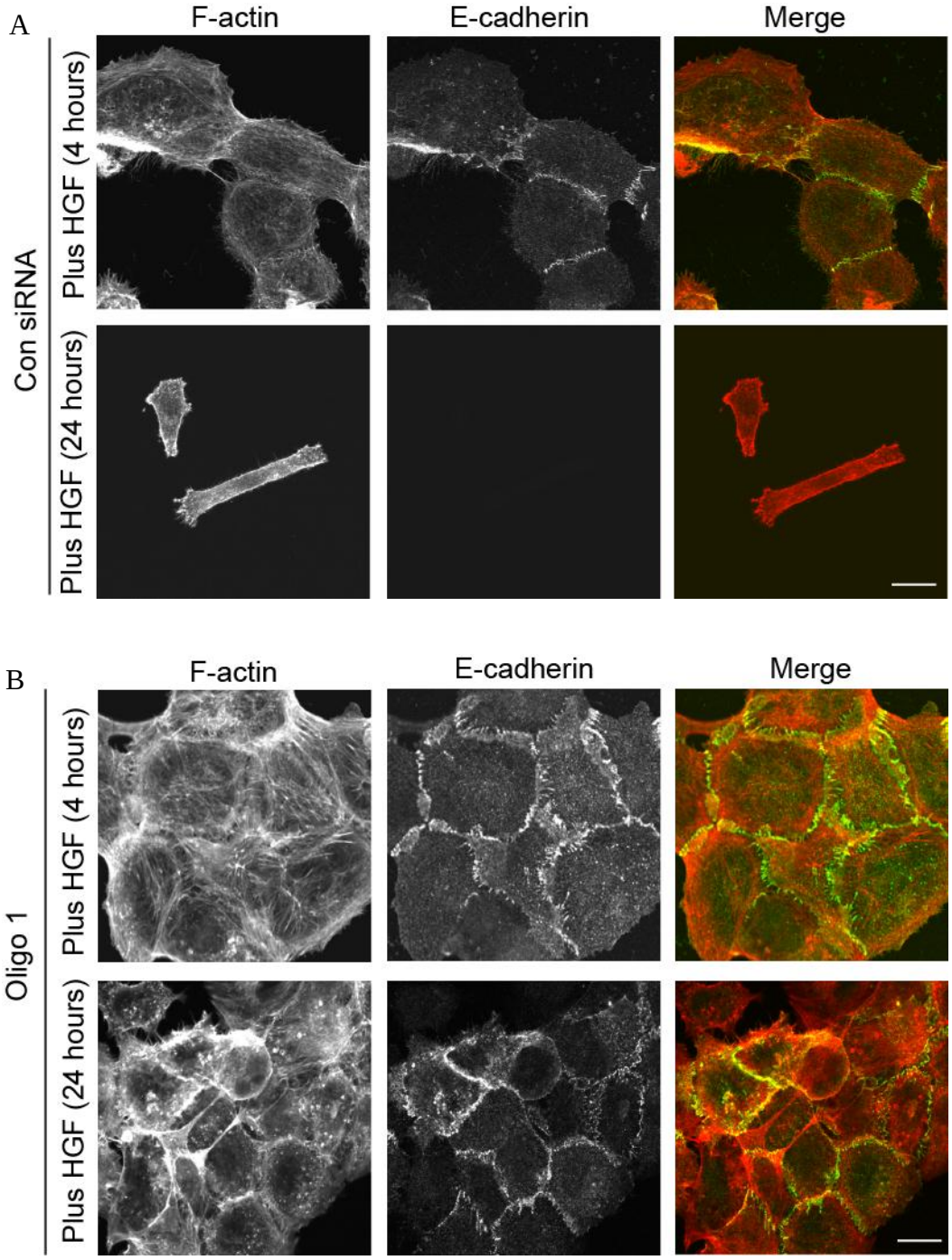

Figure 4.12 PAK6 knockdown inhibits the re-distribution of E-cadherin from cell-cell boundaries to the cytoplasm downstream of HGF in DU145 cells. A) and **B)** DU145 cells were transfected with control siRNA (Con siRNA) or PAK6 siRNA (Oligo 1) as indicated. Following 72 hours, cells were serum-starved for 24 hours and stimulated with HGF (10 ng/ml) for 4 hours and 24 hours as indicated. The cells were then fixed and labelled for E-cadherin and F-actin. In (A) and (B) cells were imaged using confocal microscopy. The images shown are representative of 3 independent experiments. Bar = 10 µm.

E-cadherin staining detected (**figure 4.12A**). In contrast, the cell borders in PAK6 knockdown cell populations were E-cadherin-positive, with distinct and extensive punctate staining following 4 hours stimulation with HGF (**figure 4.12B**). At the 24 hour time point, the cell-cell boundaries in the PAK6 knockdown cell population were still E-cadherin-positive, with a distinct localisation pattern similar to that observed following 4 hours HGF stimulation (**figure 4.12B**).

4.2.10 PAK6 localisation in DU145 cells

Taken together, with the finding that PAK6 over-expression drives the disassembly of junctions, it might be speculated that PAK6 is localised at cell junctions. To investigate PAK6 localisation within DU145 colony cells, low level expressing WT PAK6 cells were imaged as high expressing WT PAK6 cells were already escaping the cell colony. PAK6 was found to be specifically localised at cell-cell boundaries with punctate and distinct localisation (**figure 4.13, arrows**) which correlated with the pattern of E-cadherin localisation detected in these cells (**figure 4.13, arrows**). Thus, PAK6 can be detected at E-cadherin-positive cell-cell junctions. However, it is important to consider that there are potential artefacts of examining co-localisation with tagged proteins. For example, fluorophore tags such as GFP may potentially influence the localisation of a protein. In order to confirm that this is not the case between GFP-PAK6 and E-cadherin, the co-localisation between control cells transfected with GFP alone and E-cadherin could be analysed and compared to that of GFP-PAK6 expressing cells. Furthermore, Z-sections could be taken at different focal planes through the cells where GFP-PAK6 and E-cadherin appear to be co-localised. This would further help confirm that the co-localisation observed between GFP-PAK6 and E-cadherin is true.

Subsequently, the localisation of other PAK6 mutants was investigated (**figure 4.14**). As expected, the localisation of GFP control cells was nuclear and cytoplasmic (**figure 4.14**). The localisation could not be determined in colony cells expressing the S531N PAK6 mutant as even low expressing cells had already escaped from colonies (**figure 4.14**). Furthermore, these cells exhibited a rounded phenotype, unlike WT PAK6 expressing DU145 cells (**figure 4.14**). Cell rounding can be stimulated by different cellular mechanisms including the induction of contraction which leads to rounding of

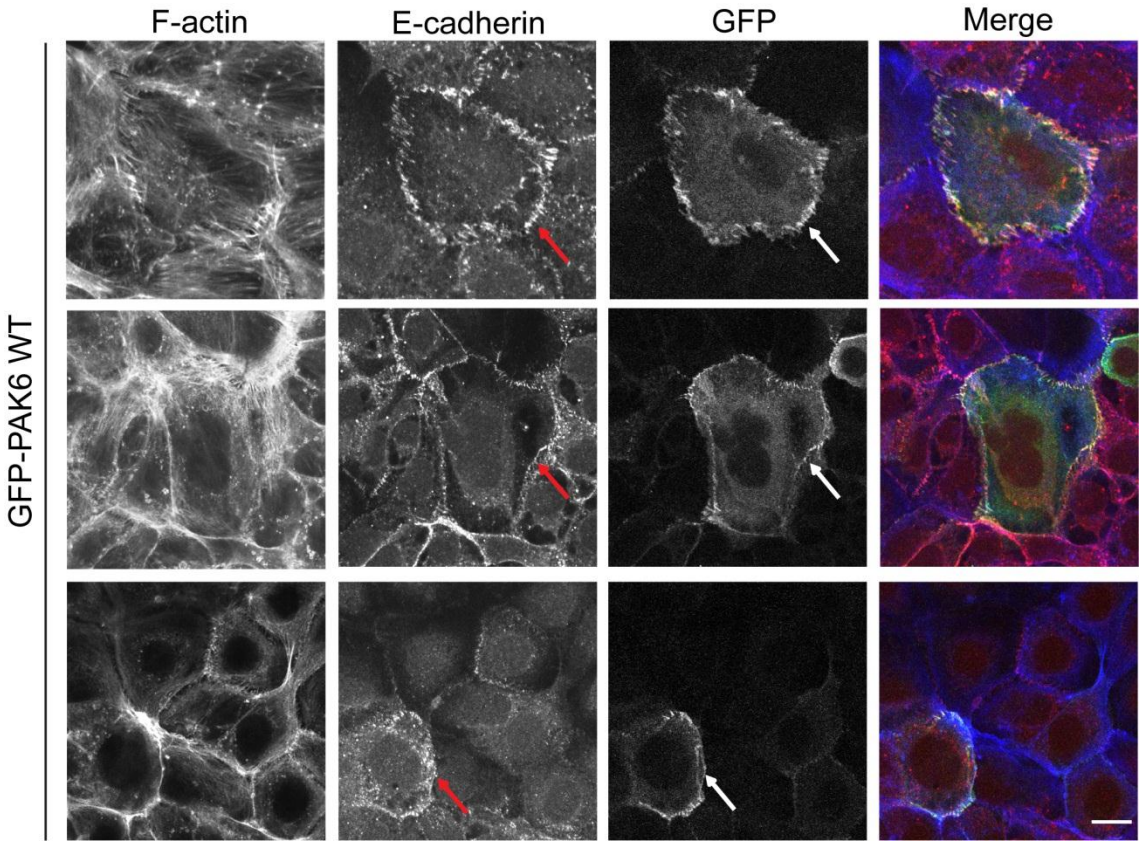

Figure 4.13 Localisation of over-expressed PAK6 in DU145 cells. DU145 cells were transfected with WT GFP-PAK6. After 24 hours, the cells were serum-starved for 24 hours. Cells were then fixed and labelled for E-cadherin and F-actin. Low level WT GFP-PAK6 expression could be detected at E-cadherin-positive cell-cell junctions (arrows). Cells were imaged using confocal microscopy and the images shown are representative of 3 independent experiments. Bar = 10 µm.

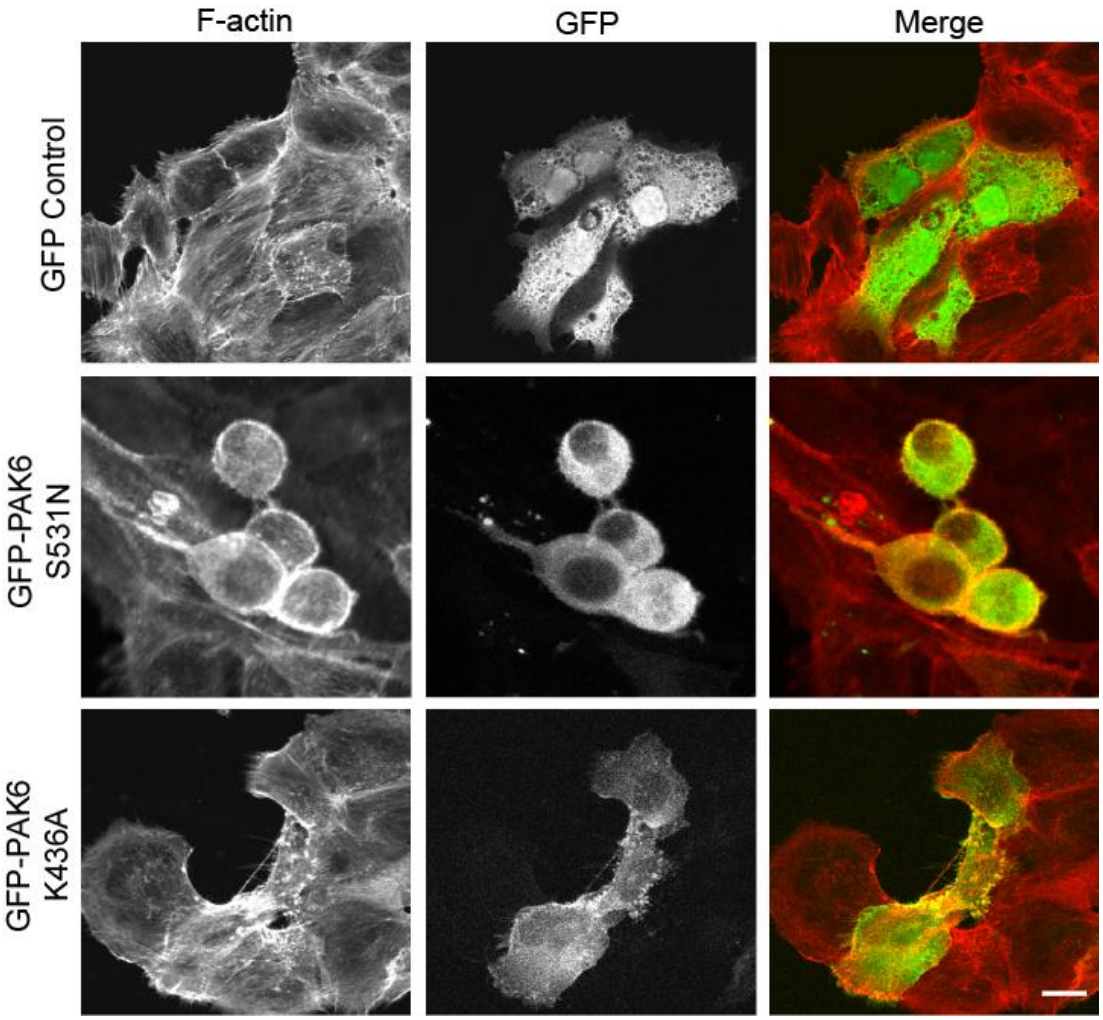

Figure 4.14 Localisation of PAK6 mutants in DU145 cells. DU145 cells were transfected with GFP control vector or GFP-PAK6 mutants as indicated. After 24 hours, the cells were serum-starved for 24 hours. Cells were then fixed and stained for F-actin and imaged using confocal microscopy. The images shown are representative of 3 independent experiments. Bar = 10 µm.

the cell body as well as during mitosis. In addition, cell rounding is characteristic of dying cells; this possibility could be excluded by the use of cell viability and cytotoxicity assays of S531N PAK6 expressing DU145 cells.

In contrast, the kinase dead mutant of PAK6, K436A, which exhibited a reduced efficiency in colony escape induction (**figure 4.7B**), was diffusely localised in the cell cytoplasm (**figure 4.14**) and was not specifically detected at cell junctions. Taken together, these results suggest that PAK6 mediates cell-cell dissociation.

4.3 Discussion

In this chapter, the potential role of the PAK family member PAK6 in growth factor-induced cell migration has been investigated using the scatter assay from chapter 3 as a model system. It has been shown that PAK6 autophosphorylation levels are increased in response to HGF in DU145 and HT29 cells, but not in response to EGF stimulation. Moreover, it has been demonstrated for the first time that PAK6 over-expression is able to induce cell elongation and cell colony escape in DU145 and HT29 colony-forming cells. In addition, siRNA knockdown of PAK6 inhibited HGF-induced cell scattering and affected E-cadherin localisation downstream of HGF stimulation. These results suggest that PAK6 plays an important role in driving cell-cell dissociation downstream of HGF.

PAK6 is known to be highly expressed in the testis and in prostate tissues, as demonstrated by Northern blot analysis (Yang et al., 2001). In this study, PAK6 was found to be expressed in DU145 prostate cancer cells, as consistent with previous reports (Callow et al., 2002; Wells et al., 2010; Yang et al., 2001), as well as in HT29 colon adenocarcinoma cells. However, PAK6 expression was lower in the HT29 cells when compared to DU145 cells. This is consistent with the reported mRNA expression levels of PAK6 in HT29 and DU145 cells (Callow et al., 2002). PAK6 is also expressed in MCF7, HS578t and MDA-MB-231 breast cancer cells, with highest PAK6 expression detected in the latter cell type (Kaur et al., 2008).

PAK6 differs from its family members in its ability to bind to the LBD of the AR and induce the suppression of AR signalling (Schrantz et al., 2004). In addition, ectopic expression of PAK6 is thought to enhance the survival of prostate cancer cells (Li et al., 2005a). In the literature, PAK6 knockdown was found to inhibit DU145 prostate cancer cell growth (Wen et al., 2009). However, the effect of PAK6 siRNA knockdown on cell migration has not been assessed. In addition, very little is known on the effect of PAK6 over-expression and PAK6 localisation in cells.

It is well established that HGF signalling plays a role in prostate cancer metastasis (Gmyrek et al., 2001). HGF stimulation significantly increased PAK6 autophosphorylation in DU145 cells, as well as in HT29 cells. Whilst HGF is also

known to induce an increase in both PAK1 and PAK4 phosphorylation levels in DU145 cells, these PAKs induce distinct functions downstream of HGF stimulation (Bright et al., 2009; Wells et al., 2010). Although phospho-PAK6 levels were increased upon HGF addition, the elevation in phospho-PAK6 detected was only modest in the DU145 cells. Interestingly, it has been shown that the HGF receptor c-Met is distributed on the basolateral membrane of polarised multi-cellular MDCK cells (Crepaldi et al., 1994). Thus it has been speculated that in colony-forming cells, only cells located at the periphery of the colony, and not those within the cell colony, have the ability to respond to HGF addition thereby accounting for a muted HGF response (Wells et al., 2002; Wells et al., 2010). Hence this theory could potentially account for, in part, the modest elevation in PAK6 phospho levels upon HGF stimulation.

The regulation of group II PAK activity and the phosphorylation sites involved has yet to be fully discerned. PAK1, the most extensively studied group I PAK, is known to have multiple autophosphorylation sites (Chong et al., 2001). Thus it is possible that PAK6 is phosphorylated downstream of HGF on residues other than serine 560, which has been tested here, and thus these results may not reflect the complete activating potential of HGF signalling on PAK6. Indeed, it has been shown here that mutating this site does not increase the kinase activity of PAK6, as consistent with previous reports (Kaur et al., 2005; Schrantz et al., 2004). In contrast, mutating serine 531 increased PAK6 kinase activity as also observed in previous work (Schrantz et al., 2004). In addition, whilst serine 560 phosphorylation is known to be required for PAK6 activation via MKK6, PAK6 is also directly activated by MKK6 at tyrosine 566 (Kaur et al., 2005). This supports a hypothesis that the phosphorylation of other residues on PAK6 is important for PAK6 activation. This hypothesis could be investigated further by designing in-house antibodies to different serine, threonine or tyrosine sites on PAK6.

The potential of EGF to stimulate PAK6 was also investigated due to its ability to induce cell-cell junction breakdown in DU145 cells (Gan et al., 2010). In contrast to HGF, EGF was unable to induce a phospho-PAK6 response at serine 560 in DU145 cells. This again may be due to the fact that PAK6 is more responsive to growth factor stimulation at other sites; or PAK6 may not be involved in EGF signalling in DU145 cells.

In this chapter, PAK6 over-expression was found to induce morphological and phenotypical changes in DU145 cells. HGF stimulation was not required for the cell shape changes induced; indeed WT PAK6 expression in serum-starved conditions was sufficient to stimulate pronounced morphological effects. The elongated phenotype observed for WT PAK6 expressing DU145 cells is novel when compared to cell shape analyses of other PAKs. WT PAK4 over-expression exhibited no effects on MDCK cell morphology in unstimulated conditions, as well as upon stimulation with HGF (Wells et al., 2002). Furthermore, WT PAK4 expression induces no cell shape changes in DU145 cells (personal communication with Dr. Wells). Consistent with this, WT PAK4 expression in unstimulated conditions induced no cell shape changes in C2C12 mouse myoblast cells (Dan et al., 2001) or NIH 3T3 mouse embryo fibroblast cells (Qu et al., 2001). The ability of WT PAK6 expressing cells to induce a morphological response may be related to the phosphorylation status of WT PAK6 and thus activity levels. WT PAK6 may be autophosphorylated under basal conditions, as has been speculated in the literature for group II PAKs (Abo et al., 1998; Pandey et al., 2002). Interestingly it has been shown here that at the residue serine 560, a predicted autophosphorylation site of PAK6, phospho-PAK6 levels are high in serum-starved DU145 cells.

The majority of PAK induced cell shape changes have been detected when the constitutively active forms of PAK1, 2 and 4 were utilised (Manser et al., 1997; Qu et al., 2001; Zeng et al., 2000). DU145 cells over-expressing the kinase active form of PAK6 were predominantly rounded in the absence of HGF. This is consistent with the cell rounding reported upon expression of activated PAK4 in mouse embryo fibroblast cells in unstimulated conditions (Dan et al., 2001). However HGF stimulation was required to induce cell rounding in MDCK (Wells et al., 2002) and DU145 (Wells et al., 2010) cells. The cell rounding phenotype observed for kinase active PAK6 expressing DU145 cells may be due to a defect in cell spreading. Indeed, it has been reported that Rat1 fibroblast cells expressing active PAK4 exhibited a diminished ability in cell spreading on fibronectin coated substratum (Qu et al., 2001). Moreover, there is evidence suggesting that PAKs play a role in cell-substratum adhesion (Manser et al., 1997; Wells et al., 2002) and cell rounding induction in cells can also be as a consequence of aberrant focal adhesion turnover (Manser et al., 1997).

One of the first characteristics of HGF-induced DU145 cell scattering is that cells become more elongated (Fram et al., 2011; Wells et al., 2005). Following HGF stimulation, cell elongation becomes more pronounced, thereby inducing cell detachment and subsequent cell colony escape (Fram et al., 2011; Wells et al., 2005). WT PAK6 was found to induce cell elongation in serum-starved conditions and these cells exhibited the ability to escape from a cell colony in the absence of HGF stimulation. This colony escape phenotype was dependent on PAK6 kinase activity, as the kinase dead mutant failed to induce efficient cell colony escape. In addition, the kinase active PAK6 mutant, S531N, induced an increase in the percentage of cells escaping a colony, even when compared to WT PAK6 cells. This correlates with the kinase activity exhibited for these derivatives of PAK6 as shown in the radioactive *in vitro* kinase assay; the S531N mutant exhibited a substantial increase in autophosphorylation and substrate phosphorylation when compared to the kinase activity of WT PAK6, whilst the kinase dead PAK6 mutant, K436A, exhibited no kinase activity. The kinase activity profiles observed for these mutants are consistent with previous reports (Kaur et al., 2005; Schrantz et al., 2004).

Colony escape mechanisms have been reported in epithelial cell colonies during epithelial cancer cell outgrowth. In one study, single cells induced to express oncogenes translocated out of the epithelial layer (Leung and Brugge, 2012). It was postulated that these cells were escaping the hostile environment of a developed epithelium (Leung and Brugge, 2012). This in turn allows for aberrant proliferation of these cells and thereby induces cancer cell progression (Leung and Brugge, 2012). In a second study, it was demonstrated that live epithelial cells are extruded from an overcrowded epithelial environment (Eisenhoffer et al., 2012). Moreover, MDCK cells expressing oncogenic Ras basally extrude from epithelial cell sheets in a model of tumour cell progression (Hogan et al., 2009).

PAK6 knockdown cells were defective in cell junction disassembly downstream of HGF stimulation, whilst PAK6 over-expression induced cell colony escape. In addition, these phenotypes were reproducible in HT29 cells. This suggests that PAK6 may have a similar role in cell-cell dissociation in different colony-forming cancer cell types. Whilst HGF-induced cell scattering was also inhibited in PAK4 knockdown DU145 cells, these

PAK4-depleted cells did not possess a defect in junction disassembly (Wells et al., 2010).

PAK1 knockdown cells exhibited a similar phenotype to that of PAK6 in DU145 cells downstream of HGF stimulation (Bright et al., 2009) and it was speculated that the inhibition of scattering was related to cell-cell adhesion dynamics (Bright et al., 2009). In contrast, HGF-induced DU145 cell scattering was not inhibited in PAK2 knockdown cells and it was proposed that depletion of PAK2 in fact promoted cell scattering in DU145 cells (Bright et al., 2009). Unfortunately, there is significant variation in the methods used to measure cell scattering in the Bright et al. study, compared to the quantification system used here. Therefore, the inhibition in HGF-induced scattering as a result of PAK1 depletion cannot be directly compared to the PAK6 knockdown phenotype observed here.

PAK6 knockdown cells retained strong localisation of E-cadherin at cell-cell junctions downstream of HGF stimulation. In addition, these cells were still in colonies following 24 hours HGF stimulation. E-cadherin, a junctional marker (Gumbiner et al., 1988) that is commonly associated with cancer progression (van Roy and Berx, 2008), is normally re-distributed from cell-cell junctions to the cytoplasm during cell-cell dissociation (Miura et al., 2001). In the Bright et al. study, whilst E-cadherin localisation was also maintained at PAK1 knockdown cell junctions, these knockdown cells appeared to be partially scattered, rather than remaining within a tight cell colony (Bright et al., 2009). Thus it could be speculated that the roles of PAK1 and PAK6 during junctional disassembly are distinct.

The work presented here suggests a novel role for PAK6 in the disruption of junctions that subsequently leads to cell-cell dissociation. Interestingly Mbt, a *Drosophila* PAK protein which shares close homology with human group II PAKs, localises at adherens junctions when activated and has been reported to induce the breakdown of these junctions during eye maturation (Menzel et al., 2008; Menzel et al., 2007; Schneeberger and Raabe, 2003). In addition, the *Xenopus* PAK4 homologue, X-PAK5, also localises at sites of cell contact and has been implicated in the cell-cell dissociation process (Faure et al., 2005). In DU145 cells, PAK4 is not required for cell-cell adhesion disassembly but is required for subsequent cell scattering (Wells et al., 2010). Thus both

of these group II PAKs may be present in the same HGF-induced signalling pathway where PAK6 lies upstream of PAK4. Indeed, in the group I PAKs, it has been hypothesised that PAK2 may exert its effects through PAK1 to modulate HGF-induced DU145 cell scattering (Bright et al., 2009).

In DU145 cells, WT PAK6 was localised to cell-cell boundaries. Very little is known about PAK6 localisation in other cell types. However, full-length PAK6 was found to be localised predominantly in the cytoplasm of non-colony forming fibroblastic CV-1 cells but PAK6 can also translocate to the nucleus with AR stimulation (Yang et al., 2001). This cytoplasmic localisation pattern was similar to that described for the localisation of kinase active (S531N) PAK6 and kinase dead (K436A) PAK6 (Schrantz et al., 2004) and over-expressed WT PAK6 in HeLa cells, which exhibit a low level of cell-cell contact sites (Lee et al., 2002). PAK6 was also found localised at the plasma membrane in HeLa cells (Lee et al., 2002). More recent work has shown that over-expressed PAK6 frequently localises to punctate formations in the cytoplasm of HeLa B cells and NCI-H1299 lung cancer cells (Shepelev and Korobko, 2012). The latter cell type is colony forming possessing high levels of cell-cell contacts, however PAK6 localisation at cell-cell junctions was not observed (Shepelev and Korobko, 2012). The difference in cell elongation and colony escape phenotypes observed between WT PAK6 and PAK6 mutant constructs in this study could potentially be accounted for by the intracellular distribution of these mutants, as the kinase dead mutant of PAK6 exhibited diffuse and cytoplasmic localisation. A junctional localisation for PAK4 in lung epithelial cells has also been reported (Wallace et al., 2010), but not in DU145 cells; however PAK4 has been localised to focal adhesions in these cells (Wells et al., 2010).

In summary, a novel role for PAK6 in HGF-induced cell scattering has been identified using over-expression and knockdown strategies. Indeed, work presented here suggests that PAK6 may mediate cell-cell junction dissolution.

4.3.1 Future work

Based on the *in vitro* kinase assay data in this chapter, it seems likely that PAK6 possesses autophosphorylation sites other than serine 560. Thus it would be interesting to deduce the location of these sites within PAK6. This could be achieved by performing an *in vitro* kinase assay using wild-type PAK6 and/or PAK6 mutants and conducting mass spectrometry phosphorylation analysis on observed phosphorylation band(s). Furthermore, as the AR is the only PAK6 substrate that has been identified (Schrantz et al., 2004) it would be interesting to investigate other potential PAK6 substrates that could potentially be involved in cell-cell junction disassembly signalling. Techniques such as mass spectrometry or a yeast two-hybrid screen could be implemented.

In this study, PAK6 knockdown in DU145 and HT29 cells led to a reduction in cell-cell junction disassembly. To confirm that this phenotype was PAK6-specific, a rescue experiment could be conducted. Furthermore, DU145 cells expressing the kinase dead mutant of PAK6, K436A, remained in cell colonies, unlike wild-type PAK6 and the kinase active form of PAK6, S531N. The localisation pattern of E-cadherin was similar to that of wild-type PAK6. Thus it would be beneficial to compare E-cadherin localisation in these cells to the other derivatives of PAK6, as well as to control cells transfected with GFP.

Chapter 5
PAK6 interaction with IQGAP1 in DU145 cells

Chapter 5 – PAK6 interaction with IQGAP1 in DU145 cells

5.1 Introduction

In cells with reduced PAK6 expression, HGF does not induce cell-cell junction dissociation (chapter 4). Moreover, PAK6 over-expression induces cell elongation and cell colony escape (chapter 4). These results suggest that PAK6 plays a role in junction disassembly. Thus to better understand how PAK6 might regulate cell-cell boundaries, potential binding partners were investigated.

There is one report in the literature that PAK6 can interact with IQGAP1 (Kaur et al., 2008), a protein known to localise to MDCK (Kuroda et al., 1996) and MCF7 (Li et al., 1999; Swart-Mataraza et al., 2002) cell-cell junctions. This putative interaction was detected in a breast cancer cell line using co-immunoprecipitation experiments (Kaur et al., 2008), but this finding has yet to be validated in other cell types. IQGAP1 is a multi-domain protein that is thought to be involved in protein-protein interactions and various signal transduction pathways (White et al., 2011). Indeed, IQGAP1 binds to Cdc42 (Kuroda et al., 1996) and is thought to act as a scaffold protein in the MAPK signalling cascade (Ren et al., 2007; Roy et al., 2005).

IQGAP1 has also been implicated in cancer cell motility and siRNA knockdown of IQGAP1 significantly decreases cancer cell migration in MCF7 breast epithelial cells (Mataraza et al., 2003b). IQGAP1 also binds to junctional-associated molecules including actin (Erickson et al., 1997) and E-cadherin (Kuroda et al., 1998) and is thought to regulate cell-cell dissociation downstream of HGF in colony-forming MDCK II cells (Fukata et al., 2001). Moreover, it has been postulated that the GTP-bound forms of Rac1 and Cdc42 are involved in cell-cell dissociation downstream of HGF stimulation by modulating the interaction of IQGAP1 with an E-cadherin-containing junctional complex (Fukata et al., 2001).

In this chapter, the aim was to further characterise the interaction between IQGAP1 and PAK6 and identify any functional relationship that may be associated with cell-cell dissociation.

5.2 Results

5.2.1 IQGAP1 expression and localisation in DU145 cells

IQGAP1 is a ubiquitously expressed protein (Weissbach et al., 1994); however its expression in prostate cancer cells has not been examined. IQGAP1 was found to be expressed in DU145 cells (**figure 5.1A**). It has been reported that IQGAP1 is enriched at cell-cell junctions in colony-forming MDCK II cells (Fukata et al., 2001). Therefore, the localisation of WT GFP-IQGAP1 was examined in DU145 cells. Consistent with previous reports (Kuroda et al., 1998), over-expressed WT IQGAP1 was detected and enriched at E-cadherin-positive junctions (**figure 5.1B**). Diffuse cytoplasmic expression was also discernible as has been observed previously (Fukata et al., 2001).

5.2.2 PAK6 interacts with IQGAP1

HEK293 cells were used for a structure-function analysis of the reported interaction between PAK6 and IQGAP1. IQGAP1 is a large (approximately 189 kDa) multi-domain scaffold protein (Briggs and Sacks, 2003; Weissbach et al., 1994) that is known to have multiple binding partners (Brown and Sacks, 2006). PAK6 is structurally similar to its family members and possesses an N-terminal PBD and a C-terminal serine/threonine kinase domain (Wells and Jones, 2010). Endogenous (co)-immunoprecipitation protocols were firstly employed, but these attempts were unsuccessful. However, endogenous PAK6 (which is expressed in HEK293 cells (**figure 5.2A**) was co-immunoprecipitated with over-expressed WT GFP-IQGAP1 in HEK293 cells (**figure 5.2B**).

Both PAK6 and IQGAP1 are reported to interact with activated Cdc42 (Hart et al., 1996; Kuroda et al., 1996; Lee et al., 2002). Thus, the interaction between IQGAP1 and PAK6 may not be direct but mediated through a joint interaction with Cdc42. Immunoprecipitation studies indicated that full-length WT IQGAP1, Cdc42-V12 and full-length WT PAK6 could be pulled down together (**figure 5.3**).

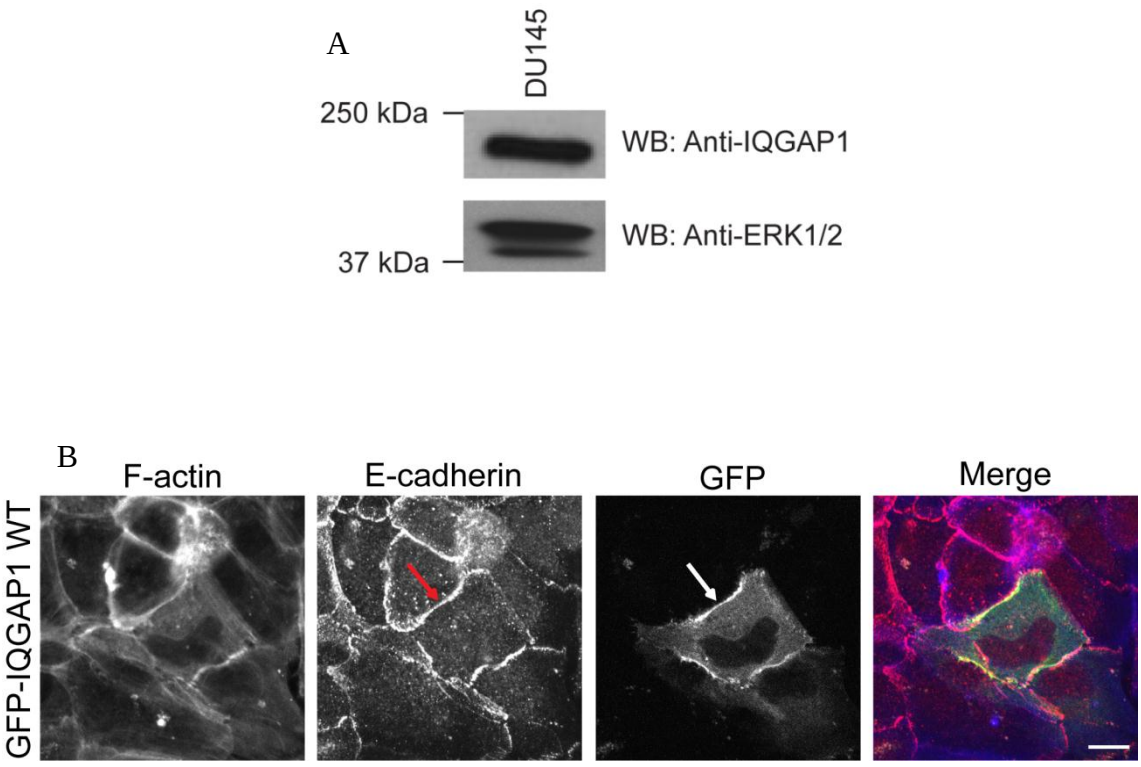

Figure 5.1 IQGAP1 expression and localisation in DU145 cells. A) DU145 whole cell lysate was immunoblotted for IQGAP1 expression using an anti-IQGAP1 antibody and for ERK1/2 using an anti-ERK1/2 antibody as a loading control. **B)** DU145 cells were transfected with WT GFP-IQGAP1. Cells were fixed and labelled for E-cadherin and F-actin and imaged using confocal microscopy. WT GFP-IQGAP1 expression could be detected at E-cadherin-positive cell-cell junctions (arrows). In (A) and (B) data are representative of 3 independent experiments. Bar = 10 µm.

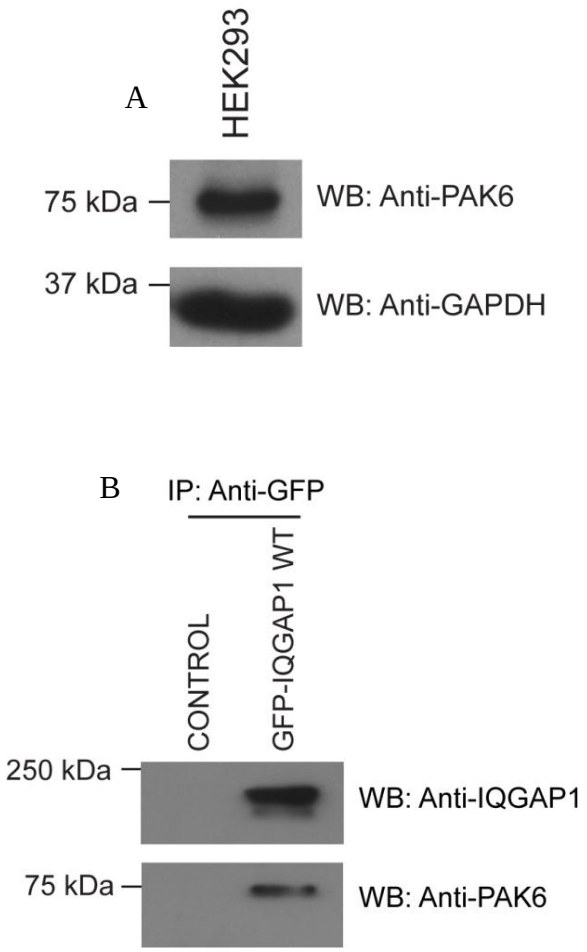

Figure 5.2 PAK6 interacts with IQGAP1. A) HEK293 whole cell lysate was immunoblotted for endogenous PAK6 using a PAK6 specific antibody and for GAPDH as a loading control. **B)** HEK293 cells were transfected with WT GFP-IQGAP1. The cells were lysed and IQGAP1 was immunoprecipitated using an anti-GFP antibody (IP) from cell lysates. The samples were immunoblotted for endogenous PAK6 using a PAK6 specific antibody and anti-GFP for WT GFP-IQGAP1. The blots in (A) and (B) are representative of 3 independent experiments.

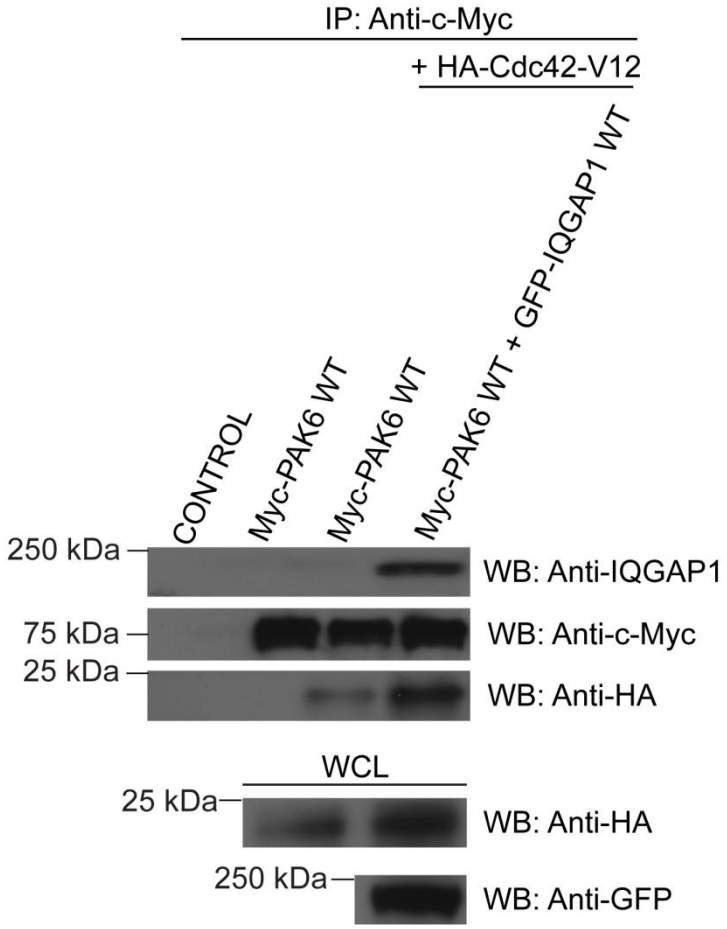

Figure 5.3 Co-immunoprecipitation of PAK6, IQGAP1 and Cdc42-V12. HEK293 cells were transfected with WT Myc-PAK6, WT GFP-IQGAP1 and HA-Cdc42-V12 as indicated. The cells were lysed and WT Myc-PAK6 was immunoprecipitated using an anti-c-Myc antibody (IP) from cell lysates. The samples were immunoblotted for over-expressed WT GFP-IQGAP1 using an anti-GFP antibody, for WT Myc-PAK6 using an anti-c-Myc antibody and for HA-Cdc42-V12 using an anti-HA antibody. Whole cell lysates (WCL) were immunoblotted using anti-HA and anti-GFP antibodies as loading controls. The blots shown are representative of 3 independent experiments.

The limitations of using co-immunoprecipitation techniques to investigate protein-protein interactions are that they do not confirm that proteins pulled down together are in fact directly interacting. For example, PAK6 may be in a binary complex with Cdc42-V12, as may IQGAP1 in **figure 5.3**. Alternative approaches that are more suitable for examining direct protein-protein interactions include protein fractionation, fluorescence resonance energy transfer (FRET) and yeast two-hybrid screening.

5.2.3 Full-length IQGAP1 interacts with the N- and C-termini of PAK6

In order to elucidate whether Cdc42 may mediate the interaction between IQGAP1 and PAK6, domain mutants of PAK6 were co-expressed with full-length WT IQGAP1 (**figure 5.4A**). Co-immunoprecipitation experiments demonstrated that full-length WT IQGAP1 bound to both the N- and C-termini of PAK6 (**figure 5.4B**). The interaction between IQGAP1 and the N-terminal domain of PAK6 may be mediated by Cdc42. However, it is also possible that the ability of IQGAP1 to interact with both the N- and C-terminal of PAK6 is due to PAK6 and/or IQGAP1 forming homodimers. Indeed it has been demonstrated that IQGAP1 self-associates in cells (Ren et al., 2005). Nevertheless, the binding of IQGAP1 to the C-terminal region of PAK6 is likely to be a direct association.

5.2.4 Full-length PAK6 interacts with the N-terminal region of IQGAP1

Having established that IQGAP1 can bind to PAK6, the interaction between full-length PAK6 and IQGAP1 domain mutants was explored. Domain mutants of IQGAP1 were co-expressed with full-length wild-type PAK6 (**figure 5.5A**). Co-immunoprecipitation experiments demonstrated that full-length wild-type PAK6 selectively interacted with the N-terminal region of IQGAP1 (**figure 5.5B**).

Subsequently, the interaction between the C-terminal region of PAK6 and a truncated N-terminal mutant of IQGAP1 was investigated. This mutant encompassed amino acids 717-863 of the N-terminal region of IQGAP1 (IQGAP1$^{717\text{-}863}$) (**figure 5.6A**) and was chosen as it included the IQ domain region of IQGAP1 (amino acids 746-856) (Brown and Sacks, 2006) but not the Cdc42 binding site (Hart et al., 1996; Mataraza et al., 2003a). This domain is known to bind a number of proteins and kinases including calmodulin (Hart et al., 1996), MEK1 and MEK2 (Roy et al., 2005). Thus the IQGAP1$^{717\text{-}863}$ mutant was used to examine the interaction between the C-terminal of

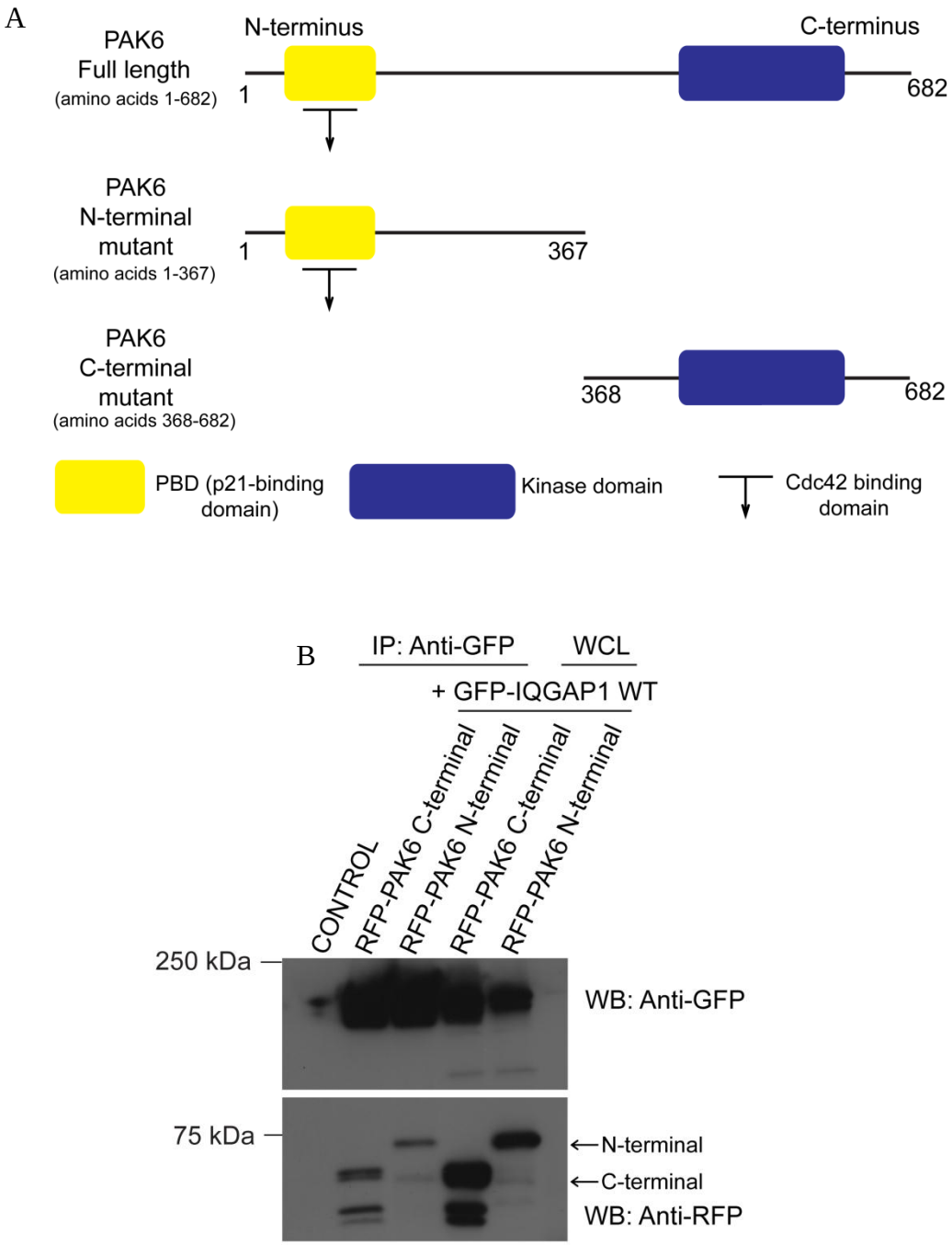

Figure 5.4 IQGAP1 interacts with the N- and C-termini of PAK6. A) Schematic illustrating full-length PAK6 (amino acids 1–682), N-terminal (amino acids 1–367) and C-terminal (amino acids 368–682) PAK6 generated constructs. These constructs were used in subsequent experiments. **B)** HEK293 cells were transfected with N- or C-terminal RFP-PAK6 mutants and WT GFP-IQGAP1 as indicated. The cells were lysed and WT GFP-IQGAP1 was immunoprecipitated using an anti-GFP antibody (IP) from cell lysates. The samples were immunoblotted for WT GFP-IQGAP1 using an anti-GFP antibody and for N- and C-terminal PAK6 mutants using an anti-RFP antibody (arrows). Whole cell lysates (WCL) were immunoblotted using anti-GFP and anti-RFP antibodies as loading controls (arrows). The blots shown are representative of 3 independent experiments.

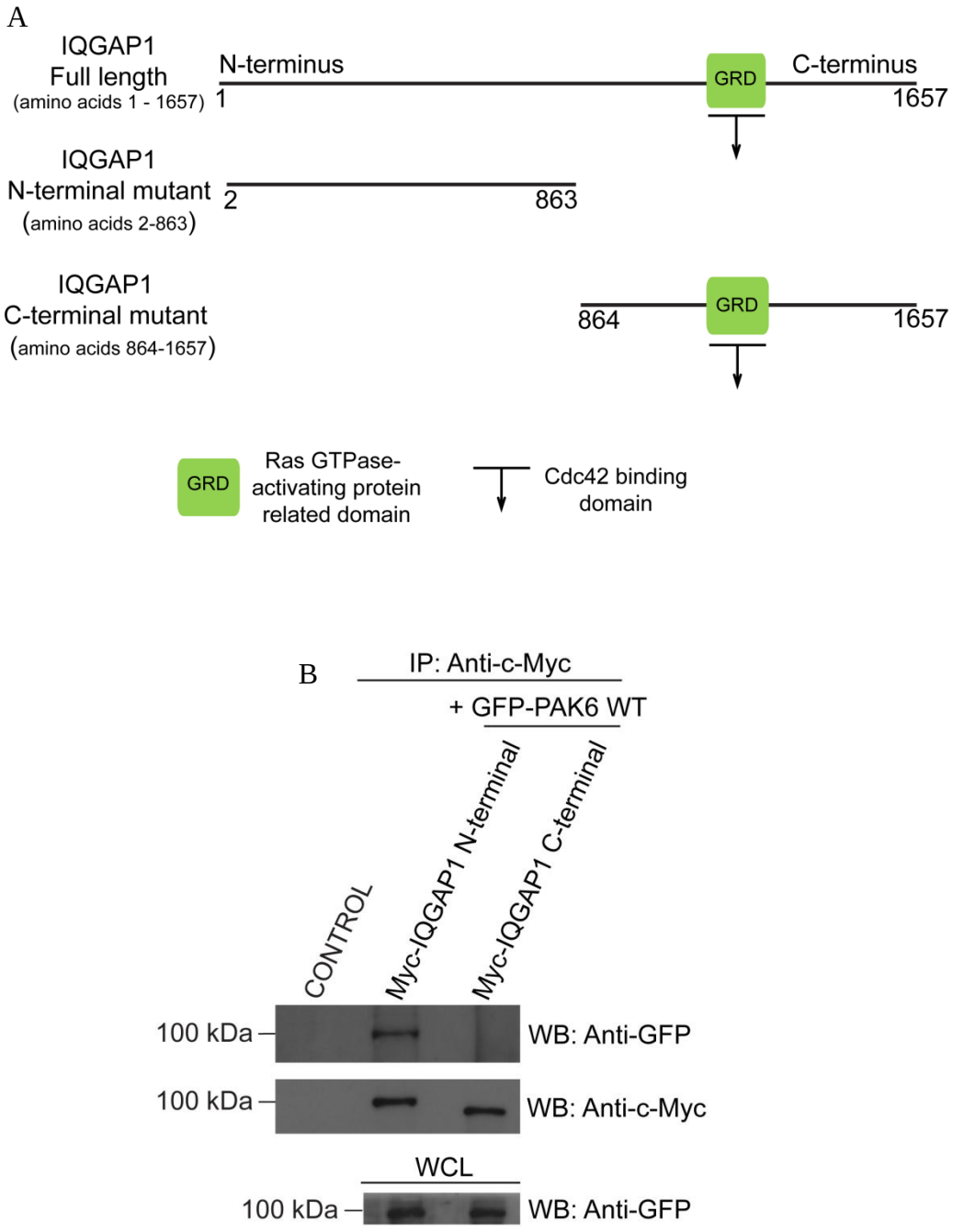

Figure 5.5 PAK6 selectively binds to the N-terminal region of IQGAP1. A) Schematic illustrating full-length IQGAP1 (amino acids 1–1657), N-terminal IQGAP1 (amino acids 2–863) and C-terminal IQGAP1 (amino acids 864-1657) constructs. These constructs were used in subsequent experiments. **B)** HEK293 cells were transfected with N- or C- terminal Myc-IQGAP1 mutants and WT GFP-PAK6 as indicated. The cells were lysed and N- and C-terminal IQGAP1 mutants were immunoprecipitated using an anti-c-Myc antibody (IP) from cell lysates. The samples were immunoblotted for WT GFP-PAK6 using an anti-GFP antibody and for N- and C-terminal Myc-IQGAP1 mutants using an anti-c-Myc antibody. Whole cell lysates (WCL) were immunoblotted using an anti-GFP antibody as a loading control. The blots shown are representative of 3 independent experiments.

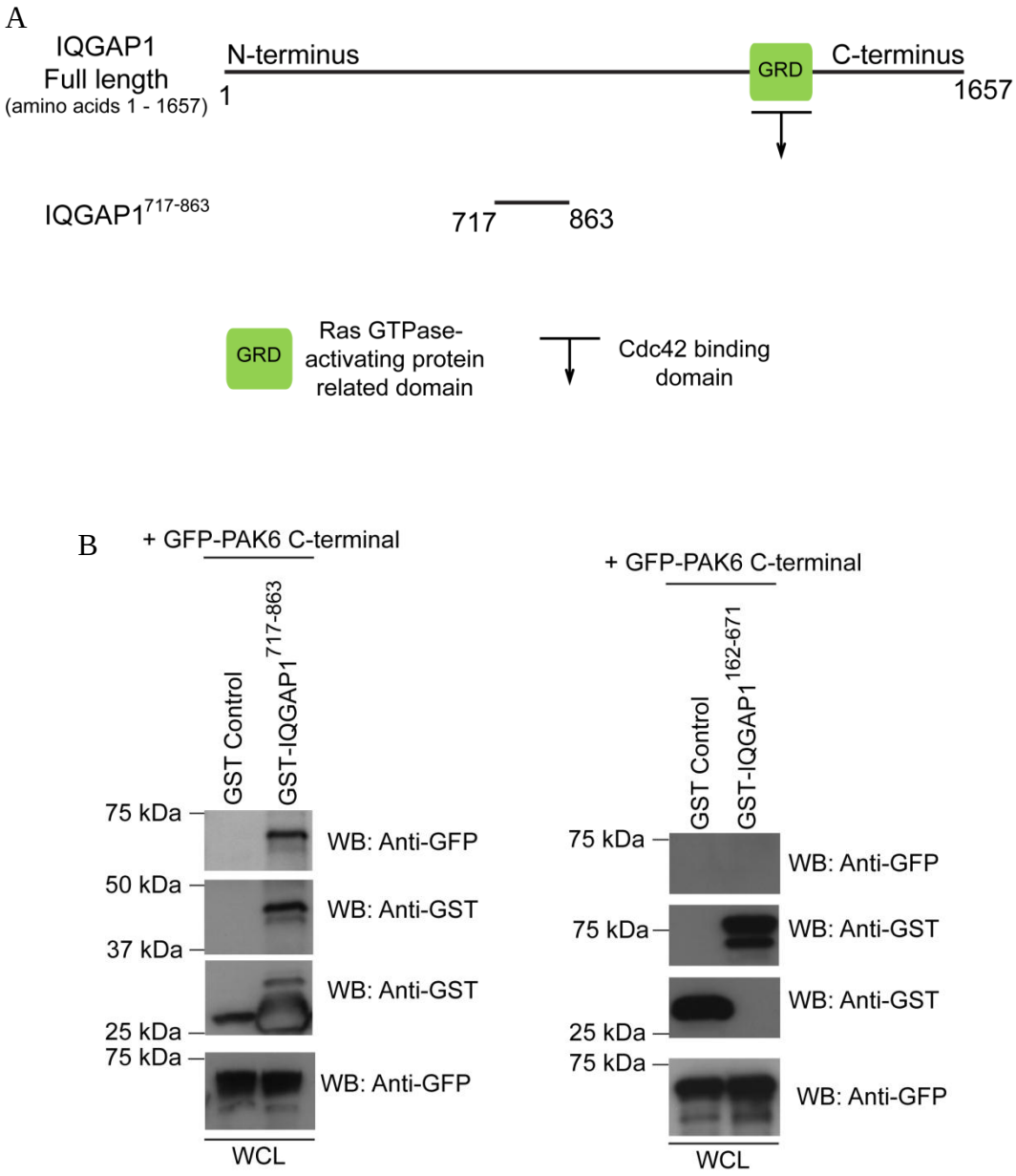

Figure 5.6 The C-terminal region of PAK6 interacts with amino acids 717-863 in the N-terminal region of IQGAP1. A) Schematic illustrating full-length IQGAP1 (amino acids 1–1657) and the truncated N-terminal mutant of IQGAP1 (amino acids 717–863). To protein purify GST-IQGAP1 (GST-IQGAP1$^{717-863}$) *E. coli* BL21-A1 cells were transformed with the expression plasmid and grown to mid-log phase. Protein expression was induced with 0.05% L-Arabinose overnight at 20ºC. **B)** HEK293 cells were transfected with C-terminal GFP-PAK6 mutant as indicated. Cell lysates were subjected to a GST pulldown assay using GST-IQGAP1$^{717-863}$ or GST-IQGAP1$^{162-671}$. GST was used as a control. The samples were immunoblotted for the C-terminal GFP-PAK6 mutant using an anti-GFP antibody and for GST-IQGAP1$^{717-863}$ or GST-IQGAP1$^{162-671}$ and GST alone (control) using an anti-GST antibody. Whole cell lysate samples (WCL) were immunoblotted using an anti-GFP antibody as a loading control. The blots shown are representative of 3 independent experiments.

PAK6 and this region of IQGAP1. This truncated IQGAP1 mutant interacted with the C-terminal PAK6 mutant (**figure 5.6B**). In contrast, PAK6 did not interact with a truncated N-terminal mutant of IQGAP1 encompassing amino acids 162-671 **figure 5.6B**. In summary, the C-terminal half of PAK6 interacts with amino acids 717-863 within the N-terminal region of IQGAP1. Furthermore, Cdc42-V12 was co-immunoprecipitated with PAK6 and IQGAP1. A potential structural conformation between these 3 proteins is illustrated in **figure 5.7**.

Having confirmed the interaction between IQGAP1 and PAK6 in HEK293 cells, an interaction using DU145 cells was explored. Full-length GST-PAK6 bound to endogenous IQGAP1 when using DU145 cells (**Figure 5.8**).

5.2.5 IQGAP1 induces morphological changes and colony escape when expressed alone and when co-expressed with PAK6 in DU145 cells

PAK6 is localised to cell-cell junctions and PAK6 over-expression induces cell elongation in DU145 cells (chapter 4). IQGAP1 is also localised at cell-cell junctions (**figure 5.1B**) and has been found to interact with PAK6 (**figure 5.8**) in these cells. Therefore, the effect of WT IQGAP1 over- expression on DU145 cells was compared to the morphological changes already described for PAK6 (**figure 4.6**). Control cells transfected with GFP were not significantly different in shape when compared to untransfected cells (**figure 5.9A**). WT IQGAP1 expressing DU145 cells exhibited significantly higher elongation ratios when compared to GFP control cells under serum-starved conditions **(figures 5.9A** and **5.9B**). This was similar to the cell shape changes observed for WT PAK6 expressing cells (**figures 4.6A** and **4.6C**). Moreover, when WT GFP-IQGAP1 was co-expressed with WT RFP-PAK6 under these conditions, this elongation phenotype was further enhanced to a significant level when compared to cells expressing WT GFP-IQGAP1 alone (**figures 5.9A** and **5.9B**). WT RFP-PAK6 exhibited similar elongation ratios and localisation as that of WT GFP-PAK6 in DU145 cells (data not shown).

Over-expression of WT PAK6 not only induced cell elongation but also cell colony escape (**figure 4.7**). Having established that WT IQGAP1 also induced cell elongation in DU145 cells, the effect on colony behaviour was also investigated. There was no

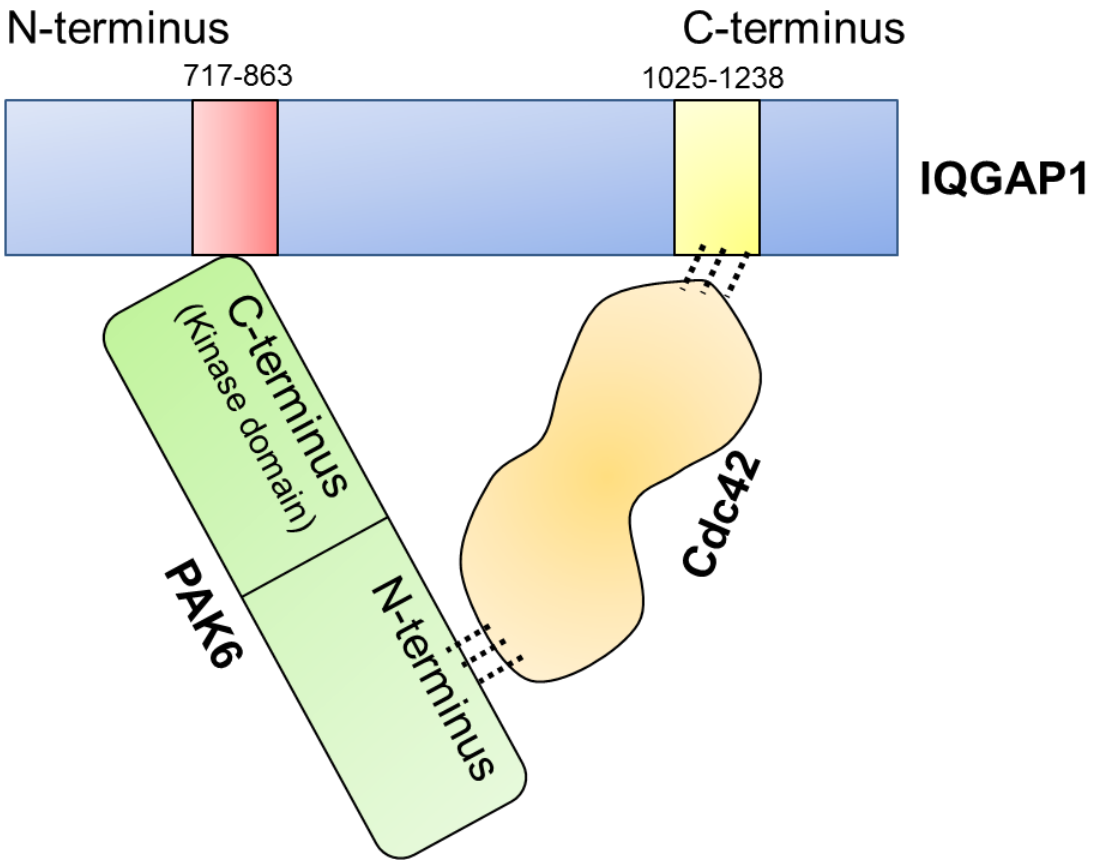

Figure 5.7 Schematic to illustrate the proposed conformation of the interaction between PAK6, **IQGAP1 and active Cdc42**. The C-terminal region of PAK6 interacts with IQGAP1 via amino acids 717-863. Cdc42-V12 was co-immunoprecipitated with these two proteins. GTP-bound Cdc42 is known to interact with PAK6 (Lee et al., 2002) presumably via its N-terminal region, similar to its family members (Abo et al., 1998). IQGAP1 interacts with active Cdc42 via its GRD region (amino acids 1025-1238) in the C-terminal domain (Hart et al., 1996; Mataraza et al., 2003a). Dashed lines represent interactions proposed in the literature as described.

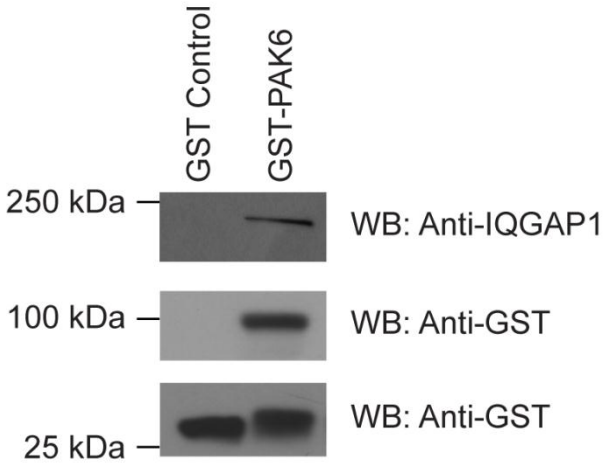

Figure 5.8 PAK6 interacts with IQGAP1 in DU145 cells. DU145 cells were cultured in 10% FBS serum for 48 hours. Cells were then lysed and subjected to a GST-PAK6 pulldown assay. GST was used as a control. The samples were immunoblotted for endogenous IQGAP1 using an anti-IQGAP1 antibody and for GST-PAK6 and GST alone (control) using an anti-GST antibody as indicated. The blots shown are representative of 3 independent experiments.

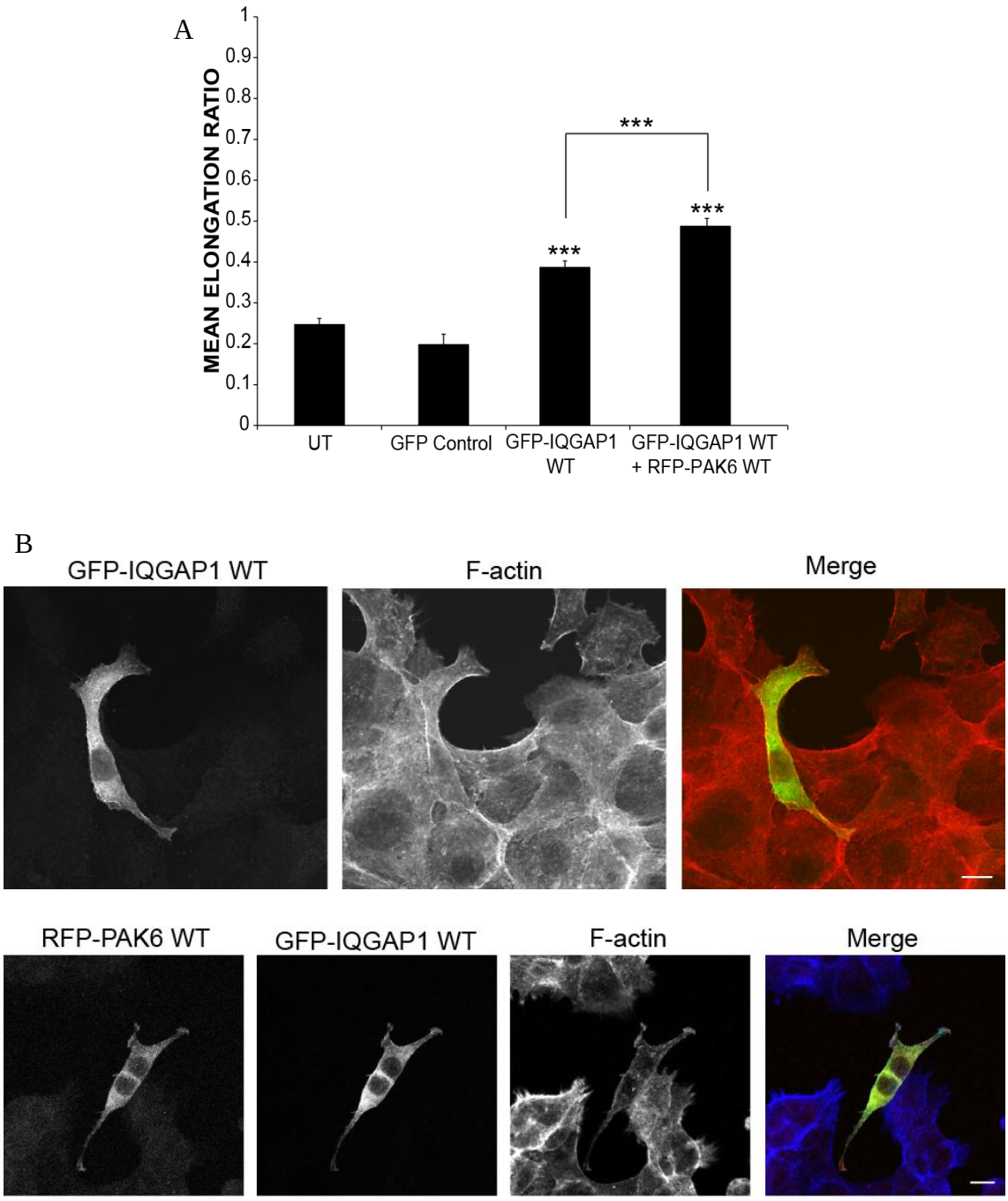

Figure 5.9 IQGAP1 over-expression and co-expression with PAK6 induces morphological changes in DU145 cells. A) DU145 cells were transfected with GFP control vector or WT GFP-IQGAP1 or co-transfected with WT RFP-PAK6 and WT GFP-IQGAP1. Untransfected cells (UT) were treated in the same manner. After 24 hours, cells were serum-starved for 24 hours. Cells were then fixed and stained for F-actin. Shape analysis was performed on the cells using Image J to determine the elongation ratio. **B)** F-actin stained DU145 cells transfected with WT GFP-IQGAP1 or co-transfected with WT RFP-PAK6 and WT GFP-IQGAP1 from (A) were imaged using confocal microscopy. In (A) the mean elongation ratio was calculated for 110 cells per condition over 3 independent experiments. Statistical significance compared with GFP control cells (unless otherwise indicated) was calculated using Student's *t*-test; ***, $P < 0.0005$. Bar = 10 µm.

significant difference in cell colony escape between untransfected and GFP control expressing cells (data not shown). However, reminiscent of WT PAK6 expressing DU145 cells (**figure 4.7**), WT IQGAP1 expressing cells and cells co-expressing WT IQGAP1 and WT PAK6 were uncoupled from neighbouring cells and were no longer within the cell colony (**figure 5.10**). Based on the cell shape and colony escape data, IQGAP1, like PAK6, may be driving colony escape in DU145 cells.

5.2.6 There is an optimal interaction between PAK6 and IQGAP1 following 4 hours HGF stimulation

When cell colonies are responding to HGF, cell-cell dissociation is required (**figure 3.1**). Given that PAK6 and IQGAP1 interact in DU145 cells, and that these proteins function additively to increase cell-cell dissociation, it might be speculated that PAK6 and IQGAP1 interact in an HGF-dependent manner.

Endogenous IQGAP1 was pulled down with GST-PAK6 when growing DU145 cells were used (**figure 5.11A**), as previously shown (**figure 5.8**). Upon serum-starvation, this interaction decreased, although not to a significant level (**figures 5.11A** and **5.11B**). Earlier studies had shown that PAK6 autophosphorylation at serine 560 was elevated following 5, 15 and 30 minutes HGF stimulation (**figures 4.2A** and **4.2B**). Therefore, the level of interaction between PAK6 and IQGAP1 was investigated during early HGF stimulation time points. Although not significant, a small increase in the level of interaction between GST-PAK6 and endogenous IQGAP1 was observed following 30 and 60 minutes HGF stimulation when compared to serum-starved conditions (**figures 5.11A** and **5.11B**). However it is important to note that the input protein levels of endogenous IQGAP1 may be lower in serum-starved conditions when compared to grow conditions. This may influence the level of interaction observed between GST-PAK6 and endogenous IQGAP1. Furthermore, there are limitations in using immobilized GST-PAK6 to detect endogenous protein interactions. Firstly, in contrast to endogenous IQGAP1, GST-PAK6 was not exposed to the variation in conditions, for example serum-starvation and HGF stimulation. In addition, GST-PAK6 may have become saturated with bound endogenous protein which will influence the GST-PAK6-IQGAP1 binding profiles that were observed. Lastly, the GST-PAK6 used was expressed in bacteria and not mammalian cells and thus it could potentially be in quite an inert state. Taken together, there are a number of factors that may influence the

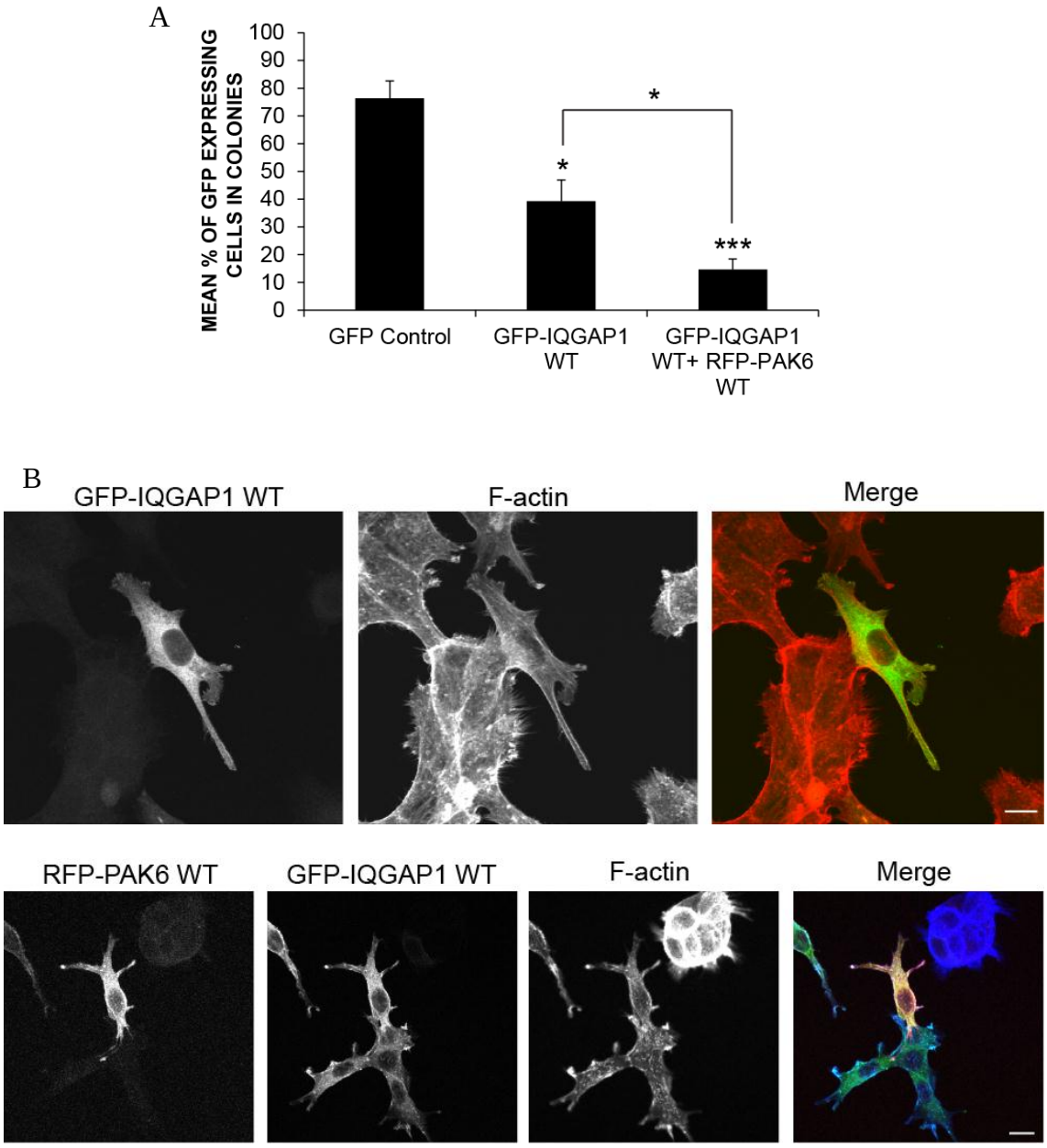

Figure 5.10 IQGAP1 over-expression and co-expression with PAK6 induces colony escape in DU145 cells. A) DU145 cells were transfected with GFP control vector or WT GFP-IQGAP1 or co-transfected with WT RFP-PAK6 and WT GFP-IQGAP1. After 24 hours, cells were serum-starved for 24 hours and then fixed and stained for F-actin. The % of GFP expressing cells present within a colony for each condition was calculated. A cell escaping a colony was defined as either greater than 50% of the cell body perimeter detached from the neighbouring cell(s), cells already escaped from a colony and exhibiting 100% dissociation from the neighbouring cell(s) or cells in a different plane to the underlying cell colony. **B)** F-actin stained DU145 cells transfected with WT GFP-IQGAP1 or co-transfected with WT RFP-PAK6 and WT GFP-IQGAP1 from (A) were imaged using confocal microscopy. In (A) the mean % of GFP expressing cells in colonies was calculated for 110 cells per condition over 3 independent experiments. Statistical significance compared with GFP control cells (unless otherwise indicated) was calculated using Student's *t*-test; *, $P < 0.05$, ***, $P < 0.005$. Bar = 10 µm.

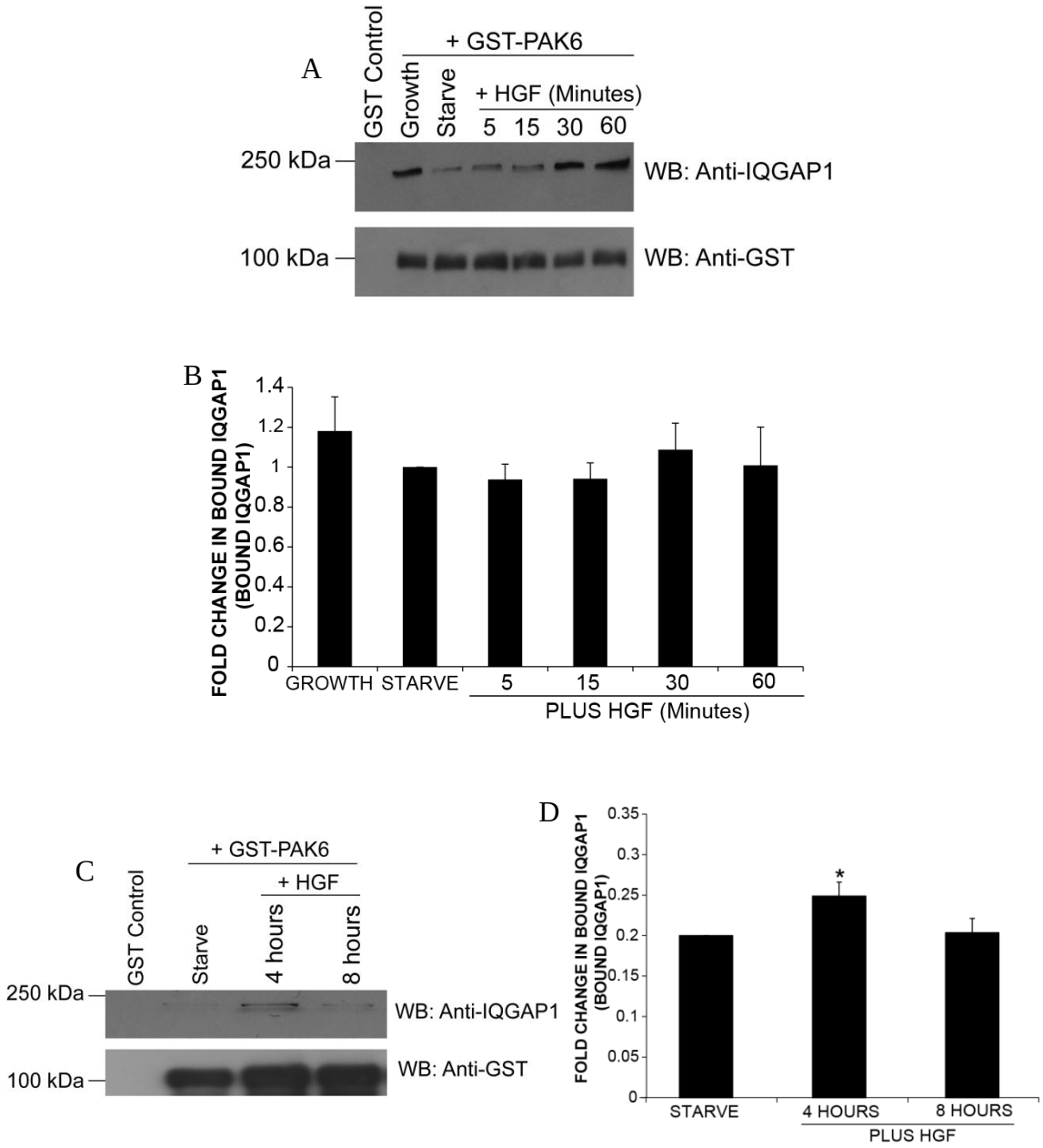

Figure 5.11 PAK6 and IQGAP1 interact downstream of HGF stimulation. A) DU145 cells were serum-starved for 24 hours or replenished with 10% FBS media (Growth). Cells were then left unstimulated (Starve) or stimulated with HGF (500 ng/ml) for the indicated time points. Cells were then lysed and subjected to a GST-PAK6 pulldown assay, using GST as a control. The samples were immunoblotted for endogenous IQGAP1 and for GST-PAK6 using an anti-GST antibody as a loading control. **B)** The level of binding between PAK6 and IQGAP1 was quantified using ANDOR IQ Technology software. **C)** DU145 cells were treated as described in (A). **D)** The level of binding was quantified as in (B). In (A) and (C) GST alone controls were GST positive as demonstrated in figures 5.6 and 5.8. In (B) and (D), the mean fold value representing the amount of bound IQGAP1 was deduced. The standard error of the mean was calculated over 3 independent experiments. Statistical significance compared with serum-starved cells (Starve) was calculated using Student's *t*-test: *, $P < 0.05$.

interaction between GST-PAK6 and endogenous IQGAP1. As cell-cell dissociation in DU145 cells responding to HGF occurs approximately 4 hours post-stimulation (**figure 3.1**), the interaction between PAK6 and IQGAP1 was also examined at later time points. A significant increase in the interaction between GST-PAK6 and endogenous IQGAP1 was observed following 4 hours HGF stimulation when compared to serum-starved conditions (**figures 5.11C** and **5.11D**), thereby correlating with HGF-induced cell-cell dissociation that occurs after 4 hours stimulation (**figure 3.1**). Furthermore, following 8 hours HGF stimulation, the interaction between these two proteins was reduced to near serum-starved levels (**figures 5.11C** and **5.11D**).

5.2.7 There is an optimal interaction between PAK6 and E-cadherin following 4 hours HGF stimulation

It has been demonstrated that the interaction between PAK6 and IQGAP1 is optimal following 4 hours stimulation with HGF (**figures 5.11C** and **5.11D**) which correlates with E-cadherin cell junction disassembly (**figure 3.1**). IQGAP1 is known to interact with E-cadherin (Kuroda et al., 1998), and it has been shown that PAK6 can localise to E-cadherin-positive junctions (**figure 4.13**). Furthermore, E-cadherin is retained at cell-cell junctions in PAK6 knockdown cells downstream of HGF (**figure 4.12B**). Therefore, the possibility of an interaction between PAK6 and E-cadherin was investigated.

In serum-starved conditions, bacterially purified GST-PAK6 bound to endogenous E-cadherin (**figure 5.12A**). Following 4 hours of HGF stimulation, where characteristically E-cadherin begins to move away from cell-cell junctions in DU145 cells (**figure 3.1**) there was a significant increase in the level of interaction between GST-PAK6 and endogenous E-cadherin when compared to serum-starved cells (**figures 5.12A** and **5.12B**). Additionally, the interaction between GST-PAK6 and E-cadherin diminished following 8 hours HGF stimulation when compared to 4 hours stimulation (**figures 5.12A** and **5.12B**), similar to the interaction trend observed between GST-PAK6 and IQGAP1 (**figures 5.11C** and **5.11D**). Furthermore, GST-PAK6, endogenous IQGAP1 and endogenous E-cadherin were pulled down together using serum-starved DU145 cells, as well as following 4 hours HGF stimulation (**figure 5.12C**). However,

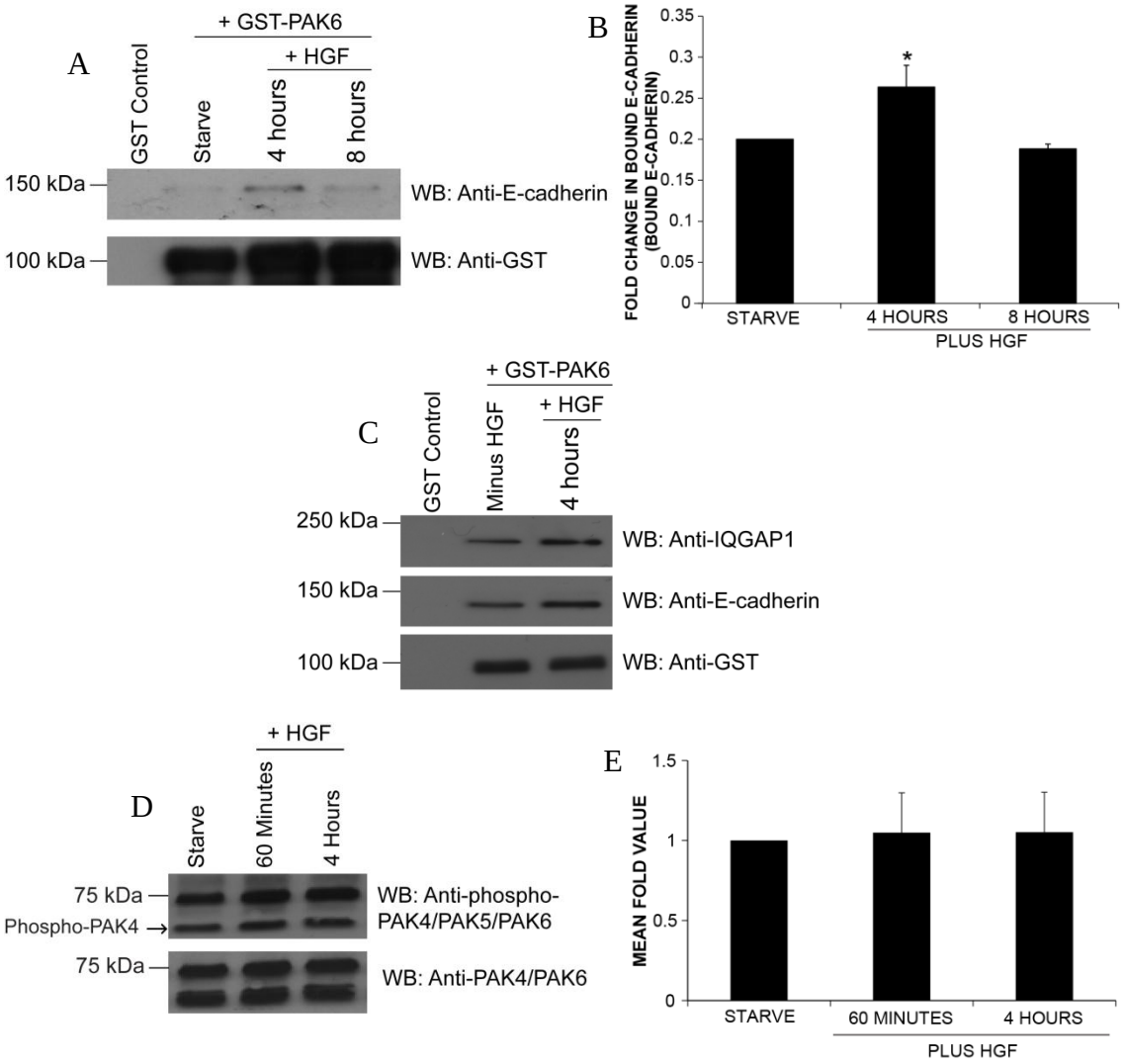

Figure 5.12 PAK6 and E-cadherin interact downstream of HGF stimulation. A) Serum-starved DU145 cells were left unstimulated (Starve) or stimulated with HGF (500 ng/ml) for 4 or 8 hours. Cells were then lysed and subjected to a GST-PAK6 pulldown assay. GST was used as a control. The samples were immunoblotted for endogenous E-cadherin and for GST-PAK6 using an anti-GST antibody as a loading control. **B)** The level of binding between PAK6 and E-cadherin was quantified using ANDOR IQ Technology software. **C)** DU145 cells were treated as described in (A) and immunoblotted for endogenous IQGAP1 and E-cadherin and for GST-PAK6 using an anti-GST antibody as a loading control. **D)** DU145 cells were seeded at a density that correlated with the HGF-induced scatter assay. Serum-starved DU145 cells were left unstimulated (Starve) or stimulated with HGF (10 ng/ml) for 60 minutes and 4 hours prior to lysis. Lysates were immunoblotted for levels of PAK6 autophosphorylation at serine 560 using a phospho-PAK4/PAK5/PAK6 antibody. Blots were re-probed for total PAK6 expression using an anti-PAK4/PAK6 antibody. **E)** Changes in the levels of autophosphorylation at serine 560 in (D) were quantified using ANDOR IQ Technology software. In (A) and (C) GST alone controls were GST positive as demonstrated in figures 5.6 and 5.8. In (B) the mean fold value representing the amount of bound E-cadherin and in (E) the changes in the level of PAK6 autophosphorylation at serine 560 were quantified. The standard error of the mean was calculated over 3 independent experiments. Statistical significance compared with serum-starved cells (Starve) was calculated using Student's *t*-test: *, $P < 0.05$.

no significant change in PAK6 autophosphorylation at serine 560 was detected at longer HGF stimulation time points, including after 4 hours (**figures 5.12D** and **5.12E**).

5.2.8 PAK6 phosphorylation levels are elevated in the presence of IQGAP1

IQGAP1 binds to the C-terminal region of PAK6 which encompasses the kinase domain (**figure 5.6**). Thus, it was hypothesised that IQGAP1 may be a substrate for PAK6. Indeed, it has been shown in the literature that IQGAP1 is phosphorylated at serine 1443, potentially by the serine/threonine kinase protein kinase C (PKC) epsilon, and this in turn can alter the function of IQGAP1 (Grohmanova et al., 2004). This hypothesis was tested using a radioactive *in vitro* kinase assay. GST-PAK6 did not phosphorylate over-expressed WT IQGAP1 *in vitro* as incorporated [γ-^{32}P] ATP was not detected at the size of WT GFP-IQGAP1 (approximately 220 kDa) or above. However, unexpectedly, the presence of WT IQGAP1 induced an increase in the phosphorylation levels of GST-PAK6, when compared to the phosphorylation levels of GST-PAK6 in the absence of WT IQGAP1 (**figure 5.13A)**. Therefore, this suggests that IQGAP1 is not a PAK6 substrate but that the presence of IQGAP1 elevates the levels of PAK6 phosphorylation.

IQGAP1 is able to interact with other kinases, such as MEK1 and MEK2, and in turn indirectly modulates their activation status (Roy et al., 2005). It has been demonstrated previously that PAK6 autophosphorylation levels at serine 560 increased upon HGF stimulation (**figure 4.2**). In addition, phosphorylation at this residue has been reported to be required for MKK6-mediated activation of PAK6 (Kaur et al., 2005). Therefore, WT or dominant-negative IQGAP1 were over-expressed with WT PAK6 and the levels of PAK6 autophosphorylation at serine 560 were examined (**figure 5.13B**). Dominant-negative IQGAP1 lacks the GRD domain, where active Cdc42 binds, and thereby reduces the level of GTP-Cdc42 bound to IQGAP1 (Swart-Mataraza et al., 2002). However, phosphorylation levels at this residue were unaltered in the presence of the IQGAP1 constructs tested (**figure 5.13B**). Thus, the presence of IQGAP1 does not affect the levels of autophosphorylation at serine 560 on PAK6, implying that IQGAP1 affects PAK6 phosphorylation levels on another site.

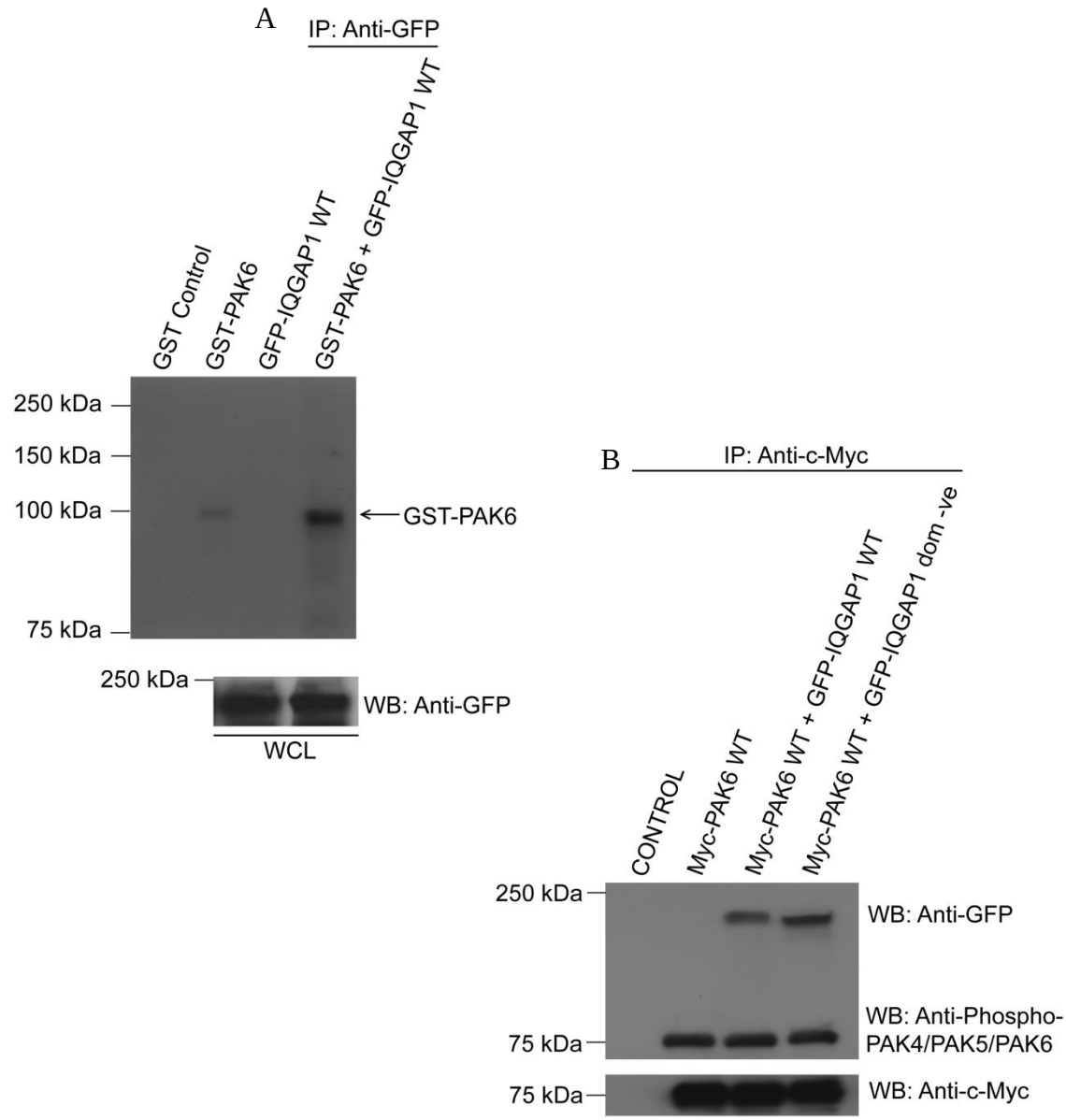

Figure 5.13 IQGAP1 expression increases PAK6 phosphorylation levels. A) HEK293 cells were transfected with WT GFP-IQGAP1 as indicated. The cells were lysed and IQGAP1 was immunoprecipitated using an anti-GFP antibody (IP) from cell lysates and mixed with or without GST-PAK6 as indicated. An *in vitro* kinase assay was performed using [γ-^{32}P] ATP. GST-PAK6 alone was also subjected to the *in vitro* kinase assay and GST was used as a control. Whole cell lysates (WCL) were immunoblotted using an anti-GFP antibody as a loading control. **B)** HEK293 cells were transfected with WT Myc-PAK6, or co-transfected with WT Myc-PAK6 and WT GFP-IQGAP1 or dominant-negative (dom –ve) GFP-IQGAP1. The cells were lysed and WT Myc-PAK6 was immunoprecipitated using an anti-c-Myc antibody (IP) from cell lysates. The samples were immunoblotted for GFP-IQGAP1 using an anti-GFP antibody and also for WT Myc-PAK6 using an anti-c-Myc antibody as a loading control. The IP samples were immunoblotted for levels of PAK6 autophosphorylation at serine 560 using a phospho-PAK4/PAK5/PAK6 antibody. In (A) and (B) the blots shown are representative of 3 independent experiments.

5.3 Discussion

In this chapter, an interaction between PAK6 and IQGAP1 has been established in DU145 cells for the first time. IQGAP1 was found to induce cell elongation and a cell colony escape phenotype in DU145 cells, similar to that observed for PAK6 expressing cells in chapter 4. Endogenous E-cadherin and IQGAP1 were pulled down with PAK6 and the association between PAK6 and these proteins was maximal following 4 hours HGF stimulation. In addition, it was demonstrated that the presence of IQGAP1 increases PAK6 phosphorylation levels.

IQGAP1 is known to be over-expressed in numerous types of cancer including colorectal (Nabeshima et al., 2002), hepatocellular (Chen et al., 2010) and ovarian carcinomas (Dong et al., 2006), as well as in breast cancer epithelial cells (Jadeski et al., 2008); however its expression in prostate cancer cells has not been documented. In this study, IQGAP1 was found to be expressed in DU145 cells.

IQGAP1 is known to bind to kinases such as ERK1/2 and MEK1/2 and these interactions are important for MAPK signalling (Roy et al., 2005). IQGAP1 also interacts with PAK6 in MCF7 breast cancer cells (Kaur et al., 2008); however the significance of this association has yet to be elucidated. An interaction between PAK6 and IQGAP1 was confirmed using an endogenous IP protocol and a GST pulldown assay. This association was detected in the absence of HGF stimulation; consistent with this, the interaction between IQGAP1 and ERK2 did not require EGF stimulation (Roy et al., 2004). However, over-expressed IQGAP1 must associate with ERK2 for the regulation of EGF-induced ERK2 stimulation (Roy et al., 2004). Therefore, it could be speculated that whilst IQGAP1 and PAK6 are able to interact in the absence of HGF stimulation, the presence of IQGAP1 may be required for HGF-induced PAK6 activation and/or for the function of PAK6 downstream of HGF.

In the GST pulldown assay, only endogenous IQGAP1, and not GST-PAK6, was exposed to serum-starved conditions and to HGF stimulation. The data presented indicates an increase in the association of IQGAP1 to GST-PAK6 upon HGF addition when compared to serum-starvation. This suggests that HGF may modulate IQGAP1 and consequently enhance its interaction with GST-PAK6. For example, HGF may

modify the conformation of IQGAP1 and thereby make the PAK6 binding site on IQGAP1 more accessible. Additionally, the presence of HGF may induce the phosphorylation of IQGAP1; indeed EGF has been shown to induce the phosphorylation of IQGAP1 at serine 1443 via protein kinase C (McNulty et al., 2011). Moreover, phosphorylation of IQGAP1 at this site was also detected upon cell-cell junction disassembly (Grohmanova et al., 2004).

Full-length IQGAP1 was found to interact with both the N- and C-terminal regions of PAK6. The N-terminal region of PAK6 possesses a PBD domain, to which the activated form of Cdc42 is known to interact (Lee et al., 2002). IQGAP1 is also known to interact with GTP-bound Cdc42 (Hart et al., 1996; Kuroda et al., 1996). It is likely that the association of full-length IQGAP1 with the N-terminal region of PAK6 is mediated by Cdc42, rather than a direct interaction. Furthermore, PAK6 may be associated with IQGAP1 and Cdc42. More recently, it has been shown that PAK6 interacts with the atypical Rho GTPase, RhoV (Shepelev and Korobko, 2012), which shares close sequence homology with Cdc42 (Aronheim et al., 1998). Thus, it could also be speculated that PAK6 may interact with both RhoV and IQGAP1. Furthermore, RhoV has also been implicated in cytoskeletal modulation (Aronheim et al., 1998).

The C-terminal kinase domain containing region of PAK6 interacted with the N-terminal of IQGAP1; this region of IQGAP1 also binds to the kinase domain of the EGFR (McNulty et al., 2011). IQGAP1 modulates the activation of the EGFR and subsequent signalling through this association (McNulty et al., 2011). Further binding studies in this chapter revealed that the C-terminal half of PAK6 bound to a region spanning the IQ domain, similar to the IQGAP1 binding reported for the kinases MEK1 and MEK2 (Roy et al., 2005). In this interaction IQGAP1 acts as a scaffold where its interaction with ERK is speculated to induce a conformational change that triggers an increased association with MEK, thereby allowing subsequent MEK-mediated ERK activation (Roy et al., 2005). It could be speculated that IQGAP1 might play a similar scaffolding role where it allows the interaction between PAK6 and a downstream substrate/upstream regulator.

This direct interaction of IQGAP1 is similar to that described for identified binding partners of other PAK family members. DGCR6L, a protein implicated in cancer

metastasis, is known to bind to the C-terminal region of PAK4 and modulate PAK4-induced cell migration, via LIM kinase 1 (LIMK1), in gastric cancer cells (Li et al., 2010). In addition, this association increased PAK4-mediated phosphorylation of LIMK1 (Li et al., 2010). In contrast, the intracellular protein nischarin modulates cell migration by binding to the C-terminal region of PAK1 in its activated conformation (Alahari et al., 2004). This in turn inhibits the ability of PAK1 to phosphorylate other proteins (Alahari et al., 2004). Thus interactions via the C-terminal of PAKs are important in signal transduction modulation.

Once the interaction between PAK6 and IQGAP1 had been examined, the functional significance of the association between these two proteins was assessed. Over-expressed WT IQGAP1 was found to induce cell elongation and colony escape in serum-starved DU145 cells. Consistent with this cell-cell dissociation phenotype of IQGAP1 expressing cells, cell-cell dissociation assays have shown that in EL cells the majority of IQGAP1 expressing cells were dissociated and visible as single cells (Kuroda et al., 1998). In contrast, control cells did not dissociate and persisted in aggregates (Kuroda et al., 1998). Thus, Kuroda et al. demonstrated that expression of IQGAP1 increased the ability of epithelial cells to detach from one another, in the absence of growth factor stimulation. This is consistent with the colony escape phenotype observed here. IQGAP1 regulates actin dynamics and the over-expression of WT IQGAP1 is also known to induce actin microspikes and filopodia in MCF7 breast cancer cells (Swart-Mataraza et al., 2002). Interestingly, IQGAP1-expressing cells appeared to exhibit a colony escape phenotype in the study by Swart-Mataraza et al.; however the authors did not comment on nor quantify this phenotype.

In this chapter not only did over-expression of IQGAP1 drive cell colony escape, but co-expression with PAK6 increased the level of cell-cell dissociation. Thus there would appear to be a synergistic relationship between these two proteins. One possibility is that IQGAP1 is a PAK6 substrate. Indeed, phosphorylation of specific residues on IQGAP1 can modify its function by altering its association with other proteins, as well as its conformation or its dimerisation, and in turn affect its interaction with the actin cytoskeleton (Grohmanova et al., 2004; Li et al., 2005b). However, no phosphorylation of IQGAP1 was detected in the presence of PAK6 using a radioactive *in vitro* kinase assay. In contrast, the presence of over-expressed IQGAP1 increased the levels of GST-

PAK6 phosphorylation in this *in vitro* kinase assay. It is unlikely that this increase in PAK6 phosphorylation levels is as a result of a second kinase bound to IQGAP1 in the immunoprecipitate as incorporation of radioactivity was not detected anywhere else on the blot. Thus, it is likely that the increase in phosphorylation of PAK6 observed in the presence of IQGAP1 is as a result of PAK6 phosphorylating itself. In addition, the presence of IQGAP1 may alter the conformation of the PAK6 kinase domain. Interestingly, a recent report has demonstrated the ability of IQGAP1 to regulate the activity of Aurora-A kinase (Yin et al., 2012), a serine/threonine kinase that has been associated with human malignancy (Wang et al., 2006). Similar to the results obtained here, over-expression of IQGAP1 is thought to increase Aurora-A phosphorylation levels (Yin et al., 2012).

Whilst IQGAP1 does not possess the ability to phosphorylate proteins, it is known to modulate the activation status of other kinases through its ability to function as a scaffold protein, for example in the MAPK signalling pathway (Roy et al., 2005). In this pathway, IQGAP1 is able to directly interact with ERK2 and modulate its activity in MCF7 cells (Roy et al., 2004). In addition, IQGAP1 plays a pivotal role in regulating the activation of MEK1, upstream of ERK1 (Roy et al., 2005). The increased autophosphorylation detected in the *in vitro* kinase assay is unlikely to be focussed on serine 560 as co-expression of IQGAP1 and PAK6 does not modulate phosphorylation levels at this site. This suggests that there are other autophosphorylation sites on PAK6. Indeed, the correlation between serine 560 autophosphorylation and activity is not clearly defined. PAK6 autophosphorylation levels at serine 560 increased downstream of HGF at early time points as described in chapter 4; however, autophosphorylation levels at this residue did not increase to a significant level after 4 hours HGF addition, when IQGAP1 and E-cadherin interactions with PAK6 are maximal. Either PAK6 activity is not regulated by phosphorylation at serine 560 or PAK6 activity is not elevated at later time points. Furthermore, an increase in PAK6 activity was not detected when point mutating the serine 560 residue (**figure 4.4**). It is also possible that transient phosphorylation of PAK6 via HGF is sufficient for downstream signal propagation or that initial serine 560 autophosphorylation induces the phosphorylation of PAK6 at other sites that are required for an optimal interaction with IQGAP1 and E-cadherin.

Both IQGAP1 and PAK6 were found to be localised at E-cadherin-positive junctions in DU145 cells. This junctional localisation of IQGAP1 has been reported in different cell types including in MDCK cells (Kuroda et al., 1996) and MCF7 cells (Li et al., 1999; Swart-Mataraza et al., 2002), as well as its co-localisation with E-cadherin at sites of cell-cell contact (Kuroda et al., 1998; Li et al., 1999). Thus, data presented here would suggest that PAK6 and IQGAP1 both mediate the dissolution of cell-cell junctions downstream of HGF. Indeed, an increased interaction between PAK6 and IQGAP1 was detected following HGF stimulation which correlated in time with cell-cell dissociation (**figure 5.11C** and **figure 3.1**). This provides further evidence that PAK6 and IQGAP1 are functioning in an HGF-dependent pathway. This is in contrast to EGF, which did not modify the association between ERK2 and IQGAP1 (Roy et al., 2004). Moreover, the maximal interaction between PAK6 and E-cadherin was also observed within the same time frame (**figure 5.12A**). Furthermore, PAK6 bound to IQGAP1 and E-cadherin downstream of HGF stimulation at this time point (**figure 5.12C**).

Data presented here argue that IQGAP1 binds to and regulates PAK6 and that PAK6 and IQGAP1 are involved in HGF-induced cell scattering in DU145 cells.

5.3.1 Future work

In this chapter, PAK6 was found to interact with IQGAP1. Cdc42-V12 was also co-immunoprecipitated with these proteins. However, co-immunoprecipitation does not represent direct associations between proteins. An approach that could be implemented to directly examine protein-protein interactions includes subcellular fractionation. Furthermore, as PAK6 and IQGAP1 both interact with the GTP-bound form of Cdc42 (Hart et al., 1996; Lee et al., 2002), it would be useful to try and elucidate if this interaction is important during the cell-cell dissociation process in DU145 cells.

The presence of IQGAP1 was found to increase PAK6 autophosphorylation levels in the *in vitro* kinase assay that was conducted. However, this assay was performed in steady-state conditions; thus it would be useful to perform this experiment in the presence of HGF at different time points, particularly following 4 hours HGF stimulation, as this was identified as a significant time point during the cell-cell dissociation process. Furthermore, the levels of endogenous IQGAP1 and E-cadherin bound to GST-PAK6 were elevated 4 hours post-HGF stimulation. Moreover, as IQGAP1 is not a kinase, it would interesting to elucidate the mechanism by which IQGAP1 induces an increase in PAK6 autophosphorylation.

Whilst PAK6 and IQGAP1 may function together during HGF-induced cell-cell contact disassembly, data from this study suggest that IQGAP1 is unlikely to be a PAK6 substrate. Thus it would be useful to isolate PAK6 substrates that may be involved in this process. For example, a potential candidate as a PAK6 substrate is p120 catenin, a junctional protein that binds E-cadherin (Daniel and Reynolds, 1995) and is important in the maintenance of cell-cell adhesivity (Davis et al., 2003), is known to bind to PAK6 and is also phosphorylated by both PAK4 and PAK5 (Wong et al., 2010).

Chapter 6
Concluding Remarks

Chapter 6 - Concluding Remarks

In this study it has been demonstrated that DU145 prostate cancer cells scatter in response to HGF stimulation and this is supported on a range of substrata. As a consequence, this scatter model was then used to investigate the potential role of PAK6 in prostate cancer cell dissemination. Depletion of PAK6 expression was found to inhibit the HGF-induced cell-cell junction dissolution and subsequent cell scattering. In contrast, over-expression of PAK6 drove cell-cell dissemination; a process dependent on PAK6 kinase activity. Furthermore, PAK6 was localised at E-cadherin-positive junctions. Subsequently, PAK6 was found to interact with the junctional protein IQGAP1, in an HGF-dependent manner. Thus, PAK6 and IQGAP1 may collaborate downstream of HGF to induce cell-cell dissociation in DU145 prostate cancer cells.

The question is how PAK6 and/or IQGAP1 achieve junction disassembly in DU145 cells. There is already considerable evidence to suggest a key role for IQGAP1 in junction disassembly in other cell types. In gastric cancer cells, junctional localisation of IQGAP1 has been linked to a reduction in E-cadherin-mediated cell-cell adhesion (Takemoto et al., 2001). IQGAP1 also localises at cell-cell junctions in MCF7 breast cancer cells (Swart-Mataraza et al., 2002) and the increased junctional localisation of this protein correlates with a reduction in E-cadherin localisation at sites of cell-cell contact in breast cancer cells (Li et al., 1999). Moreover, IQGAP1 has been shown to negatively modulate cell-cell adhesion in MDCK II colony-forming cells downstream of HGF (Fukata et al., 2001).

How IQGAP1 drives junction disassembly is not clearly elucidated. Historically, IQGAP1 was thought to contribute to a reduction in cell-cell adhesivity through its association with β-catenin (Kuroda et al., 1998). It was proposed that this interaction with β-catenin induces α-catenin displacement from the E-cadherin-β-catenin complex *in vitro* and *in vivo* (Kuroda et al., 1998) and that removal of α-catenin weakens these adhesions (Kuroda et al., 1998; Ozawa and Kemler, 1998), thereby inducing cell scattering (Fukata et al., 2001). However, more recently α-catenin dissociation from β-catenin has been linked to junction stabilisation (Benjamin and Nelson, 2008; Drees et al., 2005). Nevertheless, several studies have shown that α-catenin expression is lost in

gastric and breast scirrhous adenocarcinomas (Ochiai et al., 1994) and in human lung adenocarcinoma PC9 cells (Watabe et al., 1994); furthermore, these cell types also exhibit a scattered phenotype (Ochiai et al., 1994; Watabe et al., 1994).

Data presented here demonstrate that E-cadherin, IQGAP1 and PAK6 can be pulled down together. Thus what needs to be addressed is how PAK6 would fit into an E-cadherin-IQGAP1 cell-cell junction dissociation model. There is no evidence to suggest that IQGAP1 is a PAK6 substrate; however, it could be speculated that β-catenin may be a potential substrate for PAK6. PAK1 (Zhu et al., 2011) and PAK4 (Li et al., 2011) both phosphorylate β-catenin at serine 675. Moreover, the hyper-phosphorylation of β-catenin on serine/threonine residues has been shown to induce the loss of cell-cell junction sites in human epidermal cells (Serres et al., 1997) and Jun N-terminal kinase (JNK) phosphorylates β-catenin at serine 37 and threonine 41, which induces the loss of cell-cell contacts (Lee et al., 2009). In contrast, inhibition of JNK kinase activity leads to a reduction in the phosphorylation of β-catenin and promotes cell-cell adhesion (Lee et al., 2009).

Furthermore, the junctional protein p120 catenin also binds E-cadherin (Jou et al., 1995) and is important for the stabilisation of cell-cell junctions (Ireton et al., 2002). Indeed it has been demonstrated that siRNA-induced depletion of p120 catenin lead to the rapid turnover and degradation of E-cadherin as well as the subsequent loss of cell-cell junctions (Davis et al., 2003). Interestingly, group II PAKs were recently reported to associate with this catenin family member (Wong et al., 2010). Wong et al. demonstrated that p120 catenin interacts with PAK5 with the highest affinity, followed by PAK6, whereas p120 catenin bound PAK4 with the lowest affinity (Wong et al., 2010). However whilst an interaction between PAK6 and p120 catenin was detected, the authors only tested the phosphorylating potential of PAK4 and PAK5 (Wong et al., 2010). Activated PAK4 phosphorylated p120 catenin *in vitro* and *in vivo*, as did wild-type PAK5 (Wong et al., 2010). Thus it cannot be rules out that PAK6 may also phosphorylate p120 catenin and the interaction detected between PAK6 and p120 catenin suggests a functional relationship between these two proteins. In addition to serine/threonine phosphorylation of p120 catenin (Wong et al., 2010; Xia et al., 2003) it has also been suggested that the N-terminal region of p120 catenin, encompassing the phosphorylation domain, confers an inhibitory effect on intercellular adhesivity (Aono

et al., 1999). Taken together, it could be speculated that PAK6 phosphorylates p120 catenin which in turn triggers the degradation of E-cadherin and subsequent cell-cell dissociation.

Given the strong link between PAKs, serine/threonine phosphorylation of β-catenin and cell-cell dissociation, it might be imagined that during HGF-induced cell scattering PAK6 functions as follows (**figure 6.1**). Stimulation through HGF of cells with strong E-cadherin-positive junctions induces serine 560 autophosphorylation of PAK6 (other sites on PAK6 may also be phosphorylated as a result of HGF addition). At 4 hours post-HGF stimulation, there is an optimal interaction between E-cadherin, PAK6 and IQGAP1 which correlates with cell-cell dissociation. During the interaction between PAK6 and IQGAP1, PAK6 autophosphorylation levels are increased, which may potentially allow for increased substrate phosphorylation. Thus, the interaction between PAK6 and IQGAP1 may induce an increase in exogenous PAK6 activity. Given that IQGAP1 and E-cadherin both interact with β-catenin (Kuroda et al., 1998), PAK6 may also potentially phosphorylate β-catenin. These events may in turn trigger α-catenin dissociation from the E-cadherin-β-catenin complex, thereby inducing cell-cell dissociation. This model does speculate that PAK6 phosphorylates β-catenin and that the phosphorylation of β-catenin leads to junctional breakdown. Moreover, it favours a model where IQGAP1-mediated dissociation of α-catenin from β-catenin promotes cell-cell adhesion disassembly. However, it is important to clarify that the outcome of α-catenin dissociation from the cadherin complex has yet to be fully established.

PAK6 interacts with the GTP-bound form of Cdc42 (Lee et al., 2002) as does IQGAP1 (Hart et al., 1996). However, the interaction of active Cdc42 does not enhance the activity of PAK6 (Lee et al., 2002), which is required for cell colony escape. GTP-bound Cdc42 could potentially mediate the localisation of PAK6 at cell-cell junctions; indeed it has been reported that active Cdc42 induces the re-localisation of PAK4 (Abo et al., 1998) and X-PAK5 (Cau et al., 2001). Thus Cdc42 may be involved in the IQGAP1-PAK6-modulated cell-cell dissociation process. However, there are conflicting views as to how Cdc42 contributes to cell-cell adhesion strength modulation, which is clearly a tightly regulated and complex process (Keely et al., 1997; Kodama et al., 1999).

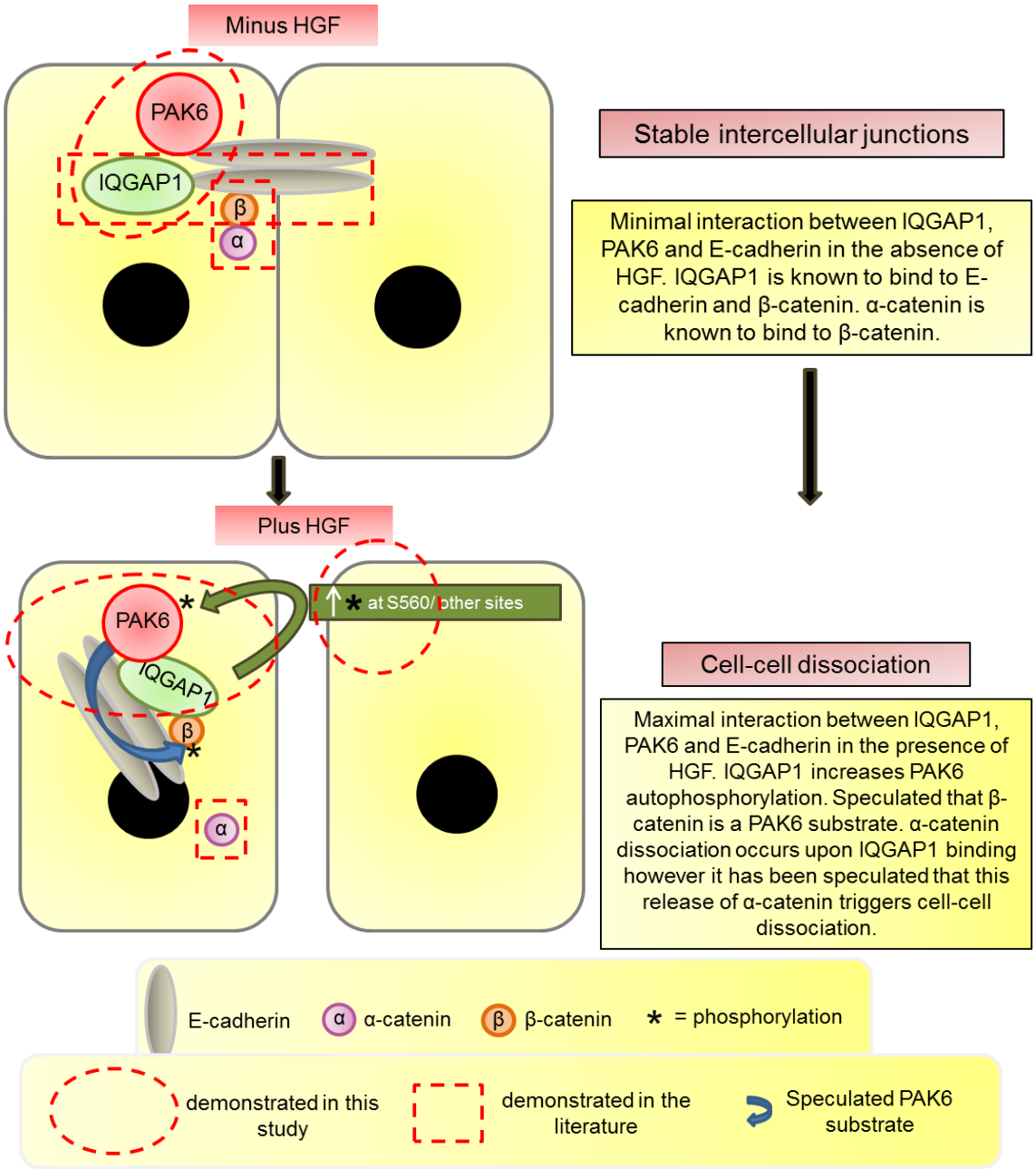

Figure 6.1 A proposed model for the role of PAK6, acting with IQGAP1, in HGF-induced cell-cell dissociation in DU145 prostate cancer cells. In the absence of HGF, there is a minimal interaction between E-cadherin-PAK6-IQGAP1 at cell-cell junctions. α-catenin is bound to β-catenin, which in turn is associated with E-cadherin, leading to strong intercellular adhesions. Upon HGF stimulation, PAK6 autophosphorylation levels are increased (other PAK6 sites may also be phosphorylated). A maximal interaction occurs between E-cadherin-PAK6-IQGAP1 (this interaction may also include β-catenin) 4 hours post-HGF stimulation. IQGAP1 increases PAK6 autophosphorylation activity and PAK6 substrate phosphorylation may also be elevated. It has been speculated here that PAK6 phosphorylates β-catenin. These events may trigger α-catenin uncouplingthereby leading to the weakening of cell-cell adhesions and subsequent cell-cell dissociation. α-catenin is known to dissociate from β-catenin; however, the consequence of this dissociation is still unclear. Thus this model speculates that α-catenin dissociation leads to cell junction disassembly.

In future studies, it would be interesting to assess whether there is an interaction between PAK6 and β-catenin, as well as whether PAK6 phosphorylates β-catenin. In addition, the association between IQGAP1 and the junctional components α-catenin, β-catenin and E-cadherin in PAK6 knockdown cells and the interaction between IQGAP1 and kinase active and kinase dead PAK6 mutants could also be investigated. Moreover, Cdc42 and PAK6-IQGAP1 interactions downstream of HGF could be examined. This would help elucidate the intricacies of the mechanism involving IQGAP1 and PAK6 in cell-cell dissociation downstream of HGF in DU145 cells.

References

Aberle, H., Butz, S., Stappert, J., Weissig, H., Kemler, R. and Hoschuetzky, H. (1994). Assembly of the cadherin catenin complex in-vitro with recombinant proteins *Journal of Cell Science* **107**, 3655-3663.

Abo, A., Qu, J., Cammarano, M. S., Dan, C. T., Fritsch, A., Baud, V., Belisle, B. and Minden, A. (1998). PAK4, a novel effector for Cdc42Hs, is implicated in the reorganization of the actin cytoskeleton and in the formation of filopodia. *Embo Journal* **17**, 6527-6540.

Adams, C. L., Chen, Y. T., Smith, S. J. and Nelson, W. J. (1998). Mechanisms of epithelial cell-cell adhesion and cell compaction revealed by high-resolution tracking of E-cadherin-green fluorescent protein. *Journal of Cell Biology* **142**, 1105-1119.

Ahlstrom, J. D. and Erickson, C. A. (2009). The neural crest epithelial-mesenchymal transition in 4D: a 'tail' of multiple non-obligatory cellular mechanisms. *Development* **136**, 1801-1812.

Ahmed, T., Shea, K., Masters, J. R. W., Jones, G. E. and Wells, C. M. (2008). A PAK4-LIMK1 pathway drives prostate cancer cell migration downstream of HGF. *Cellular Signalling* **20**, 1320-1328.

Alahari, S. K., Reddig, P. J. and Juliano, R. L. (2004). The integrin-binding protein Nischarin regulates cell migration by inhibiting PAK. *Embo Journal* **23**, 2777-2788.

Alblas, J., Ulfman, L., Hordijk, P. and Koenderman, L. (2001). Activation of RhoA and ROCK are essential for detachment of migrating Leukocytes. *Molecular Biology of the Cell* **12**, 2137-2145.

Alexander, S., Koehl, G., Hirschberg, M., Geissler, E. and Friedl, P. (2008). Dynamic imaging of cancer growth and invasion: a modified skin-fold chamber model. *Histochemistry and Cell Biology* **130**, 1147-1154.

Allen, W. E., Zicha, D., Ridley, A. J. and Jones, G. E. (1998). A role for Cdc42 in macrophage chemotaxis. *Journal of Cell Biology* **141**, 1147-1157.

Alper, O., Bergmann-Leitner, E. S., Bennett, T. A., Hacker, N. F., Stromberg, K. and Stetler-Stevenson, W. G. (2001). Epidermal growth factor receptor signaling and the invasive phenotype of ovarian carcinoma cells. *Journal of the National Cancer Institute* **93**, 1375-1384.

Altmann, K.-H. and Gertsch, J. (2007). Anticancer drugs from nature-natural products as a unique source of new microtubule-stabilizing agents. *Natural Product Reports* **24**, 327-357.

Angelucci, A., Gravina, G. L., Rucci, N., Millimaggi, D., Festuccia, C., Muzi, P., Teti, A., Vicentini, C. and Bologna, M. (2006). Suppression of EGF-R signaling reduces the incidence of prostate cancer metastasis in nude mice. *Endocrine-Related Cancer* **13**, 197-210.

Aoki, H., Yokoyama, T., Fujiwara, K., Tari, A. M., Sawaya, R., Suki, D., Hess, K. R., Aldape, K. D., Kondo, S., Kumar, R. et al. (2007). Phosphorylated Pak1 level in the cytoplasm correlates with shorter survival time in patients with glioblastoma. *Clinical Cancer Research* **13**, 6603-6609.

Aono, S., Nakagawa, S., Reynolds, A. B. and Takeichi, M. (1999). p120ctn Acts as an Inhibitory Regulator of Cadherin Function in Colon Carcinoma Cells. *The Journal of Cell Biology* **145**, 551-562.

Arias-Romero, L. E. and Chernoff, J. (2008). A tale of two Paks. *Biology of the Cell* **100**, 97-108.

Aronheim, A., Broder, Y. C., Cohen, A., Fritsch, A., Belisle, B. and Abo, A. (1998). Chp, a homologue of the GTPase Cdc42Hs, activates the JNK pathway and is implicated in reorganizing the actin cytoskeleton. *Current Biology* **8**, 1125-1128.

Artym, V. and Matsumoto, K. (2010). Imaging Cells in Three-Dimensional Collagen Matrix. *Curr Protoc Cell Biol*.

Aspenström, P., Ruusala, A. and Pacholsky, D. (2007). Taking Rho GTPases to the next level: The cellular functions of atypical Rho GTPases. *Experimental Cell Research* **313**, 3673-3679.

Bagrodia, S., Taylor, S. J., Creasy, C. L., Chernoff, J. and Cerione, R. A. (1995). Identification of a mouse p21 (Cdc42/Rac) activated kinase *Journal of Biological Chemistry* **270**, 22731-22737.

Bellovin, D. I., Bates, R. C., Muzikansky, A., Rimm, D. L. and Mercurio, A. M. (2005). Altered Localization of p120 Catenin During Epithelial to Mesenchymal Transition of Colon Carcinoma Is Prognostic for Aggressive Disease. *Cancer Research* **65**, 10938-10945.

Benjamin, J. M. and Nelson, W. J. (2008). Bench to bedside and back again: Molecular mechanisms of alpha-catenin function and roles in tumorigenesis. *Seminars in Cancer Biology* **18**, 53-64.

Bergauer, T., Krueger, U., Lader, E., Pilk, S., Wolter, I. and Bielke, W. (2009). Analysis of Putative miRNA Binding Sites and mRNA 3 ' Ends as Targets for siRNA-Mediated Gene Knockdown. *Oligonucleotides* **19**, 41-52.

Bernards, A. and Settleman, J. (2004). GAP control: regulating the regulators of small GTPases. *Trends in Cell Biology* **14**, 377-385.

Birchmeier, W. and Behrens, J. (1994). Cadherin expression in carcinomas: role in the formation of cell junctions and the prevention of invasiveness. *Biochimica et Biophysica Acta (BBA) - Reviews on Cancer* **1198**, 11-26.

Bishop, A. L. and Hall, A. (2000). Rho GTPases and their effector proteins. *Biochemical Journal* **348**, 241-255.

Bokoch, G. M., Reilly, A. M., Daniels, R. H., King, C. C., Olivera, A., Spiegel, S. and Knaus, U. G. (1998). A GTPase-independent mechanism of p21-activated kinase activation - Regulation by sphingosine and other biologically active lipids. *Journal of Biological Chemistry* **273**, 8137-8144.

Bokoch, G. M., Wang, Y., Bohl, B. P., Sells, M. A., Quilliam, L. A. and Knaus, U. G. (1996). Interaction of the Nck adapter protein with p21-activated kinase (PAK1). *Journal of Biological Chemistry* **271**, 25746-25749.

Boller, K., Vestweber, D. and Kemler, R. (1985). Cell-adhesion molecule uvomorulin is localized in the intermediate junctions of junctions of adult intestinal epithelial cells *Journal of Cell Biology* **100**, 327-332.

Bonkhoff, H., Stein, U. and Remberger, K. (1993). Differential expression of alpha-6 and alpha-2 very late antigen integrins in the normal, hyperplastic, and neoplastic prostate - simultaneous demonstration of cell-surface receptors and their extracellular ligands *Human Pathology* **24**, 243-248.

Bostner, J., Waltersson, M. A., Fornander, T., Skoog, L., Nordenskjöld, B. and Stål, O. (2007). Amplification of CCND1 and PAK1 as predictors of recurrence and tamoxifen resistance in postmenopausal breast cancer. *Oncogene* **26**, 6997-7005.

Bottaro, D. P., Rubin, J. S., Faletto, D. L., Chan, A. M. L., Kmiecik, T. E., Vandewoude, G. F. and Aaronson, S. A. (1991). Identification of the hepatocyte growth factor receptor as the c-met proto-oncogene product *Science* **251**, 802-804.

Bourguignon, L. Y. W., Gilad, E., Rothman, K. and Peyrollier, K. (2005). Hyaluronan-CD44 Interaction with IQGAP1 Promotes Cdc42 and ERK Signaling,

Leading to Actin Binding, Elk-1/Estrogen Receptor Transcriptional Activation, and Ovarian Cancer Progression. *Journal of Biological Chemistry* **280**, 11961-11972.

Braga, V. M. M., Betson, M., Li, X. D. and Lamarche-Vane, N. (2000). Activation of the small GTPase Rac is sufficient to disrupt cadherin-dependent cell-cell adhesion in normal human keratinocytes. *Molecular Biology of the Cell* **11**, 3703-3721.

Braga, V. M. M., Machesky, L. M., Hall, A. and Hotchin, N. A. (1997). The Small GTPases Rho and Rac Are Required for the Establishment of Cadherin-dependent Cell-Cell Contacts. *The Journal of Cell Biology* **137**, 1421-1431.

Briggs, M. W. and Sacks, D. B. (2003). IQGAP proteins are integral components of cytoskeletal regulation. *Embo Reports* **4**, 571-574.

Bright, M. D., Garner, A. P. and Ridley, A. J. (2009). PAK1 and PAK2 have different roles in HGF-induced morphological responses. *Cellular Signalling* **21**, 1738-1747.

Brill, S., Li, S. H., Lyman, C. W., Church, D. M., Wasmuth, J. J., Weissbach, L., Bernards, A. and Snijders, A. J. (1996). The Ras GTPase-activating-protein-related human protein IQGAP2 harbors a potential actin binding domain and interacts with calmodulin and Rho family GTPases. *Molecular and Cellular Biology* **16**, 4869-4878.

Brinkmann, V., Foroutan, H., Sachs, M., Weidner, K. M. and Birchmeier, W. (1995). Hepatocyte growth-factor/scatter factor induces a variety of tissue-specific morphogenic programs in epithelial-cells *Journal of Cell Biology* **131**, 1573-1586.

Brown, M. D. and Sacks, D. B. (2006). IQGAP1 in cellular signaling: bridging the GAP. *Trends in Cell Biology* **16**, 242-249.

Bubendorf, L., Schöpfer, A., Wagner, U., Sauter, G., Moch, H., Willi, N., Gasser, T. C. and Mihatsch, M. J. (2000). Metastatic patterns of prostate cancer: An autopsy study of 1,589 patients. *Human Pathology* **31**, 578-583.

Burbelo, P. D., Drechsel, D. and Hall, A. (1995). A conserved binding motif defines numerous candidate target proteins for both Cdc42 and Rac GTPases *Journal of Biological Chemistry* **270**, 29071-29074.

Byers, S. W., Sommers, C. L., Hoxter, B., Mercurio, A. M. and Tozeren, A. (1995). Role of E-Cadherin in the response of tumor-cell aggregates to lymphatic, venous and arterial flow - measurement of cell-cell adhesion strength *Journal of Cell Science* **108**, 2053-2064.

Callow, M. G., Clairvoyant, F., Zhu, S., Schryver, B., Whyte, D. B., Bischoff, J. R., Jallal, B. and Smeal, T. (2002). Requirement for PAK4 in the anchorage-independent growth of human cancer cell lines. *Journal of Biological Chemistry* **277**, 550-558.

Callow, M. G., Zozulya, S., Gishizky, M. L., Jallal, B. and Smeal, T. (2005). PAK4 mediates morphological changes through the regulation of GEF-H1. *Journal of Cell Science* **118**, 1861-1872.

Cameron, M. D., Schmidt, E. E., Kerkvliet, N., Nadkarni, K. V., Morris, V. L., Groom, A. C., Chambers, A. F. and MacDonald, I. C. (2000). Temporal progression of metastasis in lung: Cell survival, dormancy, and location dependence of metastatic inefficiency. *Cancer Research* **60**, 2541-2546.

Cantley, L. G., Barros, E. J., Gandhi, M., Rauchman, M. and Nigam, S. K. (1994). Regulation of mitogenesis, motogenesis, and tubulogenesis by hepatocyte growth factor in renal collecting duct cells. *American Journal of Physiology - Renal Physiology* **267**, F271-F280.

Cao, J., Chiarelli, C., Richman, O., Zarrabi, K., Kozarekar, P. and Zucker, S. (2008). Membrane Type 1 Matrix Metalloproteinase Induces Epithelial-to-

Mesenchymal Transition in Prostate Cancer. *Journal of Biological Chemistry* **283**, 6232-6240.

Carter, J. H., Douglass, L. E., Deddens, J. A., Colligan, B. M., Bhatt, T. R., Pemberton, J. O., Konicek, S., Hom, J., Marshall, M. and Graff, J. R. (2004). Pak-1 expression increases with progression of colorectal carcinomas to metastasis. *Clinical Cancer Research* **10**, 3448-3456.

Cau, J., Faure, S., Comps, M., Delsert, C. and Morin, N. (2001). A novel p21-activated kinase binds the actin and microtubule networks and induces microtubule stabilization. *The Journal of Cell Biology* **155**, 1029-1042.

Cavey, M., Rauzi, M., Lenne, P.-F. and Lecuit, T. (2008). A two-tiered mechanism for stabilization and immobilization of E-cadherin. *Nature* **453**, 751-756.

Ceteci, F., Ceteci, S., Karreman, C., Kramer, B. W., Asan, E., Göttz, R. and Rapp, U. R. (2007). Disruption of Tumor Cell Adhesion Promotes Angiogenic Switch and Progression to Micrometastasis in RAF-Driven Murine Lung Cancer. *Cancer Cell* **12**, 145-159.

Chaffer, C. L. and Weinberg, R. A. (2011). A Perspective on Cancer Cell Metastasis. *Science* **331**, 1559-1564.

Chamberlain, C. E., Kraynov, V. S., Hahn, K. M., W.E. Balch, C. J. D. and Alan, H. (2000). Imaging spatiotemporal dynamics of Rac activation in vivo with FLAIR. In *Methods in Enzymology*, vol. Volume 325, pp. 389-400: Academic Press.

Chen, F., Zhu, H. H., Zhou, L. F., Wu, S. S., Wang, J. and Chen, Z. (2010). IQGAP1 is overexpressed in hepatocellular carcinoma and promotes cell proliferation by Akt activation. *Experimental and Molecular Medicine* **42**, 477-483.

Ching, Y. P., Leong, V. Y. L., Lee, M. F., Xu, H. T., Jin, D. Y. and Ng, I. O. L. (2007). P21-activated protein kinase is overexpressed in hepatocellular carcinoma and enhances cancer metastasis involving c-Jun NH2-terminal kinase activation and paxillin phosphorylation. *Cancer Research* **67**, 3601-3608.

Ching, Y. P., Leong, V. Y. L., Wong, C. M. and Kung, H. F. (2003). Identification of an autoinhibitory domain of p21-activated protein kinase 5. *Journal of Biological Chemistry* **278**, 33621-33624.

Chong, C., Tan, L., Lim, L. and Manser, E. (2001). The mechanism of PAK activation - Autophosphorylation events in both regulatory and kinase domains control activity. *Journal of Biological Chemistry* **276**, 17347-17353.

ChrzanowskaWodnicka, M. and Burridge, K. (1996). Rho-stimulated contractility drives the formation of stress fibers and focal adhesions. *Journal of Cell Biology* **133**, 1403-1415.

Clark, E. A., Golub, T. R., Lander, E. S. and Hynes, R. O. (2000). Genomic analysis of metastasis reveals an essential role for RhoC. *Nature* **406**, 532-535.

Clark, P. (1994). Modulation of scatter factor/hepatocyte growth-factor activity by cell-substratum adhesion *Journal of Cell Science* **107**, 1265-1275.

Colombel, M., Eaton, C. L., Hamdy, F., Ricci, E., van der Pluijm, G., Cecchini, M., Mege-Lechevallier, F., Clezardin, P. and Thalmann, G. (2011). Increased expression of putative cancer stem cell markers in primary prostate cancer is associated with progression of bone metastases. *The Prostate*, n/a-n/a.

Cotteret, S., Jaffer, Z. M., Beeser, A. and Chernoff, J. (2003). p21-activated kinase 5 (Pak5) localizes to mitochondria and inhibits apoptosis by phosphorylating BAD. *Molecular and Cellular Biology* **23**, 5526-5539.

Crepaldi, T., Pollack, A. L., Prat, M., Zborek, A., Mostov, K. and Comoglio, P. M. (1994). Targeting of the SF/HGF receptor to the basolateral domain of polarized epithelial cells *Journal of Cell Biology* **125**, 313-320.

D'Souza-Schorey, C. (2005). Disassembling adherens junctions: breaking up is hard to do. *Trends in Cell Biology* **15**, 19-26.

Dan, C., Kelly, A., Bernard, O. and Minden, A. (2001). Cytoskeletal changes regulated by the PAK4 serine/threonine kinase are mediated by LIM kinase 1 and cofilin. *Journal of Biological Chemistry* **276**, 32115-32121.

Dan, C., Nath, N., Liberto, M. and Minden, A. (2002). PAK5, a new brain-specific kinase, promotes neurite outgrowth in N1E-115 cells. *Molecular and Cellular Biology* **22**, 567-577.

Daniel, J. M. and Reynolds, A. B. (1995). The tyrosine kinase substrate p120cas binds directly to E-Cadherin but not to the adenomatous polyposis-coli protein or alpha-catenin *Molecular and Cellular Biology* **15**, 4819-4824.

Davidson, B., Shih, I. M. and Wang, T. L. (2008). Different clinical roles for p21-activated kinase-1 in primary and recurrent ovarian carcinoma. *Human Pathology* **39**, 1630-1636.

Davies, G., Watkins, G., Mason, M. D. and Jiang, W. G. (2004). Targeting the HGF/SF receptor c-met using a hammerhead ribozyme transgene reduces in vitro invasion and migration in prostate cancer cells. *Prostate* **60**, 317-324.

Davis, M. A., Ireton, R. C. and Reynolds, A. B. (2003). A core function for p120-catenin in cadherin turnover. *Journal of Cell Biology* **163**, 525-534.

de Beco, S., Gueudry, C., Amblard, F. and Coscoy, S. (2009). Endocytosis is required for E-cadherin redistribution at mature adherens junctions. *Proceedings of the National Academy of Sciences* **106**, 7010-7015.

de Leeuw, W. J. F., Berx, G., Vos, C. B. J., Peterse, J. L., Van de Vijver, M. J., Litvinov, S., Van Roy, F., Cornelisse, C. J. and Cleton-Jansen, A.-m. (1997). Simultaneous loss of E-cadherin and catenins in invasive lobular breast cancer and lobular carcinoma in situ. *The Journal of Pathology* **183**, 404-411.

de Rooij, J., Kerstens, A., Danuser, G., Schwartz, M. A. and Waterman-Storer, C. M. (2005). Integrin-dependent actomyosin contraction regulates epithelial cell scattering. *Journal of Cell Biology* **171**, 153-164.

DerMardirossian, C. and Bokoch, G. M. (2005). GDIs: central regulatory molecules in Rho GTPase activation. *Trends in Cell Biology* **15**, 356-363.

Di Lullo, G. A., Sweeney, S. M., Korkko, J., Ala-Kokko, L. and San Antonio, J. D. (2002). Mapping the Ligand-binding Sites and Disease-associated Mutations on the Most Abundant Protein in the Human, Type I Collagen. *Journal of Biological Chemistry* **277**, 4223-4231.

Didsbury, J., Weber, R. F., Bokoch, G. M., Evans, T. and Snyderman, R. (1989). Rac, a novel ras-related family of proteins that are botulinum toxin substrates SUBSTRATES. *Journal of Biological Chemistry* **264**, 16378-16382.

DiMilla, P., Stone, J., Quinn, J., Albelda, S. and Lauffenburger, D. (1993). Maximal migration of human smooth muscle cells on fibronectin and type IV collagen occurs at an intermediate attachment strength. *The Journal of Cell Biology* **122**, 729-737.

Dollé, L., El Yazidi-Belkoura, I., Adriaenssens, E., Nurcombe, V. and Hondermarck, H. (2003). Nerve growth factor overexpression and autocrine loop in breast cancer cells. *Oncogene* **22**, 5592-5601.

Dong, P.-X., Jia, N., Xu, Z.-J., Liu, Y.-T., Li, D.-J. and Feng, Y.-J. (2008). Silencing of IQGAP1 by shRNA inhibits the invasion of ovarian carcinoma HO-8910PM cells in vitro. *Journal of Experimental & Clinical Cancer Research* **27**, 77.

Dong, P. X., Nabeshima, K., Nishimura, N., Kawakami, T., Hachisuga, T., Kawarabayashi, T. and Iwasaki, H. (2006). Overexpression and diffuse expression

pattern of IQGAP1 at invasion fronts are independent prognostic parameters in ovarian carcinomas. *Cancer Letters* **243**, 120-127.

Donjacour, A. A. and Cunha, G. R. (1993). Assessment of prostatic protein secretion in tissue recombinants made of urogenital sinus mesenchyme and urothelium from normal or androgen-insensitive mice. *Endocrinology* **132**, 2342-50.

Drees, F., Pokutta, S., Yamada, S., Nelson, W. J. and Weis, W. I. (2005). α-Catenin Is a Molecular Switch that Binds E-Cadherin-β-Catenin and Regulates Actin-Filament Assembly. *Cell* **123**, 903-915.

Duffy, M. J., McGowan, P. M. and Gallagher, W. M. (2008). Cancer invasion and metastasis: changing views. *Journal of Pathology* **214**, 283-293.

Dunn, G. A., Dobbie, I. M., Monypenny, J., Holt, M. R. and Zicha, D. (2002). Fluorescence localization after photobleaching (FLAP): a new method for studying protein dynamics in living cells. *Journal of Microscopy-Oxford* **205**, 109-112.

Ehrlich, J. S., Hansen, M. D. H. and Nelson, W. J. (2002). Spatio-Temporal Regulation of Rac1 Localization and Lamellipodia Dynamics during Epithelial Cell-Cell Adhesion. *Developmental Cell* **3**, 259-270.

Eisenhoffer, G. T., Loftus, P. D., Yoshigi, M., Otsuna, H., Chien, C. B., Morcos, P. A. and Rosenblatt, J. (2012). Crowding induces live cell extrusion to maintain homeostatic cell numbers in epithelia. *Nature* **484**, 546-U183.

Ellenbroek, S. I. J. and Collard, J. G. (2007). Rho GTPases: functions and association with cancer. *Clinical & Experimental Metastasis* **24**, 657-672.

Ellis, W. J., Pfitzenmaier, J., Colli, J., Arfman, E., Lange, P. H. and Vessella, R. L. (2003). Detection and isolation of prostate cancer cells from peripheral blood and bone marrow. *Urology* **61**, 277-281.

Epp, J. A. and Chant, J. (1997). An IQGAP-related protein controls actin-ring formation and cytokinesis in yeast. *Current Biology* **7**, 921-929.

Erickson, J. W., Cerione, R. A. and Hart, M. J. (1997). Identification of an actin cytoskeletal complex that includes IQGAP and the Cdc42 GTPase. *Journal of Biological Chemistry* **272**, 24443-24447.

Eswaran, J., Soundararajan, M., Kumar, R. and Knapp, S. (2008). UnPAKing the class differences among p21-activated kinases. *Trends in Biochemical Sciences* **33**, 394-403.

Farooqui, R. and Fenteany, G. (2005). Multiple rows of cells behind an epithelial wound edge extend cryptic lamellipodia to collectively drive cell-sheet movement. *Journal of Cell Science* **118**, 51-63.

Farquhar, M. G. and Palade, G. E. (1963). Junctional complexes in various epithelia. *Journal of Cell Biology* **17**, 375-412.

Faure, S., Cau, J., Barbara, P. D., Bigou, S., Ge, Q. Y., Delsert, C. and Morin, N. (2005). Xenopus p21-activated kinase 5 regulates blastomeres adhesive properties during convergent extension movements. *Developmental Biology* **277**, 472-492.

Fidler, I. J. (2003). Timeline - The pathogenesis of cancer metastasis: the 'seed and soil' hypothesis revisited. *Nature Reviews Cancer* **3**, 453-458.

Fiegen, D., Blumenstein, L., Stege, P., Vetter, I. R. and Ahmadian, M. R. (2002). Crystal structure of Rnd3/RhoE: functional implications. *Febs Letters* **525**, 100-104.

Folkman, J. (1971). Tumor Angiogenesis: Therapeutic Implications. *New England Journal of Medicine* **285**, 1182-1186.

Folkman, J., Becker, F. F. and Long, D. M. (1963). Growth and metastasis of tumor in organ culture *Cancer* **16**, 453-467.

Foster, R., Hu, K. Q., Lu, Y., Nolan, K. M., Thissen, J. and Settleman, J. (1996). Identification of a novel human rho protein with unusual properties: GTPase deficiency and in vivo farnesylation. *Molecular and Cellular Biology* **16**, 2689-2699.

Fram, S. T., Wells, C. M. and Jones, G. E. (2011). HGF-Induced DU145 Cell Scatter Assay. *Cell Migration, Methods in Molecular Biology* **769**, 31-40.

Friedl, P. and Gilmour, D. (2009). Collective cell migration in morphogenesis, regeneration and cancer. *Nature Reviews Molecular Cell Biology* **10**, 445-457.

Friedl, P., Noble, P. B., Walton, P. A., Laird, D. W., Chauvin, P. J., Tabah, R. J., Black, M. and Zänker, K. S. (1995). Migration of coordinated cell clusters in mesenchymal and epithelial cancer explants in vitro *Cancer Research* **55**, 4557-4560.

Friedl, P. and Wolf, K. (2003). Tumour-cell invasion and migration: Diversity and escape mechanisms. *Nature Reviews Cancer* **3**, 362-374.

Frixen, U. H., Behrens, J., Sachs, M., Eberle, G., Voss, B., Warda, A., Löchner, D. and Birchmeier, W. (1991). E-Cadherin-mediated cell-cell adhesion prevents invasiveness of human carcinoma cells *Journal of Cell Biology* **113**, 173-185.

Fujita, Y., Krause, G., Scheffner, M., Zechner, D., Leddy, H. E. M., Behrens, J., Sommer, T. and Birchmeier, W. (2002). Hakai, a c-Cbl-like protein, ubiquitinates and induces endocytosis of the E-cadherin complex. *Nat Cell Biol* **4**, 222-231.

Fujiuchi, Y., Nagakawa, O., Murakami, K., Fuse, H. and Saiki, I. (2003). Effect of hepatocyte growth factor on invasion of prostate cancer cell lines. *Oncology Reports* **10**, 1001-1006.

Fukata, M., Kuroda, S., Nakagawa, M., Kawajiri, A., Itoh, N., Shoji, I., Matsuura, Y., Yonehara, S., Fujisawa, H., Kikuchi, A. et al. (1999). Cdc42 and Rac1 regulate the interaction of IQGAP1 with beta-catenin. *Journal of Biological Chemistry* **274**, 26044-26050.

Fukata, M., Nakagawa, M., Itoh, N., Kawajiri, A., Yamaga, M., Kuroda, S. and Kaibuchi, K. (2001). Involvement of IQGAP1, an effector of Rac1 and Cdc42 GTPases, in cell-cell dissociation during cell scattering. *Molecular and Cellular Biology* **21**, 2165-2183.

Gabbert, H., Wagner, R., Moll, R. and Gerharz, C. D. (1985). Tumor dedifferentiation - an important step in tumor invasion. *Clinical & Experimental Metastasis* **3**, 257-279.

Gallin, W. J., Edelman, G. M. and Cunningham, B. A. (1983). Characterization of L-CAM, a major cell adhesion molecule from embryonic liver cells. *Proceedings of the National Academy of Sciences* **80**, 1038-1042.

Gan, Y., Shi, C., Inge, L., Hibner, M., Balducci, J. and Huang, Y. (2010). Differential roles of ERK and Akt pathways in regulation of EGFR-mediated signaling and motility in prostate cancer cells. *Oncogene* **29**, 4947-4958.

Garavini, H., Riento, K., Phelan, J. P., McAlister, M. S. B., Ridley, A. J. and Keep, N. H. (2002). Crystal structure of the core domain of RhoE/Rnd3: A constitutively activated small G protein. *Biochemistry* **41**, 6303-6310.

Garćia, A. J. and Boettiger, D. (1999). Integrin-fibronectin interactions at the cell-material interface: initial integrin binding and signaling. *Biomaterials* **20**, 2427-2433.

Gardiner, E. M., Pestonjamasp, K. N., Bohl, B. P., Chamberlain, C., Hahn, K. M. and Bokoch, G. M. (2002). Spatial and temporal analysis of Rac activation during live neutrophil chemotaxis. *Current Biology* **12**, 2029-2034.

Geldof, A. A., DeKleijn, M. A. T., Rao, B. R. and Newling, D. W. W. (1997). Nerve growth factor stimulates in vitro invasive capacity of DU145 human prostatic cancer cells. *Journal of Cancer Research and Clinical Oncology* **123**, 107-112.

Ghosh, S., Spagnoli, G. C., Martin, I., Ploegert, S., Demougin, P., Heberer, M. and Reschner, A. (2005). Three-dimensional culture of melanoma cells profoundly affects gene expression profile: A high density oligonucleotide array study. *Journal of Cellular Physiology* **204**, 522-531.

Gmyrek, G. A., Walburg, M., Webb, C. P., Yu, H. M., You, X. K., Vaughan, E. D., Woude, G. F. V. and Knudsen, B. S. (2001). Normal and malignant prostate epithelial cells differ in their response to hepatocyte growth factor/scatter factor. *American Journal of Pathology* **159**, 579-590.

Gnesutta, N., Qu, J. and Minden, A. (2001). The Serine/Threonine Kinase PAK4 Prevents Caspase Activation and Protects Cells from Apoptosis. *Journal of Biological Chemistry* **276**, 14414-14419.

Gong, W., An, Z., Wang, Y., Pan, X., Fang, W., Jiang, B. and Zhang, H. (2009). P21-activated kinase 5 is overexpressed during colorectal cancer progression and regulates colorectal carcinoma cell adhesion and migration. *International Journal of Cancer* **125**, 548-555.

Gorlov, I. P., Byun, J., Gorlova, O. Y., Aparicio, A. M., Efstathiou, E. and Logothetis, C. J. (2009). Candidate pathways and genes for prostate cancer: a meta-analysis of gene expression data. *Bmc Medical Genomics* **2**.

Greenburg, G. and Hay, E. D. (1982). Epithelia suspended in collagen gels can lose polarity and express characteristics of migrating mesenchymal cells *Journal of Cell Biology* **95**, 333-339.

Greene, H. S. N. (1941). Heterologous transplantation of mammalian tumors I. The transfer of rabbit tumors to alien species. *Journal of Experimental Medicine* **73**, 461-U3.

Greenman, C., Stephens, P., Smith, R., Dalgliesh, G. L., Hunter, C., Bignell, G., Davies, H., Teague, J., Butler, A., Edkins, S. et al. (2007). Patterns of somatic mutation in human cancer genomes. *Nature* **446**, 153-158.

Grohmanova, K., Schlaepfer, D., Hess, D., Gutierrez, P., Beck, M. and Kroschewski, R. (2004). Phosphorylation of IQGAP1 modulates its binding to Cdc42, revealing a new type of Rho-GTPase regulator. *Journal of Biological Chemistry* **279**, 48495-48504.

Gumbiner, B., Stevenson, B. and Grimaldi, A. (1988). The role of the cell adhesion molecule uvomorulin in the formation and maintenance of the epithelial junctional complex. *The Journal of Cell Biology* **107**, 1575-1587.

Hage, B., Meinel, K., Baum, I., Giehl, K. and Menke, A. (2009). Rac1 activation inhibits E-cadherin-mediated adherens junctions via binding to IQGAP1 in pancreatic carcinoma cells. *Cell Communication and Signaling* **7**.

Hall, A. (1998). Rho GTPases and the Actin Cytoskeleton. *Science* **279**, 509-514.

Hamanoue, M., Kawaida, K., Takao, S., Shimazu, H., Noji, S., Matsumoto, K. and Nakamura, T. (1992). Rapid and marked induction of hepatocyte growth factor during liver regeneration after ischemic or crush injury. *Hepatology* **16**, 1485-1492.

Han, G., Buchanan, G., Ittmann, M., Harris, J. M., Yu, X., DeMayo, F. J., Tilley, W. and Greenberg, N. M. (2005). Mutation of the androgen receptor causes oncogenic transformation of the prostate. *Proceedings of the National Academy of Sciences of the United States of America* **102**, 1151-1156.

Härmä, V., Virtanen, J., Mäkelä, R., Happonen, A., Mpindi, J. P., Knuuttila, M., Kohonen, P., Lötjönen, J., Kallioniemi, O. and Nees, M. (2010). A Comprehensive Panel of Three-Dimensional Models for Studies of Prostate Cancer Growth, Invasion and Drug Responses. *Plos One* **5**.

Hart, M. J., Callow, M. G., Souza, B. and Polakis, P. (1996). IQGAP1, a calmodulin-binding protein with a rasGAP-related domain, is a potential effector for cdc42Hs. *Embo Journal* **15**, 2997-3005.

He, B., You, L., Uematsu, K., Zang, K. L., Xu, Z. D., Lee, A. Y., Costello, J. F., McCormick, F. and Jablons, D. M. (2003). SOCS-3 is frequently silenced by hypermethylation and suppresses cell growth in human lung cancer. *Proceedings of the National Academy of Sciences of the United States of America* **100**, 14133-14138.

He, H., Shulkes, A. and Baldwin, G. S. (2008). PAK1 interacts with beta-catenin and is required for the regulation of the beta-catenin signalling pathway by gastrins. *Biochimica Et Biophysica Acta-Molecular Cell Research* **1783**, 1943-1954.

Heasman, S. J., Carlin, L. M., Cox, S., Ng, T. and Ridley, A. J. (2010). Coordinated RhoA signaling at the leading edge and uropod is required for T cell transendothelial migration. *The Journal of Cell Biology* **190**, 553-563.

Heasman, S. J. and Ridley, A. J. (2008). Mammalian Rho GTPases: new insights into their functions from in vivo studies. *Nature Reviews Molecular Cell Biology* **9**, 690-701.

Hegerfeldt, Y., Tusch, M., Bröcker, E. B. and Friedl, P. (2002). Collective cell movement in primary melanoma explants: Plasticity of cell-cell interaction, ss 1-integrin function, and migration strategies. *Cancer Research* **62**, 2125-2130.

Herrenknecht, K., Ozawa, M., Eckerskorn, C., Lottspeich, F., Lenter, M. and Kemler, R. (1991). The uvomorulin-anchorage protein alpha catenin is a vinculin homologue. *Proceedings of the National Academy of Sciences* **88**, 9156-9160.

Herrera, R. (1998). Modulation of hepatocyte growth factor-induced scattering of HT29 colon carcinoma cells - Involvement of the MAPK pathway. *Journal of Cell Science* **111**, 1039-1049.

Hershkoviz, R., Alon, R., Gilat, D. and Lider, O. (1992). Activated T lymphocytes and macrophages secrete fibronectin which strongly supports cell adhesion. *Cellular Immunology* **141**, 352-361.

Ho, Y. D., Joyal, J. L., Li, Z. G. and Sacks, D. B. (1999). IQGAP1 integrates Ca2+/calmodulin and Cdc42 signaling. *Journal of Biological Chemistry* **274**, 464-470.

Hogan, C., Dupré-Crochet, S., Norman, M., Kajita, M., Zimmermann, C., Pelling, A. E., Piddini, E., Baena-López, L. A., Vincent, J. P., Itoh, Y. et al. (2009). Characterization of the interface between normal and transformed epithelial cells. *Nature Cell Biology* **11**, 460-U234.

Holm, C., Rayala, S., Jirström, K., Stål, O., Kumar, R. and Landberg, G. (2006). Association between Pak1 expression and subcellular localization and tamoxifen resistance in breast cancer patients. *Journal of the National Cancer Institute* **98**, 671-680.

Hooper, S., Marshall, J. F. and Sahai, E. (2006). Tumor cell migration in three dimensions. In *Methods in Enzymology, Vol 406, Regulators and Effectors of Small Gtpases: Rho Family*, vol. 406 (eds W. E. Balch C. J. Der and A. Hall), pp. 625-643.

Hoshino, T., Shimizu, K., Honda, T., Kawakatsu, T., Fukuyama, T., Nakamura, T., Matsuda, M. and Takai, Y. (2004). A novel role of nectins in inhibition of the e-cadherin-induced activation of Rac and formation of cell-cell adherens junctions. *Molecular Biology of the Cell* **15**, 1077-1088.

Hosotani, R., Kawaguchi, M., Masui, T., Koshiba, T., Ida, J., Fujimoto, K., Wada, M., Doi, R. and Imamura, M. (2002). Expression of Integrin [alpha]V[beta]3 in Pancreatic Carcinoma: Relation to MMP-2 Activation and Lymph Node Metastasis. *Pancreas* **25**, e30-e35.

Hu, B., Shi, B. H., Jarzynka, M. J., Yiin, J. J., D'Souza-Schorey, C. and Cheng, S. Y. (2009). ADP-Ribosylation Factor 6 Regulates Glioma Cell Invasion through the IQ-Domain GTPase-Activating Protien 1-Rac1-Mediated Pathway. *Cancer Research* **69**, 794-801.

Huang, Y. T., Lai, C. Y., Lou, S. L., Yeh, J. M. and Chan, W. H. (2009). Activation of JNK and PAK2 Is Essential for Citrinin-Induced Apoptosis in a Human Osteoblast Cell Line. *Environmental Toxicology* **24**, 343-356.

Hudson, D. L. (2004). Epithelial stem cells in human prostate growth and disease. *Prostate Cancer Prostatic Dis* **7**, 188-194.

Humphrey, P. A., Zhu, X. P., Zarnegar, R., Swanson, P. E., Ratliff, T. L., Vollmer, R. T. and Day, M. L. (1995). Hepatocyte growth factor and its receptor c-MET in prostatic carcinoma *American Journal of Pathology* **147**, 386-396.

Huttenlocher, A., Ginsberg, M. H. and Horwitz, A. F. (1996). Modulation of cell migration by integrin-mediated cytoskeletal linkages and ligand-binding affinity. *Journal of Cell Biology* **134**, 1551-1562.

Huttenlocher, A. and Horwitz, A. R. (2011). Integrins in Cell Migration. *Cold Spring Harbor Perspectives in Biology* **3**.

Huynh, N., Liu, K. H., Baldwin, G. S. and He, H. (2010). P21-activated kinase 1 stimulates colon cancer cell growth and migration/invasion via ERK- and AKT-dependent pathways. *Biochimica Et Biophysica Acta-Molecular Cell Research* **1803**, 1106-1113.

Ireton, R. C., Davis, M. A., van Hengel, J., Mariner, D. J., Barnes, K., Thoreson, M. A., Anastasiadis, P. Z., Matrisian, L., Bundy, L. M., Sealy, L. et al. (2002). A novel role for p120 catenin in E-cadherin function. *The Journal of Cell Biology* **159**, 465-476.

Ishii, T., Sato, M., Sudo, K., Suzuki, M., Nakai, H., Hishida, T., Niwa, T., Umezu, K. and Yuasa, S. (1995). Hepatocyte Growth Factor Stimulates Liver Regeneration and Elevates Blood Protein Level in Normal and Partially Hepatectomized Rats. *Journal of Biochemistry* **117**, 1105-1112.

Ito, M., Nishiyama, H., Kawanishi, H., Matsui, S., Guilford, P., Reeve, A. and Ogawa, O. (2007). P21-activated kinase 1: A new molecular marker for intravesical recurrence after transurethral resection of bladder cancer. *Journal of Urology* **178**, 1073-1079.

Itoh, M., Nelson, C. M., Myers, C. A. and Bissell, M. J. (2007). Rap1 integrates tissue polarity, lumen formation, and tumorigenic potential in human breast epithelial cells. *Cancer Research* **67**, 4759-4766.

Ivascu, A. and Kubbies, M. (2006). Rapid generation of single-tumor spheroids for high-throughput cell function and toxicity analysis. *Journal of Biomolecular Screening* **11**, 922-932.

Iwanicki, M. P., Davidowitz, R. A., Ng, M. R., Besser, A., Muranen, T., Merritt, M., Danuser, G., Ince, T. and Brugge, J. S. (2011). Ovarian Cancer Spheroids Use Myosin-Generated Force to Clear the Mesothelium. *Cancer Discovery* **1**, 144-157.

Jadeski, L., Mataraza, J. M., Jeong, H. W., Li, Z. G. and Sacks, D. B. (2008). IQGAP1 stimulates proliferation and enhances tumorigenesis of human breast epithelial cells. *Journal of Biological Chemistry* **283**, 1008-1017.

Jaffer, Z. M. and Chernoff, J. (2002). p21-activated kinases: three more join the Pak. *International Journal of Biochemistry & Cell Biology* **34**, 713-717.

Jeffers, M., Rong, S. and Vande Woude, G. F. (1996). Enhanced tumorigenicity and invasion-metastasis by hepatocyte growth factor scatter factor-met signalling in human cells concomitant with induction of the urokinase proteolysis network. *Molecular and Cellular Biology* **16**, 1115-1125.

Jemal, A., Siegel, R., Ward, E., Hao, Y., Xu, J., Murray, T. and Thun, M. J. (2008). Cancer Statistics, 2008. *CA: A Cancer Journal for Clinicians* **58**, 71-96.

Johnson, M., Sharma, M. and Henderson, B. R. (2009). IQGAP1 regulation and roles in cancer. *Cellular Signalling* **21**, 1471-1478.

Jou, T. S., Stewart, D. B., Stappert, J., Nelson, W. J. and Marrs, J. A. (1995). Genetic and biochemical dissection of protein linkages in the cadherin-catenin complex *Proceedings of the National Academy of Sciences of the United States of America* **92**, 5067-5071.

Kamei, T., Matozaki, T., Sakisaka, T., Kodama, A., Yokoyama, S., Peng, Y. F., Nakano, K., Takaishi, K. and Takai, Y. (1999). Coendocytosis of cadherin and c-Met coupled to disruption of cell-cell adhesion in MDCK cells - regulation by Rho, Rac and Rab small G proteins. *Oncogene* **18**, 6776-6784.

Katayama, K. I., Melendez, J., Baumann, J. M., Leslie, J. R., Chauhan, B. K., Nemkul, N., Lang, R. A., Kuan, C. Y., Zheng, Y. and Yoshida, Y. (2011). Loss of RhoA in neural progenitor cells causes the disruption of adherens junctions and hyperproliferation. *Proceedings of the National Academy of Sciences of the United States of America* **108**, 7607-7612.

Katoh, K., Kano, Y., Amano, M., Onishi, H., Kaibuchi, K. and Fujiwara, K. (2001). Rho-kinase-mediated contraction of isolated stress fibers. *Journal of Cell Biology* **153**, 569-583.

Kaur, R., Liu, X., Gjoerup, O., Zhang, A. H., Yuan, X., Balk, S. P., Schneider, M. C. and Lu, M. L. (2005). Activation of p21-activated kinase 6 by MAP kinase kinase 6 and p38 MAP kinase. *Journal of Biological Chemistry* **280**, 3323-3330.

Kaur, R., Yuan, X., Lu, M. L. and Balk, S. P. (2008). Increased PAK6 expression in prostate cancer and identification of PAK6 associated proteins. *Prostate* **68**, 1510-1516.

Keely, P. J., Westwick, J. K., Whitehead, I. P., Der, C. J. and Parise, L. V. (1997). Cdc42 and Rac1 induce integrin-mediated cell motility and invasiveness through PI(3)K. *Nature* **390**, 632-636.

Kemler, R. and Ozawa, M. (1989). Uvomorulin-catenin complex - cytoplasmic anchorage of a Ca 2+ dependent cell adhesion molecule. *Bioessays* **11**, 88-91.

Kermorgant, S., Aparicio, T., Dessirier, V., Lewin, M. J. M. and Lehy, T. (2001). Hepatocyte growth factor induces colonic cancer cell invasiveness via enhanced motility and protease overproduction. Evidence for PI3 kinase and PKC involvement. *Carcinogenesis* **22**, 1035-1042.

Kikkawa, Y., Sanzen, N., Fujiwara, H., Sonnenberg, A. and Sekiguchi, K. (2000). Integrin binding specificity of laminin-10/11 : laminin-10/11 are recognized by alpha 3 beta 1, alpha 6 beta 1 and alpha 6 beta 4 integrins. *Journal of Cell Science* **113**, 869-876.

Kiosses, W. B., Daniels, R. H., Otey, C., Bokoch, G. M. and Schwartz, M. A. (1999). A role for p21-activated kinase in endothelial cell migration. *Journal of Cell Biology* **147**, 831-843.

Knowles, L. M., Stabile, L. P., Egloff, A. M., Rothstein, M. E., Thomas, S. M., Gubish, C. T., Lerner, E. C., Seethala, R. R., Suzuki, S., Quesnelle, K. M. et al.

(2009). HGF and c-Met Participate in Paracrine Tumorigenic Pathways in Head and Neck Squamous Cell Cancer. *Clinical Cancer Research* **15**, 3740-3750.

Knudsen, K. A., Soler, A. P., Johnson, K. R. and Wheelock, M. J. (1995). Interaction of alpha-actinin with the cadherin/catenin cell-cell adhesion complex via alpha-catenin. *Journal of Cell Biology* **130**, 67-77.

Kodama, A., Takaishi, K., Nakano, K., Nishioka, H. and Takai, Y. (1999). Involvement of Cdc42 small G protein in cell-cell adhesion, migration and morphology of MDCK cells. *Oncogene* **18**, 3996-4006.

Kovacs, E. M., Ali, R. G., McCormack, A. J. and Yap, A. S. (2002a). E-cadherin Homophilic Ligation Directly Signals through Rac and Phosphatidylinositol 3-Kinase to Regulate Adhesive Contacts. *Journal of Biological Chemistry* **277**, 6708-6718.

Kovacs, E. M., Goodwin, M., Ali, R. G., Paterson, A. D. and Yap, A. S. (2002b). Cadherin-Directed Actin Assembly: E-Cadherin Physically Associates with the Arp2/3 Complex to Direct Actin Assembly in Nascent Adhesive Contacts. *Current Biology* **12**, 379-382.

Kozma, R., Ahmed, S., Best, A. and Lim, L. (1995). The Ras-related protein Cdc42Hs and bradykinin promote formation of peripheral actin microspikes and filopodia in swiss 3T3 fibroblasts *Molecular and Cellular Biology* **15**, 1942-1952.

Krawczyk, W. S. (1971). Pattern of epidermal cell migration during wound healing *Journal of Cell Biology* **49**, 247-263.

Kraynov, V. S., Chamberlain, C., Bokoch, G. M., Schwartz, M. A., Slabaugh, S. and Hahn, K. M. (2000). Localized Rac Activation Dynamics Visualized in Living Cells. *Science* **290**, 333-337.

Kümper, S. and Ridley, A. J. (2010). p120ctn and P-Cadherin but Not E-Cadherin Regulate Cell Motility and Invasion of DU145 Prostate Cancer Cells. *Plos One* **5**, e11801.

Kuroda, S., Fukata, M., Kobayashi, K., Nakafuku, M., Nomura, N., Iwamatsu, A. and Kaibuchi, K. (1996). Identification of IQGAP as a putative target for the small GTPases, Cdc42 and Rac1. *Journal of Biological Chemistry* **271**, 23363-23367.

Kuroda, S., Fukata, M., Nakagawa, M., Fujii, K., Nakamura, T., Ookubo, T., Izawa, I., Nagase, T., Nomura, N., Tani, H. et al. (1998). Role of IQGAP1, a target of the small GTPases Cdc42 and Rac1, in regulation of E-cadherin-mediated cell-cell adhesion. *Science* **281**, 832-835.

Kurokawa, K. and Matsuda, M. (2005). Localized RhoA activation as a requirement for the induction of membrane ruffling. *Molecular Biology of the Cell* **16**, 4294-4303.

Lai, A. Z., Abella, J. V. and Park, M. (2009). Crosstalk in Met receptor oncogenesis. *Trends in Cell Biology* **19**, 542-551.

Lai, F. P., Szczodrak, M., Block, J., Faix, J., Breitsprecher, D., Mannherz, H. G., Stradal, T. E., Dunn, G. A., Small, J. V. and Rottner, K. (2008). Arp2/3 complex interactions and actin network turnover in lamellipodia. *Embo Journal* **27**, 982-992.

Lam, S., Verhagen, N. A. M., Strutz, F., Van Der Pijl, J. W., Daha, M. R. and Van Kooten, C. (2003). Glucose-induced fibronectin and collagen type III expression in renal fibroblasts can occur independent of TGF-beta 1. *Kidney International* **63**, 878-888.

Lauffenburger, D. A. and Horwitz, A. F. (1996). Cell migration: A physically integrated molecular process. *Cell* **84**, 359-369.

Lee, M. H., Koria, P., Qu, J. and Andreadis, S. T. (2009). JNK phosphorylates beta-catenin and regulates adherens junctions. *Faseb Journal* **23**, 3874-3883.

Lee, S. R., Ramos, S. M., Ko, A., Masiello, D., Swanson, K. D., Lu, M. L. and Balk, S. P. (2002). AR and ER interaction with a p21-activated kinase (PAK6). *Molecular Endocrinology* **16**, 85-99.

Lei, M., Lu, W. G., Meng, W. Y., Parrini, M. C., Eck, M. J., Mayer, B. J. and Harrison, S. C. (2000). Structure of PAK1 in an autoinhibited conformation reveals a multistage activation switch. *Cell* **102**, 387-397.

Leung, C. T. and Brugge, J. S. (2012). Outgrowth of single oncogene-expressing cells from suppressive epithelial environments. *Nature* **482**, 410-413.

Levayer, R. and Lecuit, T. (2008). Breaking down EMT. *Nat Cell Biol* **10**, 757-759.

Li, D., Liu, X., Richie, J. and Lu, M. (2005a). P21 activated protein kinase 6 (PAK6) as novel target of prostate cancer ionizing radiation resistance. *Journal of the American College of Surgeons* **201**, S94-S94.

Li, L., Luo, Q., Zheng, M., Pan, C., Wu, G., Lu, Y., Feng, B., Chen, X. and Liu, B. (2012). P21-activated protein kinase 1 is overexpressed in gastric cancer and induces cancer metastasis. *Oncology Reports*.

Li, X. D., Ke, Q., Li, Y. S., Liu, F. N., Zhu, G. and Li, F. (2010). DGCR6L, a novel PAK4 interaction protein, regulates PAK4-mediated migration of human gastric cancer cell via LIMK1. *International Journal of Biochemistry & Cell Biology* **42**, 70-79.

Li, X. Y., Bu, X., Lu, B. F., Avraham, H., Flavell, R. A. and Lim, B. (2002). The hematopoiesis-specific GTP-binding protein RhoH is GTPase deficient and modulates activities of other Rho GTPases by an inhibitory function. *Molecular and Cellular Biology* **22**, 1158-1171.

Li, Y., Shao, Y., Tong, Y., Shen, T., Zhang, J., Li, Y., Gu, H. and Li, F. (2011). Nucleo-cytoplasmic shuttling of PAK4 modulates β-catenin intracellular translocation and signaling. *Biochimica et Biophysica Acta (BBA) - Molecular Cell Research* **1823**, 465-475.

Li, Z. G., Kim, S. H., Higgins, J. M. G., Brenner, M. B. and Sacks, D. B. (1999). IQGAP1 and calmodulin modulate E-cadherin function. *Journal of Biological Chemistry* **274**, 37885-37892.

Li, Z. G., McNulty, D. E., Marler, K. J. M., Lim, L., Hall, C., Annan, R. S. and Sacks, D. B. (2005b). IQGAP1 promotes neurite outgrowth in a phosphorylation-dependent manner. *Journal of Biological Chemistry* **280**, 13871-13878.

Lippincott, J. and Li, R. (1998). Sequential assembly of myosin II, an IQGAP-like protein, and filamentous actin to a ring structure involved in budding yeast cytokinesis. *Journal of Cell Biology* **140**, 355-366.

Liu, H., Radisky, D. C., Wang, F. and Bissell, M. J. (2004). Polarity and proliferation are controlled by distinct signaling pathways downstream of PI3-kinase in breast epithelial tumor cells. *Journal of Cell Biology* **164**, 603-612.

Lo, C. M., Wang, H. B., Dembo, M. and Wang, Y. L. (2000). Cell movement is guided by the rigidity of the substrate. *Biophysical Journal* **79**, 144-152.

Long, R. M., Morrissey, C., Fitzpatrick, J. M. and Watson, R. W. G. (2005). Prostate epithelial cell differentiation and its relevance to the understanding of prostate cancer therapies. *Clinical Science* **108**, 1-11.

Lozano, E., Frasa, M. A. M., Smolarczyk, K., Knaus, U. G. and Braga, V. M. M. (2008). PAK is required for the disruption of E-cadherin adhesion by the small GTPase Rac. *Journal of Cell Science* **121**, 933-938.

Lu, W. G., Katz, S., Gupta, R. and Mayer, B. J. (1997). Activation of Pak by membrane localization mediated by an SH3 domain from the adaptor protein Nck. *Current Biology* **7**, 85-94.

Lu, Z. M., Jiang, G. Q., Blume-Jensen, P. and Hunter, T. (2001). Epidermal growth factor-induced tumor cell invasion and metastasis initiated by dephosphorylation and downregulation of focal adhesion kinase. *Molecular and Cellular Biology* **21**, 4016-4031.

Luzzi, K. J., MacDonald, I. C., Schmidt, E. E., Kerkvliet, N., Morris, V. L., Chambers, A. F. and Groom, A. C. (1998). Multistep nature of metastatic inefficiency - Dormancy of solitary cells after successful extravasation and limited survival of early micrometastases. *American Journal of Pathology* **153**, 865-873.

Machacek, M., Hodgson, L., Welch, C., Elliott, H., Pertz, O., Nalbant, P., Abell, A., Johnson, G. L., Hahn, K. M. and Danuser, G. (2009). Coordination of Rho GTPase activities during cell protrusion. *Nature* **461**, 99-103.

Madaule, P. and Axel, R. (1985). A novel Ras-related gene family *Cell* **41**, 31-40.

Maeno, Y., Moroi, S., Nagashima, H., Noda, T., Shiozaki, H., Monden, M., Tsukita, S. and Nagafuchi, A. (1999). α-Catenin-Deficient F9 Cells Differentiate into Signet Ring Cells. *The American Journal of Pathology* **154**, 1323-1328.

Manser, E., Chong, C., Zhao, Z. S., Leung, T., Michael, G., Hall, C. and Lim, L. (1995). Molecular coloning of a new member of the p21-Cdc42/Rac-activated kinase (PAK) family *Journal of Biological Chemistry* **270**, 25070-25078.

Manser, E., Huang, H. Y., Loo, T. H., Chen, X. Q., Dong, J. M., Leung, T. and Lim, L. (1997). Expression of constitutively active alpha-PAK reveals effects of the kinase on actin and focal complexes. *Molecular and Cellular Biology* **17**, 1129-1143.

Manser, E., Leung, T., Salihuddin, H., Zhao, Z. S. and Lim, L. (1994). A brain serine threonine protein kinase activated by Cdc42 and Rac1 *Nature* **367**, 40-46.

Manser, E., Loo, T. H., Koh, C. G., Zhao, Z. S., Chen, X. Q., Tan, L., Tan, I., Leung, T. and Lim, L. (1998). PAK kinases are directly coupled to the PIX family of nucleotide exchange factors. *Molecular Cell* **1**, 183-192.

Martin, G. A., Bollag, G., McCormick, F. and Abo, A. (1995). A novel serine kinase activated by rac1/CDC42Hs-dependent autophosphorylation related to PAK65 and STE20 *Embo Journal* **14**, 4385-4385.

Massie, C. E., Lynch, A., Ramos-Montoya, A., Boren, J., Stark, R., Fazli, L., Warren, A., Scott, H., Madhu, B., Sharma, N. et al. (2011). The androgen receptor fuels prostate cancer by regulating central metabolism and biosynthesis. *EMBO J* **30**, 2719-2733.

Mataraza, J. M., Briggs, M. W., Li, Z., Frank, R. and Sacks, D. B. (2003a). Identification and characterization of the Cdc42-binding site of IQGAP1. *Biochemical and Biophysical Research Communications* **305**, 315-321.

Mataraza, J. M., Briggs, M. W., Li, Z. G., Entwistle, A., Ridley, A. J. and Sacks, D. B. (2003b). IQGAP1 promotes cell motility and invasion. *Journal of Biological Chemistry* **278**, 41237-41245.

McAteer, J. A., Evan, A. P. and Gardner, K. D. (1987). Morphogenetic clonal growth of kidney epithelial cell line MDCK. *Anatomical Record* **217**, 229-239.

McCabe, N. P., De, S., Vasanji, A., Brainard, J. and Byzova, T. V. (2007). Prostate cancer specific integrin alpha v beta 3 modulates bone metastatic growth and tissue remodeling. *Oncogene* **26**, 6238-6243.

McInnes, I. B., AlMughales, J., Field, M., Leung, B. P., Huang, F. P., Dixon, R., Sturrock, R. D., Wilkinson, P. C. and Liew, F. Y. (1996). The role of interleukin-15 in T-cell migration and activation in rheumatoid arthritis. *Nature Medicine* **2**, 175-182.

McNeal, J. E. (1969). Origin and development of carcinoma in prostate *Cancer* **23**, 24-34.

McNeal, J. E. (1988). Normal histology of the prostate *American Journal of Surgical Pathology* **12**, 619-633.

McNulty, D. E., Li, Z. G., White, C. D., Sacks, D. B. and Annan, R. S. (2011). MAPK Scaffold IQGAP1 Binds the EGF Receptor and Modulates Its Activation. *Journal of Biological Chemistry* **286**, 15010-15021.

Menzel, N., Melzer, J., Waschke, J., Lenz, C., Wecklein, H., Lochnit, G., Drenckhahn, D. and Raabe, T. (2008). The Drosophila p21-activated kinase Mbt modulates DE-cadherin-mediated cell adhesion by phosphorylation of Armadillo. *Biochemical Journal* **416**, 231-241.

Menzel, N., Schneeberger, D. and Raabe, T. (2007). The Drosophila p21 activated kinase Mbt regulates the actin cytoskeleton and adherens junctions to control photoreceptor cell morphogenesis. *Mechanisms of Development* **124**, 78-90.

Miura, H., Nishimura, K., Tsujimura, A., Matsumiya, K., Matsumoto, K., Nakamura, T. and Okuyama, A. (2001). Effects of hepatocyte growth factor on E-cadherin-mediated cell-cell adhesion in DU145 prostate cancer cells. *Urology* **58**, 1064-1069.

Mizuno, M., Fujisawa, R. and Kuboki, Y. (2000). Type I collagen-induced osteoblastic differentiation of bone-marrow cells mediated by collagen-α2β1 integrin interaction. *Journal of Cellular Physiology* **184**, 207-213.

Mommaerts, W. (1952). The molecular transformation of actin .2. the polymerisation process. *Journal of Biological Chemistry* **198**, 459-467.

Mullins, R. D., Heuser, J. A. and Pollard, T. D. (1998). The interaction of Arp2/3 complex with actin: Nucleation, high affinity pointed end capping, and formation of branching networks of filaments. *Proceedings of the National Academy of Sciences of the United States of America* **95**, 6181-6186.

Munemitsu, S., Innis, M. A., Clark, R., McCormick, F., Ullrich, A. and Polakis, P. (1990). Molecular cloning and expression of a G25K cDNA, the human homolog of the yeast cell cycle gene CDC42. *Molecular and Cellular Biology* **10**, 5977-5982.

Nabeshima, K., Inoue, T., Shimao, Y., Okada, Y., Itoh, Y., Seiki, M. and Koono, M. (2000). Front-cell-specific expression of membrane-type 1 matrix metalloproteinase and gelatinase a during cohort migration of colon carcinoma cells induced by hepatocyte growth factor/scatter factor. *Cancer Research* **60**, 3364-3369.

Nabeshima, K., Shimao, Y., Inoue, T. and Koono, M. (2002). Immunohistochemical analysis of IQGAP1 expression in human colorectal carcinomas: its overexpression in carcinomas and association with invasion fronts. *Cancer Letters* **176**, 101-109.

Nakamura, T., Nishizawa, T., Hagiya, M., Seki, T., Shimonishi, M., Sugimura, A., Tashiro, K. and Shimizu, S. (1989). Molecular cloning and expression of human hepatocyte growth factor *Nature* **342**, 440-443.

Nakano, T., Tani, M., Ishibashi, Y., Kimura, K., Park, Y. B., Imaizumi, N., Tsuda, H., Aoyagi, K., Sasaki, H., Ohwada, S. et al. (2003). Biological properties and gene expression associated with metastatic potential of human osteosarcoma. *Clinical & Experimental Metastasis* **20**, 665-674.

Nakaya, Y., Sukowati, E. W., Wu, Y. and Sheng, G. J. (2008). RhoA and microtubule dynamics control cell-basement membrane interaction in EMT during gastrulation. *Nature Cell Biology* **10**, 765-775.

Nekrasova, T., Jobes, M. L., Ting, J. H., Wagner, G. C. and Minden, A. (2008). Targeted disruption of the Pak5 and Pak6 genes in mice leads to deficits in learning and locomotion. *Developmental Biology* **322**, 95-108.

Niranjan, B., Buluwela, L., Yant, J., Perusinghe, N., Atherton, A., Phippard, D., Dale, T., Gusterson, B. and Kamalati, T. (1995). HGF/SF: a potent cytokine for mammary growth, morphogenesis and development. *Development* **121**, 2897-2908.

Nishimura, K., Kitamura, M., Miura, H., Nonomura, N., Takada, S., Takahara, S., Matsumoto, K., Nakamura, T. and Matsumiya, K. (1999). Prostate stromal cell-derived hepatocyte growth factor induces invasion of prostate cancer cell line DU145 through tumor-stromal interaction. *Prostate* **41**, 145-153.

Nobes, C. D. and Hall, A. (1995). Rho,Rac and Cdc42 GTPases regulate the assembly of multimolecular focal complexes associated with actin stress fibers, lamellipodia, and filopodia *Cell* **81**, 53-62.

Nobes, C. D. and Hall, A. (1999). Rho GTPases control polarity, protrusion, and adhesion during cell movement. *Journal of Cell Biology* **144**, 1235-1244.

Nobes, C. D., Lauritzen, I., Mattei, M. G., Paris, S., Hall, A. and Chardin, P. (1998). A new member of the Rho family, Rnd1, promotes disassembly of actin filament structures and loss of cell adhesion. *Journal of Cell Biology* **141**, 187-197.

Noritake, J., Fukata, M., Sato, K., Nakagawa, M., Watanabe, T., Izumi, N., Wang, S. J., Fukata, Y. and Kaibuchi, K. (2004). Positive role of IQGAP1, an effector of Rac1, in actin-meshwork formation at sites of cell-cell contact. *Molecular Biology of the Cell* **15**, 1065-1076.

Noritake, J., Watanabe, T., Sato, K., Wang, S. and Kaibuchi, K. (2005). IQGAP1: a key regulator of adhesion and migration. *Journal of Cell Science* **118**, 2085-2092.

Nose, A., Nagafuchi, A. and Takeichi, M. (1988). Expressed recombinant cadherins mediate cell sorting in model systems *Cell* **54**, 993-1001.

O'Sullivan, G. C., Tangney, M., Casey, G., Ambrose, M., Houston, A. and Barry, O. P. (2007). Modulation of p21-activated kinase 1 alters the behavior of renal cell carcinoma. *International Journal of Cancer* **121**, 1930-1940.

Ochiai, A., Akimoto, S., Shimoyama, Y., Nagafuchi, A., Tsukita, S. and Hirohashi, S. (1994). Frequent loss of alpha-catenin expression in scirrhous carcinomas with scattered cell growth. *Japanese Journal of Cancer Research* **85**, 266-273.

Ohkubo, T. and Ozawa, M. (1999). p120(ctn) binds to the membrane-proximal region of the E-cadherin cytoplasmic domain and is involved in modulation of adhesion activity. *Journal of Biological Chemistry* **274**, 21409-21415.

Ortonne, J.-P., Löning, T., Schmitt, D. and Thivolet, J. (1981). Immunomorphological and ultrastructural aspects of keratinocyte migration in epidermal wound healing. *Virchows Archiv* **392**, 217-230.

Ozawa, M. and Kemler, R. (1998). Altered Cell Adhesion Activity by Pervanadate Due to the Dissociation of α-Catenin from the E-Cadherin-Catenin Complex. *Journal of Biological Chemistry* **273**, 6166-6170.

Palacios, F. and D'Souza-Schorey, C. (2003). Modulation of Rac1 and ARF6 Activation during Epithelial Cell Scattering. *Journal of Biological Chemistry* **278**, 17395-17400.

Palecek, S. P., Loftus, J. C., Ginsberg, M. H., Lauffenburger, D. A. and Horwitz, A. F. (1997). Integrin-ligand binding properties govern cell migration speed through cell-substratum adhesiveness. *Nature* **385**, 537-540.

Pandey, A., Dan, I., Kristiansen, T. Z., Watanabe, N. M., Voldby, J., Kajikawa, E., Khosravi-Far, R., Blagoev, B. and Mann, M. (2002). Cloning and characterization of PAK5, a novel member of mammalian p21-activated kinase-II subfamily that is predominantly expressed in brain. *Oncogene* **21**, 3939-3948.

Pantel, K., Aignherr, C., Köllermann, J., Caprano, J., Riethmüller, G. and Köllermann, M. W. (1995). Immunocytochemical detection of isolated tumour cells in bone marrow of patients with untreated stage C prostatic cancer. *European Journal of Cancer* **31A**, 1627-1632.

Pantel, K., Enzmann, T., Köllermann, J., Caprano, J., Riethmüller, C. and Köllermann, M. W. (1997). Immunocytochemical monitoring of micrometastatic disease: Reduction of prostate cancer cells in bone marrow by androgen deprivation. *International Journal of Cancer* **71**, 521-525.

Parr, C., Davies, G., Nakamura, T., Matsumoto, K., Mason, M. D. and Jiang, W. G. (2001). The HGF/SF-induced phosphorylation of paxillin, matrix adhesion, and invasion of prostate cancer cells were suppressed by NK4, an HGF/SF variant. *Biochemical and Biophysical Research Communications* **285**, 1330-1337.

Parri, M. and Chiarugi, P. (2010). Rac and Rho GTPases in cancer cell motility control. *Cell Communication and Signaling* **8**.

Parrini, M. C., Lei, M., Harrison, S. C. and Mayer, B. J. (2002). Pak1 kinase homodimers are autoinhibited in trans and dissociated upon activation by Cdc42 and Rac1. *Molecular Cell* **9**, 73-83.

Patel, S., Takagi, K., Suzuki, J., Imaizumi, A., Kimura, T., Mason, R. M., Kamimura, T. and Zhang, Z. (2005). RhoGTPase activation is a key step in renal epithelial mesenchymal transdifferentiation. *Journal of the American Society of Nephrology* **16**, 1977-1984.

Patel, V., Hood, B. L., Molinolo, A. A., Lee, N. H., Conrads, T. P., Braisted, J. C., Krizman, D. B., Veenstra, T. D. and Gutkind, J. S. (2008). Proteomic analysis of laser-captured paraffin-embedded tissues: A molecular portrait of head and neck cancer progression. *Clinical Cancer Research* **14**, 1002-1014.

Paterson, H. F., Self, A. J., Garrett, M. D., Just, I., Aktories, K. and Hall, A. (1990). Microinjection of recombinant p21rho induces rapid changes in cell morphology *Journal of Cell Biology* **111**, 1001-1007.

Patrawala, L., Calhoun-Davis, T., Schneider-Broussard, R. and Tang, D. G. (2007). Hierarchical organization of prostate cancer cells in xenograft tumors: The CD44(+)alpha 2 beta 1(+) cell population is enriched in tumor-initiating cells. *Cancer Research* **67**, 6796-6805.

Perl, A. K., Wilgenbus, P., Dahl, U., Semb, H. and Christofori, G. (1998). A causal role for E-cadherin in the transition from adenoma to carcinoma. *Nature* **392**, 190-193.

Pertz, O., Hodgson, L., Klemke, R. L. and Hahn, K. M. (2006). Spatiotemporal dynamics of RhoA activity in migrating cells. *Nature* **440**, 1069-1072.

Peruzzi, B. and Bottaro, D. P. (2006). Targeting the c-Met signaling pathway in cancer. *Clinical Cancer Research* **12**, 3657-3660.

Peters, J. H., Sporn, L. A., Ginsberg, M. H. and Wagner, D. D. (1990). Human endothelial cells synthesize, process, and secrete fibronectin molecules bearing an alternatively spliced type III homology (ED1) *Blood* **75**, 1801-1808.

Pilot, F., Philippe, J.-M., Lemmers, C. and Lecuit, T. (2006). Spatial control of actin organization at adherens junctions by a synaptotagmin-like protein. *Nature* **442**, 580-584.

Pollard, T. D. and Borisy, G. G. (2003). Cellular motility driven by assembly and disassembly of actin filaments. *Cell* **113**, 549-549.

Potempa, S. and Ridley, A. J. (1998). Activation of both MAP kinase and phosphatidylinositide 3-kinase by Ras is required for hepatocyte growth factor scatter factor-induced adherens junction disassembly. *Molecular Biology of the Cell* **9**, 2185-2200.

Prescott, M. F., McBride, C. K. and Court, M. (1989). Development of intimal lesions after leukocyte migration into the vascular wall *American Journal of Pathology* **135**, 835-846.

Puto, L. A., Pestonjamasp, K., King, C. C. and Bokoch, G. M. (2003). p21-activated kinase 1 (PAK1) interacts with the Grb2 adapter protein to couple to growth factor signaling. *Journal of Biological Chemistry* **278**, 9388-9393.

Qiu, R. G., Abo, A., McCormick, F. and Symons, M. (1997). Cdc42 regulates anchorage-independent growth and is necessary for Ras transformation. *Molecular and Cellular Biology* **17**, 3449-3458.

Qu, J., Cammarano, M. S., Shi, Q., Ha, K. C., De Lanerolle, P. and Minden, A. (2001). Activated PAK4 regulates cell adhesion and anchorage-independent growth. *Molecular and Cellular Biology* **21**, 3523-3533.

Rabinovitz, I., Nagle, R. B. and Cress, A. E. (1995). Integrin alpha 6 expression in human prostate carcinoma cells is associated with a migratory and invasive phenotype in vitro and in vivo *Clinical & Experimental Metastasis* **13**, 481-491.

Raftopoulou, M. and Hall, A. (2004). Cell migration: Rho GTPases lead the way. *Developmental Biology* **265**, 23-32.

Raghavan, S., Shen, C. J., Desai, R. A., Sniadecki, N. J., Nelson, C. M. and Chen, C. S. (2010). Decoupling diffusional from dimensional control of signaling in 3D culture reveals a role for myosin in tubulogenesis. *Journal of Cell Science* **123**, 2877-2883.

Rayala, S. K., Talukder, A. H., Balasenthil, S., Tharakan, R., Barnes, C. J., Wang, R. A., Aldaz, M., Khan, S. and Kumar, R. (2006). P21-activated kinase 1 regulation of estrogen receptor-alpha activation involves serine 305 activation linked with serine 118 phosphorylation. *Cancer Research* **66**, 1694-1701.

Ren, J.-G., Li, Z., Crimmins, D. L. and Sacks, D. B. (2005). Self-association of IQGAP1. *Journal of Biological Chemistry* **280**, 34548-34557.

Ren, J. G., Li, Z. G. and Sacks, D. B. (2007). IQGAP1 modulates activation of B-Raf. *Proceedings of the National Academy of Sciences of the United States of America* **104**, 10465-10469.

Ren, Y., Li, R., Zheng, Y. and Busch, H. (1998). Cloning and characterization of GEF-H1, a microtubule-associated guanine nucleotide exchange factor for Rac and Rho GTPases. *Journal of Biological Chemistry* **273**, 34954-34960.

Reynolds, A. B., Daniel, J. M., Mo, Y. Y., Wu, J. and Zhang, Z. (1996). The novel catenin p120(cas) binds classical cadherins and induces an unusual morphological phenotype in NIH3T3 fibroblasts. *Experimental Cell Research* **225**, 328-337.

Ridley, A. J. (2011). Life at the Leading Edge. *Cell* **145**, 1012-1022.

Ridley, A. J., Comoglio, P. M. and Hall, A. (1995). Regulation of scatter factor/hepatocyte growth factor responses by Ras, Rac, and Rho in MDCK cells *Molecular and Cellular Biology* **15**, 1110-1122.

Ridley, A. J. and Hall, A. (1992). The small GTP-binding protein rho regulates the assembly of focal adhesions and actin stress fibers in response to growth factors *Cell* **70**, 389-399.

Ridley, A. J., Paterson, H. F., Johnston, C. L., Diekmann, D. and Hall, A. (1992). The small GTP-binding protein rac regulates growth factor-induced membrane ruffling *Cell* **70**, 401-410.

Ridley, A. J., Schwartz, M. A., Burridge, K., Firtel, R. A., Ginsberg, M. H., Borisy, G., Parsons, J. T. and Horwitz, A. R. (2003). Cell migration: Integrating signals from front to back. *Science* **302**, 1704-1709.

Rimm, D. L., Koslov, E. R., Kebriaei, P., Cianci, C. D. and Morrow, J. S. (1995). Alpha(1)(E)-catenin is an actin-binding and actin-bundling protein mediating the attachment of F-actin to the membrane adhesion complex. *Proceedings of the National Academy of Sciences of the United States of America* **92**, 8813-8817.

Rosenow, F., Ossig, R., Thormeyer, D., Gasmann, P., Schlüter, K., Brunner, G., Haier, J. and Eble, J. A. (2008). Integrins as Antimetastatic Targets of RGD-Independent Snake Venom Components in Liver Metastasis. *Neoplasia* **10**, 168-176.

Rossman, K. L., Der, C. J. and Sondek, J. (2005). GEF means go: Turning on Rho GTPases with guanine nucleotide-exchange factors. *Nature Reviews Molecular Cell Biology* **6**, 167-180.

Roy, M., Li, Z. G. and Sacks, D. B. (2004). IQGAP1 binds ERK2 and modulates its activity. *Faseb Journal* **18**, C165-C165.

Roy, M., Li, Z. G. and Sacks, D. B. (2005). IQGAP1 is a scaffold for mitogen-activated protein kinase signaling. *Molecular and Cellular Biology* **25**, 7940-7952.

Royal, I., Lamarche-Vane, N., Lamorte, L., Kaibuchi, K. and Park, M. (2000). Activation of Cdc42, Rac, PAK, and Rho-kinase in response to hepatocyte growth factor differentially regulates epithelial cell colony spreading and dissociation. *Molecular Biology of the Cell* **11**, 1709-1725.

Royal, I. and Park, M. (1995). Hepatocyte growth factor-induced scatter of Madin Darby canine kidney cells requires phosphatidylinositol 3-kinase *Journal of Biological Chemistry* **270**, 27780-27787.

Royer, C. and Lu, X. (2011). Epithelial cell polarity: a major gatekeeper against cancer? *Cell Death and Differentiation* **18**, 1470-1477.

Ruggiero, F., Champliaud, M. F., Garrone, R. and Aumailley, M. (1994). Interactions between cells and collagen V molecules or single chains involve distinct mechanisms *Experimental Cell Research* **210**, 215-223.

Sahai, E. (2007). Illuminating the metastatic process. *Nature Reviews Cancer* **7**, 737-749.

Sahai, E. and Marshall, C. J. (2003). Differing modes of tumour cell invasion have distinct requirements for Rho/ROCK signalling and extracellular proteolysis. *Nature Cell Biology* **5**, 711-719.

Sander, E. E., van Delft, S., ten Klooster, J. P., Reid, T., van der Kammen, R. A., Michiels, F. and Collard, J. G. (1998). Matrix-dependent Tiam1/Rac signaling in epithelial cells promotes either cell-cell adhesion or cell migration and is regulated by phosphatidylinositol 3-kinase. *Journal of Cell Biology* **143**, 1385-1398.

Schmelz, M., Cress, A. E., Scott, K. M., Bürger, F., Cui, H. Y., Sallam, K., McDaniel, K. M., Dalkin, B. L. and Nagle, R. B. (2002). Different phenotypes in human prostate cancer: alpha 6 or alpha 3 integrin in cell-extracellular adhesion sites. *Neoplasia* **4**, 243-254.

Schmidt-Mende, J., Geering, B., Yousefi, S. and Simon, H. U. (2010). Lysosomal degradation of RhoH protein upon antigen receptor activation in T but not B cells. *European Journal of Immunology* **40**, 525-529.

Schmidt, C., Bladt, F., Goedecke, S., Brinkmann, V., Zschiesche, W., Sharpe, M., Gherardi, E. and Birchmeier, C. (1995). Scatter factor/hepatocyte growth factor is essential for liver development *Nature* **373**, 699-702.

Schneeberger, D. and Raabe, T. (2003). Mbt, a Drosophila PAK protein, combines with Cdc42 to regulate photoreceptor cell morphogenesis. *Development* **130**, 427-437.

Schneider, L., Cammer, M., Lehman, J., Nielsen, S. K., Guerra, C. F., Veland, I. R., Stock, C., Hoffmann, E. K., Yoder, B. K., Schwab, A. et al. (2010). Directional Cell Migration and Chemotaxis in Wound Healing Response to PDGF-AA are Coordinated by the Primary Cilium in Fibroblasts. *Cellular Physiology and Biochemistry* **25**, 279-292.

Schrantz, N., Correia, J. D., Fowler, B., Ge, Q. Y., Sun, Z. J. and Bokoch, G. M. (2004). Mechanism of p21-activated kinase 6-mediated inhibition of androgen receptor signaling. *Journal of Biological Chemistry* **279**, 1922-1931.

Sells, M. A., Knaus, U. G., Bagrodia, S., Ambrose, D. M., Bokoch, G. M. and Chernoff, J. (1997). Human p21-activated kinase (Pak1) regulates actin organization in mammalian cells. *Current Biology* **7**, 202-210.

Serres, M., Grangeasse, C., Haftek, M., Durocher, Y., Duclos, B. and Schmitt, D. (1997). Hyperphosphorylation of beta-catenin on serine-threonine residues and loss of cell-cell contacts induced by calyculin A and okadaic acid in human epidermal cells. *Experimental Cell Research* **231**, 163-172.

Shadidi, K. R., Thompson, K. M., Henriksen, J. E., Natvig, J. B. and Aarvak, T. (2002). Association of antigen specificity and migratory capacity of memory T cells in rheumatoid arthritis. *Scandinavian Journal of Immunology* **55**, 274-283.

Shen, M. M. and Abate-Shen, C. (2010). Molecular genetics of prostate cancer: new prospects for old challenges. *Genes & Development* **24**, 1967-2000.

Shepelev, M. and Korobko, I. (2012). Pak6 protein kinase is a novel effector of an atypical Rho family GTPase Chp/RhoV. *Biochemistry (Moscow)* **77**, 26-32.

Shibamoto, S., Hayakawa, M., Takeuchi, K., Hori, T., Miyazawa, K., Kitamura, N., Johnson, K. R., Wheelock, M. J., Matsuyoshi, N., Takeichi, M. et al. (1995). Association of p120, a tyrosine kinase substrate, with E-Cadherin/catenin complexes *Journal of Cell Biology* **128**, 949-957.

Shimamura, K. and Takeichi, M. (1992). Local and transient expression of E-cadherin involved in mouse embryonic brain morphogenesis *Development* **116**, 1011-&.

Siu, M. K. Y., Wong, E. S. Y., Chan, H. Y., Kong, D. S. H., Woo, N. W. S., Tam, K. F., Ngan, H. Y. S., Chan, Q. K. Y., Chan, D. C. W., Chan, K. Y. K. et al. (2010). Differential expression and phosphorylation of Pak1 and Pak2 in ovarian cancer: effects on prognosis and cell invasion. *International Journal of Cancer* **127**, 21-31.

Small, J. V., Isenberg, G. and Celis, J. E. (1978). Polarity of actin at the leading edge of cultured cells *Nature* **272**, 638-639.

Small, J. V., Stradal, T., Vignal, E. and Rottner, K. (2002). The lamellipodium: where motility begins. *Trends in Cell Biology* **12**, 112-120.

Stanley, F. M. (2007). Insulin-increased prolactin gene expression requires actin treadmilling: Potential role for p21 activated kinase. *Endocrinology* **148**, 5874-5883.

Steeg, P. S. (2003). Metastasis suppressors alter the signal transduction of cancer cells. *Nat Rev Cancer* **3**, 55-63.

Stockton, R. A., Schaefer, E. and Schwartz, M. A. (2004). p21-activated kinase regulates endothelial permeability through modulation of contractility. *Journal of Biological Chemistry* **279**, 46621-46630.

Stoker, M. (1989). Effect of scatter factor on motility of epithelial cells and fibroblasts *Journal of Cellular Physiology* **139**, 565-569.

Stoker, M., Gherardi, E., Perryman, M. and Gray, J. (1987). Scatter factor is a fibroblast-derived modulator of epithelial cell mobility *Nature* **327**, 239-242.

Stoker, M. and Perryman, M. (1985). An epithelial scatter factor released by embryo fibroblasts *Journal of Cell Science* **77**, 209-223.

Stolz, D. B. and Michalopoulos, G. K. (1994). Comparative effects of hepatocyte growth factor and epidermal growth factor on motility, morphology, mitogenesis, and signal transduction of primary rat hepatocytes *Journal of Cellular Biochemistry* **55**, 445-464.

Straub, F. B. (1943). Actin, II. *Stud. Inst. Med. Chem.Univ. Szeged*, 23-37.

Sugiyama, N., Varjosalo, M., Meller, P., Lohi, J., Hyytiainen, M., Kilpinen, S., Kallioniemi, O., Ingvarsen, S., Engelholm, L. H., Taipale, J. et al. (2010). Fibroblast Growth Factor Receptor 4 Regulates Tumor Invasion by Coupling Fibroblast Growth Factor Signaling to Extracellular Matrix Degradation. *Cancer Research* **70**, 7851-7861.

Swaminathan, G. and Cartwright, C. A. (2011). Rack1 promotes epithelial cell-cell adhesion by regulating E-cadherin endocytosis. *Oncogene* **31**, 376-389.

Swart-Mataraza, J. M., Li, Z. G. and Sacks, D. B. (2002). IQGAP1 is a component of Cdc42 signaling to the cytoskeleton. *Journal of Biological Chemistry* **277**, 24753-24763.

Taherian, A., Li, X. L., Liu, Y. Q. and Haas, T. A. (2011). Differences in integrin expression and signaling within human breast cancer cells. *Bmc Cancer* **11**.

Takaishi, K., Sasaki, T., Kotani, H., Nishioka, H. and Takai, Y. (1997). Regulation of cell-cell adhesion by Rac and Rho small G proteins in MDCK cells. *Journal of Cell Biology* **139**, 1047-1059.

Takeichi, M. (1977). Functional correlation between cell adhesive properties and some cell surface proteins *Journal of Cell Biology* **75**, 464-474.

Takemoto, H., Doki, Y., Shiozaki, H., Imamura, H., Utsunomiya, T., Miyata, H., Yano, M., Inoue, M., Fujiwara, Y. and Monden, M. (2001). Localization of IQGAP1 is inversely correlated with intercellular adhesion mediated by e-cadherin in gastric cancers. *International Journal of Cancer* **91**, 783-788.

Tanihara, H., Sano, K., Heimark, R. L., St john, T. and Suzuki, S. (1994). Cloning of five human cadherins clarifies characteristic features of cadherin extracellular domain and provides further evidence for 2 structurally different types of cadherin *Cell Adhesion and Communication* **2**, 15-26.

Tay, H. G., Ng, Y. W. and Manser, E. (2010). A Vertebrate-Specific Chp-PAK-PIX Pathway Maintains E-Cadherin at Adherens Junctions during Zebrafish Epiboly. *Plos One* **5**, e10125.

Tcherkezian, J. and Lamarche-Vane, N. (2007). Current knowledge of the large RhoGAP family of proteins. *Biology of the Cell* **99**, 67-86.

Teo, M., Manser, E. and Lim, L. (1995). Identification and molecular cloning of a p21 (Cdc42/Rac1)-activated serine/threonine kinase that is rapidly activated by thrombin in platelets *Journal of Biological Chemistry* **270**, 26690-26697.

Theriot, J. A. and Mitchison, T. J. (1991). Actin microfilament dynamics in locomoting cells *Nature* **352**, 126-131.

Thoreson, M. A., Anastasiadis, P. Z., Daniel, J. M., Ireton, R. C., Wheelock, M. J., Johnson, K. R., Hummingbird, D. K. and Reynolds, A. B. (2000). Selective uncoupling of p120(ctn) from E-cadherin disrupts strong adhesion. *Journal of Cell Biology* **148**, 189-201.

Tillotson, J. K. and Rose, D. P. (1991). Endogenous secretion of epidermal growth factor peptides stimulates growth of DU145 prostate cancer cells. *Cancer Letters* **60**, 109-112.

Timms, B. G. (2008). Prostate development: a historical perspective. *Differentiation* **76**, 565-577.

Toiyama, Y., Yasuda, H., Saigusa, S., Matushita, K., Fujikawa, H., Tanaka, K., Mohri, Y., Inoue, Y., Goel, A. and Kusunoki, M. (2011). Co-expression of hepatocyte growth factor and c-Met predicts peritoneal dissemination established by autocrine hepatocyte growth factor/c-Met signaling in gastric cancer. *International Journal of Cancer*, 2912-2921.

Tomura, M., Honda, T., Tanizaki, H., Otsuka, A., Egawa, G., Tokura, Y., Waldmann, H., Hori, S., Cyster, J. G., Watanabe, T. et al. (2010). Activated regulatory T cells are the major T cell type emigrating from the skin during a cutaneous immune response in mice. *The Journal of Clinical Investigation* **120**, 883-893.

Tomura, M., Yoshida, N., Tanaka, J., Karasawa, S., Miwa, Y., Miyawaki, A. and Kanagawa, O. (2008). Monitoring cellular movement in vivo with photoconvertible fluorescence protein "Kaede" transgenic mice. *Proceedings of the National Academy of Sciences of the United States of America* **105**, 10871-10876.

Trusolino, L., Cavassa, S., Angelini, P., Ando, M., Bertotti, A., Comoglio, P. M. and Boccaccio, C. (2000). HGF/scatter factor selectively promotes cell invasion by increasing integrin avidity. *Faseb Journal* **14**, 1629-1640.

Tse, J. M., Cheng, G., Tyrrell, J. A., Wilcox-Adelman, S. A., Boucher, Y., Jain, R. K. and Munn, L. L. (2011). Mechanical compression drives cancer cells toward invasive phenotype. *Proceedings of the National Academy of Sciences* **109**, 911-916.

Tsingotjidou, A. S., Zotalis, G., Jackson, K. R., Sawyers, C., Puzas, J. E., Hicks, D. G., Reiter, R. and Lieberman, J. R. (2001). Development of an animal model for prostate cancer cell metastasis to adult human bone. *Anticancer research* **21**, 971-8.

Turner, T., Chen, P., Goodly, L. J. and Wells, A. (1996). EGF receptor signaling enhances in vivo invasiveness of DU-145 human prostate carcinoma cells. *Clinical & Experimental Metastasis* **14**, 409-418.

Vadlamudi, R. K., Li, F., Barnes, C. J., Bagheri-Yarmand, R. and Kumar, R. (2004). p41-Arc subunit of human Arp2/3 complex is a p21-activated kinase-1-interacting substrate. *Embo Reports* **5**, 154-160.

van de Wijngaart, D. J., van Royen, M. E., Hersmus, R., Pike, A. C. W., Houtsmuller, A. B., Jenster, G., Trapman, J. and Dubbink, H. J. (2006). Novel FXXFF and FXXMF motifs in androgen receptor cofactors mediate high affinity and specific interactions with the ligand-binding domain. *Journal of Biological Chemistry* **281**, 19407-19416.

van Leenders, G., van Balken, B., Aalders, T., Hulsbergen-van de Kaa, C., Ruiter, D. and Schalken, J. (2002). Intermediate cells in normal and malignant prostate epithelium express C-MET: Implications for prostate cancer invasion. *Prostate* **51**, 98-107.

van Leenders, G. J. L. H., Sookhlall, R., Teubel, W. J., de Ridder, C. M. A., Reneman, S., Sacchetti, A., Vissers, K. J., van Weerden, W. and Jenster, G. (2011). Activation of c-MET Induces a Stem-Like Phenotype in Human Prostate Cancer. *Plos One* **6**, e26753.

van Roy, F. and Berx, G. (2008). The cell-cell adhesion molecule E-cadherin. *Cellular and Molecular Life Sciences* **65**, 3756-3788.

Vasilyev, A., Liu, Y., Mudumana, S., Mangos, S., Lam, P.-Y., Majumdar, A., Zhao, J., Poon, K.-L., Kondrychyn, I., Korzh, V. et al. (2009). Collective Cell Migration Drives Morphogenesis of the Kidney Nephron. *PLoS Biol* **7**, e1000009.

Vaughan, R. B. and Trinkaus, J. P. (1966). Movements of epithelial cell sheets in vitro *Journal of Cell Science* **1**, 407-&.

Vestweber, D. and Kemler, R. (1984). Rabbit antiserum against a purified surface glycoprotein decompacts mouse preimplantation embryos and reacts with specific adult tissues *Experimental Cell Research* **152**, 169-178.

Vilas, G. L., Corvi, M. M., Plummer, G. J., Seime, A. M., Lambkin, G. R. and Berthiaume, L. G. (2006). Posttranslational myristoylation of caspase-activated p21-activated protein kinase 2 (PAK2) potentiates late apoptotic events. *Proceedings of the National Academy of Sciences of the United States of America* **103**, 6542-6547.

Virtanen, I., Korkohen, M., Laitinen, L., Ylänne, J., Kariniemi, A.-L. and Gould, V. E. (1990). Integrins in human cells and tumors. *Cell Differentiation and Development* **32**, 215-227.

Vogt, F., Zernecke, A., Beckner, M., Krott, N., Bosserhoff, A.-K., Hoffmann, R., Zandvoort, M. A. M. J., Jahnke, T., Kelm, M., Weber, C. et al. (2008). Blockade of Angio-Associated Migratory Cell Protein Inhibits Smooth Muscle Cell Migration and Neointima Formation in Accelerated Atherosclerosis. *J Am Coll Cardiol* **52**, 302-311.

Wallace, S. W., Durgan, J., Jin, D. and Hall, A. (2010). Cdc42 Regulates Apical Junction Formation in Human Bronchial Epithelial Cells through PAK4 and Par6B. *Molecular Biology of the Cell* **21**, 2996-3006.

Wang, R. A., Mazumdar, A., Vadlamudi, R. K. and Kumar, R. (2002). P21-activated kinase-1 phosphorylates and transactivates estrogen receptor-alpha and promotes hyperplasia in mammary epithelium. *Embo Journal* **21**, 5437-5447.

Wang, S. J., Watanabe, T., Noritake, J., Fukata, M., Yoshimura, T., Itoh, N., Harada, T., Nakagawa, M., Matsuura, Y., Arimura, N. et al. (2007). IQGAP3, a novel effector of Rac1 and Cdc42, regulates neurite outgrowth. *Journal of Cell Science* **120**, 567-577.

Wang, X., Julio, M. K.-d., Economides, K. D., Walker, D., Yu, H., Halili, M. V., Hu, Y.-P., Price, S. M., Abate-Shen, C. and Shen, M. M. (2009). A luminal epithelial stem cell that is a cell of origin for prostate cancer. *Nature* **461**, 495-500.

Wang, X. X., Liu, R., Jin, S. Q., Fan, F. Y. and Zhan, Q. M. (2006). Overexpression of Aurora-A kinase promotes tumor cell proliferation and inhibits apoptosis in esophageal squamous cell carcinoma cell line. *Cell Res* **16**, 356-366.

Wang, Y. P., Yu, Q. J., Cho, A. H., Rondeau, G., Welsh, J., Adamson, E., Mercola, D. and McClelland, M. (2005). Survey of differentially methylated promoters in prostate cancer cell lines. *Neoplasia* **7**, 748-760.

Watabe, M., Nagafuchi, A., Tsukita, S. and Takeichi, M. (1994). Induction of polarized cell-cell association and retardation of growth by activation of the E-cadherin-catenin adhesion system in a dispersed carcinoma line *Journal of Cell Biology* **127**, 247-256.

Wegner, A. (1976). Head to tail polymerization of actin *Journal of Molecular Biology* **108**, 139-150.

Weidner, K. M., Behrens, J., Vandekerckhove, J. and Birchmeier, W. (1990). Scatter factor: molecular characteristics and effect on the invasiveness of epithelial cells *Journal of Cell Biology* **111**, 2097-2108.

Weissbach, L., Settleman, J., Kalady, M. F., Snijders, A. J., Murthy, A. E., Yan, Y. X. and Bernards, A. (1994). Identification of a human RasGAP-related protein containing calmodulin-binding motifs *Journal of Biological Chemistry* **269**, 20517-20521.

Wells, C. M., Abo, A. and Ridley, A. J. (2002). PAK4 is activated via PI3K in HGF-stimulated epithelial cells. *Journal of Cell Science* **115**, 3947-3956.

Wells, C. M., Ahmed, T., Masters, J. R. W. and Jones, G. E. (2005). Rho family GTPases are activated during HGF-stimulated prostate cancer-cell scattering. *Cell Motility and the Cytoskeleton* **62**, 180-194.

Wells, C. M. and Jones, G. E. (2010). The emerging importance of group II PAKs. *Biochemical Journal* **425**, 465-473.

Wells, C. M., Whale, A. D., Parsons, M., Masters, J. R. W. and Jones, G. E. (2010). PAK4: a pluripotent kinase that regulates prostate cancer cell adhesion. *Journal of Cell Science* **123**, 1663-1673.

Wen, X. Q., Li, X. J., Liao, B., Liu, Y., Wu, J. Y., Yuan, X. X., Ouyang, B., Sun, Q. P. and Gao, X. (2009). Knockdown of p21-activated Kinase 6 Inhibits Prostate Cancer Growth and Enhances Chemosensitivity to Docetaxel. *Urology* **73**, 1407-1411.

Whale, A., Hashim, F. N., Fram, S., Jones, G. E. and Wells, C. M. (2011). Signalling to cancer cell invasion through PAK family kinases. *Frontiers in Bioscience-Landmark* **16**, 849-864.

White, C. D., Erdemir, H. H. and Sacks, D. B. (2011). IQGAP1 and its binding proteins control diverse biological functions. *Cellular Signalling* **24**, 826-834.

Witkowski, C. M., Rabinovitz, I., Nagle, R. B., Affinito, K. S. D. and Cress, A. E. (1993). Characterization of integrin subunits, cellular adhesion and tumorgenicity of four human prostate cell lines *Journal of Cancer Research and Clinical Oncology* **119**, 637-644.

Wong, L. E., Reynolds, A. B., Dissanayaka, N. T. and Minden, A. (2010). p120-catenin is a binding partner and substrate for Group B Pak kinases. *Journal of Cellular Biochemistry* **110**, 1244-1254.

Wu, X. and Frost, J. A. (2006). Multiple Rho proteins regulate the subcellular targeting of PAK5. *Biochemical and Biophysical Research Communications* **351**, 328-335.

www.harvardprostateknowledge.org/prostate-basics.

Wyckoff, J. B., Jones, J. G., Condeelis, J. S. and Segall, J. E. (2000). A critical step in metastasis: In vivo analysis of intravasation at the primary tumor. *Cancer Research* **60**, 2504-2511.

Xia, X., Mariner, D. J. and Reynolds, A. B. (2003). Adhesion-Associated and PKC-Modulated Changes in Serine/Threonine Phosphorylation of p120-Cateninâ€ *Biochemistry* **42**, 9195-9204.

Yamada, S., Pokutta, S., Drees, F., Weis, W. I. and Nelson, W. J. (2005). Deconstructing the Cadherin-Catenin-Actin Complex. *Cell* **123**, 889-901.

Yamashiro, S., Noguchi, T. and Mabuchi, I. (2003). Localization of two IQGAPs in cultured cells and early embryos of Xenopus laevis. *Cell Motility and the Cytoskeleton* **55**, 36-50.

Yamazaki, D., Kurisu, S. and Takenawa, T. (2009). Involvement of Rac and Rho signaling in cancer cell motility in 3D substrates. *Oncogene* **28**, 1570-1583.

Yang, F., Lio, X. Y., Sharma, M. J., Zarnegar, M., Lim, B. and Sun, Z. (2001). Androgen receptor specifically interacts with a novel p21-activated kinase, PAK6. *Journal of Biological Chemistry* **276**, 15345-15353.

Yap, A. S., Niessen, C. M. and Gumbiner, B. M. (1998). The juxtamembrane region of the cadherin cytoplasmic tail supports lateral clustering, adhesive strengthening, and interaction with p129(ctn). *Journal of Cell Biology* **141**, 779-789.

Yilmaz, M. and Christofori, G. (2009). EMT, the cytoskeleton, and cancer cell invasion. *Cancer and Metastasis Reviews* **28**, 15-33.

Yin, N., Shi, J., Wang, D., Tong, T., Wang, M., Fan, F. and Zhan, Q. (2012). IQGAP1 interacts with Aurora-A and enhances its stability and its role in cancer. *Biochemical and Biophysical Research Communications*.

Yoshida, C. and Takeichi, M. (1982). Teratocarcinoma cell adhesion: Identification of a cell-surface protein involved in calcium-dependent cell aggregation. *Cell* **28**, 217-224.

Zaman, M. H., Trapani, L. M., Siemeski, A., MacKellar, D., Gong, H., Kamm, R. D., Wells, A., Lauffenburger, D. A. and Matsudaira, P. (2006). Migration of tumor cells in 3D matrices is governed by matrix stiffness along with cell-matrix adhesion and proteolysis *Proceedings of the National Academy of Sciences of the United States of America* **103**, 13897-13897.

Zegers, M. M. P., Forget, M. A., Chernoff, J., Mostov, K. E., ter Beest, M. B. A. and Hansen, S. H. (2003). Pak1 and PIX regulate contact inhibition during epithelial wound healing. *Embo Journal* **22**, 4155-4165.

Zeng, Q., Lagunoff, D., Masaracchia, R., Goeckeler, Z., Côté, G. and Wysolmerski, R. (2000). Endothelial cell retraction is induced by PAK2 monophosphorylation of myosin II. *Journal of Cell Science* **113**, 471-482.

Zhang, L., Luo, J., Wan, P., Wu, J., Laski, F. and Chen, J. (2011). Regulation of cofilin phosphorylation and asymmetry in collective cell migration during morphogenesis. *Development* **138**, 455-464.

Zhang, M., Siedow, M., Saia, G. and Chakravarti, A. (2009). Inhibition of p21-activated kinase 6 (PAK6) increases radiosentivity of prostate cancer cells. *Proceedings of the American Association for Cancer Research Annual Meeting* **50**, 962.

Zhao, Z. S., Manser, E., Chen, X. Q., Chong, C., Leung, T. and Lim, L. (1998). A conserved negative regulatory region in alpha PAK: Inhibition of PAK kinases reveals their morphological roles downstream of Cdc42 and Rac1. *Molecular and Cellular Biology* **18**, 2153-2163.

Zhao, Z. S., Manser, E., Loo, T. H. and Lim, L. (2000). Coupling of PAK-interacting exchange factor PIX to GIT1 promotes focal complex disassembly. *Molecular and Cellular Biology* **20**, 6354-6363.

Zhou, W., Grandis, J. R. and Wells, A. (2006). STAT3 is required but not sufficient for EGF receptor-mediated migration and invasion of human prostate carcinoma cell lines. *British Journal of Cancer* **95**, 164-171.

Zhu, G., Wang, Y., Huang, B., Liang, J., Ding, Y., Xu, A. and Wu, W. (2011). A Rac1/PAK1 cascade controls β-catenin activation in colon cancer cells. *Oncogene* **31**, 1001-1012.

Appendices

Appendix 1 – PCR amplification primer sequences

Full-length PAK6 (amino acids 1–682)

*att*B1 Forward primer: **5'**-GGGG ACA AGT TTG TAC AAA AAA GCA GGC TTG ATG TTC CGC AAG AAA AAG AAG AAA-**3'**

*att*B2 Reverse primer: **5'**-GGGG A CCA CTT TGT ACA AGA AAG CTG GGT C TCA GCA GGT GGA GGT CTG CTT TCG-**3'**

N-terminal PAK6 mutant (amino acids 1–367)

*att*B1 Forward primer: **5'**-GGGG ACA AGT TTG TAC AAA AAA GCA GGC TTG ATG TTC CGC AAG AAA AAG AAG AAA-**3'**

*att*B2 Reverse primer: **5'**-GGG GAC CAC TTT GTA CAA GAA AGC TGG GTC TCA CTG GGG CAG GTA CAG GTT GCT GGT-**3'**

C-terminal PAK6 mutant (amino acids 368–682)

*att*B1 Forward primer: **5'**-GGG GAC AAG TTT GTA CAA AAA AGC AGG CTT GGA CCT GGA CCC CAC GGT TGC CAA GGG TGC C-**3'**

*att*B2 Reverse primer: **5'**-GGGG A CCA CTT TGT ACA AGA AAG CTG GGT C TCA GCA GGT GGA GGT CTG CTT TCG-**3'**

Mutagenic primers

S560E PAK6 mutant (predicted PAK6 autophosphorylation site)

Forward primer: **5'**-CGT CCC TAA GAG GAA GGA GCT GGT GGG AAC CCC CT-**3'**

Reverse primer: **5'**-AGG GGG TTC CCA CCA GCT CCT TCC TCT TAG GGA CG-**3'**

S531N PAK6 mutant (Kinase active PAK6 mutant)

Forward primer: **5'**-GGG ACA TCA AGA GTG ACA ACA TCC TGC TGA CCC TCG-**3'**

Reverse primer: **5'**-CGA GGG TCA GCA GGA TGT TGT CAC TCT TGA TGT CCC-**3'**

K436A PAK6 mutant (Kinase dead PAK6 mutant)

Forward primer: **5'**-CGC CAG GTG GCC GTC GCG ATG ATG GAC CTC AG-**3'**

Reverse primer: **5'**-CTG AGG TCC ATC ATC GCG ACG GCC ACC TGG CG-**3'**

Sequencing Primers

Primer	Sequence
P19 Forward	**5'**-GTA ACA TCA GAG ATT TTG AGA CAC-**3'**
P20 Reverse	**5'**-TCG CGT TAA CGC TAG CAT GGA TC-**3'**
Internal PAK6	**5'**-CCT AGC CCT AAG ACC CGG G-**3'**
GST GEX-5 Forward	**5'**-GGG CTG GCA AGC CAC GTT TGG TG-**3'**
GST T7 terminator Reverse	Primer provided by Eurofins MWG Operon
pEGFP-C1 Forward	Primer provided by Eurofins MWG Operon
pEGFP-C1 Reverse	Primer provided by Eurofins MWG Operon

Appendix 2 - siRNA oligonucleotide sequences

Control siRNA (non-silencing)

Target sequence: AAT TCT CCG AAC GTG TCA CGT

PAK6 siRNA (Oligonucleotide 1)

Target sequence: GGC UAU UCC GAA GCA UGU Utt

PAK6 siRNA (Oligonucleotide 2)

Target sequence: CCA AUG GGC UGG CUG CAAA

Appendix 3 - Figure legends for movies 1-5

Movie 1
DU145 cells were left for 48 hours to form colonies and were then serum-starved for 24 hours. Cells were then filmed for 24 hours at 5 minute intervals using phase-contrast time-lapse microscopy (see **section 2.2.10**). Movie is representative of 3 independent experiments.

Movie 2
DU145 cells were left for 48 hours to form colonies and were then serum-starved for 24 hours. Cells were then stimulated with HGF (10 ng/ml) and filmed for 24 hours at 5 minute intervals using phase-contrast time-lapse microscopy (see **section 2.2.10**). Movie is representative of 3 independent experiments.

Movies 3PC and 3G
EGFP lentiviral vector expressing DU145 cells were seeded into a 98% collagen I and a 2% matrigel 3D matrix and left for one week to form colonies. Cells were then serum-starved for 24 hours prior to filming. Cells were filmed for 24 hours at 5 minute intervals. Cells were filmed using phase-contrast (PC) and GFP fluorescence (G) time-lapse microscopy (see **section 2.2.10**). Movies are representative of 3 independent experiments.

Movies 4PC and 4G
EGFP lentiviral vector expressing DU145 cells were seeded into a 98% collagen I and a 2% matrigel 3D matrix and left for one week to form colonies. Cells were serum-starved for 24 hours and then stimulated with HGF (500 ng/ml) for 48 hours. Cells were then filmed for 24 hours at 5 minute intervals using phase-contrast (PC) and GFP fluorescence (G) time-lapse microscopy (see **section 2.2.10**). Movies are representative of 3 independent experiments.

Movies 5PC and 5G
DU145 cells were transfected with WT GFP-PAK6. Cells were immediately filmed for 24 hours at 5 minute intervals using phase-contrast (PC) and GFP fluorescence (G) time-lapse microscopy (see **section 2.2.10**). Movies are representative of 3 independent experiments.